Graduate School for Cellular and Biomedical Sciences

University of Bern

Identification and Targeting of Novel Mechanisms for Treatment of Castration Resistant Prostate Cancer (CRPC)

PhD Thesis submitted by

Katyayani Sharma

for the degree of

PhD in Biochemistry and Molecular Biology

Supervisor

Prof. Dr. Amit V Pandey

Pediatric Endocrinology, Department of Pediatrics,
Faculty of Medicine of the University of Bern

Co-advisor

Prof. Dr. med Jean-Marc Nuoffer

Institute of Clinical Chemistry, University Hospital Bern,
Faculty of Medicine of the University of Bern

b
UNIVERSITÄT
BERN

UNIVERSITÄT
BERN

Accepted by the Faculty of Medicine, the Faculty of Science and the Vetsuisse Faculty of the University of Bern at the request of the Graduate School for Cellular and Biomedical Sciences

Bern, Dean of the Faculty of Medicine

Bern, Dean of the Faculty of Science

Bern, Dean of the Vetsuisse Faculty Bern

UNIVERSITÄT
BERN

PhD Thesis Committee

Supervisor:

Prof. Dr. Amit V Pandey
Department of Pediatric Endocrinology, Faculty of Medicine, University Children's Hospital, University of Bern
Translational Hormone Research, Department of Biomedical Research, University of Bern

Co-supervisor:

Prof. Dr. med Jean-Marc Nuoffer
Institute of Clinical Chemistry, University Hospital Bern,
Faculty of Medicine, University of Bern

GCB Mentor:

Prof. Dr. Ren-Wang Peng
Division of General Thoracic Surgery, University Hospital Bern
Department of Biomedical Research (DBMR), University of Bern

External co-referee:

Prof Pieter Swart
Department of Biochemistry, Stellenbosch University, South Africa

Acknowledgements

I would like to express my sincere gratitude to my supervisor, Dr Amit V Pandey for giving me the opportunity to pursue my doctoral studies in University of Bern, Switzerland. Without his constant support and advice, this endeavor would not have been possible. I am grateful for his encouragement towards participating in different national and international conferences that not only helped me to present my research work but also gave me an incredible chance to visit different parts of the world which has brought about a positive change in my personality.

A special mention goes to the Swiss Government Excellence Scholarship (ESKAS), for all the financial support and help right before and after my arrival to Bern till the end of my studies. Especially Jasmin Fallahi and Chantal Hinni, I appreciate their assistance in all the matters concerning living in Bern. I am extremely grateful to Dr Christa E. Flueck, for her insightful guidance regarding my research projects which has always expanded my knowledge. I would like to extend my heartfelt thanks to my GCB mentor, Prof Reng-Wang Peng for his excellent suggestions that helped me in completing my project. I also want to acknowledge the collaborators from Poland and Denmark, who have significantly contributed to carry out a major portion of my doctoral research. I would also like to extend my genuine appreciation to Kay Sauter and Silvia Rihs, for their assistance in all the lab related work and experimental support. I am grateful to Shaheena, Patricia, Emanuele, Stathis, Idoia, Natalia and Jibira for helping me to carry out my research experiments. I will be always thankful to all my lab members for their constant help and motivation which helped me tremendously to deal with the challenges during my PhD journey. I am deeply thankful to all my professors and teachers for their strong belief in me that has been a guiding light for my entire academic career.

I am blessed to have constant love and emotional support from family and friends both in Bern and back home in India. I am immensely thankful to Kiran, Shripriya, Meghranjana, Mohanna, Disha and Aryavrat for all the trips and fun during our Indian festival celebrations which did not let me to miss home that much. I am thankful to Gayatri, Vidhi and Ayushi for the long talks during weekends which brought a great relief from the mundane life and kept me sane in difficult times. Last but never the least, my mother has been a pillar of strong emotional support throughout my life. I am indebted forever to her teachings and values that has always inspired me to become a better person in life. With a significant role in enhancing my scientific knowledge, my PhD journey has taught me the values of patience, perseverance, and endurance.

"The only true wisdom is in knowing you know nothing.
The only true freedom comes from knowledge."
Socrates

ABSTRACT

Prostate cancer (PCa) is a major cause of cancer-related deaths in men. Its prevalence varies by region, with higher rates in North America, Europe, and Australia. The incidence of prostate cancer tends to increase with age, making it particularly relevant in aging populations. PCa cells are stimulated by Androgens through intracellular Androgen Receptor (AR). AR acts as a transcriptional activator for the expression of genes responsible for growth and survival of the tumor (Tan et al., 2015). Therefore, lowering the levels of Androgens in circulation and/or blocking AR is the most employed method for treatment of PCa (Harris et al., 2009). However, during metastatic conditions such as Castration Resistance Prostate Cancer (CRPC), the tumor cells develop mechanisms to evade androgen dependency for their growth and survival. These mechanisms include expression of AR variants which bind to androgen precursors of adrenal origin and *de novo* intra tumoral androgen production. Therefore, androgen biosynthesis seems to be the key target for treatment of Castration Resistant Prostate Cancer (R. Bruce Montgomery et al., 2008).

In humans, androgens are primarily produced in the male testis, female ovaries, and adrenal glands. Androgens control male sex traits and development as well as influence female sexual behavior. The Zona Reticularis (ZR) of adrenal cortex produces dehydroepiandrosterone (DHEA) and its sulphate, DHEAS. DHEA(S) acts as precursors for production of androgens (testosterone and androstenedione). An essential enzyme that plays an important role in adrenal androgen production is cytochrome P450c17 (encoded by CYP17A1). CYP17A1 localized in the endoplasmic reticulum, can catalyze both 17α-hydroxylase and 17,20 lyase reactions (Zuber et al., 1986). It is known that CYP17A1 is the qualitative controller of steroidogenesis. The 17, 20 lyase activity of CYP17A1 is supported by at least three factors. First, the amount of POR for electron transfer (Flück et al., 2004), second, presence of allosteric activator microsomal CYB5 (Pandey & Miller, 2005b; Storbeck et al., 2013; Yin et al., 2015), and third, phosphorylation of the CYP17A1 protein at serine residues (Petra Kempná et al., 2010; Amit V. Pandey et al., 2003; Pandey & Miller, 2005b; Tee et al., 2008).

Given the major role of CYP17A1 in androgen production, finding specific CYP17A1 inhibitors for clinical use is of great interest. Abiraterone is a CYP17A1 inhibitor already in use for prostate cancer treatment but unfortunately it also alters activities of other CYP enzymes (Attard et al., 2008; Yin & Hu, 2014). Recent identification of an active site mutation in humans that specifically abolishes 17,20 lyase activity of human CYP17A1, provides hope for design of specific CYP17A1 inhibitors (Fernández-Cancio et al., 2018). Therefore, with new drug development strategies more selective CYP17A1 17,20 lyase inhibitors are currently being designed and tested. In addition, the focus is on finding molecules that do not

resemble steroid hormones and should not be metabolized into androgen like molecules, which could act as strong inducers of androgen receptor mediated signaling.

In this thesis, we report outcomes resulting from screening a number of small molecule inhibitors that could be developed as potential selective inhibitors of CYP17A1 lyase activity. This included computationally designed and chemically synthesized small molecules that were predicted to bind to the active site of CYP17A1 in a similar way as Abiraterone and native substrates of the enzyme. Also, the possible role of Endocrine disruptors in the regulation of androgen production was explored through screening essential oil metabolites and certain plant extracts for inhibition of CYP17A1 activity. Few case reports have suggested that long term exposure to certain natural products can be causative environmental factors contributing towards increased risk of cancer (Ramsey et al., 2019; Ramsey et al., 2020). Therefore, findings from this work can help in providing structural leads for designing better and efficient inhibitors of CYP17A1.

Another way to target CYP17A1 lyase activity is to understand mechanisms involved in the regulation of CYP17A1 activity through phosphorylation. It has been shown that the increased production of adrenal and ovarian C19 steroids may be regulated through an unknown signal transduction pathway that ultimately enhances the Ser/Thr phosphorylation of CYP17A1 (Zhang et al., 1995). In a recent finding, CYP17A1 was found to be phosphorylated by p38α in a manner that selectively enhances its 17,20 lyase activity. This suggests possibility that other kinases may also play a role in this process. In addition, a protein phosphatase, PP2A dephosphorylated CYP17A1, that can in turn be inhibited by the phosphoprotein SET (A. V. Pandey et al., 2003). ROCK1, a protein previously associated with CYP17A1 phosphorylation might act as an upstream scaffolding protein in a MAPK pathway. The involvement of these kinases or phosphatases have helped in prediction of a signaling cascade leading to phosphorylation of CYP17A1 (Tee & Miller, 2013). Therefore, finding the missing links in these pathways can provide insight into mechanism involved in regulation of CYP17A1 activity.

We have identified a potential role of PLK1 in this signaling cascade. A continuous deprivation of PLK1 resulted in decreased CYP17A1 lyase activity. Additionally, a transcriptomic analysis was performed to find out differentially expressed kinases and phosphatases expressed in case of PCa and PCOS. Overexpression of these genes in human adrenal cell line caused changes in the lyase activity. A protein-protein interaction database search suggested that these proteins can interact with the proteins in the previously predicted signaling cascade. If validated, known inhibitors of these proteins can be exploited to selectively inhibit CYP17A1 lyase activity.

Understanding the regulatory mechanisms of 17,20 lyase activity is important for the understanding of hyperandrogenic disorders such as premature, exaggerated adrenarche and the polycystic ovary syndrome (PCOS) (Essah et al., 2006). Development of drugs to reduce the levels of circulating androgens without affecting cortisol levels can overcome the side effects of currently used drugs. Moreover, this property can also be used to treat androgen excess disorders such as PCOS and premature adrenarche offers a broader therapeutic application in context of overall reproductive health.

Table of Contents

Acknowledgements **7**
Abstract **9**
Table of Contents **13**
List of Figures and Tables **15**
List of Abbreviations **16**
Introduction **19**
1. Prostate Cancer (PCa) ***21***
1.1. Epidemiology 21
1.2. History 21
1.3. Risk factors 22
1.4. Pathophysiology 23
1.5. Clinical manifestation 26
1.6. Diagnosis 26
1.7. Classical Treatment 27
2. Human Steroid Biosynthetic Pathway (Steroidogenesis) ***30***
2.1. Introduction 30
2.2. Chemistry of Steroidogenesis 30
2.3. Cytochrome P450 enzymes (CYPs) 32
2.4. Androgen synthesis and Cytochrome P450 c17 (CYP17A1) 32
2.5. Role of CYP17A1 in Estrogen synthesis and PCOS 33
2.6. Role of CYP17A1 in Hyperandrogenic disorders 34
2.7. Regulation of CYP17A1 activity 34
Hypothesis **39**
Aims **39**
Materials and methods **41**
3. Experimental details ***43***
3.1. General Laboratory Practice 43
3.2. Handling of Radioactive materials 43
3.3. Preparation of cell culture media, buffers, and other reagents 43
3.4. Cell culture 45
3.5. Cell Viability Assays 48

3.6. General Protocol for cell-based enzyme assay 50
3.7. Transformation of competent cells 55
3.8. Maxi-Prep for Plasmid 56
3.9. Transient transfection 57
3.10. Stable transfection 58
3.11 siRNA transfection 59
3.12 Statistical analysis 60
Results 61
Chapter 1 65
Screening computationally designed and chemically synthesized compounds against CYP17A1 activity. 65
Section A: Synthesis and Structure-Activity Relationships of Novel Non-Steroidal CYP17A1 Inhibitors as Potential Prostate Cancer Agents 67
Section B: Exploring the Potential of Sulfur Moieties in Compounds Inhibiting Steroidogenesis 69
Chapter 2 71
Endocrine Disrupting Chemical as structural cues for the development of inhibitors of CYP17A1 activity 71
Section C: Essential oil components may act as antiandrogen compounds in prostate cancer by inhibition of steroidogenic cytochrome P450 activities. 73
Section D: Effect of crude extracts from plant tissue of Ghost pepper and Vietnamese coriander on CYP17A1 activity. 75
Chapter 3 81
Study the role of specific Kinases and Phosphatases involved in the regulation of CYP17A1 lyase activity. 81
Section E: Effect of selected kinases and phosphatases in the regulation of CYP17A1 activity 83
Section F: Effect of PLK1 in the regulation of CYP17A1 activity. 87
General discussion 93
References 95
Curriculum Vitae 111
List of Publications 113
Appendix I 115
Appendix II 117

List of Figures and Tables

Figure 1: *Schematic Representation of Human Steroidogenic Pathway in a simplified form, depicting the major Cytochrome P450s involved.* ***31***

Figure 2: *Animated representation of interaction between P450c17, POR and Cytochrome B5 during an enzymatic reaction.* ***36***

Figure 3 *Outline of common steps followed to assay CYP17A1 enzyme activity.* ***51***

Figure 4 *Schematic representation of the 17,20-lyase reaction.* ***53***

Figure 5 *Inhibition of CYP17A1 Hydroxylase activity by test compounds for 24 hours in NCI H295R cells.* ***76***

Figure 6: *Steroid profile by LC-MS in cells treated with 50 µg/mL extracts for 24 hours.* ***77***

Figure 7: *Cell viability assay performed in LNCaP cells to determine the effect of increasing concentration of the extracts on tumor growth for a duration of 24 hours.* ***78***

Figure 8: *Gene Map of pcDNA 3.1 plasmid (GenScript) used in transfection experiments.* ***83***

Figure 9: *Inhibition of CYP17A1 Lyase activity in transiently transfected NCI H295R cells with plasmids of Kinases and Phosphatases at 48, 72 and 96 hours.* ***84***

Figure 10: *Inhibition of CYP17A1 activity by PLK1 inhibitor.* ***88***

Figure 11: *Inhibition of CYP17A1 Lyase activity by test compounds at 10 µM concentration for 3h in NCI H295R cells.* ***89***

Figure 12: *PLK1 knock-down in NCI H295R cells transfected with siPLK1 using Lipofectamine 2000 reagent.* ***90***

Figure 13: *PLK1 inhibits cellular growth of LNCaP cells in a dose-dependent manner with an IC50 at 11.6 µM.* ***91***

Figure 14: *Signaling pathway involving different protein kinases and phosphatases in post translational regulation of CYP17A1.* ***92***

Table 1*: Small molecule inhibitors from Boehringer Ingelheim. Selective PLK1 inhibitor, BI 2536 were used to test CYP17A1 activity in NCI H295R cell line.* *87*

List of Abbreviations

ABT	Abiraterone
ACTH	Adrenocorticotropic Hormone
ADT	Androgen Deprivation Therapy
ANOVA	Analysis of Variance
AR	Androgen Receptor
ARE	Androgen Response Element
BRCA	Breast Cancer genes
cAMP	cyclic Adenosine monophosphate
CDK	Cyclin Dependent Kinase
CPR/POR	Cytochrome P450 Reductase
CRPC	Castration Resistance Prostate Cancer
CYB5	Cytochrome B5
CYP	Cytochrome P450
DHEA	Dehydroepiandrosterone
DHEAS	Dehydroepiandrosterone sulfated form
DHT	Dihydrotestosterone
DMSO	Dimethyl sulfoxide
DNA	Deoxyribonucleotide acid
DUSP	Dual Specificity Phosphatase
EDTA	Ethylenediamine tetra acetic acid
EOs	Essential Oils
FAD	Flavin adenine dinucleotide
FDX	Ferredoxin
FDXR	Ferredoxin reductase
FMN	Flavin mononucleotide
GFP	Green Fluorescent Protein
GnRH	Gonadotropin Releasing Hormone
GSK	Glycogen Synthase Kinase
HEPES	4-(2-hydroxyethyl)-1-piperazineethanesulfonic acid
HSD	Hydroxysteroid dehydrogenase
IC50	Inhibitory Concentration 50
IUPAC	International Union of Pure and Applied Chemistry
LB	Luria Bertani

LC	Liquid Chromatography
LH	Luteinizing hormone
LHRH	Luteinizing hormone-releasing hormone
MAPK	Mitogen-activated protein kinase
MTT	3-(4,5-dimethylthiazol-2-yl)-2,5-diphenyltetrazolium bromide
NADPH	Nicotinamide adenine dinucleotide phosphate hydrogen.
PBS	Phosphate buffered saline
PCa	Prostate Cancer
PCOS	Polycystic ovary syndrome
PLK	Polo-like kinase
POR/CPR	P450 Oxidoreductase
PP/PPP	Protein phosphatase
Preg	Pregnenolone
Prog	Progesterone
17OH-Preg	17α-hydroxy pregnenolone
17OH-Prog	17α-hydroxy progesterone
RNA	Ribonucleotide acid
ROCK	Rho-associated protein kinase
SF-1	Steroidogenic Factor-1
SREBP	Sterol regulatory element binding protein
SULT2A1	Sulfotransferase Family 2A Member 1
TLC	Thin Layer Chromatography
UV	Ultraviolet
ZF	Zona fasciculata
ZG	Zona glomerulosa
ZR	Zona reticularis

UNIVERSITÄT
BERN

INTRODUCTION

1. Prostate Cancer (PCa)

It is a prevalent malignancy that arises from the prostate gland, an essential component of the male reproductive system. It primarily affects older men, with most cases occurring in individuals over 50 years of age. PCa is a significant global health concern, with substantial morbidity and mortality rates (Giwercman & Giwercman, 2000). The disease is characterized by its potential to exhibit diverse clinical behavior, ranging from slow-growing, indolent tumors to aggressive, rapidly spreading cancers. Understanding the etiology, risk factors, pathogenesis, and diagnostic strategies for PCa is crucial for effective management and the development of targeted therapies.

1.1. Epidemiology

With about 1.4 million new cases and 375,000 deaths worldwide, PCa is the second most frequent cancer and the fifth leading cause of cancer death among men. The occurrence of PCa differs across various ethnic groups and geographical regions. The most affected are black men and the prevalence rate are 3 times higher in developed countries than in developing countries, probably due to longer life expectancy. Countries in sub-Saharan Africa, the Caribbean, and Central and South America as well as Sweden have the highest number of PCa-related deaths (Rawla, 2019; Taitt, 2018).

1.2. History

The first detailed description of Prostate was documented by the Venetian anatomist Niccolò Massa in the 16th century, however, PCa was not discovered until 1853 by J. Adams, a surgeon at The London Hospital (Denmeade & Isaacs, 2002; Lytton, 2001). The first successful radical prostatectomy (complete removal of the prostate gland) was performed in 1904 by Hugh Hampton Young (Lepor, 2005). Terence Millin, an Irish urologist revolutionized prostate surgery for both benign and malignant diseases. By the end of the 1920s, there were 3 main operations to relieve bladder outflow obstruction because of prostatic enlargement (O'Brien et al., 2009). The introduction of transurethral resection of the prostate (TURP) in the 1930s provided a less invasive option for managing prostate enlargement and early-stage cancer with maintenance of penile function (Walsh et al., 1983). This marked a significant advancement in the surgical treatment of PCa, although it was still a high-risk procedure with substantial effects. In 1941, Charles B. Huggins conducted studies that utilized estrogen to counter testosterone production in men with metastatic PCa. This groundbreaking approach of "chemical castration" earned Huggins the prestigious 1966 Nobel Prize in Physiology and Medicine (Huggins & Hodges, 1972). In a parallel breakthrough, Andrzej W. Schally and Roger Guillemin explained the significance of the gonadotropin-releasing hormone (GnRH) in reproduction, leading to their joint receipt of the 1977 Nobel Prize in Physiology and Medicine. The development of GnRH receptor agonists, including leuprolide and goserelin ensued new

approach towards PCa treatment (Schally et al., 1971). The 21st century has seen a focus on understanding the genetics and molecular biology of PCa. Advances in targeted therapies, immunotherapy, and precision medicine has gained preference for the treatment of PCa.

1.3. Risk factors

PCa is a complex disease influenced by various genetic, environmental, and lifestyle factors.

1.3.1. Age: Age is the most significant risk factor for prostate cancer. The incidence of prostate cancer increases with age, particularly after the age of 50. This suggests that cumulative exposure to risk factors over time contributes to the development of the disease (Hankey et al., 1999).

1.3.2. Genetics and Family History: Family history plays a role in prostate cancer risk. Having a first-degree relative (father or brother) with prostate cancer increases the risk. Certain genetic mutations and variations have also been linked to an elevated risk of developing prostate cancer (Zeegers et al., 2003).

1.3.3. Race and Ethnicity: Prostate cancer is more common in certain racial and ethnic groups. African American men have the highest incidence of prostate cancer, followed by Caucasian men. Asian and Hispanic men have lower incidence rates (Rawla, 2019).

1.3.4. Hormonal Factors: Androgens, including testosterone, play a crucial role in the development and growth of the prostate. Men with higher levels of testosterone might be at a slightly increased risk. This is supported by observations that prostate cancer risk decreases after surgical or medical castration (Gann, 2002).

1.3.5. Dietary Factors: Diet may influence prostate cancer risk. Diets high in red meat, particularly processed meats, and low in fruits, vegetables, and whole grains have been associated with a higher risk. Obesity might also contribute to an increased risk of aggressive prostate cancer (Bylsma & Alexander, 2015).

1.3.6. Environmental Factors: Exposure to certain environmental factors, such as toxins or chemicals, might increase the risk of prostate cancer. However, the specific mechanisms behind these associations are not yet fully understood (Ferrís et al., 2011).

1.3.7. Genetic factors: While often associated with breast and ovarian cancers, mutations in the Breast Cancer, (BRCA1 and BRCA2) genes also increase the risk of prostate cancer in men. These mutations impair DNA repair mechanisms, increasing the likelihood of cancer development (Nyberg et al., 2020). Certain mutations in the genes like Homeobox transcription factor (HOXB13), Microseminoprotein-B (MSMB), elaC homolog-2/hereditary prostate cancer (ELAC2/HPC2), Ribonuclease L (RNASEL); Ataxia-Telangiectasia and Mantle Cell Lymphoma Serine-Threonine Kinase (ATM), Tumor suppressor (TP53), proto-oncogene (MYC) and androgen-regulated homeodomain gene (NKX3.1) have been linked to an increased risk of PCa (Ewing et al., 2012; Gurel et al., 2010; Karlsson et al., 2021; Maxwell et al., 2022; Meyer et al., 2010; Qiu et al., 2022; Sjöblom et al., 2016; Wang et al., 2001).

1.4. Pathophysiology

1.4.1. Tumor initiation and progression: PCa develops when abnormal cells within the prostate gland undergo uncontrolled proliferation, leading to the formation of a tumor. The prostate gland is located in the male pelvis at the base of the penis, below the urinary bladder and immediately anterior to the rectum. Prostate cancer is categorized as an adenocarcinoma, a type of cancer originating from glandular tissues. It initiates when regular cells within the prostate gland, responsible for producing semen, undergo genetic mutations, transforming into cancerous cells. The peripheral zone of the prostate gland is where adenocarcinoma is predominantly observed. Initially, minute clusters of cancer cells remain confined within structurally normal prostate gland, a condition referred to as carcinoma in situ or prostate intraepithelial neoplasia (PIN). While not definitively proven as a precursor, PIN is closely linked to the presence of cancer. Over time, these cancerous cells undergo rapid multiplication, infiltrating the adjacent prostate tissue (known as the stroma) and forming a distinct tumor. Eventually, this tumor might enlarge significantly, invading neighboring organs like the seminal vesicles or the rectum. Alternately, the cancer cells could develop the capability to migrate through the bloodstream and the lymphatic system leading to metastasis. Among the common sites of metastasis are bones and lymph nodes. With local progression, the cancer may also extend to the rectum, bladder, and lower ureters. It's thought that the path of metastasis to the bones occurs via the venous route, as the prostatic venous plexus, which drains the prostate, is interconnected with the vertebral veins (Castillejos-Molina & Gabilondo-Navarro, 2016).

1.4.2. Role of Androgens: Apart from mutations or alterations in the genetic make-up of prostate cells, abnormal levels of the male sex hormone, Androgen contributes to the progression of PCa. Androgens play a vital role in the normal development and function of the prostate gland (Mustafa et al., 2016). Androgens are also responsible for secondary sex characteristics in males and act as precursor for sex hormone, Estrogen in females. The synthesis of androgens occurs primarily in the testes, where Leydig cells produce testosterone under the regulation of luteinizing hormone (LH) secreted by the pituitary gland. Testosterone is transported via the bloodstream to the prostate, where it is converted into the more potent and biologically active form, Dihydrotestosterone (DHT), by the enzyme 5-alpha-reductase. DHT exerts its effects on prostate cells by binding to and activating the androgen receptor (AR), a transcription factor that modulates gene expression involved in cell growth, differentiation, and survival (Bluemn & Nelson, 2012).

1.4.3. Castration-resistant Prostate Cancer (CRPC): Initially, cancer cells remain dependent on androgens for growth and survival, and this dependence is exploited therapeutically through Androgen Deprivation Therapy (ADT), which aims to suppress

androgen production or block androgen receptor activation. ADT effectively reduces tumor burden and slows disease progression in most patients. However, over time, PCa cells may adapt and develop mechanisms to overcome androgen deprivation, leading to a more aggressive form of the disease known as Castration-resistant PCa. In CRPC, despite low circulating levels of androgens, cancer cells find alternative pathways to sustain androgen signaling.

There are several mechanisms that contribute to the development of CRPC:

- **Androgen Receptor Mutations**: Cancer cells can acquire mutations in the AR that make it more sensitive to lower levels of androgens or even allow it to be activated by ligands other than Androgens.
- **Intra-tumoral Androgen Production**: Some cancer cells start producing androgens de novo, allowing them to sustain growth even when systemic androgen levels are low.
- **Alternative Signaling Pathways**: Cancer cells may find ways to grow by activating other growth-promoting pathways that are not dependent on androgens.
- **Androgen Receptor Amplification**: Tumor cells might increase the number of androgen receptors on their surface, making them more responsive to even trace amounts of androgens.
- **Epithelial-Mesenchymal Transition (EMT):** This is a process by which cancer cells become more aggressive and invasive. During EMT, cancer cells can lose their dependence on androgens for growth.

1.4.4. Role of Genetic mutations:

1.4.4.1. Tumor suppressor genes: Mutations in genes like Rb (retinoblastoma), CDKN2, and p53, which have been detected in both hereditary and non-hereditary (sporadic) cancer cases, are not commonly changed during the initial stages of prostate cancer development. However, these mutations have been observed to undergo alterations in advanced prostate cancer cases (MacGrogan & Bookstein, 1997).

1.4.4.2. Oncogenes: Growth factors such as Insulin like Growth Factor, (IGF), human epidermal growth factor (Her2-Neu), Fibroblast growth factors (TGF-β), Vascular endothelial growth factor, and Phosphoinositide-3 Kinase have been implicated in PCa development. It acts as an endocrine hormone and activates several downstream signaling pathways involved in antiapoptotic and proneoplastic processes. Her2-Neu facilitates androgen independent activation of AR, thus playing a crucial role in metastasis of tumor (Dasgupta et al., 2012; Reynolds & Kyprianou, 2006).

1.4.4.3. DNA repair genes: AR transcriptional activity is important for normal prostate development as well as tumor development. Defects in DNA repair mechanisms can alter the expression of AR related genes and affect the overall signaling pathway leading to

abnormal development of prostate cells. Several DNA repair genes like BRCA2 and BRCA1, Cyclin-dependent kinase (CDK12), Serine-threonine kinase (ATM), cell cycle checkpoint regulator (RAD51C) have been associated with prostate cancer (Mateo et al., 2017).

1.4.4.4. Epigenetic changes: Hypermethylation of the promoter region of several genes repress activity of tumor suppression and cell cycle regulation. Genes such as adenomatous polyposis coli (APC) , Retinoic acid receptor (RARβ), Ras association domain family (RASSF1), Cyclin D2 family (CCND2), Cyclin dependent kinase (CDKN1B) have been studied for its role in PCa development (Albany et al., 2011).

1.4.4.5. Androgen Receptor mutations: The AR belongs to a nuclear receptor superfamily which includes the estrogen, progesterone, glucocorticoid, and thyroid hormone receptors. The AR gene is located on chromosome X (Xq11-12) comprising 8 exons. AR has four regions: the N-terminal, an NH2 terminal transactivation domain (NTD) encoded by exon 1, a DNA-binding domain (DBD) encoded by exons 2–3, a hinge region encoded by exon 4, and a ligand binding domain (LBD) encoded by exons 5–6 which results in the production of an 11 kDa protein. Upon binding of testosterone or DHT to the ligand-binding domain, AR undergoes a conformational alteration. Then it relocates to the nucleolus, where it dimerizes and subsequently attaches to the androgen-response element (ARE) located in the promoter and enhancer regions of specific genes. This binding is facilitated by the zinc-finger present in the DBD of the receptor (Fujita & Nonomura, 2019).

- **Point mutations** such as T878A, F876L, L702H in the LBD or NTD domain of AR gene renders the receptor to lose its ligand specificity resulting in activation of AR by other steroids such as progesterone and estrogen. These mutations are also responsible for resistance towards AR antagonists like enzalutamide, flutamide, and bicalutamide used in the treatment of PCa (Azad et al., 2015).

- **Gain of function Mutations** lead to the overexpression of AR and enable tumor cells transform to an androgen independent mechanism to grow and proliferate. Overexpression of genes encoding enzymes like 3β-hydroxysteroid dehydrogenase type 1 (HSD3β), Cytochrome P450 (CYP17A1, CYP11A1), aldo-keto reductase family 1 member C3 (AKR1C3), involved in production of androgen and its precursor tends to over activate AR (Chang et al., 2013; R. B. Montgomery et al., 2008). This facilitates the tumor cell to grow independent of circulating adrenal androgens. It is a common mechanism observed in the case of an advanced form of PCa, known as Castration Resistant PCa (Cai et al., 2011) .

1.5. Clinical manifestation

Although not specific, some symptoms may imply onset of benign state of prostate tumor, these might include frequent urination, nocturia (heightened urination during the night), challenges in initiating and sustaining a consistent urine flow, presence of blood in urine (hematuria), and discomfort during urination (dysuria) (Hamilton et al., 2006; Kim & Kim, 2017). Urinary issues are most common due to the proximity of the prostate gland to the prostatic urethra. Alterations within the gland have a direct impact on urinary capabilities. As the vas deferens releases seminal fluid into the prostatic urethra, and the prostate gland contributes to semen composition, PCa can additionally lead to challenges related to sexual function. These might encompass difficulties in attaining an erection or experiencing painful ejaculation (Hyun, 2012). Advanced PCa has the potential to metastasize to different body regions, potentially leading to supplementary symptoms. Among these, the prevalent indication is discomfort in the bones, frequently observed in the spine, pelvic area, or ribs. When cancer migrates to bones like the femur, it generally affects the proximal or adjacent sections of the bone. Furthermore, prostate cancer located in the spinal region can exert pressure on the spinal cord, inducing sensations of tingling, leg weakness, and difficulties with urinary and bowel control (Leslie et al., 2023). In its advanced stages, the condition might also bring about fatigue due to reduced red blood cell levels.

1.6. Diagnosis

1.6.1. Medical History and Physical Examination: A healthcare provider will start by taking a detailed medical history and conducting a physical examination. This may involve discussing any symptoms you're experiencing and your risk factors for PCa.

1.6.2. Imaging Studies: The identification of prostate irregularities can be done through a digital rectal examination. A type of cystoscopy, involving the insertion of a slender, flexible camera tube through the urethra, enables visualizing the interior of the bladder and urinary tract. Transrectal ultrasonography employs sound waves emitted from a probe in the rectum to generate an image of the prostate. Prostate Magnetic Resonance Imaging (MRI) outperforms ultrasounds in depicting soft tissues with greater precision. Presently, MRI serves as advanced diagnostic tool for prostate biopsy by either merging MRI with ultrasound or employing MRI-guided procedures independently (Descotes, 2019; Ghadimi & Sapra, 2023).

1.6.3. Biopsy: In the process of a biopsy, either a urologist or a radiologist acquires tissue specimens from the prostate by means of the rectum. A biopsy gun is employed to swiftly insert and withdraw specialized hollow-core needles, usually ranging from three to six needles on each side of the prostate. The use of antibiotics is recommended to mitigate

potential complications like fever, urinary tract infections, and sepsis. Subsequently, the collected tissue samples undergo analysis to ascertain the presence of cancer cells and to assess their microscopic characteristics (Shariat & Roehrborn, 2008; Streicher et al., 2019).

1.6.4. Prostate Specific Antigen (PSA): A blood test measures the level of PSA, a protein (Serine protease) produced by the prostate gland. PSA is naturally present in small amounts in the blood, and its main function is to liquefy semen, aiding in the movement of sperm. Elevated PSA levels can indicate the possibility of PCa, though other factors like age, prostate size, and infection can also influence PSA levels. PSA serves as a prominent biomarker for PCa, but sometimes its specificity is constrained due to the frequent occurrence of falsely elevated values in individuals with benign prostatic hyperplasia (BPH) (Stenman et al., 1999).

1.6.5. Gleason score: A grading system used to evaluate the aggressiveness of prostate cancer based on the microscopic appearance of cancer cells in a tissue biopsy sample. The Gleason score is named after Dr. Donald Gleason, who developed the system in the 1960s. The score is determined by examining the patterns of cancer cells under a microscope and assigning two grades. The sum of these two grades constitutes the Gleason score, which can range from 2 to 10. Lower Gleason scores (6 or below) indicate less aggressive while higher Gleason scores (8, 9, or 10) indicate more aggressive form with a higher potential for rapid spread.(Epstein et al., 2016; Gordetsky & Epstein, 2016)

1.6.6. Determination of Stages: If PCa is confirmed, additional tests may be performed to determine the stage of the cancer which indicates its size, extent of spread, and whether it has metastasized to other parts of the body. The primary system used for staging PCa is developed by the American Joint Committee on Cancer and the Union for International Cancer Control. Based on Gleason score, PCa is categorized into 4 stages (I-IV) with certain tumor characteristics defined by TNM (Tumor, Node, Metastasis) system (Cheng et al., 2012; Telloni, 2017).

1.7. Classical Treatment

1.7.1. Androgen Deprivation Therapy (ADT): This aims to reduce the levels of androgens that fuel the growth of prostate cancer cells. It can involve medications that suppress hormone production or block hormone receptors and surgical methods to lower testosterone levels.

1.7.2. Surgical Castration (Orchiectomy): A surgical procedure that entails the removal of the testes, which was performed as a straightforward operation. The basic form of orchidectomy is conducted through the scrotum and was historically a prominent method of hormonal control in treating patients with PCa that had progressed locally. However,

this has been gradually replaced by a reversal and less invasive hormonal treatments like GnRH agonists or antagonists (Okoye & Saikali, 2023).

1.7.3. Hormone Therapy: Diethylstilbestrol, a semi-synthetic estrogen compound, emerged as an early nonsurgical choice in PCa treatment. Its extensive use has been restricted due to notable cardiovascular and thromboembolic risks. Cyproterone acetate is a steroidal anti-androgen which inhibits the interaction of androgens with AR and reduce serum testosterone levels through a mild anti-gonadotropic effect towards LH (Hellerstedt & Pienta, 2002). LHRH (Luteinizing Hormone releasing hormone) agonists such as leuprolide and goserelin operate through a negative-feedback process. This process triggers an initial rise in testosterone levels, which could worsen clinical symptoms of PCa. On the other hand, GnRH antagonists provide consistent hormonal suppression without the initial testosterone surge linked to LHRH agonists (Kluth et al., 2014). This form of treatment is occasionally referred to as medical castration, as it effectively decreases androgen levels comparable to orchiectomy. However, use of hormone therapy is limited as it has been associated with acute and long-term side effects, such as hyperlipidemia, fatigue, hot flashes, flare effect, osteoporosis, insulin resistance, cardiovascular disease, anemia, and sexual dysfunction (Seidenfeld et al., 2000).

1.7.4. Chemotherapy: This treatment uses drugs to kill rapidly dividing cancer cells. Chemotherapy is often used in more advanced stages of prostate cancer when hormone therapy is no longer effective. Docetaxel is regarded as the primary standard treatment which functions by binding to β-tubulin, preventing microtubule depolymerization during mitotic cell division and initiates apoptosis. However, the activation of Docetaxel relies significantly on CYP3A, a group of Cytochrome P450 proteins involved in drug metabolism. The development of resistance to Docetaxel has been linked to relapse. This resistance is associated with an increased upregulation of the multidrug resistance (MDR1) gene (Zhu et al., 2013). Cabazitaxel represents a second-generation treatment designed to counteract resistance to docetaxel (Abidi, 2013).

1.7.5. Radiation Therapy:

1.7.5.1. External Beam Radiation Therapy (EBRT): High-energy beams are directed at the prostate from outside the body to destroy cancer cells.

1.7.5.2. Brachytherapy: Radioactive seeds or sources are implanted directly into the prostate, delivering targeted radiation to the tumor.

1.7.5.3. Proton Therapy: A type of radiation therapy that uses protons instead of X-rays to treat cancer cells.

Radiation therapy, when combined with ADT, is recognized as an effective treatment for intermediate-risk and high-risk PCa. This approach is well-suited for mitigating the

spread of cancer cells to other parts of the body. Compared to surgical intervention, it addresses early-stage cancer and presents fewer associated risks. Additionally, it can alleviate symptoms like bone and joint pain. Some of the side effects of radiation therapy include urinary urgency and frequency, erectile dysfunction, painful urination, diarrhea, and inflammation of the rectal lining (proctitis) (Budäus et al., 2012; Martin & D'Amico, 2014).

1.7.6. Immunotherapy: Sipuleucel-T stimulate the immune system to recognize and attack cancer cells. Delivered through vaccination, the process involves harvesting a patient's dendritic cells, cultivating them with a PCa-associated antigen and subsequently reintroducing the engineered product to the patient. Another antigen used, PA2024, is a synthetic combination protein containing prostatic acid phosphatase (PAP), a protein expressed in most prostate adenocarcinomas and specific to prostate tissue, along with granulocyte macrophage colony-stimulating factor (GM-CSF), a cytokine that aids in the maturation and activation of immune cells against PCa cells. Although sipuleucel-T does not exhibit evident anticancer effects, there have been instances of remarkable responses to this vaccine reported in case studies (Bilusic et al., 2017; Fay & Graff, 2020) .

1.7.7. Bone-Targeted Therapy: The most common location for PCa metastasis are bones. Medication like Bisphosphonates, the synthetic non-hydrolysable analogs of pyrophosphate with structural similarity to inorganic phosphate, is used to control metastasized PCa cells. The receptor activator of nuclear factor-kappa B (RANK) is a transmembrane receptor found on osteoclast precursor cells, while its ligand (RANKL) is expressed by osteoblasts and bone marrow stromal cells. When RANKL binds to RANK, it triggers the maturation, activation, and survival of osteoclasts. Denosumab, a human monoclonal antibody developed to attach and counteract RANKL. This action effectively hinders the function of osteoclasts, preventing both widespread bone resorption and localized bone damage. Thus, helping in reducing bone pain and the risk of fractures (Deng et al., 2014).

1.7.8. Recent Advances in Targeted Drug Therapeutics

Use of single treatment approach leads to a substantial reduction of circulating testosterone levels. However, residual amount of circulating testosterone remains due to the peripheral conversion of adrenal steroids to testosterone contributing to the development of resistance to these therapies. A combination of these therapies still improves patient survival but only for few months and with risk of relapse of disease. In case of CRPC, adaptation of tumor cells to survive independent of androgen often surpasses these therapies. In addition, there is no respite from adverse side-effects associated with above treatment procedures.

Whether it is increased sensitivity to androgens or androgen-like ligands or de novo intra-tumoral androgen production, studying the regulation of androgen production is crucial for developing effective therapeutic strategies. Targeting androgen production has been the most employed therapeutic approach for PCa treatment, with drugs such as anti-androgens, AR antagonists, and inhibitors of androgen synthesis demonstrating efficacy in various stages of the disease. Ongoing research continues to explore novel approaches to disrupt androgen signaling and overcome treatment resistance in PCa and CRPC, with the ultimate goal of improving patient outcomes and survival (Dai et al., 2023)

2. Human Steroid Biosynthetic Pathway (Steroidogenesis)

2.1. Introduction

A complex process by which the body synthesizes steroids, a group of lipid molecules that play crucial roles in various physiological processes, including regulating metabolism, inflammation, and reproductive functions. The synthesis of steroids primarily occurs in specialized endocrine glands and tissues, with the adrenal glands and gonads (testes and ovaries) being the major sites of steroid production. A common precursor, Pregnenolone produce mineralocorticoids, glucocorticoids, and androgens (sex steroids). These hormones regulate processes such as salt-water balance, glucose metabolism, and sexual development respectively. The adrenal gland produces these distinct steroid groups within specific layers of the cortex: the zona glomerulosa (ZG), the zona fasciculata (ZF), and the zona reticularis (ZR) respectively. In contrast, the testes and ovaries exclusively synthesize sex steroids, namely testosterone in males and estradiol in females.

2.2. Chemistry of Steroidogenesis

The first rate-limiting step in biosynthesis of all steroid hormones is the cleavage of the cholesterol side chain by the mitochondrial P450 enzyme CYP11A1 system (CYP11A1-FDX-FDXR) also called P450scc, to convert cholesterol into pregnenolone (Preg) **(*Figure 1*).**

Cholesterol is transported into the mitochondria by a protein called the Steroidogenic Acute Regulatory protein (StAR). The basic structure of all the steroids including Cholesterol is derived from a cyclopentanoperhydrophenanthrene, having 17 carbons arranged in a three six-member carbon rings (named as A-C) and a five-member carbon ring (named as D according to IUPAC).

Preg, the first 21-carbon steroid precursor, can take one of two pathways:

- it may undergo 17α-hydroxylation, resulting in 17α-hydroxypregnenolone (17OH-Preg), through the action of the CYP17A1 enzyme.
- Alternatively, it can be converted into progesterone (Prog) with the help of the 3ß-hydroxysteroid dehydrogenase (HSD3B2) enzyme.

Prog can then undergo further transformations into aldosterone through a series of sequential reactions catalyzed by the CYP21A2 and CYP11B1/2 enzymes. Additionally, Prog gets converted to 17 hydroxyprogesterone (17OH-Prog) by CYP17A1, via the Δ4 pathway.

Alternatively, the Δ5 pathway leads to the conversion of 17OH-Preg to dehydroepiandrosterone (DHEA) through the 17,20-lyase activity of CYP17A1. Subsequently, DHEA is converted to DHEA sulfate (DHEA-S) by sulfonyltransferase (SULT2A1). To a lesser extent, DHEA is converted to androstenedione (Δ4A) by HSD3B2 and further to testosterone by AKR1C3 (HSD17B5). The 19-carbon products of Δ5 pathway are collectively known as Androgen precursors.

It is important to note here that in human ovary, the synthesis of Estrogen precursors occurs via the Δ5 pathway, where Δ4A and Testosterone is converted to Estrone and Estradiol through the action of Aromatase enzyme (Andersen & Ezcurra, 2014).

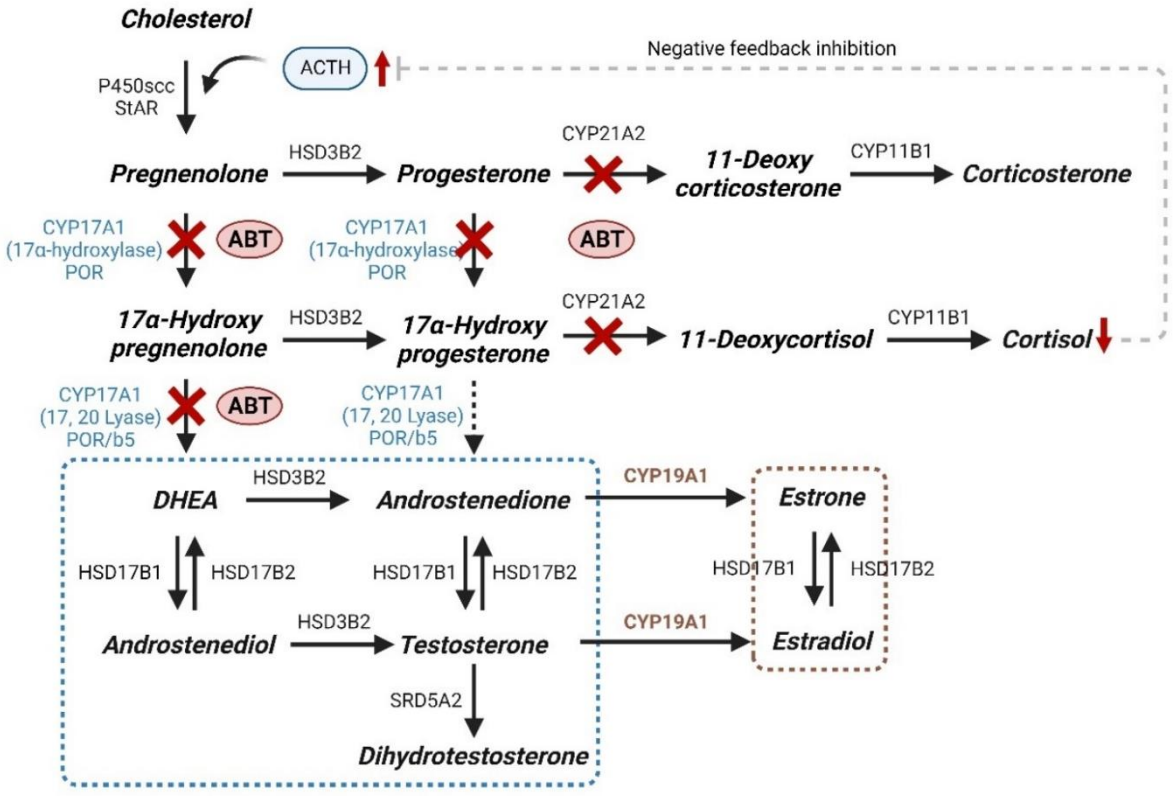

Figure 1: *Schematic Representation of Human Steroidogenic Pathway in a simplified form, depicting the major Cytochrome P450s involved. The diagram also shows the target sites of a common CYP17A1 inhibitor, Abiraterone. Created by BioRender.com*

2.3. Cytochrome P450 enzymes (CYPs)

These are enzymes belonging to superfamily of Hemoproteins found across species. These enzymes play a pivotal role in catalyzing reactions that utilize molecular oxygen to oxidize a diverse range of substrates involved in metabolism of drugs, lipids, and steroid synthesis. CYPs can also be categorized based on their location of action. In corticosteroid synthesis, five specific CYP450 enzymes are involved: CYP11A1 (cholesterol side-chain cleavage), CYP11B1 (steroid 11β-monooxygenase), and CYP11B2 that are located within the mitochondria, while CYP17A1 (P450 17α-hydroxylase-17,20-lyase) and CYP21A2 (Steroid-21-hydroxylase) are found in the endoplasmic reticulum, where they are referred to as microsomal CYPs. Within the adrenal glands and gonads, these enzymes facilitate a monooxygenase reaction. This process involves the incorporation of an oxygen atom into the steroid substrate R-H, with the assistance of an electron donor, typically nicotinamide adenine dinucleotide phosphate (NADPH). Importantly, the precise position and orientation of the resulting hydroxyl group are unique to each specific enzyme. The basic chemical equation is as follows (Guengerich, 2018).

$$NAD(P)H + O_2 + R\text{-}H \rightarrow NAD(P)^+ + H_2O + R\text{-}O$$

Mitochondrial and microsomal CYPs adapt different mechanism to carry out oxidation reaction. Mitochondrial enzymes receive electrons through an electron transfer chain. Initially, two electrons are transferred to the flavoprotein adrenodoxin reductase (FDXR) when bound to NADPH. These electrons are then relayed to adrenodoxin (FDX1), a non-heme iron-sulfur protein. Adrenodoxin transfers the electrons to the heme iron within the CYP450 enzyme before eventually transferring them to the substrate. In contrast, microsomal CYP450 enzymes employ a single flavoprotein known as P450 oxidoreductase (POR), which contains two flavin molecules: flavin adenine dinucleotide (FAD) and flavin mononucleotide (FMN) for the transfer of two electrons, one at a time to its respective substrate. In case of CYP17A1, a soluble Cytochrome b_5 also participate in the electron transfer mechanism to facilitate the 17,20 Lyase reaction. These distinct electron transport mechanisms may have a significant impact on regulating enzymatic activity of different CYPs (Yoshimoto & Auchus, 2015).

2.4. Androgen synthesis and Cytochrome P450 c17 (CYP17A1)

The zona reticularis of adrenal cortex produces the androgens namely, DHEA and its sulfate DHEA(S). DHEA(S) acts as precursors for production of androgens and estrogens (Kempná et al., 2015).

- An essential enzyme that plays an important role in adrenal androgen production is cytochrome P450c17 (encoded by CYP17A1 gene). CYP17A1 localized in the endoplasmic

reticulum, can catalyze both 17α-hydroxylase and 17,20 lyase reactions. It is known that CYP17A1 is the qualitative controller of steroidogenesis. Through its characteristic dual activity, it catalyzes both 17alpha-hydroxylase and 17,20-lyase reaction to produce 17OH-Preg or 17OH-Prog and DHEA respectively. In humans the conversion of 17OH-Preg to DHEA is preferred pathway than conversion of 17OH-Prog to Δ4A.

- Another enzyme important for androgen production is HSD3B2. It competes with CYP17A1 and SULT2A1 in ZR for substrates such as Preg, 17OH-Preg and DHEA to synthesis Prog, 17OH-Prog and Δ4A respectively.

- The ZR contains limited activity of type 5 17β-hydroxysteroid dehydrogenase (AKR1C3), which results in the production of minor quantities of the potent androgen, testosterone. However, even small quantities of testosterone, has approximately ten times greater potency when interacting with the androgen receptor compared to Δ4A.

- Furthermore, peripheral tissues expressing enzymes such as 3β-hydroxysteroid dehydrogenase type 1 (HSD3B1) and/or 17β-hydroxysteroid dehydrogenases (HSD17B) can convert circulating androgen precursors to potent forms (Simard et al., 2005).

- Similarly, androgen production in Leydig cells of the testes follows the delta 5 pathway, resulting in the production of DHEA from Preg. Significant expression of HSD3B2 and type 3 17β-hydroxysteroid dehydrogenase (HSD17B3) but no SULT2A1 results only in conversions of DHEA into Δ4A or androstenediol and subsequently into testosterone.

- During the prenatal stage of development, the human fetal adrenal glands exhibit a steroidogenic enzyme expression pattern that closely resembles the zona reticularis. These fetal adrenal glands produce significant quantities of DHEA-S. However, shortly after birth, this fetal organ undergoes differentiation and is substituted by a two-layer adrenal cortex, comprised of the Zona Glomerulosa and Zona Fasciculata. Initially, ZG primarily synthesizes mineralocorticoids, while ZF focuses on glucocorticoid production. The formation of the third layer, ZR, in the adrenal cortex is a gradual process that occurs postnatally. It becomes active in the synthesis of androgens during a physiological event known as Adrenarche, which typically occurs around the ages of 6 to 8 years (Miller, 2009; Miller & Auchus, 2011). It's worth noting that adrenarche is a unique phenomenon exclusive to higher primates and humans (Cutler et al., 1978; Smail et al., 1982).

2.5. Role of CYP17A1 in Estrogen synthesis and PCOS

In the ovarian theca cell, Pregnenolone, originating from the granulosa cell, undergoes a conversion to DHEA in a manner like that observed in the ZR and Leydig cells due to CYP17A1 activity. HSD3B2 further transforms DHEA into Δ4A. This Δ4A can then either be returned to the granulosa cell for use as a substrate in estrogen production or released into circulation

in small quantities (Cui et al., 2013; Gowtham Kumar et al., 2022). An early and pronounced onset of adrenarche can potentially result in hyperandrogenic condition like polycystic ovary syndrome (PCOS). Conditions of PCOS are very much similar to PCa, where high levels of androgens can be found in blood circulation. This indicates a prominent role of CYP17A1 in the pathophysiology of both PCa and PCOS (Carey et al., 1994). Therefore, a better understanding of mechanisms of androgen production through CYP17A1 enzyme activity can help in developing therapeutics (Baston & Leroux, 2007). This thesis primarily focuses on PCa and CRPC but will address from time to time the effect of therapeutics use to target CYP17A1 in the pathogenesis of PCOS.

2.6. Role of CYP17A1 in Hyperandrogenic disorders

Congenital adrenal hyperplasia (CAH) is an autosomal recessive disorder caused due to defect in genes encoding enzymes of steroidogenesis. Although the classic form is caused due to mutation in CYP21A2 leading to impaired cortisol and aldosterone production. The absence of 21-hydroxylase activity directs the synthetic pathway towards the production of excessive androgens through CYP17A1 activity. This can lead to various symptoms and complications, including virilization (masculinization) of female genitalia, early development of male secondary sexual characteristics in both sexes, and other androgen-related issues.

2.7. Regulation of CYP17A1 activity

The regulation of CYP17A1 activity involves multiple factors and mechanisms. These can be loosely divided into following categories:

2.7.1. Transcriptional Regulation: The transcription of the CYP17A1 gene is tightly regulated by a combination of transcription factors, hormonal signals, and epigenetic modifications. Various transcription factors, including SF-1 (steroidogenic factor-1) and DAX-1 (dosage-sensitive sex reversal, adrenal hypoplasia critical region, on chromosome X, gene 1), play a crucial role in regulating CYP17A1 gene expression (Hanley et al., 2001). SF-1 is particularly important as it acts as a master regulator of steroidogenesis and binds to the SF-1 response element in the CYP17A1 promoter. Another family of transcription factors known as GATA are found to be involved in regulation of CYP17A1 gene expression in the adrenal cortex. GATA-6 or GATA-4 in complex with specificity protein, Sp1 helps in constitutive expression of CYP17A1 (Flück & Miller, 2004).

- Sterol regulatory element binding protein 1c (SREBP1c), are group of transcription factors which also acts as cholesterol sensors. In the presence of sphingosine-1-phosphate, SREBP1c translocate to the nucleus upon cleavage and activates the transcription of CYP17A1 (Ozbay et al., 2006; Sewer & Jagarlapudi, 2009).

- Epigenetic changes, such as DNA methylation and histone modifications, can also influence the accessibility of the CYP17A1 promoter to transcription factors (Martinez-Arguelles & Papadopoulos, 2010).

- Transcriptional regulation of CYP17A1 can vary depending on the tissue type and hormonal signals present. For example, in the adrenal cortex, Adrenocorticotropic Hormone (ACTH) plays a significant role in stimulating CYP17A1 transcription, while in gonads, luteinizing hormone is a key regulator. Upon binding to its receptor, ACTH activates G protein-coupled receptors such as melanocortin 2 receptor (MC2R) leading to the production of cyclic adenosine monophosphate (cAMP) inside the cell. cAMP activates protein kinase A (PKA), which in turn phosphorylates and activates SF-1. Activated SF-1 then binds to the CYP17A1 promoter, promoting gene transcription (Ruggiero & Lalli, 2016). Additionally, ACTH levels are regulated through a negative feedback inhibition by adrenal cortisol involving the hypothalamic-pituitary-adrenal (HPA) axis (Melau et al., 2021).

2.7.2. Protein-Protein interaction

2.7.2.1. Presence of POR: Cytochrome P450 enzymes are considered external monooxygenases, relying on interactions with electron-transporting proteins to obtain electrons from reduced coenzymes such as NAD(P)H. In microsomal systems, these electrons are efficiently transferred from NADPH through POR also known as Cytochrome P450 Reductase (CPR) containing FAD and FMN domains (*Figure 2*). Initial investigations have indicated that the connection between microsomal CYPs and their redox partner CPR is primarily dictated by electrostatic attractions due to the positively charged proximal surface near the CYP heme and the negatively charged FMN and FAD/NADPH domains of CPR (Shen & Strobel, 1993; Shimizu et al., 1991). Minor alterations in structure, like the substitution of a single amino acid, can yield profound impacts on the capacity of CPR to effectively transfer electrons to a specific CYP isoform. Recent investigations have delved into the influence of genetic diversity within the human CPR gene on specific CYP-mediated metabolism. Pathogenic mutations in POR gene, especially in its FMN, FAD and NADPH binding domain cause severe disruption in the activity of several CYP450 including CYP17A1. For instance, P228L, R316W, G413S, and G504R have been reported to severely affect the CYP17A1 activity. (Kandel & Lampe, 2014) (Bernhardt & Neunzig, 2021; Huang et al., 2005).

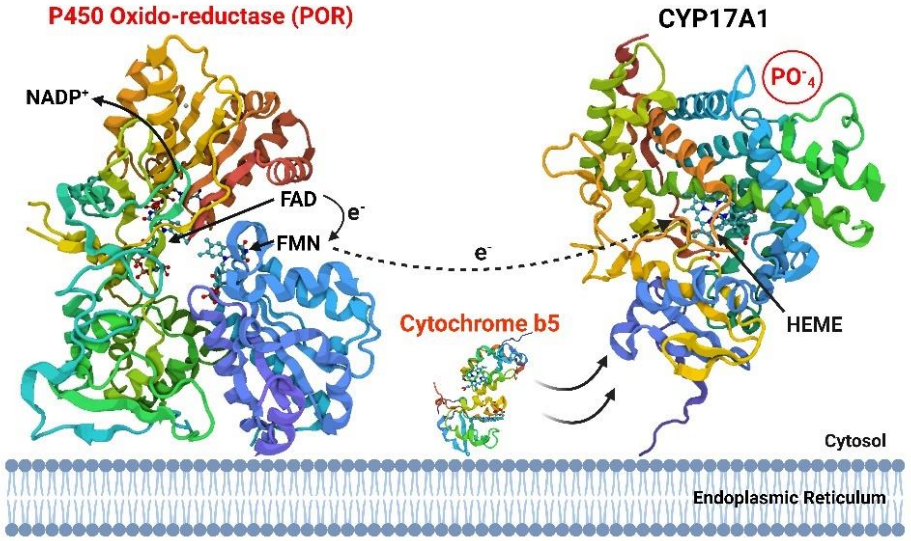

***Figure 2**: Animated representation of interaction between CYP17A1, POR and Cytochrome B5 during an enzymatic reaction. Transfer of electrons from reducing equivalent, NADPH is facilitated by the FAD and FMN domain of the redox partner, POR. Cytochrome B5 enhances the allosteric arrangement of the enzyme and substrate. Phosphorylation at Ser/Thr residues regulates the 17,20 Lyase activity of CYP17A1. Created by BioRender.com*

2.7.2.2. Presence of Cytochrome b_5: Cytochrome b_5 (CYB5) is a small, heme-containing protein that plays a crucial role in various enzymatic reactions, particularly those involving cytochrome P450 enzymes. The presence of CYB5 can enhance the catalytic activity of CYP17A1. CYB5 functions as an allosteric modulator facilitating the interaction between CYP17A1 and POR (***Figure 2***). The conformational change in the presence of CYB5 favors the positioning of the steroid substrate for C17-C20 cleavage in 17,20-lyase reaction (Katagiri et al., 1995; Miller et al., 1997). A homozygous W27X mutation results in loss of function of CYB5 leading to disruption of 17,20-lyase activity of CYP17A1 showing the importance of CYB5 (Kok et al., 2010). While CYP17A1 is expressed in both the human zona fasciculata and zona reticularis and remains relatively stable with age, the expression of cytochrome b_5 increases in the adrenal zona reticularis at the onset of adrenarche. This coincides with the rise in adrenal 17,20 lyase activity and the secretion of 19-carbon steroids such as DHEA and androstenedione. Similarly, cytochrome b_5 is present in gonadal cells responsible for sex steroid production, including testicular Leydig cells, follicular theca cells, theca lutein cells, and ovarian stroma. Therefore, differential expression of CYB5 is also a medium to regulate the production of androgens.

2.7.3. Post-translational regulation: CYP17A1 can be regulated through phosphorylation of the protein at specific serine and threonine residues. Phosphorylation can either enhance or inhibit the enzyme's activity, depending on the specific residue and the kinase involved. For example, phosphorylation by PKA can stimulate CYP17A1's 17α-hydroxylase activity, while phosphorylation by protein kinase C (PKC) can have inhibitory effects. The differential expression of kinases/phosphatases in a cell-specific manner and at various developmental stages determines the pattern of steroid hormones (Pandey & Miller, 2005a). Tee and Miller showed that the phosphorylation by p38α increased the 17,20-Lyase activity 2-fold (Tee & Miller, 2013). Similarly, Phosphatases, such as protein phosphatase 1 (PP1) and protein phosphatase 2A (PP2A), have been showed to dephosphorylate CYP17A1 leading to reduction in the lyase activity (A. V. Pandey et al., 2003). Therefore, the balance between phosphorylation and dephosphorylation of CYP17A1 is critical for its function. These post-translational modifications help regulate the enzyme's role in steroid biosynthesis, allowing the cell to respond to hormonal signals and maintain the proper balance of androgens and glucocorticoids. The specific serine and threonine residues targeted by kinases and phosphatases, as well as the precise effects of these modifications on CYP17A1's activity, may vary depending on the cellular context and hormonal signals.

HYPOTHESIS

Due to its pivotal involvement in sex steroid synthesis, its relevance in hyperandrogenic conditions, and its potential as a therapeutic target for cancers dependent on sex steroids, the 17,20 lyase activity of human CYP17A1 has garnered heightened interest.

Moreover, PCa is driven by its sensitivity to androgens. Historically, treatments have focused on eliminating androgens from the bloodstream. These approaches range from as basic as castration to more modern methods like blocking androgen synthesis or receptor binding. However, these treatments have limited long-term effectiveness and possess safety concerns due to following reasons:

- non-specific mode of action inhibiting both CYP17A1 hydroxylase and lyase activity
- cross reactivity towards other CYP enzymes involved in steroidogenesis
- transformation into androgen-like metabolites

Therefore, mechanisms involved in the regulation of CYP17A1 activity specifically its 17,20-lyase activity can be potential therapeutic targets for the treatment of hyperandrogenic diseases like PCa and PCOS. The work done in this thesis explore some of these different mechanisms for the inhibition of CYP17A1 activity in three different chapters (objectives). The major focus will be on inhibition of CYP17A1 activity, specially 17,20-lyase activity for development of drugs against PCa. Additionally, the potential of these mechanisms involved in CRPC and PCOS will also be described as needed.

AIMS

- To develop small molecule inhibitors for specific inhibition of CYP17A1 17,20 lyase activity

  OBJECTIVE 1 - Screening computationally designed and chemically synthesized compounds against CYP17A1 activity.

  OBJECTIVE 2 – Endocrine Disrupting Chemical as structural cues for the development of inhibitors of CYP17A1 activity.

- To identify novel pathways involved in the regulation of CYP17A1 through post-translational mechanisms.

  OBJECTIVE 3 - Study the role of specific Kinases and Phosphatases involved in the regulation of CYP17A1 lyase activity.

MATERIALS AND METHODS

3. Experimental details

This section offers an in-depth overview of the standard laboratory protocols and experimental techniques employed in conducting the research outlined in this thesis. While some of these methods are shared across multiple chapters, there are dedicated materials and methods sections within each respective section.

3.1. General Laboratory Practice

Throughout all procedures, personal protective equipment (PPE) like laboratory coat and latex powder-free gloves were worn. Laboratory facemasks, protective eyewear, and fume hoods were utilized as needed. Adherence to safety protocols in handling hazardous substances were observed following the DBMR Safety Guidelines. The equipment and reagents used to carry out scientific experiments were of the highest available grades. Chemical were properly labelled and stored according to the safety data sheets by the manufacturer. These general laboratory practices are essential for promoting a safe, efficient, and productive research environment while ensuring the reliability of scientific data and results.

3.2. Handling of Radioactive materials

Experiments involving the use of radioactive materials were performed in compliance with the Radiation Safety rules under the supervision of DBMR Radiation Safety Officer. Safety training courses were attended before starting any radioactivity related work. A designated controlled workplace was utilized to perform all the experiments. Dosimeter was worn all the time to record the exposure to any radiation. User Log sheets were maintained to control the usage of radiation amount within the prescribed limits. Waste management were done according to type of nuclides and their combustibility. Wipe tests were regularly performed to detect surface contamination in case of any spillage.

3.3. Preparation of cell culture media, buffers, and other reagents

3.3.1. NCI H295R Complete media: To 500 mL base medium, Dulbecco's Modified Eagle's Medium, DMEM/Ham's F-12 medium 1X (1:1 Mix) containing L-glutamine, 15 mM HEPES, 0.5 mM sodium pyruvate and 1200 mg/L sodium bicarbonate (31330-038, Gibco™, Thermo Fisher Scientific, Waltham, MA, USA) 500 µL of 0.00625 mg/mL insulin, 0.00625 mg/mL transferrin, 6.25 ng/mL selenium, 1.25 mg/mL bovine serum albumin, 0.00535 mg/mL linoleic acid in the form of ITS Premix (354350, Corning™, Manassas, VA, USA) was added to final concentration of 0.1%. The addition of sodium bicarbonate in the base medium is intended for incubation of cell culture in 5% CO_2 atmosphere. 5 mL of 10000 µg/mL Penicillin and 10000 µg/mL Streptomycin (P/S) (15140-122, Gibco™, Thermo Fisher Scientific, Waltham, MA, USA) was added to a final concentration of 1%. Finally, 25 ml of

Nu-I serum (355500, Corning™, Manassas, VA, USA) was added to make up to 5% concentration.

3.3.2. LNCaP Complete media: For a final concentration 10 mM HEPES, 5ml of 1M HEPES was added to Roswell Park Memorial Institute, RPMI-1640 Medium containing 2mM L-glutamine, 4500 mg/L glucose, 1500 mg/L sodium bicarbonate (21870-034, Gibco™, Thermo Fisher Scientific, Waltham, MA, USA). 5 mL of 100 mM Sodium pyruvate (11360070, Gibco™, Thermo Fisher Scientific, Waltham, MA, USA) was added for a final concentration of 1 mM. 50 mL of Fetal Bovine Serum, FBS (Gibco™, Thermo Fisher Scientific, Waltham, MA, USA) was added to achieve a final concentration of 10%. FBS obtained from the manufacturer was heat-inactivated by incubating at 56°C in water bath for 1 hour prior to use. For final concentration of 1%, 5 mL of P/S was added to the mix (15140-122, Gibco™, Thermo Fisher Scientific, Waltham, MA, USA).

3.3.3. COS-1 Complete media: To 500 mL of base media, DMEM (1X) with High Glucose, Glutamine, Phenol Red, no HEPES and no Sodium pyruvate (41965-039, Gibco™, Thermo Fisher Scientific, Waltham, MA, USA), 5 mL of P/S was added for final concentration of 1%. 50 mL of heat inactivated FBS was added for 10% concentration.

3.3.4. Reagents

3.3.4.1. 5 mg/mL MTT stock solution: 50 mg MTT powder (Sigma-Aldrich®, St. Louis, MO, USA) was weighed and dissolved in 10 mL of 1X PBS buffer (available from Institut für Spitalpharmazie, Inselgruppe, Bern, Switzerland). The solution was sterile filtered with help of 0.22 µm Millex® Syringe Filters (Merck, Millipore, Darmstadt, Germany). For experiments, the stock solution was diluted in Opti-MEM™ I Reduced Serum Medium, no phenol red (11058021, Gibco™, Thermo Fisher Scientific, Waltham, MA, USA) to avoid optical interference (Ghasemi et al., 2021). A final concentration of 0.5 mg/ml was used for cell viability assays in a 96 well plate format. The stock solution can be stored at -20°C for long term. The dilutions with the culture medium should be freshly prepared. Minimum exposure to light is recommended while handling the dye.

3.3.4.2. 0.5 mg/mL Resazurin salt stock solution: 5 mg Resazurin sodium salt (R7017, Sigma-Aldrich®, St. Louis, MO, USA) was dissolved in 10 mL PBS. The solution was sterile filtered and accordingly diluted in culture media to obtain a final concentration of 0.05 mg/mL for the assay.

3.3.4.3. Stock solutions of test compounds and drugs: Abiraterone acetate (MedChemExpress®, Lucerna Chem AG, Lucerne, Switzerland) and test compounds in solid form were weighed and dissolved in suitable solvent, DMSO (Sigma-Aldrich®, St. Louis, MO, USA) or Ethanol (absolute ≥99.8%, Sigma-Aldrich®, St. Louis, MO, USA) to

obtain a 10 to 30 mM stock solutions. These solutions were diluted to appropriate working solutions to obtain a final concentration of nanomolar to micromolar range in 1 mL or 0.5 mL cell culture. 1mM stock solution of Trilostane (commercially available as tablets from Modrenal® Bioenvision, NY, USA) and Anastrozole (AstraZeneca, in form of commercially available drug, Arimidex) was prepared by weighing an appropriate amount and dissolving in DMSO.

3.3.4.4. 5% Charcoal/0.5% Dextran: 50 g of activated Charcoal (Merck AG, Darmstadt, Germany) was weighed. 5 g of dextran (Sigma-Aldrich®, St. Louis, MO, USA] was weighed and dissolved in 100 mL distilled water. This solution was added to the charcoal and the volume were made upto 1L. A suspension solution was obtained which were homogenized using magnetic stirrer before adding it to the sample media.

3.3.4.5. Potassium Phosphate buffer: 174.18 g of di-Potassium hydrogen phosphate, K_2HPO_4 (≥99 %, p.a., anhydrous, Carl Roth® GmbH + Co. KG Karlsruhe, Germany) was weighed and dissolved in 1L distilled water to obtain 1M concentration. Similarly, 1M solution of Potassium dihydrogen phosphate, KH_2PO_4 (≥99 %, p.a., 136.09 g/mol, Carl Roth® GmbH + Co. KG Karlsruhe, Germany) was prepared separately. 80.2 mL K_2HPO_4 was mixed with 19.8 mL KH_2PO_4 to obtain 100 mM phosphate buffer. The pH was adjusted to 7.4 and the final volume was made up to 1L.

3.4. Cell culture

3.4.1. General practice: All the work related to cell culturing were carried out under sterile conditions within Class II biological vertical laminar flow safety cabinets (BioWizard Silver Line Biosafety Cabinet, Kojair Tech, Finland). Before and after each use, these cabinets were meticulously cleaned using 70% ethanol and distilled water. UV light was kept on for 20 minutes at the end of the day for complete sterilization of the laminar flow. Liquid waste was decontaminated using 10% Incidin™ Pro (EcoLab GmbH, Switzerland) while plastics were disposed in a container for incineration. The cells were grown as a monolayer in sterile culture flasks or dishes of various sizes (25cm^2, 75cm^2, and 150cm^2) all equipped with vented caps (Corning Life Sciences, Amsterdam, Netherlands). Cultures were maintained in a humidified chamber at 37°C with a 5% CO_2 atmosphere.

3.4.2. Cell lines:

3.4.2.1. NCI H295R (ATCC® CRL2128™): In 1990, Gazdar et al. developed human adrenocortical cell line, NCI-H295, derived in 1980 from a 48-year-old woman diagnosed with primary adrenal cortical carcinoma Following surgical resection and subsequent processing, these cultured cells underwent extensive long-term cultivation over several years. Through radioimmunoassay and mass spectrometry, it was reported that these cells demonstrated the capacity to synthesize all major adrenal steroids like

corticosteroids, mineralocorticoids, androgens, and estrogens. Since then, NCI-H295 have been developed into various sub-strains (H295A, H295R, H295RA, HAC13, HAC15, and HAC50) and has become the most widely employed model to study adrenal steroidogenesis (Gazdar et al., 1990) (K. E. M. Ahmed et al., 2018). NCI-H295R cell line has been adapted from the original strain by employing different growth conditions to promote adherence to culture plates and reduce cell cycle durations. Compared to the original H295 cell line, H295R cells exhibit a compact adherent monolayer growth pattern and a decreased population doubling time from five to two days (Hornsby & McAllister, 1991). The original strain demonstrated no response to hormonal stimulation by ACTH, Angiotensin II (ANG II) and potassium ion (K^+) signals (Staels et al., 1993). NCI-H295R cell strain has been characterized to determine the responsiveness to ACTH, ANG II, and K^+ signals. While responsiveness of the cells towards ANG II and K^+ signals can be used to study the mechanisms regulating aldosterone production, however, poor ACTH response is a drawback in these cells to study the regulation of cortisol production. Therefore, addition of either forskolin (to activate adenylylcyclase) or cAMP analogues are needed to examine cAMP dependent signaling pathways (Bird et al., 1993; Mountjoy et al., 1994; Rainey et al., 1993). NCI H295R cells also show influence of culture conditions like growth medium in the production of steroids. Studies have shown that serum starvation increases the production of androgens along with CYP17A1 lyase activity in NCI H295R cells (P. Kempná et al., 2010). NCI H295R was obtained from the American Type Culture Collection (ATCC® CRL2128™), Manassas, VA, USA. Cells were grown in complete media described in section 3.3.1.1 at 37°C in a humid atmosphere with a constant supply of 5% carbon dioxide to maintain the physiological pH (Kurlbaum et al., 2020).

3.4.2.2. LNCaP clone FGC (ATCC® CRL1740™): This cell line was established by cultivating explants of needle biopsy specimens obtained from a **L**ymph **N**ode metastasis of PCa. The LNCaP-FGC cell line was adapted from rapidly growing colony of original LNCaP cells. These cells exhibit responsiveness to 5α-dihydrotestosterone (DHT), as indicated by their ability to modulate growth and produce acid phosphatase. Furthermore, they express Prostate-Specific Antigen and Prostatic Acid Phosphatase (PAP), and possess Androgen Receptors (Horoszewicz et al., 1980; Okada et al., 1976; van Steenbrugge et al., 1989). In our work the LNCaP cells were used to study cell cytotoxic effects in the presence of small molecule drugs. Standard test conditions using MTT-based assay have been established in these cell lines by Romijn et al (Romijn et al., 1988). They do not form a uniform monolayer but instead grow in clusters, which results in formation of aggregates through repeated pipetting during subculture preparation. Their adhesion to the substrate is only minimal, preventing them from reaching confluence, and they rapidly lower the pH of the medium. Cell cultures were maintained in complete media

according to section 3.3.1.2. Cells from passage 12-30 were used in experiments as previously described (Wu et al., 2013).

3.4.2.3. COS1 (ATCC® CRL-1650™): This cell line was established through the transformation of monkey epithelial; CV-1 cell line using a defective mutant of simian virus, SV40 containing a minor deletion in its origin of replication. This ensured that there is no growth of the infectious viruses even after prolonged culture. The acronym "COS" was designated due to cells being **C**V-1 (simian) in **O**rigin and carrying the **S**V40 genetic material. COS-1 cells exhibit the expression of nuclear large T antigen and all the requisite proteins essential for the replication of appropriate circular genomes. Any plasmid containing an SV40 replication origin, when introduced into COS-1 cells, undergoes replication to achieve a high copy number. Consequently, the transfected cells will also express any gene located on the plasmid, driven by a suitable eukaryotic promoter. This results in a transient high-level expression of the gene of interest (Hancock, 1992). Therefore, this this cell line was used to generate stable cell lines in our experiments. The cells were grown in DMEM (1X) supplemented with 10% FBS and 1% P/S.

3.4.3. Maintenance of cell lines: Cells were regularly passaged when they reached an approximately 80% confluence level. The culture medium was removed, and the cells were washed with an appropriate volume of commercially available sterile phosphate-buffered saline, PBS solution (1X) [available from (Institut für Spitalpharmazie, Inselgruppe, Bern, Switzerland). The volume of PBS depended on the size of the flask, typically ranging from 6 to 10 ml. To detach the cells from the flask, up to 5 ml of 0.25% Trypsin-EDTA solution (Gibco™, Thermo Fisher Scientific Inc.) was added. The cells were then incubated at 37ºC for 2-4 minutes. Trypsin-EDTA solution was subsequently neutralized by adding an equal volume of complete growth medium. The cells were then transferred to a sterile falcon tube and pelleted through centrifugation at 1500 rpm (rotations per minute) for 5 minutes. The supernatant was discarded, and the cell pellet was resuspended in an appropriate volume of fresh complete growth medium, depending on the desired sub-cultivation ratio. Typically, the complete growth medium was changed every 2-3 days depending on the cell line.

3.4.4. Cryopreservation: It is a technique to protect organelles, cells, tissues, or any biological structures by damages such as osmotic shock caused by extreme low temperature. For extended storage, cells were collected following the procedure outlined in Section 3.3.3. However, they were resuspended in complete growth medium that included sterile 10% (v/v) dimethyl sulfoxide, DMSO. This addition of cryoprotective agent served to prevent the formation of ice crystals. For sensitive cell lines like NCI H295R, 7.5% Nu-I serum was also added. The resulting cell suspensions were divided into 2 ml cryogenic

vials (Thermo Scientific™ Nunc™ Biobanking and Cell Culture Cryogenic Tubes) and gradually cooled at a constant rate of -1°C per minute to reach -80°C. This controlled cooling was achieved using Isopropyl alcohol (ROTISOLV® Pestilyse® ≥99,8 %, Carl Roth® GmbH + Co. KG Karlsruhe, Germany) filled in a Thermo Scientific™ Mr. Frosty™ Freezing Container (NALGENE™, Thermo Fisher Scientific Inc). Subsequently, the vials were placed in -130°C freezer for long-term storage. To resuscitate cells from cryopreservation, the vials were thawed in a 37°C water bath, and the suspension was quickly transferred to a culture plate containing complete growth medium. The cells were then allowed to attach to the plate. The media was changed the following day and according to confluency the cells were sub-cultured as mentioned in earlier (Jang et al., 2017).

3.4.5. Cell counting: An essential step involved in all the experimental protocols is the assessment of cell counts prior before starting downstream procedures that requires precise and uniform number of cells. Having an accurate count of input cells holds significant value for standardizing experiments such as transfection, studies related to cell proliferation and viability, enzyme assays and protein production. Cell counting can be carried out manually using a hemocytometer, or by using an automated cell counter. In recent times, automated cell counting has emerged as an advanced substitute from the traditional hemocytometer-based cell counting method delivering more accurate, unbiased, and reproducible outcomes in a fraction of the time required for manual counting (Fagète et al., 2019). Cell suspension was obtained from the pellet by resuspending it in 1-5 ml of complete medium as described in Section 3.3.3. 10 µl of 0.4% Trypan blue dye (from BioRad) was added to 10 µl of cell suspension and mixed gently. The dye is used as a stain to detect live cells based on the reactivity of the negatively charged chromophore towards internal side of the membrane. Therefore, the dye can only stain dead cells in comparison to live cells where the cell membrane remains intact (Kwizera et al., 2018). 10 µl of this mixture is released into the well of a dual chamber cell counting slide (from BioRad). The slide is then inserted into Bio-Rad TC20™ Automated Benchtop Counter (Bio-Rad Laboratories, Inc.) for counting. The measurement range is $5 \times 10^4 – 1 \times 10^7$ cells/ml and 6 – 50 µm cell diameter. Having information about the cell count per milliliter in the cell suspension allowed for plating of cells at the desired density.

3.5. Cell Viability Assays

These assays are frequently employed to screen libraries of compounds, assessing whether the tested molecules influence cell proliferation or exhibit direct cytotoxic effects that can ultimately result in cell death. The assays used in our experiments are based on colorimetric and fluorescent signals to monitor viable cells. In general, Percentage cell viability was calculated as 100% × (absorbance of treated cells – absorbance of background controls) /

(absorbance of matched DMSO concentration controls – absorbance of background controls)(Larsson et al., 2020).

3.5.1. MTT assay: The MTT, 3-(4,5-dimethylthiazol-2-yl)-2,5-diphenyltetrazolium bromide reduction assay was the first homogeneous method developed for assessing cell viability in a 96-well format, particularly suited for high-throughput screening (Mosmann, 1983) . This assay involves preparing the MTT substrate in a physiologically balanced solution, typically at a final concentration of 0.2 - 0.5 mg/ml and adding it to cells in culture. The cells are then incubated for a duration ranging from 1 to 4 hours. MTT is positively charged and can readily penetrate viable eukaryotic cells. The amount of formazan produced, presumably directly proportional to the number of viable cells, is quantified by measuring changes in absorbance at 570 nm using a plate reading spectrophotometer (SpectraMax M2, Bucher Biotec, Basel Switzerland). The mechanism behind MTT reduction into formazan is likely associated with reactions involving NADH or similar reducing molecules that transfer electrons to MTT. The formazan product accumulates as an insoluble precipitate within cells and is also deposited near the cell surface and in the culture medium. Various solubilizing agents including the use of acidified isopropanol, DMSO, dimethylformamide, Sodium Dodecyl Sulfate, and combinations of detergent and organic solvents are used to dissolve the formed crystals. The signal generated in the MTT assay depends on several factors, including the concentration of MTT, the incubation period's duration, the number of viable cells, and their metabolic activity. All these parameters should be considered when optimizing assay conditions to achieve a detectable level of product above background (Larsson et al., 2020). Due to MTT's cytotoxic nature, the assay should be considered an endpoint assay. Suspected chemical interference from test compounds can be verified by measuring absorbance values from control wells without cells, incubated with culture medium containing MTT and various concentrations of the test compound (Riss et al., 2004).

3.5.2. Resazurin assay: Resazurin serves as a cell-permeable redox indicator and is utilized using methods as in case of tetrazolium compounds. Resazurin can be dissolved in physiological buffers, forming a deep, blue-colored solution, which can then be directly introduced to cells in culture in a homogeneous manner. Viable cells with active metabolism possess the ability to reduce resazurin into the resorufin product, characterized by its pink color and fluorescence. The quantity of resorufin generated is directly proportional to the number of viable cells, and this can be quantified using a microplate fluorometer equipped with a 560 nm excitation / 590 nm emission filter set. While it's possible to measure resorufin quantification through changes in absorbance, this method is less common because it is considerably less sensitive compared to fluorescence measurements. The resazurin reduction assay offers slightly greater sensitivity than

tetrazolium reduction assays, and it has been widely employed high-throughput screening applications. Other key advantages of the resazurin reduction assay include its cost-effectiveness and the homogeneous composition with culture medium. Furthermore, resazurin assays can be combined with other methods, like measuring caspase activity, to gain more insights into the mechanisms underlying cytotoxicity. However, the resazurin assay has its disadvantages, including the potential for fluorescent interference from the compounds being tested and often overlooked, the direct toxic effects on cells. Prolonged exposure of cells to resazurin, lasting several hours or even days, can lead to observable changes in cell morphology, indicating interference with normal cell function. Therefore, optimization of incubation time becomes essential to avoid reagent toxicity (Kamiloglu et al., 2020; Larsson et al., 2020; Riss et al., 2004).

3.6. General Protocol for cell-based enzyme assay

In general, NCI H295R cells were seeded overnight in a 12-well plate at a cell density of 0.5 X 10^6 cells per well. Appropriate concentrations of test compounds were added to respective wells containing fresh medium and incubated for 4-24 hours. The preferred duration for drug treatment was set at 4 hours because the test compounds were hypothesized to target enzyme activity rather than having any drastic effect on basic cellular functions such as gene expression. Solvents such as DMSO or Ethanol were used to prepare dilutions for test compounds. Therefore, these were used as Controls in all the assays. Currently approved drugs known to inhibit the activity of a particular CYP enzyme under investigation were used as Positive control. For example, in case of CYP17A1 and CYP19A1, Abiraterone acetate and Anastrozole were used as positive control (Malikova et al., 2017). Appropriate radiolabeled substrates were used to determine a specific enzyme activity. The amount of enzyme activity was detected and measured as percentage of radioactivity incorporated into the product with respect to the total radioactivity (***Figure 3***) (Castaño et al., 2019; Udhane et al., 2016).

3.6.1. Isolation of Steroids from media: After appropriate incubations, steroids were extracted from the media using suitable mixture of organic solvents. Typically, to 1mL of sample media, 4mL of organic mixture (4 times the volume of media) was added. Steroids soluble in the organic phase were separated out and left overnight for evaporation under a constant flow of air. Steroids are small molecules featuring 4-membered hydrocarbon ring system. Therefore, they tend to exhibit greater solubility in organic solvent compared to aqueous fluids found in tissues. The choice for organic solvents for extraction is based on the specific chemical properties of the steroids and the scale and intent of the isolation process. Organic compounds in water-based samples have been extracted through a classical technique known as liquid-liquid extraction (LLE), which is also the most employed method for preparing samples from H295R incubation medium (Abdel-Khalik et al., 2013). This method is based on the differences in solubility and distribution of the solute between

the two immiscible liquid phases. LLE can serve various purposes, such as enhancing selectivity by isolating the analyte from interfering matrix components or improving selectivity by concentrating the analyte from a large sample volume (Silvestre et al., 2009). The current solvent system used in our experiments, Ethyl acetate and Isooctane (1:1 v/v) was developed from a series of trials with different combinations of organic reagents like methylene chloride, methanol, ethyl ether, acetic acid, benzene and acetone.(Brown & Fishman, 2000).

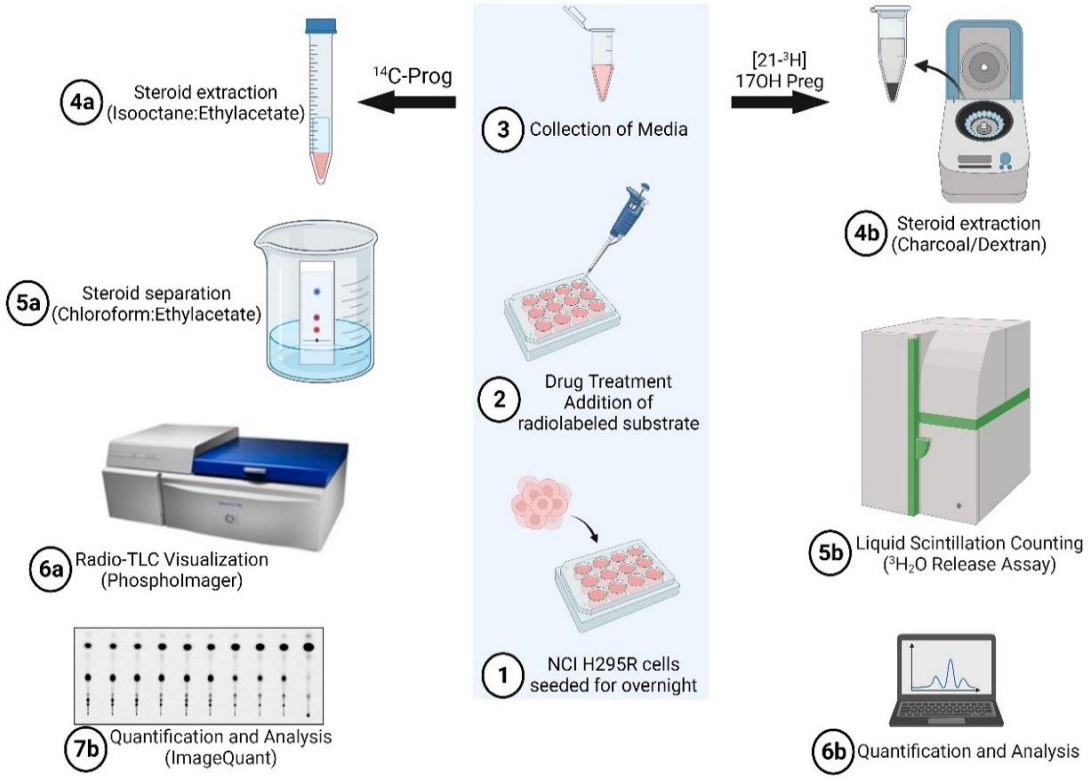

Figure 3 *Outline of common steps followed to assay CYP17A1 enzyme activity. Based on the type of radionuclide and substrate used, two approaches, a., and b., were employed to detect the radioactive signals and subsequent analysis of data. Created by BioRender.com*

3.6.2. Separation of steroids using Thin Layer Chromatography (TLC): This technique falls under the category of solid-liquid chromatography. In this method, a polar absorbent serves as the stationary phase, while the mobile phase can consist of a single solvent or a mixture of solvents. The typical stationary phase employed in TLC is silica gel, characterized by the empirical formula SiO_2. Silica gel surfaces are typically occupied by oxygen atoms bonded to protons, resulting in the presence of hydroxyl groups, which render the silica gel surface highly polar. As a consequence, organic analytes with polar functional groups exhibit strong interactions with the surface of silica gel particles, whereas organic analytes

lacking polar moieties interact only weakly. For a TLC experiment, the choice of elution solvent plays a pivotal role. For most organic analytes, a common elution solvent consists of a combination of hexane and ethyl acetate, ethyl acetate-dichloromethane, methanol-dichloromethane, methanol-water (Marston, 2011; Santiago & Strobel, 2013). Chloroform-Ethyl acetate, 3:1 (Carl Roth® GmbH + Co. KG Karlsruhe, Germany) was chosen as elution solvent used in our experiments. Whatman filter paper was inserted along the inner wall of a glass chamber to ensure that the atmosphere becomes saturated with solvent vapor. About 200 mL of the elution solvent was filled inside the chamber such that the lower part of filter paper is in contact with the solvent. On the TLC plate (Silica gel coated aluminum plate; Supelco® Analytics, Sigma Aldrich Chemie GmbH, Germany), approximately 3cm from the bottom, samples were loaded in a straight line. The samples were dissolved in highly volatile polar solvent, Methylene chloride (Carl Roth® GmbH + Co. KG Karlsruhe, Germany). Using a micro capillary, a very small volume of the sample (1 µL) was applied onto the marked positions on the TLC plate. The spots should be under 3 mm in diameter and allowed to evaporate for a few seconds. TLC plate was placed in the elution chamber, ensuring that the sample spots are at the bottom and above the level of the elution solvent. Sample containing a mixture of steroids were allowed to run until the solvent front reached the top of the TLC plate. The TLC plate was air-dried to evaporate the solvent. Since the steroids used in our experiments were radiolabeled, the TLC was visualized using autoradiography explained in the next section.

3.6.3. Visualization of TLC using Autoradiography: Since the widespread adoption of TLC in the early 1960s, significant advancements have been achieved in the quantitative radio-assay of TLC plates. Autoradiography is the most widely used method of locating radio labelled compounds on TLC plates. The autoradiographic technique can detect all low-energy β-emitters effectively, and monitoring tritiated compounds on TLC plates is more convenient than on paper chromatograms. However, for ^{3}H, extended exposure times exceeding two weeks are typically required. Additionally, the use of an intermediate protective layer is not needed. In contrast, for compounds labeled with ^{14}C, ^{35}S, and ^{36}Cl, exposure times of 1 or 2 days yield satisfactory results. The standard procedure involves placing the TLC plate in direct contact with Storage Phosphor-screen (Storage Phosphor Screen BAS-IP TR 2040 E Tritium Screen, 20 × 40 cm, Cytiva Life Sciences). Cassettes designed to accommodate 20 x 20 cm TLC plates are available from photographic suppliers. The cassettes facilitate the contact between the TLC plate and the screen with proper alignment and provide dark environment for exposure. The limit of detection depends on the amount and type of radioisotope and the duration of exposure. In any mixture of labeled compounds to be separated, it's probable that the compounds will exist at varying concentrations in terms of radioactivity. Therefore, it's advisable to select an exposure time

that is sufficiently long to enable the detection of compounds present in lower concentrations ("Chapter 4 Radio-thin-layer chromatography," 1978). The ionizing radiation emitted by the radioactive isotopes interacts with the phosphor screen. This excites the phosphor crystals layer on the screen causing them to absorb energy. In the imager, a laser or other light source scans the screen. This stimulation causes the trapped electrons in the phosphor to return to their ground state, emitting visible light in the process. A detector in the imager collects the emitted visible light and converts it into an electronic signal. This signal is then processed and used to create a digital image. The imager is equipped with software that allows for the quantification and analysis of the radioactive signals in terms of intensity (Leblans et al., 2011).

3.6.4. Tritiated water (^3H_2O) release assay: This method was employed in case when the radioactive product of enzyme reaction was soluble in aqueous phase. During CYP17A1 lyase action, the substrate 17α-hydroxy pregnenolone gets converted into DHEA and an equimolar amount of acetic acid in form of acetate. When a specific radiolabeled substrate, [21-^{3}H]-17α-hydroxy pregnenolone (SA 15 Ci/mmol; Conc. 1 mCi/mL; American Radiolabeled Chemicals Inc., St. Louis, MO, USA) is used for enzyme assay, the tritium ion at C21 position is transferred to the acetate ion imparting radioactivity to the water-soluble part of sample media.

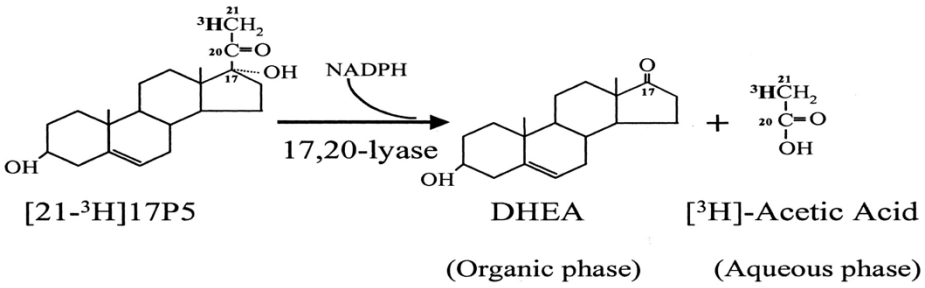

Figure 4 *Schematic representation of the 17,20-lyase reaction. Metabolism of [21-3H]17P5 by CYP17A1 releases [^{3}H] acetate that is recovered in the aqueous phase after enzymatic cleavage of the sidechain of the substrate. Copyright © 2003 by The Endocrine Society (*Morán et al., 2003*).*

Steroids in the media are precipitated out with help of activated charcoal (HERBERT et al., 1965; Morán et al., 2003). The radioactivity in the supernatant can be measured with help of Liquid scintillation counting, LSC (MicroBeta2® Plate Counter, PerkinElmer Inc. Waltham, MA, USA). It is a widely used technique in radiochemistry and radiobiology for measuring samples containing β-emitting or low-energy γ-emitting radionuclides. The radioactive sample to be measured is dissolved or suspended in a liquid scintillation cocktail (ROTISZINT®eco plus., Carl Roth® GmbH + Co. KG Karlsruhe, Germany). This cocktail has three components: an aromatic solvent, a surfactant or detergent and the scintillators. The aromatic solvent possesses π electrons, which facilitates in the transfer of energy from radioactive decay. The surfactant helps in formation of a stable

microemulsion, especially when aqueous samples are involved. This stability is essential for consistent and reliable performance throughout the counting period. When a β-particle interacts with a scintillator molecule, it imparts energy to the molecule. The scintillator molecules become excited and then quickly return to their ground state, emitting photons in the process. The emitted photons enter a photomultiplier tube which amplifies the photons and convert them into electrical signals. The amplitude if this signal is proportional to the radioactivity in the sample. Liquid scintillation counters are calibrated to convert these counts into units of radioactivity, such as disintegrations per minute (DPM) or becquerels (Bq) (Shapira & Perkins, 1960; Wiegman et al., 1975).

3.6.5. Steroid profiling by Liquid Chromatography – Mass Spectrometry: Experiments measuring the presence of steroid in sample media through mass spectrometry followed the same protocol as standard enzyme assay, with the exception that 1 µM of non-radioactive (unlabeled) steroids were utilized instead of [^{3}H]-labeled steroids. The basic principle underlying mass spectrometry (MS) involves the generation of multiple ions from a sample, their subsequent separation in an electromagnetic field based on their mass-to-charge (m/z) ratios which can correspond to their relative abundances in a mixture (Wudy et al., 2018). For small metabolites like steroids, MS is used in combination with either gas chromatography or liquid chromatography (LC). When used in combination MS serves as a detector (Soldin & Soldin, 2009). In general, internal standards in form of stable isotopes are required to track characteristic signals (Owen & Keevil, 2012). The main advantage of LC-MS over other analytical methods is the non-requirement of radioactive labelling. The approach to analyze steroids in a sample like cell culture media can be targeted or untargeted and qualitative or quantitative. LC-MS is the most commonly used technique in clinical settings to analyze glucocorticoids, mineralocorticoids, androgens, and estrogens. LC-MS provides more accurate, precise and sensitive detection method in comparison to other analytical techniques for steroid determination (Kareem Eldin Mohammed Ahmed et al., 2018; Shackleton et al., 1990).

3.6.6. Aromatase assay in JEG3 microsomes: Aromatase activity was quantified by assessing the quantity of ^3H_2O generated from the [1β-^{3}H]-androstenedione substrate. This assay relies on the fact that aromatase catalyzes the stereospecific cleavage of the covalent bond between the carbon atom at position 1 and the hydrogen located on the β side of the steroid ring system during the aromatization of the A-ring. The techniques employed for this approach was similar to the assay described in Section 3.5.4. Use of human placental microsomes to assay aromatase activity was developed during 1974 to 1980 (Reed & Ohno, 1976) (Thompson & Siiteri, 1974). This system provides a direct and rapid assay for evaluating enzymatic turnover. Microsomes resembles closely to the cellular arrangement in which CYP19A1 is anchored to the endoplasmic reticulum

membrane through its N-terminal sequence. NADPH or a system to regenerate NADPH is used to provide the necessary reducing equivalents for enzymatic activity. (İnce Ergüç et al., 2022). Microsomal fractions were isolated from JEG3 Human Choriocarcinoma derived cell line (ATCC® HTB36™) as they express several steroid enzymes including CYP19A1 along with genes for the production of progesterone, Human chorionic gonadotropin (hCG) and other placental hormones (Sun et al., 1998). The reaction mixture containing the microsomes, substrate and NADPH were prepared in Potassium phosphate buffer maintained at appropriate pH to provide cellular like environment as described earlier (Castaño et al., 2019).

3.7. Transformation of competent cells

Following procedure (Malke, 1990) was followed:

- 0.5 M KCl, 0.15 M $CaCl_2$, 0.25 M $MgCl_2$ was prepared from stocks of 4 M KCl, 1 M $CaCl_2$, 1 M $MgCl_2$ for 5X KCM solution. 20 µl of 5X KCM was pipetted out in a 1.5 ml Eppendorf-tube kept on ice.

- 1-2 µl of about 50-100 ng Plasmid-DNA, pcDNA 3.1 was added to the tube. pcDNA™3.1 is 5.4 kb vectors that is designed for high-level stable and transient expression of gene of interest in mammalian cells (Chen & Okayama, 1987).

- The final volume was made up to 100 µl with MilliQ water. DH5α competent cells (Subcloning Efficiency™, Thermo Fisher Scientific) was thawed on ice without mixing by pipette or vortex. DH5α is the commonly used laboratory E. coli strains to maintain and amplify small plasmid DNA (Thomason et al., 2014).

- 100 µl of thawed cells was added into the Plasmid-DNA mixture. This mixture containing DH5α cells was incubated for 20 minutes on ice.

- Followed by 10 minutes of incubation at room temperature, 1 ml of Luria Bertani (LB) medium was added to the tube and incubated for 1 hour on a microtube shaker at 37ºC at maximum speed. The medium was prepared by dissolving appropriate amount of commercially available LB powder (Carl Roth® GmbH + Co. KG Karlsruhe, Germany) in distilled water and autoclaved for experimental use. It is the most widely used medium for the growth of bacteria (Bertani, 1951).

- Cells were centrifuged down at low speed for 2 minutes. The medium was removed, and cells were resuspended in the remaining volume. The cell suspension was applied on an LB-Agar plate containing 100 µg/mL Carbenicillin. Carbenicillin is potent selective agent used to grow transformed bacterial cells (Korpimäki et al., 2003). The culture plate was incubated overnight at 37ºC.

3.8. Maxi-Prep for Plasmid

The preparation and isolation of plasmid of interest (pcDNA 3.1) were carried out according to Sigma's GenElute HP Plasmid Maxiprep Kit. It offers simple, rapid, and cost-effective method for isolating plasmid DNA from recombinant E. coli cultures. The protocol (Birnboim & Doly, 1979) was carried out in following steps:

- A single colony from a freshly streaked plate was picked and inoculated in 3 to 5 ml LB medium containing Carbenicillin. The culture was grown at 37°C for about 8 hours while shaking at 250–300 rpm.
- The appropriate amount of starter culture was determined by measuring the absorbance of the overnight culture at 600 nm and diluted in LB medium. The culture was incubated at 37 °C for 12 to 16 hours while shaking at 250–300 rpm.
- 150 mL of an overnight culture was centrifuged at 5000 x g for 10 minutes. The supernatant was discarded.
- 12 ml of Resuspension/RNase A Solution was added to the obtained bacterial pellet and resuspended by pipetting up and down.
- The resuspended cells were lysed by adding 12 ml of Lysis Solution and the contents were mixed by gentle inversion. The mixture was left undisturbed for 3 to 5 minutes until it becomes clear and viscous.
- Meanwhile, a filter syringe was set up by removing the plunger and placing the barrel in a rack so that the syringe barrel is upright.
- The mixture containing lysed cells were neutralized by adding 12 ml of chilled Neutralization Solution gently invert 4 to 6 times until a white aggregate appears.
- 9 mL of Binding Solution was added and mixed by inversion and poured into the barrel of the filter syringe. The lysate was allowed to sit for 5 minutes until the white aggregate floats on top.
- GenElute HP Maxiprep Binding Column was inserted into a 50 mL collection tube. 12 mL of the Column Preparation Solution was added to the column and centrifuged at 3000 x g for 2 minutes. The eluted solution was discarded.
- The filter syringe barrel was placed over the Binding Column and the plunger was pressed gently to expel half of the cleared lysate into the column. To stop the flow of the remaining lysate the plunger was pulled up to avoid overfilling of the column.
- The column was centrifuged at 3000 x g for 2 minutes. The eluent was discarded. The above step was repeated multiple times until the rest of the cleared lysate was utilized.

- 12 ml of Wash Solution 1 was added to the column and centrifuged at 3000 x g for 2 minutes. The eluent was discarded.
- 12 ml of Wash Solution 2 was added to the column and centrifuged at 3000 x g for 5 minutes. The eluent was discarded.
- The binding column was transferred to a clean 50 mL collection tube. 3 mL of Elution Solution was added to the column.
- To recover plasmid, the column with the collection tube unit was centrifuged at 3000 x g or 1000 x g for 5 minutes.
- The eluate was transferred to a clean centrifuge tube. If required, the volume was made to 100 µL by adding sterile water. 10 µL (0.1X volume) of 3.0 M Sodium Acetate Buffer Solution (pH 5.2) and 220 µL (2X volume) of 100% ethanol was added. The mixture was mixed well by inversion and centrifuged at 15,000 x g at 4 °C for 30 minutes. The supernatant was discarded carefully without disturbing the pellet with help of a micropipette.
- DNA pellet was washed with 0.5 mL of 70% ethanol and centrifuged as before for 10 minutes. The supernatant was removed, and the remaining ethanol was evaporated under air.
- The DNA pellet was resuspended in 50 µL sterile water (MilliQ).
- Purity and quantity of the plasmid DNA was determined using a NanoDrop® UV-Visible Spectrophotometer (Thermofisher Scientific). The ratio of absorbance at (A260−A320)/(A280−A320) should be 1.8 to 2.0.

Stocks of Maxi-prep cDNA plasmids purchased from GenScript was prepared as follows: The sample tube was centrifuged 10,000 rpm/7500 x g for 2 minutes. 100 µl of sterile water was added, vortexed gently and incubated at 50°C for 15 min. The solution was mixed gently and centrifuged at 10,000 rpm for 2 minutes. 20 µl of aliquots were prepared to be stored at -20ºC.

3.9. Transient transfection

Invitrogen™ Lipofectamine™ 2000 Transfection Reagent and the prescribed protocol was followed to perform transfection in mammalian cells.

- One day before transfection, 0.5 x 10^6 cells/well in 1 mL of growth medium was seeded in a 12-well-plate so that cells become 70-90% confluent at the time of transfection.
- Serum free medium (Gibco™ Opti-MEM™ I Reduced Serum Medium) without antibiotics was used to dilute the plasmid DNA and Lipofectamine reagent.

- For each replicate, 0.5 µg of plasmid DNA was diluted in 100 µl of Reduced Serum Medium and mixed gently.
- 4 µl of Lipofectamine 2000 reagent was mixed separately with 100 µl of reduced serum medium and incubated for 5 minutes at room temperature.
- The ratio of DNA (µg) and Lipofectamine reagent (µl) was optimized according to the recommended amount based on relative surface area.
- After the 5-minute incubation, both complexes were combined by gentle mixing and incubated for maximum 20 minutes at room temperature.
- 200 µl of above mixture was added to each well dropwise, containing cells with freshly added reduced serum medium. The contents were mixed gently by moving the plate back and forth.
- 6 hours post transfection, media was replaced by complete growth medium.
- Cells were visualized under microscope using a GFP control plasmid 24-48 hours post transfection.
- After successful transfection, cells were treated with appropriate reagents to perform further assays as needed.

3.10. Stable transfection

The pcDNA^{TM}3.1 contain the neomycin resistance gene for selection of stable cell lines using neomycin (Geneticin®) (Southern & Berg, 1982). For stable transfection, COS-1 cells were used due to their properties explained in ***Section 3.4.2.3***

3.10.2 Kill curve: To successfully generate a stable cell line expressing the gene of interest, the optimal concentration of Geneticin® (G418, Fisher Scientific) was determined. A kill curve follows a dose-response approach, involving the treatment of cells to progressively higher antibiotic concentrations (0.1 -2.0 mg/mL) to determine the minimum amount required for complete cell death within one-week. 0.15 x 10^6 cells/well was seeded in 0.5 mL complete growth medium one day prior to introducing antibiotic selection. Cells should have reached high confluence (~60-80%) before antibiotic treatment. Media containing selection antibiotic was changed every 2-3 days for up to a week. The culture was examined every day for signs of visual toxicity and the antibiotic dose was defined as follows:

- Low dose - the antibiotic concentration at which minimal visual toxicity is apparent even after 7 days of antibiotic selection.
- Optimal dose - the lowest antibiotic concentration at which all cells are dead after one week of antibiotic selection.

- High dose - the antibiotic concentration at which visual toxicity is evident within the first 2-3 days of antibiotic selection.

3.10.3 Selection of clones by serial dilution: The transfection protocol was followed as described in Section 3.9. 48 hours after transfection, the cells were treated with complete growth medium containing 500 µg/mL of Geneticin®. The cells were grown into appropriate confluency under Geneticin pressure. The cells were trypsinized and subjected to counting to determine the cell density. This protocol is adapted from Corning Incorporated Life Sciences.

- 200 µL of 2 X 10^4 cells/mL suspension (4000 cells) was added to the first well (A1) of a 96-well plate.
- Using a multi-channel micropipette, 100 µL of culture medium was added except to well A1. This medium could be conditioned medium obtained from cultures grown for 24 hours.
- 100 µL of the contents of well A1 is transferred to well B1 and mixed well by pipetting up and down. This step was repeated for the 1:2 dilution down the entire first column discarding 100 µL of cell suspension from the last well (H1) to maintain the total volume in each well at 200 µL.
- Using a multi-channel pipette, 100 µL of cell suspension from the first column was transferred to the next column for 1:2 dilution. This step was repeated across the entire plate up till the last column while discarding 100 µL of cell suspension from the last column to maintain 200 µL/well.
- Wells containing single clones were selected and grown under constant pressure of Geneticin.
- Upon reaching confluency, these cells were transferred to larger plates starting from 12-well plate for further expansion and cryopreservation.

3.11 siRNA transfection

Short interfering RNA (siRNA) technology is a powerful molecular tool used in scientific research for gene expression regulation. siRNAs work by triggering the RNA interference (RNAi) pathway. This involves association of Dicer endonuclease with double stranded RNA to generate small functional siRNA through cleavage. The guide strand of the siRNA is loaded onto the RNA-induced silencing complex (RISC), which unwinds the siRNA and uses the guide strand to recognize and bind to the complementary mRNA of the target gene. Once bound, the mRNA is cleaved or translationally repressed, leading to reduced expression of the target gene (Agrawal et al., 2003). Typically, siRNA of 21 to 23 nucleotides in length is used to

selectively silence or downregulate the expression of specific genes in a cell line. These are designed to improve the specificity and efficiency of siRNA with reduced off-targets (Elbashir et al., 2001). In our experiments, Lipofectamine 2000 reagent was used to transfect cells with 27-mer siRNA like the protocol from Section 3.9.

3.12 Statistical analysis

We conducted statistical analysis using Microsoft Excel and Prism 3.0 Graph Pad software. All findings are presented as mean values with standard error of the mean (SEM) unless otherwise specified. In our in vitro experiments, we carried out a minimum of three technical replicates for one to three independent occasions. The analysis of in vitro results involved the use of either unpaired Student's t-test or one-sample t-test, as indicated. For the assessment of results encompassing multiple groups, we employed one-way analysis of variance (ANOVA). We applied a 90% confidence interval, with statistical significance considered at a p-value of <0.05.

UNIVERSITÄT
BERN

RESULTS

AIM: To develop small molecule inhibitors for specific inhibition of CYP17A1 17,20 lyase activity.

Background

Early Non-specific P450 Inhibitors: Initially, compounds like **ketoconazole** were created with the intention of serving as broad-spectrum P450 inhibitors. Consequently, it led to the inhibition of 17-hydroxylase activity, along with impaired CYP11A1, CYP21A2, CYP11B1, and CYP19 activities. The lack of specificity of this drug renders it unsafe for long term therapy (Gal & Orly, 2014).

General CYP17A1 Inhibitors:
The development of more recent CYP17A1-targeted inhibitors, such as **Abiraterone**, has provided a significant advancement. Abiraterone exhibits a higher degree of selectivity toward CYP17A1 compared to ketoconazole. The primary site of action of Abiraterone is the inhibition of 17α-hydroxylase activity. However, an off-target inhibition of CYP21A2 results in elevated ACTH levels due to the absence of cortisol feedback. This can be reversed in clinical practice by co-administering glucocorticoids like prednisone. However, recent data even suggests that prednisone itself may stimulate the mutant AR, undermining the purpose of prednisone co-therapy. Although abiraterone represents a significant leap in available therapy, it does not yet exhibit the expected profile of a truly selective 17,20 lyase inhibitor (Attard et al., 2012; Stein et al., 2014).

Another drug possessing similar properties is **Orteronel (TAK-700).** Extensive research has been conducted on this compound including in H295R cells. Direct comparison of TAK-700 and Abiraterone demonstrated similar effectiveness in inhibiting DHEA production indicating some specificity for lyase inhibition compared to ketoconazole. However, both TAK-700 and abiraterone exhibited a dose-dependent effect on cortisol levels (Yamaoka et al., 2012).

Selective CYP17A1 lyase inhibitors:
In cases of selective lyase deficiency resulting from a CYP17A1 mutation, it is evident that 17-hydroxylase activity can still be maintained at around 65% even when 17,20 lyase activity is significantly inhibited. Therefore, it is unlikely that the ideal drug would surpass these established thresholds. For tumors expressing mutant AR, the primary objective of any therapeutic approach is to deprive the tumor of C19 androgens. However, this must be achieved without causing a pronounced surge in ACTH, which could otherwise lead to elevated levels of early ZF alternate pathway steroids such as pregnenolone and progesterone.

Achieving this balance is essential to avoid the necessity of using prednisone to suppress these unwanted effects (Bird & Abbott, 2016).

Galeterone (TOK-001) has been suggested to function both as CYP17A1 inhibitor and an AR antagonist. There is less publicly accessible information regarding its impact on steroid profiles, whether in vitro or in vivo. Although a crystal structure of CYP17A1 has been documented with abiraterone and galeterone, there seems to be no difference in the substrate orientation in either instance. Additionally, it has been suggested that the primary mode of action for galeterone may be at the level of the AR. Notably, clinical trial data indicate that there is no more need of co-administration of prednisone (Njar & Brodie, 2015).

VT464 is another newly developed compound, believed to function as a selective lyase inhibitor. A preliminary review of the data released indicates that the IC50 for human CYP17 lyase activity is ten times lower than that for hydroxylase (Yin & Hu, 2014). Given that the current data about CYP17A1 inhibitors indicates towards the lack of specificity towards CYP17A1 lyase activity and adverse side-effects in terms of cross reactivity with other CYPs. This compels us to look for true inhibitors of CYP17A1 lyase activity. Therefore, this section deals about screening of small molecule inhibitors which are designed and synthesized chemically by our collaborators. The in silico molecular modelling is done by bioinformatician. Brief details about the molecular docking and prediction of best candidates for cell-based screening is explained in the attached papers in form of ***Chapter 1*** and ***Chapter 2***. Additional information regarding computational modelling can be found in Appendix I section. All the cell-based screening of compounds and in vitro experiments are performed according to the experimental details described in ***Section 3***. Preliminary data from experiments with crude extract of two plant tissues is reported in form of small chapter 3. The background and approach are similar to Chapter 2.

Chapter 1

Screening computationally designed and chemically synthesized compounds against CYP17A1 activity.

Section A: Synthesis and Structure-Activity Relationships of Novel Non-Steroidal CYP17A1 Inhibitors as Potential Prostate Cancer Agents

Status: Published

My Contributions in the paper:

All the in vitro experiments were performed by me. This includes:

- Maintenance of cell culture: NCI H295R cell line
- Cell-based enzyme assays - CYP17A1 17α-Hydroxylase activity, CYP17A1 17,20Lyase activity.
- Dose response experiments in NCI H295R cells

Writing:

Section 2 (Material and Methods): Assay of CYP17A1 activities

Figures:

- Figure 2: Inhibition of CYP17A1 17α-hydroxylase activity by compounds 1–20 at 10 µM concentration.
- Figure 3: Determination of IC50 of compounds 2, 12, and 20 for inhibition of the 17α-hydroxylase activity of CYP17A1.
- Figure 5: Inhibition of CYP17A1 lyase reaction by compounds 2,12 and 20.

Statistical analysis for enzyme assays and generating graphs for Figure 2, 3 and 5.

biomolecules

MDPI

Article

Synthesis and Structure–Activity Relationships of Novel Non-Steroidal CYP17A1 Inhibitors as Potential Prostate Cancer Agents

Tomasz M. Wróbel [1,2,*], Oksana Rogova [1], Katyayani Sharma [3,4], Maria Natalia Rojas Velazquez [3,4], Amit V. Pandey [3,4], Flemming Steen Jørgensen [1], Frederic S. Arendrup [5], Kasper L. Andersen [5] and Fredrik Björkling [1]

1 Department of Drug Design and Pharmacology, University of Copenhagen, Universitetsparken 2, DK-2100 Copenhagen, Denmark; oksana.rogova@chem.lu.se (O.R.); fsj@sund.ku.dk (F.S.J.); fb@sund.ku.dk (F.B.)
2 Department of Synthesis and Chemical Technology of Pharmaceutical Substances, Medical University of Lublin, Chodźki 4a, 20093 Lublin, Poland
3 Division of Pediatric Endocrinology, Department of Pediatrics, University Children's Hospital Bern, 3010 Bern, Switzerland; katyayani.sharma@dbmr.unibe.ch (K.S.); maria.rojasvelazquez@students.unibe.ch (M.N.R.V.); amit@pandeylab.org (A.V.P.)
4 Department of Biomedical Research, University of Bern, 3010 Bern, Switzerland
5 Biotech Research and Innovation Centre (BRIC), University of Copenhagen, Ole Maaløes Vej 5, DK-2200 Copenhagen, Denmark; frederic.arendrup@bric.ku.dk (F.S.A.); kasper.andersen@bric.ku.dk (K.L.A.)
* Correspondence: tomasz.wrobel@umlub.pl; Tel.: +48-814487273

Citation: Wróbel, T.M.; Rogova, O.; Sharma, K.; Rojas Velazquez, M.N.; Pandey, A.V.; Jørgensen, F.S.; Arendrup, F.S.; Andersen, K.L.; Björkling, F. Synthesis and Structure–Activity Relationships of Novel Non-Steroidal CYP17A1 Inhibitors as Potential Prostate Cancer Agents. *Biomolecules* **2022**, *12*, 165. https://doi.org/10.3390/biom12020165

Academic Editor: Alessandro Alaimo

Received: 20 December 2021
Accepted: 18 January 2022
Published: 20 January 2022

Abstract: Twenty new compounds, targeting CYP17A1, were synthesized, based on our previous work on a benzimidazole scaffold, and their biological activity evaluated. Inhibition of CYP17A1 is an important modality in the treatment of prostate cancer, which remains the most abundant cancer type in men. The biological assessment included CYP17A1 hydroxylase and lyase inhibition, CYP3A4 and P450 oxidoreductase (POR) inhibition, as well as antiproliferative activity in PC3 prostate cancer cells. The most potent compounds were selected for further analyses including in silico modeling. This combined effort resulted in a compound (comp **2**, IC_{50} 1.2 μM, in CYP17A1) with a potency comparable to abiraterone and selectivity towards the other targets tested. In addition, the data provided an understanding of the structure–activity relationship of this novel non-steroidal compound class.

Keywords: cytochrome P450 17A1; CYP17A1; prostate cancer; enzyme inhibition

1. Introduction

Prostate cancer (PCa) remains the most common type of cancer diagnosed in men [1]. While the localized disease can be treated with surgery or radiation therapy, androgen deprivation therapy (ADT) is engaged when cancer spreads. ADT continues to be the cornerstone of prostate cancer treatment. Despite treatment, eventually, the disease develops into castration-resistant prostate cancer (CRPC), consequently yielding a poor patient prognosis.

Current discovery efforts towards new therapies focus on androgen receptor (AR) signaling. Those endeavors introduced the next-generation AR antagonists represented by enzalutamide and apalutamide [2]. Other notable discoveries include proteolysis-targeting chimeras (PROTACs), poly ADP-ribose polymerase (PARP) [3] inhibitors, histone deacetylase (HDAC) inhibitors [4], and various forms of immunotherapy [5]. The emergence of novel targets such as fatty-acid binding protein 5 (FABP5) [6] also illustrates the progress that has been made in the field of prostate cancer. However, despite these efforts, PCa still presents a significant problem.

In addition to the interventions mentioned above, cytochrome P450 17A1 (CYP17A1) inhibition has in recent years received increased attention as a valid treatment modality. CYP17A1 is a dual-function oxygenase membrane-bound enzyme that catalyzes the biosynthesis of steroids [7–9]. Its dual activity stems from the ability to produce precursors for glucocorticoids via 17α-hydroxylase reaction and androgens/estrogens via 17,20-lyase reaction [10]. Therefore, CYP17A1 is an attractive target for the treatment of prostate cancers that proliferate in response to androgens [11]. CYP17A1 is required in both the "classic" and "back-door" pathways of steroid biosynthesis, and by its inhibition, the production of androgens can be limited [12,13].

In our previous work, we identified hit compounds based on a benzimidazole/indole scaffold with satisfactory properties (Figure 1) [14]. Encouraged by these early results, we set off to explore related analogs in search of an optimized molecule and to analyze the structure–activity relationships. Here, we present the synthesis of 20 novel derivatives and their biological evaluation together with computational analysis. The compounds were designed to determine how the following modifications influence the inhibitory activity of CYP17A1, and compound properties: (a) substituent on benzimidazole moiety, to increase compound polarity; (b) introduction of selected heterocycles; (c) replacing linker nitrogen atom with oxygen bridging the aromatic moieties; (d) introduction of more sp^3 carbons to improve physico-chemical properties; (e) addition of bulk to the middle-linker part of the molecules to take advantage of hydrophobic space in a binding pocket. In addition, assays with PC3 cells, which display a high degree of metastatic potential and tumorigenicity, were performed to see if the compounds would affect hormone-insensitive cells, thus implying an additional mechanism of action.

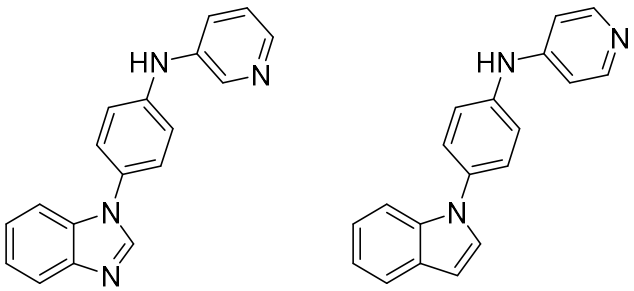

Figure 1. Early hit compounds identified in the previous study.

2. Materials and Methods

2.1. Synthesis

All reagents and solvents were used as purchased from commercial sources and reactions were carried out under anhydrous and air-free conditions unless stated otherwise. Reaction conditions and yields were not optimized. Dry column vacuum chromatography (DCVC) was performed with silica gel 60 (15–40 μm, Merck KGaA, Darmstadt, Germany). Ion exchange chromatography was performed on ISOLUTE® MP-TsOH columns (sulfonated macroporous polystyrene resin, 500 mg, 6 mL, Biotage, Uppsala, Sweden). ^{1}H and ^{13}C spectra were recorded on 600 MHz Bruker Avance III HD, 400 MHz WB Bruker Avance, or 300 MHz Bruker Fourier spectrometers (Bruker, Billerica, MA, USA). Coupling constants (J) are reported in Hertz (Hz). Chemical shifts are reported in parts per million (ppm, δ scale) relative either to an internal standard (TMS) or residual solvent peak. High-resolution mass spectroscopy (HRMS) was carried out on a Bruker Solarix XR 7T ESI/MALDI-FT-ICR with positive MALDI ionization mode using NaTFA cluster-ions for external calibration or Bruker microTOF-Q II with ESI ion source mass spectrometers (Bruker, Billerica, MA, USA). Data obtained were processed in Bruker DataAnalysis Software. Analytical HPLC was carried out on Dionex UltiMate HPLC system (Thermo-Fisher, Waltham, MA, USA) consisting of LPG-3400A pump, WPS-3000SL autosampler, and DAD-3000D diode array detector using Gemini-NX C18 column (4.6 mm × 250 mm, 3 μm, 110 Å) or Kinetex PS18 column (2.1 mm × 100 mm, 2.6 μM, 100 Å). Preparative HPLC was carried out on a Dionex

UltiMate HPLC system consisting of HPG-3200BX pump, Rheodyne 9725i injector, 10 mL loop, MWD-3000 detector, and FCA_Multi automated fraction collector using Gemini-NX C18 (21.2 mm × 250 mm, 5 µm, 110 Å). Data were acquired and processed using the Chromeleon software (Thermo Fisher Scientific).

2.2. Assays

Assay of CYP17A1 activities: Assay of CYP17A1 17α-hydroxylase and 17,20 lyase activities were performed as described previously [15,16]. The 17α-hydroxylase activity was measured by conversion of Prog to 17OH-Prog, while production of DHEA from 17OH-Preg was used for monitoring the 17,20 lyase activity of CYP17A1. For the 17-hydroxylase reaction, radiolabeled [^{14}C]-PROG (20,000 cpm/reaction) was used as a tracer. Steroids were extracted and separated by thin-layer chromatography (TLC) on silicagel (SIL G/UV_{254}) TLC plates (Macherey-Nagel, Oensingen, Switzerland) as previously described [16–18]. The separated steroids were visualized on a Fuji FLA-7000 PhosphoImager (Fujifilm, Dielsdorf, Switzerland) and quantified using Multi Gauge software (Fujifilm, Dielsdorf, Switzerland). Steroid conversion was calculated as a percentage of incorporated radioactivity into a specific steroid product to total radioactivity measured for the whole sample (internal control). For the 17,20 lyase activity of CYP17A1, a water release assay was used. We used 17OH-Preg labeled with [^{3}H] at the C21 position, which upon conversion to DHEA releases an equimolar amount of [^{3}H] H_2O. Tritiated water is separated and measured by scintillation counting based on a method described by Simpson for the assay of aromatase activity [19].

Assay of CYP3A4 activity: The activity of the major drug-metabolizing enzyme CYP3A4 in the presence of selected compounds was tested using the fluorogenic substrate BOMCC (7-Benzyloxy-4-trifluoromethylcoumarin) (Invitrogen Corp, Carlsbad, CA, USA) as described earlier [20]. In vitro CYP3A4 assays were performed using a liposome system consisting of POR, CYP3A4 and cytochrome b_5 at a ratio of 4:1:1 (POR:CYP3A4:b_5). Reconstitution of liposomes was carried out as described before [21]. The final assay mixture consisted of liposomes and proteins (80 pmol POR: 20 pmol CYP3A4: 20 pmol b_5), 2.5 mM $MgCl_2$, 2.5 µM GSH and 20 µM BOMCC in 50 mM HEPES buffer and the reaction volume was 200 µL. The catalytic reaction was initiated by the addition of NADPH to 1 mM final concentration and fluorescence was monitored on a Spectramax M2e plate reader (Molecular Devices, Sunnyvale, CA, USA) at an excitation wavelength of 415 nm and emission wavelength of 460 nm for BOMCC metabolism.

Assay of P450 oxidoreductase (POR) activity: POR assay was performed as described previously, using purified human POR [22]. The activity of the bacterially expressed POR was tested for its ability to reduce resazurin into resorufin, which is highly fluorescent. The reaction was performed in triplicate in 96-well format using a microplate reader (Molecular Devices, Sunnyvale, CA, USA). The reaction components were 10 µM resazurin, 100 ng of POR in 50 mM Tris-HCL (pH 7.8) containing 150 mM NaCl. NADPH was added at a concentration of 100 µM as the source of electrons to start the reaction, and the change in emission (570 nm excitation, 585 nm emission for resorufin) was monitored for 30 min.

Antiproliferation assay: PC-3 prostate cancer-derived cells were propagated in RPMI-1640, GlutaMAX + 25 mM HEPES (Gibco) supplemented with 100 U/mL penicillin, 100 mg/mL streptomycin (P/S) (Gibco), and 6% (PC-3) fetal bovine serum (FBS) (HyClone). Cells were grown to approximately 80% confluence and harvested by 0.25% Trypsin/EDTA (Gibco) treatment. The released cells were counted and seeded in 384-well plates (Falcon, ref. 353962). The cells were allowed to settle for 24 h, after which cell numbers in 44 wells/cell line of one plate were determined (T_0). In parallel, the indicated compounds (10 mM stock in DMSO) or DMSO alone were delivered to cells in three replicate 384-well plates by acoustic droplet ejection using an Echo 550 Liquid Handler (Labcyte) for a final concentration of 0–25 µM compound and 0.25% DMSO. Cells were then incubated for an additional 72 h before determining end-point cell numbers. CellTiter-Glo 2.0 (Promega) luminescent cell viability assay was used as a proxy for cell number according to manufacturer instructions.

Luminescence was measured with a 384-well plate reader on a SpectraMax Paradigm using Softmax Pro 6.5.1 software. Liquid handling in cell seeding and CellTiter GLO addition was performed on a MicroLab STARlet liquid handling workstation with a CO-RE 384 probe head (Hamilton Company, Reno, NV, USA).

2.3. Molecular Modeling

For the cross-docking, the ligands were extracted from their respective protein structures and prepared for docking by the LigPrep procedure in Maestro (v. 9.8, Schrodinger 2018-3 release, Schrödinger, LLC, New York, NY, USA, 2014) securing proper atom and bond typing, protonation and partial atomic charges [23]. The remaining compounds were constructed in Maestro and prepared for docking in a similar way. The proteins were extracted from the Protein DataBank [24] and subjected to the Protein Preparation procedure [23] to secure proper protonation and hydrogen bonding.

The GOLD (Genetic Optimization for Ligand Docking) program version 5.6 [25] was used for docking. Binding sites were defined by a 20 Å sphere centered at the Fe atom in the heme group. Ligands were docked with the slow genetic algorithm using the CYP450 version of the ChemScore scoring function [26,27]. Ten poses were sampled and analyzed for each docking.

The MD simulations were performed with the Desmond program (version 3.6, Schrödinger, LLC) using the OPLS4 force field [28]. The protein-ligand complexes were embedded in an orthorhombic box of SPC water molecules with a 10 Å buffer size between protein and box boundary using the Desmond system builder. The MD systems comprised approximately 70,000 atoms, including approximately 7500 atoms for the protein including the heme group, 36 atoms for the ligand, one chloride ion to neutralize the system, and approximately 21,000 water molecules. The systems were equilibrated prior to the production runs applying the Desmond default equilibration protocol. Subsequently, the systems were simulated for 100 ns and 100 frames collected.

3. Results and Discussion

3.1. Synthesis

A total of 20 new compounds were synthesized using the previously described method [14]. Briefly, indole or benzimidazole were N-arylated and the resulting bromide intermediate was subjected to Buchwald–Hartwig coupling with amines to obtain compounds **1**–**8** (Scheme 1). Access to compounds **9**–**11** was realized via intermediates that had reversed polarity for Buchwald–Hartwig coupling (Scheme 2). Using heterocyclic bromides, as coupling partners, required switching to tBuBrettPhos as a ligand and LHMDS as a base. Compound **12** was obtained from a phenol intermediate, which was synthesized employing Chan–Lam reaction (Scheme 3). Since different tautomeric forms of 5-substituted benzimidazole may react, two distinct isomers can be obtained [29]. Indeed, after transforming 5-methoxybenzimidazole into its N-arylated derivative, two regioisomers (5-methoxy and 6-methoxy) readily separable by chromatography were produced. Similar results were obtained with 5-aminobenzimidazole. Structures of these isomers were identified by NMR spectroscopy employing NOE experiments. Eventually, these intermediates were converted into the final compounds **13**–**16** via established chemistry. Coupling of compounds **15** and **16** required prior protection of the amino group, which was achieved with the Boc group (Scheme 4). Compounds **17**–**20** were synthesized in a similar fashion utilizing nitro compounds for the first step arylation, followed by catalytic reduction and finally Buchwald–Hartwig coupling (Scheme 5).

The final compounds were fully characterized by ^{1}HNMR and ^{13}CNMR spectroscopy, as well as HRMS spectrometry, and were found to be >99% pure (HPLC). Detailed synthetic procedures, spectra, and HPLC chromatograms can be found in Supplementary Materials.

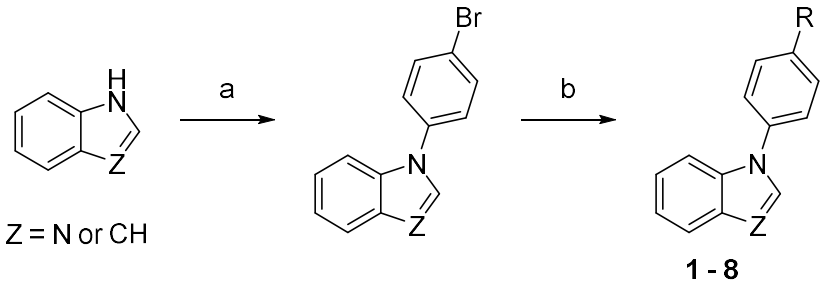

Compound	Z	R	Compound	Z	R
1	N	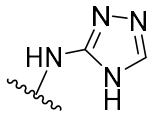	**5**	N	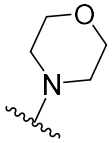
2	N	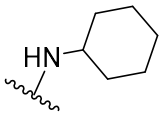	**6**	N	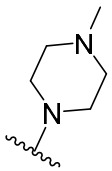
3	N	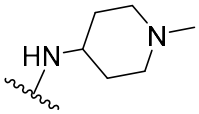	**7**	N	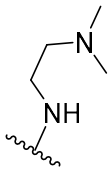
4	N	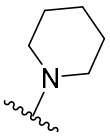	**8**	CH	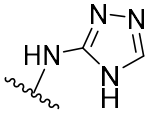

Scheme 1. Synthesis of compounds **1**–**8**. Reaction conditions: (a) 1-bromo-4-fluorobenzene, K_3PO_4, DMF, 150–160 °C, 53–78%; (b) amine, precatalyst Pd G1 or G3, tBuXPhos, NaOtBu, THF or tBuOH, 21–73%.

3.2. Biological Evaluation

The obtained compounds were subjected to initial screening for inhibition of CYP17A1 activity at a fixed concentration (10 μM) (Figure 2). Most compounds did not display improved activity over the previous hits [14]. However, we observed substantial activity in the case of compounds **2**, **12,** and **20**. Compound **2** was the most potent and comparable to abiraterone used as a reference compound in this assay. These three most potent compounds were selected for more rigorous testing comprising determination of IC_{50}, selectivity towards CYP isoform CYP3A4, the ability to inhibit cytochrome P450 reductase (POR) and the ability to inhibit the lyase reaction of CYP17A1. Compounds **2**, **12** and **20** displayed IC_{50} of 1.2, 3.4 and 2.6 μM, respectively, in the inhibition of the CYP17A1 17α-hydroxylase activity (Figure 3). All three selected compounds exhibited selectivity vs. CYP3A4 (**2**: 104 ± 4%, **12**: 75 ± 5% and **20**: 117 ± 8% compared to untreated control) and importantly they do not appear to inhibit POR (**2**: 93 ± 9%, **12**: 103 ± 9% and **20**: 88 ± 16% compared to untreated control) (Figure 4), suggesting a targeted activity towards CYP17A1. Finally, checking compounds **2**, **12** and **20** against the lyase reaction, unfortunately, revealed

little influence compared to abiraterone (**2**: 78 ± 10%, **12**: 77 ± 4% and **20**: 82 ± 5% of untreated control, compared to 5 ± 2% activity observed for abiraterone) (Figure 5).

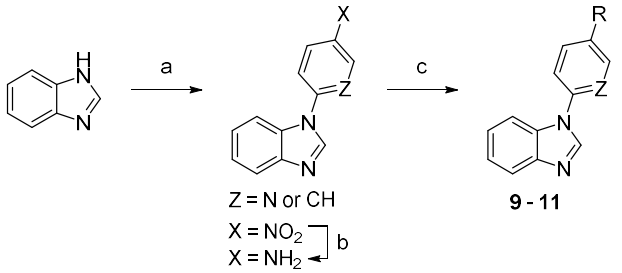

Compound	Z	R
9	CH	
10	CH	
11	N	

Scheme 2. Synthesis of compounds **9**–**11**. Reaction conditions: (a) 1-fluoro-4-nitrobenzene, K_3PO_4, DMF 150 °C, 66% or 2-fluoro-5-nitropyridine, K_3PO_4, DMSO, rt, 74%; (b) 10% Pd/C, MeOH, rt, 82%; (c) bromide, precatalyst Pd G3, tBuBrettPhos, LHMDS, THF, 60 °C, 4–15%.

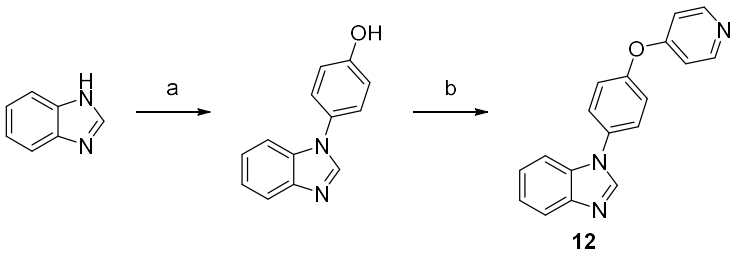

Scheme 3. Synthesis of compound **12**. Reaction conditions: (a) 4-hydroxyphenylboronic acid, O_2, Cu_2S, TMEDA, MeOH, rt, 71%; (b) 4-bromopyridine hydrochloride, NaOtBu, DMF, 150 °C, 32%.

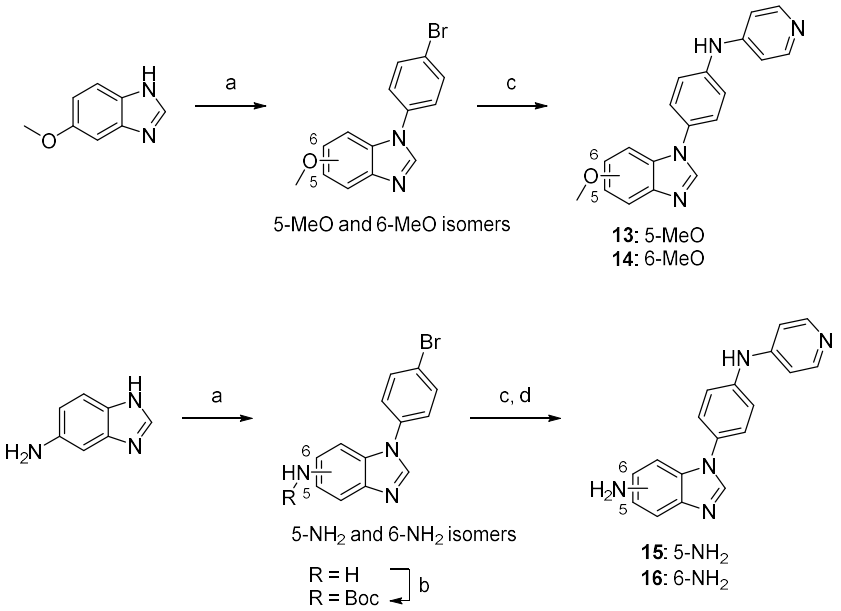

Scheme 4. Synthesis of compounds **13**–**16**. Reaction conditions: (a) 1-bromo-4-fluorobenzene, K_3PO_4, DMF, 160 °C, 5–44%; (b) Boc_2O, TEA, tBuOH, 40 °C, 74–90%; (c) 4-aminopyridine, precatalyst Pd G1, tBuXPhos, NaOtBu, tBuOH, 70 °C, 11–50%; (d) TFA, DCM, 23–50% (over two steps, c and d).

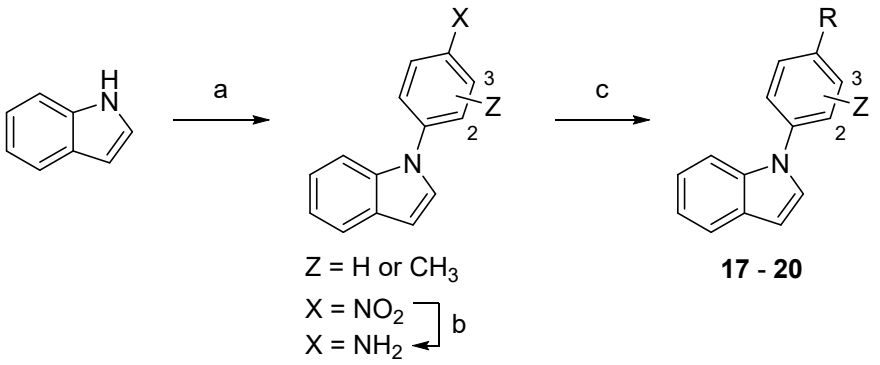

Compound	Z	R
17	H	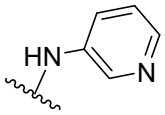
18	3-CH_3	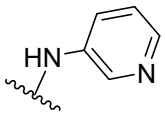
19	H	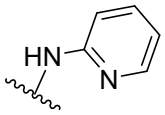
20	2-CH_3	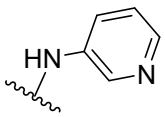

Scheme 5. Synthesis of compounds **17**–**20**. Reaction conditions: (a) 1-fluoro-4-nitrobenzene or fluoronitrotoluene, K_3PO_4, DMF, 160 °C, 18–93%; (b) 10% Pd/C, MeOH, rt, 91–96%; (c) 2- or 4-aminopyridine, precatalyst Pd G3, tBuXPhos, NaOtBu, THF, MW 100 °C, 23–32%.

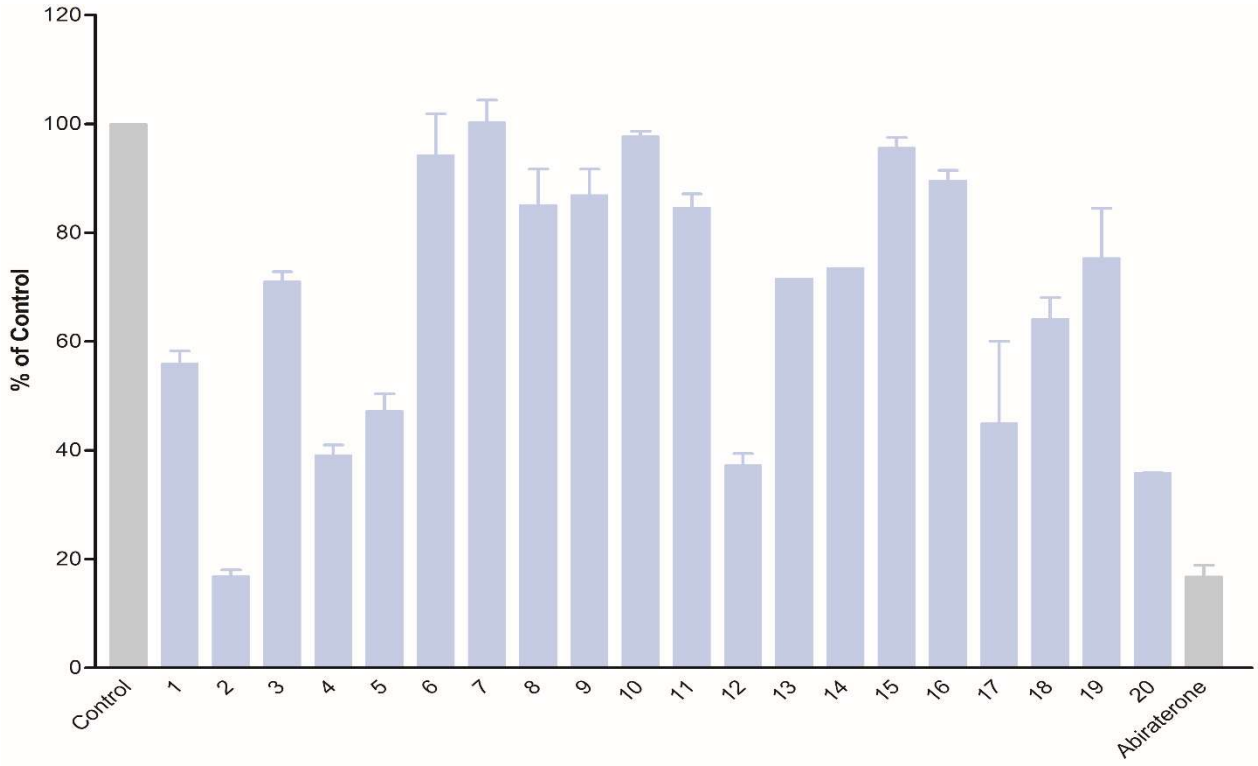

Figure 2. Inhibition of CYP17A1 17α-hydroxylase activity by compounds **1**–**20** at 10 μM concentration.

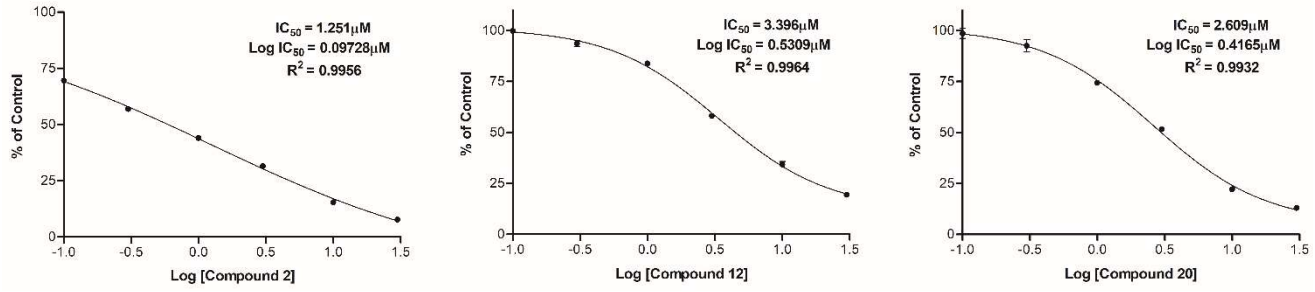

Figure 3. Determination of IC_{50} of compounds **2**, **12,** and **20** for inhibition of the 17α-hydroxylase activity of CYP17A1.

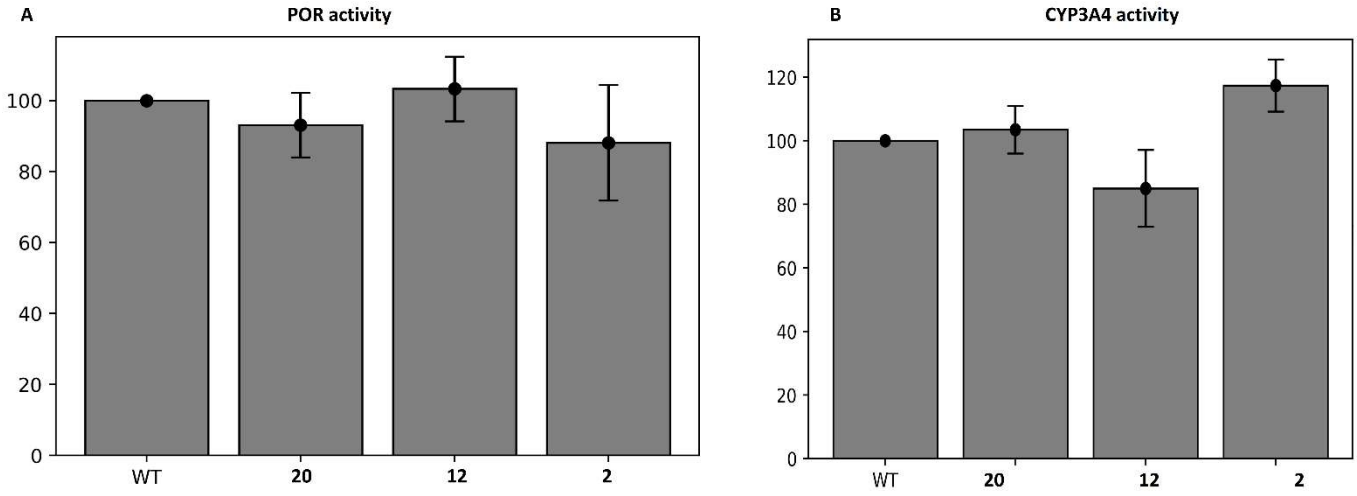

Figure 4. The activity of compounds **2**, **12,** and **20** towards POR (**A**) and CYP3A4 (**B**).

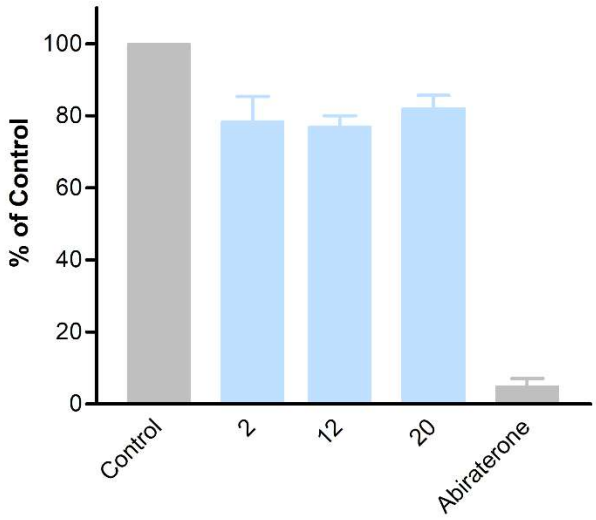

Figure 5. Inhibition of CYP17A1 lyase reaction by compounds **2**, **12,** and **20**.

These results highlight several features regarding the structural composition of the compounds. Introduction of the cyclohexane ring in **2** had the most profound effect and **2** showed similar potency to abiraterone. The presence of an aliphatic ring presumably allows for better allocation in the hydrophobic binding region. This is further corroborated when comparing **2** to **3**. Both compounds have similar shapes, but compound **3** contains a protonable amine embedded into cyclohexane. This modification causes a significant loss of activity. Compound **7,** which contains a flexible chain ending with a tertiary amine is devoid of any activity, indicating that the presence of a ring system is a necessary requirement.

When the ring system is directly connected to the benzene linker, the activity is attenuated as observed with compounds **4** and **5**, the effect being more pronounced in the latter. Similar to the pattern observed with compound **3** in relation to compound **2**, we observed a sharp drop in activity when an amine moiety was introduced, evidenced by the low activity of compound **6**. Embedding polar fragments and increasing the number of sp^3 carbons was aimed at improving the drug-likeness of our molecules [30]. Interestingly, replacing the nitrogen atom, primarily serving as a part of a linker, with an oxygen atom gave compound **12**, which was among the three most potent compounds investigated in this work. Here, we hypothesize that an analog containing a 3-pyridyl fragment instead of 4-pyridyl would have been even more potent as corroborated by computational analyses. Unfortunately, this analog was not obtained due to difficulty in chemical synthesis. Exploration of different heterocyclic ring systems did not deliver compounds with significant potency. However, it is noteworthy that in those cases a benzimidazole fragment was superior to indole, as evidenced when comparing the activity of **1** to the activity of **8**. Upon considering the structure of a five-membered ring attached to the linker, it is evident that a molecule with triazole fragment (**1**) exerts stronger inhibitory activity than molecules with imidazole (**9** and **10**). Comparison of two imidazole-containing compounds suggests that 2-imidazolyl (**9**) is preferred to 4-imidazolyl (**10**), although both compounds displayed very weak activity. The importance of having a more hydrophobic middle part of a molecule is indicated by compound **11**. This nitrogen-rich molecule has pyridine as the linker and displayed decreased activity compared to its benzene analog **1**. Compounds **13–16** were designed to explore the effect of substituting benzimidazole with various polar groups. It was hoped that by doing so we would make possible hydrogen bonding to Asn202 in helix F, as observed in the X-ray structure of CYP17A1 bound to abiraterone [7]. This operation did not bring a significant boost in the activity. However, it can be noted that the methoxy group (**13** and **14**) was a better choice than the amino group (**15** and **16**), regardless of the substitution pattern present in these two pairs of analogs. Lastly, we wanted to explore the effect of adding an extra methyl group to the benzene linker, taking advantage of the hydrophobic region of the binding site. The so-called "magic methyl" effect, which involves the addition of a single methyl group in the "right" location on a molecule can result in a significant activity boost [31,32]. In our case, we were able to obtain compounds **18** and **20** bearing this substituent. Interestingly, only **20** displayed significant activity. This compound has a methyl group that is ortho to the indole ring and is the second most potent compound in this series. In comparison, compound **18** was less active. In that case, the methyl group is meta to the indole ring, which seemingly has less influence and conformational benefit, as evidenced by our computational analysis. The activities of compounds **17** and **19** deliver further rationale for designing compounds with a 3-pyridyl substitution pattern instead of 2-pyridyl. As shown by our calculations and previous studies, compounds with a 2-pyridyl moiety adopt unfavourable binding poses.

Although we were unable to obtain compounds with significantly improved activities compared to the initial hits [14], we were nevertheless happy to observe that our design was still selective for CYP17A1 versus CYP3A4, as indicated by the assay performed on the three most potent compounds (Figure 4B). CYP3A4 is the major drug-metabolizing enzyme in the liver that has broad specificity and can also metabolize steroids [33]. A severe impact on CYP3A4 is, therefore, considered a negative criterion for compounds targeting another P450 enzyme. While CYP3A4 itself does not show much variability in humans, like CYP2D6 and CYP2C19, variations in POR have been shown to alter the activity of CYP3A4 with potentially negative consequences [20,21,33,34]. Furthermore, these compounds also do not influence POR activity (Figure 4A). This is important because all microsomal P450s depend on POR for the supply of electrons and severe disruption of POR activities may affect all microsomal P450 enzymes with serious consequences [35]. Recently, the modulation of some P450 activities by binding to POR has been reported, indicating that a direct impact on the conformation or activity of POR may also influence P450 enzymes [22].

Since our research efforts are aimed at prostate cancer, we were also interested in evaluating our compounds in the PC3 prostate cancer cell line. This cell line is hormone insensitive and presents no AR [36]; thus, any effect observed on cell growth might be attributed to additional mechanisms of action. Indeed, we observed a negative growth rate inhibition (GR) value for compounds **1**, **9**, **14,** and **16** when tested at 25 μM concentration (Figure 6, Supplementary Materials). The negative GR values indicate that the compounds are cytotoxic [37]. These compounds did not exhibit significant inhibition of CYP17A1; therefore, it is likely that they exert a different mechanism of action responsible for the observed cytotoxicity. They were more cytotoxic than the DNA replication inhibitor 5-fluorouracil used as a reference compound in this assay. Moreover, abiraterone, which was also used as a reference compound, had a very small effect on PC3 proliferation.

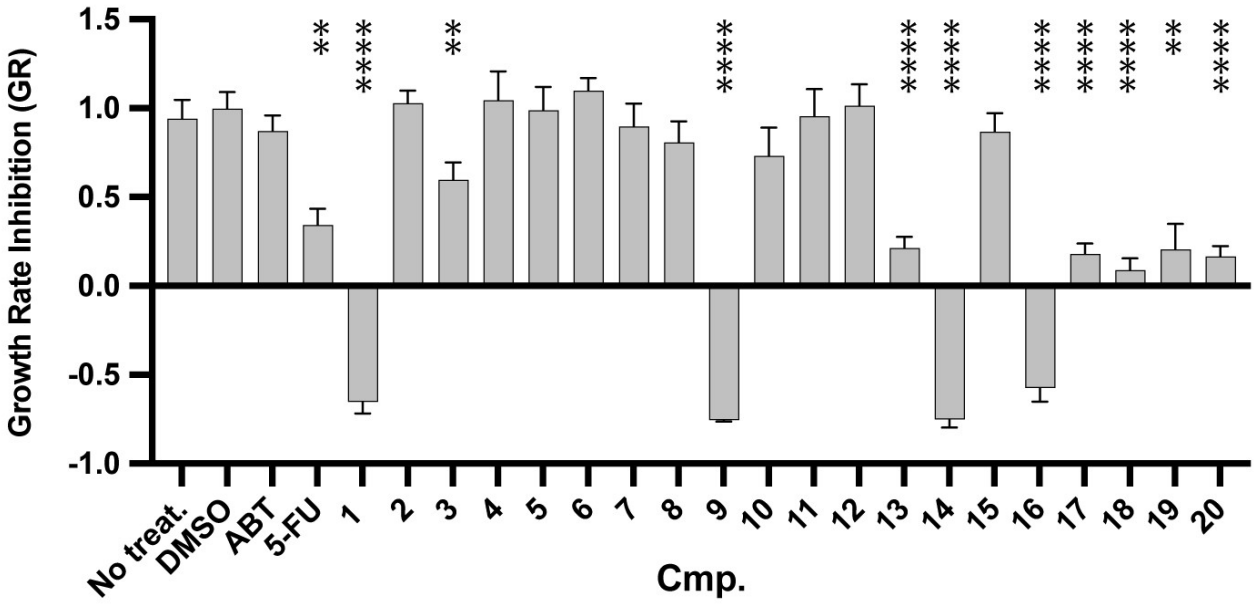

Figure 6. Growth rate inhibition (GR) of compounds **1**–**20**. All compounds were tested at 25 μM, with DMSO as a control and 5-fluorouracil (5-FU) and abiraterone (ABT) as reference compounds. The sign of the GR value relates directly to response phenotype: Values between 0 and 1 show partial growth inhibition, a value of 0 equals cytostasis, and values between 0 and −1 show that compounds are cytotoxic. Significant differences of growth in presence of compounds compared to DMSO were determined by the T-test and indicated by asterisks: ** $p < 0.01$, **** $p < 0.0001$.

3.3. Molecular Modeling

The three compounds, **2**, **12,** and **20**, showing the highest affinity for the CYP17A1 enzyme were subjected to a molecular modeling analysis to determine their potential binding mode. The compounds represent different combinations of ring systems yielding three different scaffolds. Compounds **2** and **20** only contain a single potential heme-coordinating moiety, a benzimidazole and a pyridine moiety, respectively. Compound **12** contains both these ring systems and, accordingly, this compound may bind to CYP17A1 in two different modes.

We selected the five recently determined experimental structures of the A105L mutant of CYP17A1 as the target for our docking studies since they represent structures of CYP17A1 in complex with an inhibitor, abiraterone (4NKV), two hydroxylase substrates, pregnenolone (4NKW) and progesterone (4NKX), and two lyase substrates, 17α-hydroxyprogesterone (4NKY) and 17α-hydroxypregnenolone (4NKZ) [38].

Initially, we performed a cross-docking study of the five substrates in each of the protein structures to test if the docking software was able to identify the correct binding mode for these ligands. Inspection of the docking scores (Figure 7) shows that abiraterone binds significantly better (>10 kcal/mol) to all five protein structures. It is also interesting

to note that the hydroxylase substrates generally bind better than the lyase substrates. The high degree of similarity in binding scores between the five proteins is probably a consequence of the experimental structures being nearly identical.

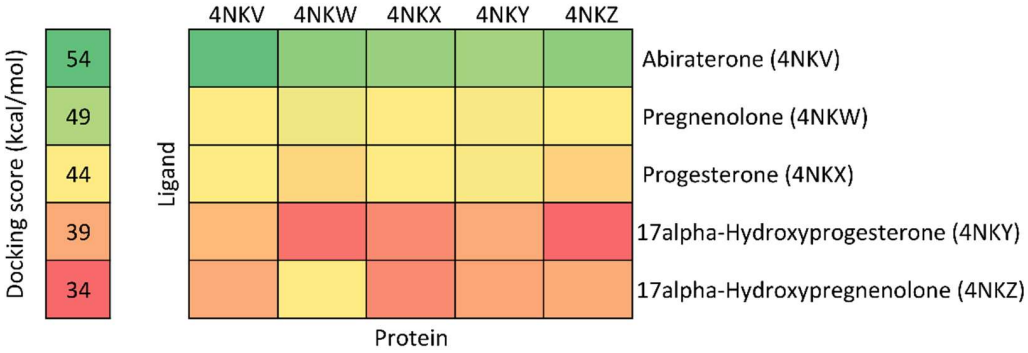

Figure 7. Heat map showing the docking scores for cross-docking of substrates into the experimentally determined CYP17A1 structures.

Initially, we docked all 20 compounds to the five CYP17A1 structures, but since we observed nearly identical results for the five structures, we only describe the results for docking into the 4NKV structure.

The docking of **2** yields poses with the nitrogen lone pair on the benzimidazole ring pointing towards the Fe atom in the heme moiety (Fe···N = 2.5 Å). The binding mode of **2** is similar to the binding mode we previously identified for the structurally related compound (**1d** in [14]) with the cyclohexane ring located in a shallow hydrophobic cavity formed by Leu105, Ile205, and Ile206, which confirms that the enzyme may accommodate different hydrophobic moieties in this part of the active site (Figure 8A). The benzimidazole ring is also located nearly identical to the benzimidazole ring in the CYP17A1–galeterone complex (PDB 3SWZ) [7]. We also observed hydrogen bonding between Asp298 and the amine situated between the aromatic and aliphatic rings (O···N = 3.1 Å). Hydrogen bonding to Asp298 has also been observed in the structure of (S)-orteronel [39] complexed with CYP17A1 (PDB 5IRQ) [40]. Recently, Fehl et al. designed inhibitors derived from abiraterone with polar substituents on the B ring in the steroid framework, which formed hydrogen bonds to Asp298 (PDB 6CHI and 6CIR) [41].

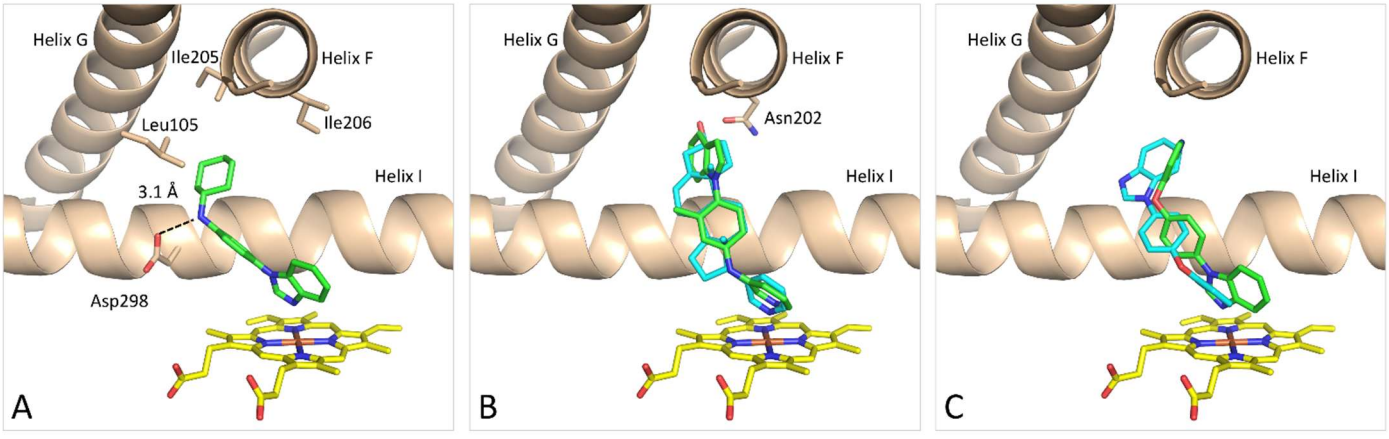

Figure 8. Preferred binding mode predicted by the GOLD docking program of compound **2** (green) (**A**), **20** (green) in comparison with abiraterone (cyan) (**B**) and **12** in two docking poses (pose #1 green and pose #2 cyan) (**C**). Coloring: protein is beige; heme is yellow; and all heteroatoms are colored based on type.

The docking of **20** showed, as expected, that the pyridine nitrogen coordinated to the Fe atom in the heme group with a Fe···N distance of 2.5 Å (Figure 8B). Comparison with

the X-ray structures of the CYP17A1–abiraterone complexes (PDB 3RUK and 4NKV) [7,38] revealed that the pyridine rings in the two structures overlap and that the benzene ring in **20** occupies the same space as the C ring of the steroid moiety of abiraterone. The methyl group in **20** was originally introduced to fill the hydrophobic cavity occupied by the B ring of abiraterone. It is possible that the position of the indole moiety relative to the benzene ring is caused by steric repulsion from that methyl group. Another possibility relies simply on a better fit to the upper part of the cavity. In any case, the indole moiety occupies the same space as the A ring and the C10 methyl group in the abiraterone structure. The docking of **20** also suggests that adding a polar substituent on the indole ring could make hydrogen bonding to Asn202, as observed in the CYP17A1–abiraterone complexes.

Compound **12** contains both a pyridine and a benzimidazole system and, accordingly, two possible binding modes are theoretically possible (Figure 8C). The docking revealed these with moieties coordinating to the Fe in the heme group with Fe···N = 2.4 Å (benzimidazole) and 2.5 Å (pyridine), respectively, referred to as pose #1 and pose #2. For compound **12**, pose #1 the benzimidazole system is located similarly to the benzimidazole system in the galeterone complex (3SWZ) [7], but in the opposite end of the compound, the pyridine is not close enough to make a contact to Asn202 as observed for galeterone. There are distinct differences in the orientation of the pyridine ring in pose #2 and in the abiraterone complexes 3RUK and 4NVK relative to the heme system. The 4-substituted pyridine ring requires more space above the heme group to adopt an ideal orthogonal orientation [42]. It suggests that the 3-substituted pyridine is the preferred moiety relative to the 2- and 4-substituted systems.

To investigate the stability of the protein–ligand complexes described above, we have subjected these to molecular dynamics (MD) simulations without any constraints, allowing both the protein and the ligands to move freely. The Fe···N distance is an important parameter when considering if the docking poses were realistic. The results of these short MD simulations revealed that all four complexes appeared to be stable (Figure 9). Although the Fe···N distance for **20** displayed extreme values for six frames around 80 ns, where the pyridine ring changed orientation and lost contact with the Fe atom, the original distance on approx. 2.4 Å was quickly re-established. The average Fe···N (benzimidazole) distances are 2.42 ± 0.11 Å and 2.44 ± 0.1 Å for compound **2** and **12**, respectively. The corresponding Fe···N (pyridine) distances are 2.42 ± 0.13 Å and 2.43 ± 0.11 Å for **12** and **20** (excluding the six frames around 80 ns).

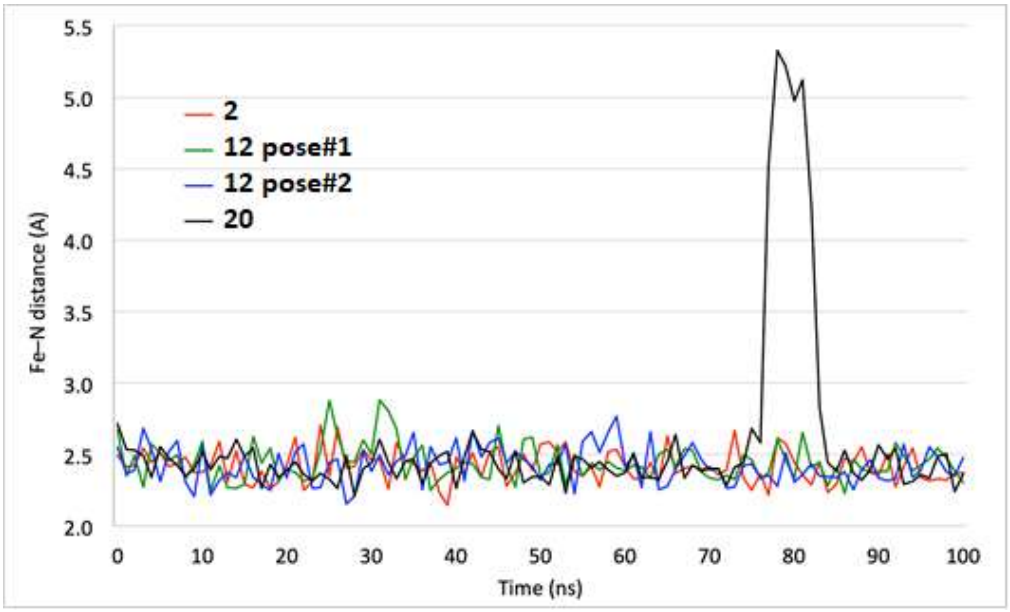

Figure 9. Fe···N distances for the four CYP17A1–ligand complexes during the 100 ns molecular dynamics simulations.

The MD simulations confirm that the docking complexes represent low energy structures and may represent likely binding modes for the compounds, which we hope to confirm by ongoing efforts to get crystals and subsequently determine X-ray structures of some of our compounds. Computational analyses indicate that benzimidazole and pyridine fragments are important pharmacophores when considering the design of CYP17A1 binders. In the case of the pyridyl fragment, the preferred substitution pattern is 3-pyridyl over 4-pyridyl, with 2-pyridyl being unable to coordinate the Fe atom in heme effectively.

4. Conclusions

A series of compounds based on benzimidazole and indole scaffolds were synthesized and evaluated as inhibitors of CYP17A1 hydroxylase and lyase activity. Selected compounds were further assessed as inhibitors of CYP3A4 and P450 oxidoreductase (POR). Three compounds, **2**, **12,** and **20**, were found to be potent inhibitors of CYP17A1 hydroxylase activity, with an IC_{50} of 1.2, 3.4 and 2.6 μM, respectively. Although they were not able to inhibit the CYP17A1 lyase catalyzed reaction, they were nevertheless selective towards CYP17A1, as indicated by their low influence on CYP3A4 and POR. Compound **2** displayed inhibitory potency comparable to the clinically used compound abiraterone in the CYP17A1 hydroxylase assay. Compounds **1**, **9**, **14** and **16** were cytotoxic towards PC3 cancer cell lines. However, as these compounds were much less potent in the CYP17A1 hydroxylase assay, the cytotoxicity is tentatively mediated through another mechanism of action, not further explored in this study. Finally, analysis of the SAR of the new compounds provided valuable information for further design of this class of compounds.

Supplementary Materials: The following supporting information can be downloaded at: https://www.mdpi.com/article/10.3390/biom12020165/s1.

Author Contributions: Conceptualization, T.M.W.; Formal analysis, T.M.W., A.V.P., F.S.J., K.L.A. and F.B.; Funding acquisition, T.M.W.; Investigation, T.M.W., O.R., K.S., M.N.R.V., A.V.P., F.S.J., F.S.A., K.L.A. and F.B.; Methodology, T.M.W., O.R., K.S., M.N.R.V., A.V.P., F.S.J., F.S.A., K.L.A. and F.B.; Writing—original draft, T.M.W.; Writing—review and editing, T.M.W., A.V.P., F.S.J., K.L.A. and F.B. All authors have read and agreed to the published version of the manuscript.

Funding: This research was funded by the Narodowe Centrum Nauki grant Sonata 16 2020/39/D/NZ7/00572 (T.M.W.). K.S. and M.N.R.V. are funded by Swiss Government Excellence Scholarships, Grant numbers 2019.0385 and 2020.0557.

Institutional Review Board Statement: Not applicable.

Informed Consent Statement: Not applicable.

Data Availability Statement: The data presented in this study are available in the Supplementary Materials here and are also available on request from the corresponding author.

Acknowledgments: We thank Emily Scott and her team for the initial work and for her support. We thank Scott Lowe for proofreading the manuscript.

Conflicts of Interest: The authors declare no conflict of interest. The funders had no role in the design of the study; in the collection, analyses, or interpretation of data; in the writing of the manuscript, or in the decision to publish the results.

References

1. Siegel, R.L.; Miller, K.D.; Fuchs, H.E.; Jemal, A. Cancer Statistics, 2021. *CA Cancer J. Clin.* **2021**, *71*, 7–33. [CrossRef] [PubMed]
2. Velho, P.I.; Anna, P.T.S.; da Silva, R.F.P.; Ferreira, R.D.P.; Venero, F.C. The development of apalutamide for the treatment of prostate cancer. *Expert Opin. Drug Discov.* **2021**, *16*, 217–226. [CrossRef]
3. Risdon, E.N.; Chau, C.H.; Price, D.K.; Sartor, O.; Figg, W.D. PARP Inhibitors and Prostate Cancer: To Infinity and Beyond BRCA. *Oncologist* **2021**, *26*, e115–e129. [CrossRef] [PubMed]
4. Rana, Z.; Diermeier, S.; Hanif, M.; Rosengren, R.J. Understanding Failure and Improving Treatment Using HDAC Inhibitors for Prostate Cancer. *Biomedicines* **2020**, *8*, 22. [CrossRef] [PubMed]
5. Rathi, N.; McFarland, T.R.; Nussenzveig, R.; Agarwal, N.; Swami, U. Evolving Role of Immunotherapy in Metastatic Castration Refractory Prostate Cancer. *Drugs* **2021**, *81*, 191–206. [CrossRef] [PubMed]

6. O'Sullivan, S.E.; Kaczocha, M. FABP5 as a novel molecular target in prostate cancer. *Drug Discov. Today* **2020**, *25*, 2056–2061. [CrossRef]
7. DeVore, N.M.; Scott, E.E. Structures of cytochrome P450 17A1 with prostate cancer drugs abiraterone and TOK-001. *Nature* **2012**, *482*, 116–119. [CrossRef] [PubMed]
8. Nakajin, S.; Hall, P.F.; Onoda, M. Testicular microsomal cytochrome P-450 for C21 steroid side chain cleavage. Spectral and binding studies. *J. Biol. Chem.* **1981**, *256*, 6134–6139. [CrossRef]
9. Chung, B.C.; Picado-Leonard, J.; Haniu, M.; Bienkowski, M.; Hall, P.F.; Shively, J.E.; Miller, W.L. Cytochrome P450c17 (steroid 17 alpha-hydroxylase/17,20 lyase): Cloning of human adrenal and testis cDNAs indicates the same gene is expressed in both tissues. *Proc. Natl. Acad. Sci. USA* **1987**, *84*, 407–411. [CrossRef]
10. Nakajin, S.; Shively, J.E.; Yuan, P.M.; Hall, P.F. Microsomal cytochrome P-450 from neonatal pig testis: Two enzymatic activities (17 alpha-hydroxylase and c17,20-lyase) associated with one protein. *Biochemistry* **1981**, *20*, 4037–4042. [CrossRef]
11. Yin, L.; Hu, Q. CYP17 inhibitors—abiraterone, C17,20-lyase inhibitors and multi-targeting agents. *Nat. Rev. Urol.* **2013**, *11*, 32–42. [CrossRef]
12. Bird, I.M.; Abbott, D.H. The hunt for a selective 17,20 lyase inhibitor; learning lessons from nature. *J. Steroid Biochem. Mol. Biol.* **2016**, *163*, 136–146. [CrossRef]
13. Flück, C.E.; Meyer-Boni, M.; Pandey, A.V.; Kempna, P.; Miller, W.L.; Schoenle, E.J.; Biason-Lauber, A. Why boys will be boys: Two pathways of fetal testicular androgen biosynthesis are needed for male sexual differentiation. *Am. J. Hum. Genet.* **2011**, *89*, 201–218. [CrossRef]
14. Wróbel, T.M.; Rogova, O.; Andersen, K.L.; Yadav, R.; Brixius-Anderko, S.; Scott, E.E.; Olsen, L.; Jørgensen, F.S.; Björkling, F. Discovery of Novel Non-Steroidal Cytochrome P450 17A1 Inhibitors as Potential Prostate Cancer Agents. *Int. J. Mol. Sci.* **2020**, *21*, 4868. [CrossRef] [PubMed]
15. Parween, S.; Fernandez-Cancio, M.; Benito-Sanz, S.; Camats, N.; Velazquez, M.N.R.; Lopez-Siguero, J.P.; Udhane, S.S.; Kagawa, N.; Fluck, C.E.; Audi, L.; et al. Molecular Basis of CYP19A1 Deficiency in a 46,XX Patient With R550W Mutation in POR: Expanding the PORD Phenotype. *J. Clin. Endocrinol. Metab.* **2020**, *105*, e1272–e1290. [CrossRef] [PubMed]
16. Udhane, S.S.; Dick, B.; Hu, Q.; Hartmann, R.W.; Pandey, A.V. Specificity of anti-prostate cancer CYP17A1 inhibitors on androgen biosynthesis. *Biochem. Biophys. Res. Commun.* **2016**, *477*, 1005–1010. [CrossRef]
17. Zhang, L.H.; Rodriguez, H.; Ohno, S.; Miller, W.L. Serine phosphorylation of human P450c17 increases 17,20-lyase activity: Implications for adrenarche and the polycystic ovary syndrome. *Proc. Natl. Acad. Sci. USA* **1995**, *92*, 10619–10623. [CrossRef]
18. Pandey, A.V.; Miller, W.L. Regulation of 17,20 lyase activity by cytochrome b5 and by serine phosphorylation of P450c17. *J. Biol. Chem.* **2005**, *280*, 13265–13271. [CrossRef]
19. Lephart, E.D.; Simpson, E.R. Assay of aromatase activity. *Methods Enzymol.* **1991**, *206*, 477–483. [PubMed]
20. Flück, C.E.; Mullis, P.E.; Pandey, A.V. Reduction in hepatic drug metabolizing CYP3A4 activities caused by P450 oxidoreductase mutations identified in patients with disordered steroid metabolism. *Biochem. Biophys. Res. Commun.* **2010**, *401*, 149–153. [CrossRef]
21. Udhane, S.S.; Parween, S.; Kagawa, N.; Pandey, A.V. Altered CYP19A1 and CYP3A4 Activities Due to Mutations A115V, T142A, Q153R and P284L in the Human P450 Oxidoreductase. *Front. Pharmacol.* **2017**, *8*, 580. [CrossRef] [PubMed]
22. Jensen, S.B.; Thodberg, S.; Parween, S.; Moses, M.E.; Hansen, C.C.; Thomsen, J.; Sletfjerding, M.B.; Knudsen, C.; Del Giudice, R.; Lund, P.M.; et al. Biased cytochrome P450-mediated metabolism via small-molecule ligands binding P450 oxidoreductase. *Nat. Commun.* **2021**, *12*, 2260. [CrossRef] [PubMed]
23. Sastry, G.M.; Adzhigirey, M.; Day, T.; Annabhimoju, R.; Sherman, W. Protein and ligand preparation: Parameters, protocols, and influence on virtual screening enrichments. *J. Comput. Aided Mol. Des.* **2013**, *27*, 221–234. [CrossRef] [PubMed]
24. Berman, H.M.; Battistuz, T.; Bhat, T.N.; Bluhm, W.F.; Bourne, P.E.; Burkhardt, K.; Feng, Z.; Gilliland, G.L.; Iype, L.; Jain, S.; et al. The Protein Data Bank. *Acta Crystallogr. D Biol. Crystallogr.* **2002**, *58*, 899–907. [CrossRef] [PubMed]
25. Jones, G.; Willett, P.; Glen, R.C.; Leach, A.R.; Taylor, R. Development and validation of a genetic algorithm for flexible docking. *J. Mol. Biol.* **1997**, *267*, 727–748. [CrossRef] [PubMed]
26. Verdonk, M.L.; Cole, J.C.; Hartshorn, M.J.; Murray, C.W.; Taylor, R.D. Improved protein-ligand docking using GOLD. *Proteins* **2003**, *52*, 609–623. [CrossRef] [PubMed]
27. Kirton, S.B.; Murray, C.W.; Verdonk, M.L.; Taylor, R.D. Prediction of binding modes for ligands in the cytochromes P450 and other heme-containing proteins. *Proteins* **2005**, *58*, 836–844. [CrossRef]
28. Lu, C.; Wu, C.; Ghoreishi, D.; Chen, W.; Wang, L.; Damm, W.; Ross, G.A.; Dahlgren, M.K.; Russell, E.; Von Bargen, C.D.; et al. OPLS4: Improving Force Field Accuracy on Challenging Regimes of Chemical Space. *J. Chem. Theory Comput.* **2021**, *17*, 4291–4300. [CrossRef] [PubMed]
29. Wright, J.B. The Chemistry of the Benzimidazoles. *Chem. Rev.* **1951**, *48*, 397–541. [CrossRef]
30. Lovering, F.; Bikker, J.; Humblet, C. Escape from Flatland: Increasing Saturation as an Approach to Improving Clinical Success. *J. Med. Chem.* **2009**, *52*, 6752–6756. [CrossRef]
31. Leung, C.S.; Leung, S.S.F.; Tirado-Rives, J.; Jorgensen, W.L. Methyl Effects on Protein–Ligand Binding. *J. Med. Chem.* **2012**, *55*, 4489–4500. [CrossRef] [PubMed]
32. Barreiro, E.J.; Kümmerle, A.E.; Fraga, C.A.M. The Methylation Effect in Medicinal Chemistry. *Chem. Rev.* **2011**, *111*, 5215–5246. [CrossRef] [PubMed]

33. Klein, K.; Zanger, U.M. Pharmacogenomics of Cytochrome P450 3A4: Recent Progress Toward the "Missing Heritability" Problem. *Front. Genet.* **2013**, *4*, 12. [CrossRef]
34. Velazquez, M.N.R.; Parween, S.; Udhane, S.S.; Pandey, A.V. Variability in human drug metabolizing cytochrome P450 CYP2C9, CYP2C19 and CYP3A5 activities caused by genetic variations in cytochrome P450 oxidoreductase. *Biochem. Biophys. Res. Commun.* **2019**, *515*, 133–138. [CrossRef] [PubMed]
35. Pandey, A.V.; Flück, C.E. NADPH P450 oxidoreductase: Structure, function, and pathology of diseases. *Pharmacol. Ther.* **2013**, *138*, 229–254. [CrossRef]
36. Cunningham, D.; You, Z. In vitro and in vivo model systems used in prostate cancer research. *J. Biol. Methods* **2015**, *2*, e17. [CrossRef]
37. Hafner, M.; Niepel, M.; Chung, M.; Sorger, P.K. Growth rate inhibition metrics correct for confounders in measuring sensitivity to cancer drugs. *Nat. Methods* **2016**, *13*, 521–527. [CrossRef]
38. Petrunak, E.M.; DeVore, N.M.; Porubsky, P.R.; Scott, E.E. Structures of Human Steroidogenic Cytochrome P450 17A1 with Substrates. *J. Biol. Chem.* **2014**, *289*, 32952–32964. [CrossRef]
39. Yamaoka, M.; Hara, T.; Hitaka, T.; Kaku, T.; Takeuchi, T.; Takahashi, J.; Asahi, S.; Miki, H.; Tasaka, A.; Kusaka, M. Orteronel (TAK-700), a novel non-steroidal 17,20-lyase inhibitor: Effects on steroid synthesis in human and monkey adrenal cells and serum steroid levels in cynomolgus monkeys. *J. Steroid Biochem. Mol. Biol.* **2012**, *129*, 115–128. [CrossRef]
40. Petrunak, E.M.; Rogers, S.A.; Aubé, J.; Scott, E.E. Structural and Functional Evaluation of Clinically Relevant Inhibitors of Steroidogenic Cytochrome P450 17A1. *Drug Metab. Dispos.* **2017**, *45*, 635–645. [CrossRef]
41. Fehl, C.; Vogt, C.D.; Yadav, R.; Li, K.; Scott, E.E.; Aubé, J. Structure-Based Design of Inhibitors with Improved Selectivity for Steroidogenic Cytochrome P450 17A1 over Cytochrome P450 21A2. *J. Med. Chem.* **2018**, *61*, 4946–4960. [CrossRef] [PubMed]
42. Bonomo, S.; Hansen, C.H.; Petrunak, E.M.; Scott, E.E.; Styrishave, B.; Jørgensen, F.S.; Olsen, L. Promising Tools in Prostate Cancer Research: Selective Non-Steroidal Cytochrome P450 17A1 Inhibitors. *Sci. Rep.* **2016**, *6*, 29468. [CrossRef] [PubMed]

Section B: Exploring the Potential of Sulfur Moieties in Compounds Inhibiting Steroidogenesis

Status: Published

My Contributions in the paper:

In vitro experiments:

- Maintenance of cell culture: NCI H295R cell line and LNCaP cell line
- Cell-based enzyme assays - CYP17A1 17α-Hydroxylase activity, CYP17A1 17,20 Lyase activity.
- Treatment of cells and preparation of media for steroid profiling by LC/MS
- Cell viability assays

Writing:
Section 2.4 (Biology): Chemicals, Cell lines and culture, Cell viability assays, CYP17A1 and CYP21A2 enzyme activity, Statistical analysis

Figures:

- Figure 3: Inhibition of CYP17A1 hydroxylase activity (A) and lyase activity (B).
- Figure 5: Inhibition of CYP21A2, CYP3A4, POR
- Figure 8: LNCaP cell viability in presence of compounds 3a-d and 4a-d.

Statistical analysis for enzyme assays and generating graphs for Figures.

biomolecules

MDPI

Article

Exploring the Potential of Sulfur Moieties in Compounds Inhibiting Steroidogenesis

Tomasz M. Wróbel [1,2,*], Katyayani Sharma [3,4,5], Iole Mannella [6], Simonetta Oliaro-Bosso [6], Patrycja Nieckarz [1], Therina Du Toit [3,4], Clarissa Daniela Voegel [4,7], Maria Natalia Rojas Velazquez [3,4,5], Jibira Yakubu [3,4,5], Anna Matveeva [3,4,5], Søren Therkelsen [2], Flemming Steen Jørgensen [2], Amit V. Pandey [3,4], Agnese C. Pippione [6], Marco L. Lolli [6], Donatella Boschi [6] and Fredrik Björkling [2]

1 Department of Synthesis and Chemical Technology of Pharmaceutical Substances, Medical University of Lublin, Chodźki 4a, 20093 Lublin, Poland
2 Department of Drug Design and Pharmacology, University of Copenhagen, Jagtvej 160, 2100 Copenhagen, Denmark
3 Department of Pediatrics, Division of Endocrinology, Diabetology and Metabolism, University Children's Hospital, University of Bern, 3010 Bern, Switzerland
4 Translational Hormone Research Program, Department of Biomedical Research, University of Bern, 3010 Bern, Switzerland
5 Graduate School for Cellular and Biomedical Sciences, University of Bern, 3012 Bern, Switzerland
6 Department of Drug Science and Technology, University of Turin, 10125 Turin, Italy
7 Department of Nephrology and Hypertension, University Hospital Inselspital, University of Bern, 3010 Bern, Switzerland
* Correspondence: tomasz.wrobel@umlub.pl; Tel.: +48-81-448-7273

Abstract: This study reports on the synthesis and evaluation of novel compounds replacing the nitrogen-containing heterocyclic ring on the chemical backbone structure of cytochrome P450 17α-hydroxylase/12,20-lyase (CYP17A1) inhibitors with a phenyl bearing a sulfur-based substituent. Initial screening revealed compounds with marked inhibition of CYP17A1 activity. The selectivity of compounds was thereafter determined against cytochrome P450 21-hydroxylase, cytochrome P450 3A4, and cytochrome P450 oxidoreductase. Additionally, the compounds showed weak inhibitory activity against aldo-keto reductase 1C3 (AKR1C3). The compounds' impact on steroid hormone levels was also assessed, with some notable modulatory effects observed. This work paves the way for developing more potent dual inhibitors specifically targeting CYP17A1 and AKR1C3.

Keywords: CYP17A1; AKR1C3; prostate cancer; enzyme inhibition

Citation: Wróbel, T.M.; Sharma, K.; Mannella, I.; Oliaro-Bosso, S.; Nieckarz, P.; Du Toit, T.; Voegel, C.D.; Rojas Velazquez, M.N.; Yakubu, J.; Matveeva, A.; et al. Exploring the Potential of Sulfur Moieties in Compounds Inhibiting Steroidogenesis. *Biomolecules* **2023**, *13*, 1349. https://doi.org/10.3390/biom13091349

Academic Editor: Vladimir N. Uversky

Received: 31 July 2023
Revised: 29 August 2023
Accepted: 31 August 2023
Published: 5 September 2023

1. Introduction

Cancer remains a major health problem and is the second leading cause of death. Of particular concern is the rising incidence of prostate cancer (PCa) from 2014 to 2019 after two decades of decline [1]. Despite significant advancements in treatment options for PCa, there is still an urgent need for the development of more effective therapies. Advanced disease can progress into castration-resistant prostate cancer (CRPC) which is characterized by poor prognosis [2]. The androgen receptor (AR) signaling pathway plays a crucial role in the development and progression of PCa [3]. Androgens, such as testosterone (T) and dihydrotestosterone (DHT), bind to the AR and activate downstream signaling pathways, leading to the growth and survival of PCa cells. Therefore, targeting the AR signaling pathway has been the focus of therapeutic strategies for PCa. Among the potential targets in prostate cancer, cytochrome P450 17α-hydroxylase/17,20-lyase (CYP17A1) is a key enzyme involved in the biosynthesis of androgens. It catalyzes two essential reactions in androgen biosynthesis: a 17α-hydroxylation and a 17,20-lyase reaction (Figure 1). The inhibition of CYP17A1 results in decreased androgen production and has emerged as a promising strategy for the treatment of PCa (Figure 2) [4]. CYP17A1 inhibitors can be

classified into two categories: steroidal represented by abiraterone, and nonsteroidal [5]. Abiraterone is the only CYP17A1 inhibitor that has been approved as a drug for clinical use in the treatment of CRPC. However, the development of resistance to abiraterone occurs with time, and, therefore, alternative CYP17A1 inhibitors might circumvent this issue. Nonsteroidal inhibitors, such as seviteronel or orteronel, have shown promising results in preclinical studies [6,7]. Unfortunately, none of these compounds have reached clinical practice [8].

PCa progression and aggressiveness have also been associated with elevated levels of the aldo-keto reductase 1C3 (AKR1C3) enzyme, another important enzyme in the steroidogenesic pathway to potent androgens (Figure 1) [9,10]. Recent studies have shown that PCa cells grown in the presence of abiraterone acquire resistance to this drug through increasing intracrine androgen synthesis and overexpressing *AKR1C3*. This discovery provided a preclinical proof-of-principle for investigating the combination of targeting AKR1C3 drugs (e.g., indomethacin) with abiraterone or other cancer chemotherapeutics for CRPC treatment [11,12].

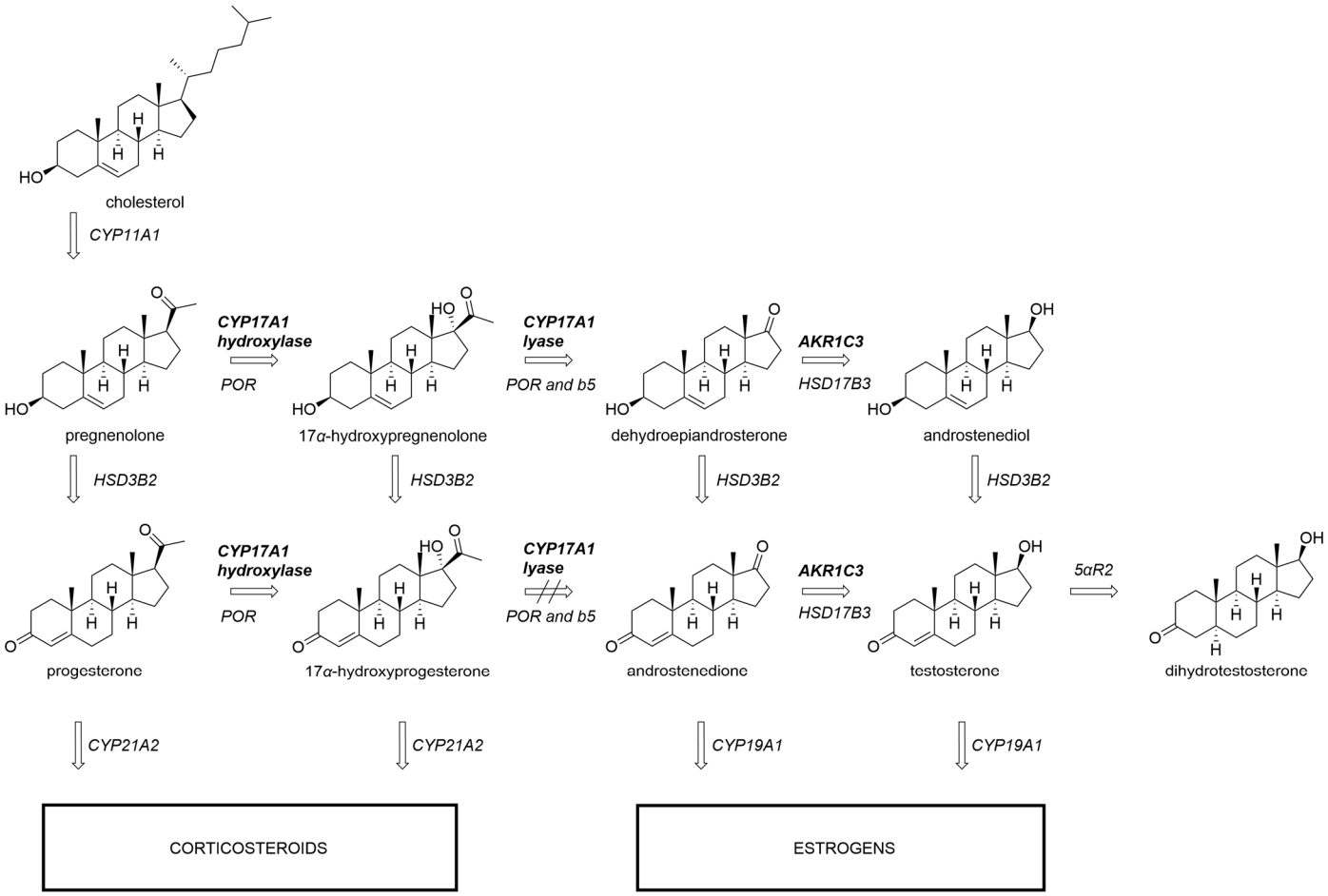

Figure 1. Androgen production depends on CYP17A1 17α-hydroxylase and 17,20-lyase activity. While the transformation of 17α-hydroxypregnenolone to dehydroepiandrosterone can be readily catalyzed by CYP17A1, the analogous reaction with 17α-hydroxyprogesterone is inefficient in humans. AKR1C3 participates in further downstream transformations towards testosterone. CYP11A1, CYP17A1, CYP19A1, CYP21A2, cytochrome P450 enzymes; AKR1C3, aldo-keto reductase family 1 member C3; 5αR2, 5α-reductase type 2; POR, cytochrome P450 oxidoreductase; b5, cytochrome b5.

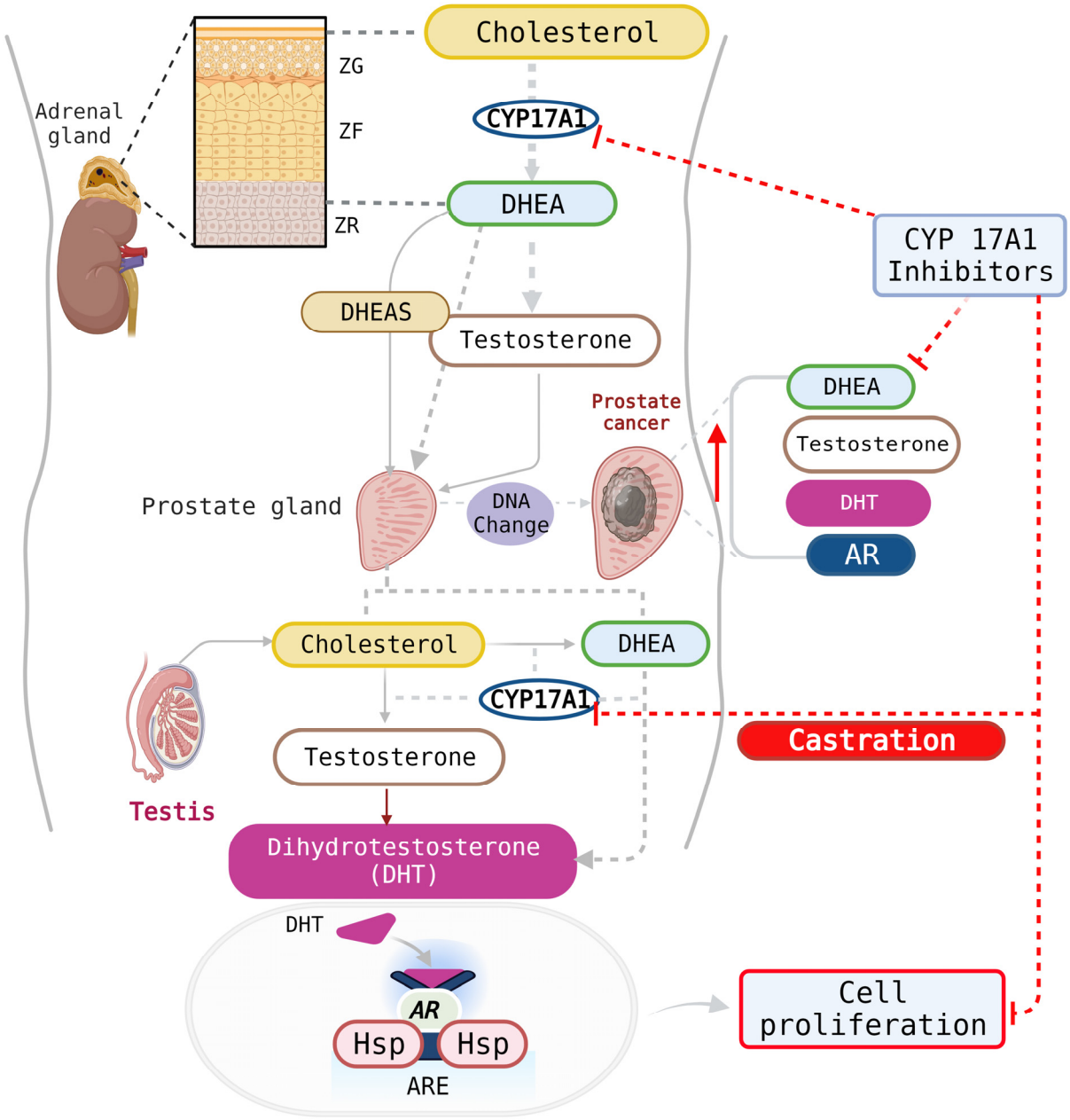

Figure 2. CYP17A1 inhibitors can impact androgen production in the testes and the adrenal glands. Additionally, PCa cells express high levels of the AR and can produce their own androgens in patients who have been otherwise castrated. AR, androgen receptor; Hsp, heat-shock proteins, ARE, androgen response element; DHEA, dehydroepiandrosterone; DHEAS, dehydroepiandrosterone-sulfate; DHT, dihydrotestosterone; ZG, zona glomerulosa; ZF, zona fasciculata; ZR, zona reticularis. Created with Biorender.com (accessed on 30 August 2023).

The common structural feature of nearly all CYP17A1 inhibitors is the presence of a sp^2-hybridized nitrogen atom in a heteroaromatic system. The lone pair on the nitrogen coordinates with the iron in the heme prosthetic group, thus blocking enzyme activity. Pyridine and imidazole moieties have been used extensively for that purpose because they offer the most favorable binding energy based on density functional theory (DFT) calculations [13,14]. Other nitrogen-bearing heterocycles have found their way into the design of many CYP17A1 inhibitors. However, they are less common. While the field appears to be biased towards the utilization of the nitrogen, other atoms can be potentially used for the purpose of coordination with the heme iron. For instance, curcumin and

theaflavin have been described as capable of CYP17A1 inhibition [15,16]. Both compounds do not contain nitrogen atoms and can only coordinate to the heme via oxygen atoms. When curcumin was docked to the PDB ID: 3RUK model, it exhibited a similar binding pose to steroid substrates, with its phenolic oxygen positioned 2.4 Å away from the heme iron [15,16]. There are also examples of the sulfur atom interacting with the heme. The bacterial CYP BM3 (CYP102A1) mutant M11 structure displays the anionic form of the sulfhydryl group in dithiothreitol coordinating to the heme with a 2.3 Å Fe-S distance [17]. A few nitric oxide synthase inhibitors based on thioethers have demonstrated type II binding to the heme group, with some sulfur atoms in these inhibitors coordinating to the heme iron with Fe-S distances of approximately 2.7 Å, as observed in X-ray crystallography [18,19].

Except for limited efforts of introducing sulfur-containing moieties into a steroidal CYP17A1 inhibitor, to the best of our knowledge, there have been no similar attempts to design non-steroidal inhibitors [20]. Therefore, we were interested in probing potential interactions between sulfenyl and sulfinyl groups with the heme iron of CYP17A1. In the current work, we present the design, synthesis, and evaluation of sulfur-based CYP17A1 non-steroidal inhibitors.

2. Materials and Methods

2.1. Chemistry

All reagents were obtained from commercial sources and used as received without additional purification. NMR spectra were acquired using a Bruker AVANCE III 600 MHz spectrometer equipped with a BBO broadband probe and referenced to either TMS or residual solvent peak. HRMS spectra were recorded using a Bruker microTOF-Q II spectrometer. HPLC analysis was run on a Thermo-Fisher Ultimate 3000 RS chromatograph using a generic gradient of 20% to 100% acetonitrile in water on a C18 column.

2.2. General Procedure to Obtain Compounds **3a** *to* **3d**

A dry vial was evacuated/backfilled with argon three times and charged with 3-bromothioanisole **2a** or 4-bromothioanisole **2b** (223 mg, 1.10 mmol), t-BuXPhos Pd G3 (40 mg, 0.05 mmol), t-BuXPhos (21 mg, 0.05 mmol), benzimidazole **1a** or indole **1b** (246 mg, 1 mmol), and t-BuONa (240 mg, 2.5 mmol). For indole derivatives, the reaction was conducted in t-BuOH (3 mL) and in the case of benzimidazole derivatives, THF (2 mL) was used. The reaction was microwaved at 100 °C for 1 h. It was then diluted with EtOAc (25 mL) and filtered through a silica plug. The crude product was purified via flash chromatography on silica as indicated below.

2.2.1. *N*-(4-(1H-Benzo[d]imidazol-1-yl)phenyl)-3-(methylthio)aniline (**3a**)

Elution with EtOAc/heptane yielded orange oil (81 mg, 24%) which can be triturated with EtOAc and recrystallized from MeOH to obtain solid material. ^{1}H NMR (600 MHz, DMSO) δ 8.54 (s, 1H), 8.46 (s, 1H), 7.79–7.74 (m, 1H), 7.56 (dt, *J* = 8.1, 0.9 Hz, 1H), 7.54–7.50 (m, 2H), 7.34–7.25 (m, 4H), 7.22 (t, *J* = 7.9 Hz, 1H), 7.00 (t, *J* = 2.0 Hz, 1H), 6.95 (ddd, *J* = 8.1, 2.3, 0.9 Hz, 1H), 6.78 (ddd, *J* = 7.8, 1.8, 0.9 Hz, 1H), 2.47 (s, 3H). ^{13}C NMR (151 MHz, DMSO) δ 143.5, 143.3, 143.2, 142.9, 139.0, 133.5, 129.7, 127.7, 125.1, 123.1, 122.1, 119.7, 117.8, 117.4, 114.3, 113.6, 110.5, 14.6. HRMS (ESI) $[M+H]^+$ calc. 332.1216, exp. 332.1216.

2.2.2. *N*-(4-(1H-Benzo[d]imidazol-1-yl)phenyl)-4-(methylthio)aniline (**3b**)

Elution with EtOAc/heptane and trituration with ether/hexane yielded a beige solid (19 mg, 6%) which can be further recrystallized from EtOAc/hexane. ^{1}H NMR (600 MHz, DMSO) δ 8.50 (s, 1H), 8.45 (s, 1H), 7.78–7.74 (m, 1H), 7.56–7.53 (m, 1H), 7.51–7.47 (m, 2H), 7.33–7.28 (m, 2H), 7.28–7.21 (m, 5H), 7.16–7.11 (m, 2H), 2.44 (s, 3H). ^{13}C NMR (151 MHz, DMSO) δ 143.5, 143.3, 140.6, 133.6, 128.9, 128.0, 127.3, 125.1, 123.1, 122.0, 119.7, 118.3, 116.8, 110.5, 16.5 HRMS (ESI) $[M+H]^+$ calc. 332.1216, exp. 332.1220.

2.2.3. *N*-(4-(1H-Indol-1-yl)phenyl)-3-(methylthio)aniline (**3c**)

Elution with EtOAc/heptane yielded red oil (72 mg, 22%) which can be recrystallized from MeOH by slow evaporation to obtain solid material. ^{1}H NMR (600 MHz, $CDCl_3$) δ 7.67 (ddd, *J* = 7.8, 1.3, 0.7 Hz, 1H), 7.49 (dt, *J* = 8.2, 0.9 Hz, 1H), 7.34–7.29 (m, 2H), 7.25 (d, *J* = 3.2 Hz, 1H), 7.22–7.12 (m, 3H), 7.12–7.07 (m, 2H), 6.95 (t, *J* = 2.0 Hz, 1H), 6.82 (dt, *J* = 7.8, 2.0 Hz, 2H), 6.64 (dt, *J* = 3.2, 0.7 Hz, 1H), 5.73 (s, 1H), 2.43 (d, *J* = 0.6 Hz, 3H). ^{13}C NMR (151 MHz, $CDCl_3$) δ 143.4, 141.5, 139.9, 136.3, 133.2, 129.9, 129.1, 128.3, 125.8, 122.3, 121.2, 120.3, 119.3, 118.9, 115.7, 114.8, 110.6, 103.1, 15.8. HRMS (ESI) $[M+H]^+$ calc. 331.1263, exp. 331.1269.

2.2.4. *N*-(4-(1H-Indol-1-yl)phenyl)-4-(methylthio)aniline (**3d**)

Elution with EtOAc/heptane yielded clear oil (13 mg, 4%) which can be recrystallized from MeOH to obtain solid material. ^{1}H NMR (600 MHz, $CDCl_3$) δ 7.68 (dt, *J* = 7.8, 1.0 Hz, 1H), 7.49 (dd, *J* = 8.3, 1.0 Hz, 1H), 7.37–7.33 (m, 2H), 7.30–7.24 (m, 3H), 7.21 (ddd, *J* = 8.3, 7.0, 1.3 Hz, 1H), 7.17–7.11 (m, 3H), 7.07 (d, *J* = 8.1 Hz, 2H), 6.65 (dd, *J* = 3.2, 0.8 Hz, 1H), 5.96 (s, 0H), 2.47 (s, 3H). ^{13}C NMR (151 MHz, $CDCl_3$) δ 141.7, 140.6, 136.2, 133.0, 130.1, 129.6, 129.0, 128.2, 125.8, 122.1, 121.0, 120.1, 119.1, 118.2, 110.4, 102.9, 17.6. HRMS (ESI) $[M+H]^+$ calc. 331.1263, exp. 331.1270.

2.3. General Procedure to Obtain Compounds **4a** *to* **4d**

To a stirred solution of the sulfide (1 eq) in phenol (12 eq) at 40 °C, 30% aq. H_2O_2 (2 eq) was added and the reaction was stirred for 5 min. The excess H_2O_2 was quenched with saturated aq. Na_2SO_3 solution, and the phenol was neutralized with 10% aq. NaOH. The product was extracted three times with EtOAc, and the combined organics were washed with aq. NaOH and dried with $MgSO_4$. The crude product was purified using flash chromatography on silica, as described below.

2.3.1. *N*-(4-(1H-Benzo[d]imidazol-1-yl)phenyl)-3-(methylsulfinyl)aniline (**4a**)

Elution with EtOAc yielded a white solid (44mg, 39%). ^{1}H NMR (600 MHz, DMSO) δ 8.85 (s, 1H), 8.49 (s, 1H), 7.79–7.75 (m, 1H), 7.59–7.54 (m, 3H), 7.49–7.42 (m, 2H), 7.36–7.25 (m, 5H), 7.11 (ddd, *J* = 7.7, 1.7, 0.9 Hz, 1H), 2.76 (s, 3H). ^{13}C NMR (151 MHz, DMSO) δ 148.1, 144.5, 144.1, 143.8, 142.7, 134.0, 130.7, 128.9, 125.7, 123.7, 122.7, 120.3, 118.8, 118.6, 115.1, 111.1, 111.0, 43.8. HRMS (ESI) $[M+H]^+$ calc. 348.1165, exp. 348.1177.

2.3.2. *N*-(4-(1H-Benzo[d]imidazol-1-yl)phenyl)-4-(methylsulfinyl)aniline (**4b**)

Elution with MeOH/DCM yielded a white solid (30 mg, 15%). ^{1}H NMR (600 MHz, DMSO) δ 8.93 (s, 1H), 8.49 (s, 1H), 7.81–7.75 (m, 1H), 7.62–7.54 (m, 5H), 7.39–7.35 (m, 2H), 7.34–7.26 (m, 4H), 2.71 (s, 3H). ^{13}C NMR (151 MHz, DMSO) δ 146.2, 144.1, 143.8, 142.3, 136.0, 134.0, 129.2, 126.0, 125.6, 123.8, 122.7, 120.3, 119.2, 116.7, 111.1, 43.6. HRMS (ESI) $[M+H]^+$ calc. 348.1165, exp. 348.1178.

2.3.3. *N*-(4-(1H-Indol-1-yl)phenyl)-3-(methylsulfinyl)aniline (**4c**)

Elution with MeOH/DCM and trituration with ether yielded a solid product (37 mg, 16%). ^{1}H NMR (600 MHz, DMSO) δ 8.78 (s, 1H), 7.65 (d, *J* = 7.8 Hz, 1H), 7.57 (d, *J* = 3.2 Hz, 1H), 7.54–7.39 (m, 5H), 7.36–7.30 (m, 2H), 7.29–7.23 (m, 1H), 7.23–7.15 (m, 1H), 7.14–7.05 (m, 2H), 6.67 (d, *J* = 3.3 Hz, 1H), 2.75 (s, 3H). ^{13}C NMR (151 MHz, DMSO) δ 148.0, 144.9, 141.5, 135.9, 132.4, 130.7, 129.2, 129.1, 125.7, 122.5, 121.3, 120.4, 118.9, 118.4, 114.7, 110.8, 110.6, 103.3, 43.8. HRMS (ESI) $[M+H]^+$ calc. 347.1213, exp. 347.1208

2.3.4. *N*-(4-(1H-Indol-1-yl)phenyl)-4-(methylsulfinyl)aniline (**4d**)

Elution with EtOAc/heptane and trituration with ether yielded a pale yellow solid (30 mg, 32%). ^{1}H NMR (600 MHz, DMSO) δ 8.81 (s, 1H), 7.68–7.63 (m, 1H), 7.61–7.56 (m, 3H), 7.53–7.47 (m, 3H), 7.36–7.32 (m, 2H), 7.29–7.24 (m, 2H), 7.19 (ddd, *J* = 8.3, 7.0, 1.3 Hz, 1H), 7.12 (ddd, *J* = 7.9, 7.0, 1.0 Hz, 1H), 6.67 (dd, *J* = 3.3, 0.8 Hz, 1H), 2.71 (s, 3H). ^{13}C NMR

(151 MHz, DMSO) δ 146.6, 141.1, 135.8, 135.6, 132.8, 129.2, 129.1, 126.0, 125.6, 122.5, 121.3, 120.4, 119.6, 116.3, 110.8, 103.4, 43.6. HRMS (ESI) $[M+H]^+$ calc. 347.1213, exp. 347.1227

2.4. Biology

Chemicals: Trilostane was obtained from the extraction of the commercially available tablets Modrenal® (Bioenvision, New York, NY, USA). Abiraterone acetate was purchased from MedChemExpress®, Lucerna Chem AG (Lucerne, Switzerland). Radiolabeled substrates, Progesterone [4-^{14}C] (SA 55mCi/mmol; Conc. 0.1mCi/mL); 17α-Hydroxypregnenolone [21-^{3}H] (SA 15Ci/mmol; Conc. 1 mCi/mL) and 17α-Hydroxyprogesterone [1, 2, 6, 7-^{3}H] (SA 60 Ci/mmol; Conc. 1 mCi/mL) were obtained from American Radiolabeled Chemicals Inc. (St. Louis, MO, USA). Non-radiolabeled standard substrates, Progesterone, 17α-Hydroxypregnenolone, and 17α-Hydroxyprogesterone; 3-(4,5-Dimethyl-2-thiazolyl)-2,5-diphenyl-2H-tetrazolium bromide (MTT); Dimethyl sulfoxide (DMSO) and Dextran were purchased from Sigma-Aldrich® (St. Louis, MO, USA). Organic solvents such as Isooctane, Ethyl acetate, and Chloroform/Trichloromethane were acquired from Carl Roth® GmbH + Co. KG (Karlsruhe, Germany). Activated Charcoal was obtained from Merck AG (Darmstadt, Germany). For the mass spectrometric analysis of steroids, all LC-MS grade solvents were from Biosolve (Valkensaard, The Netherlands) and steroid standards were from obtained as certified reference solutions from Cerillant (Round Rock, TX, USA) or from Steraloids (Newport, RI, USA).

Cell lines and culture: The human adrenocortical carcinoma cell line NCI H295R was obtained from the American Type Culture Collection (ATCC® CRL2128™), Manassas, VA, USA [21]. Cells between passages 12 and 24 were cultivated in DMEM/Ham's F-12 medium (1:1 Mix) supplemented with L-glutamine and 15 mM HEPES (Gibco™, Thermo Fisher Scientific, Waltham, MA, USA) along with 5% Nu-Serum I; 0.1% insulin, transferrin, selenium in the form of ITS Premix (Corning™, Manassas, VA, USA) and 1% penicillin–streptomycin (Gibco™, Thermo Fisher Scientific, Waltham, MA, USA) at 37 °C in a humid atmosphere with a constant supply of 5% carbon dioxide to maintain the physiological Ph [22]. The Lymph Node Carcinoma of the Prostate (LNCaP) clone FGC cell line was purchased from American Type Culture Collection (ATCC) (ATCC®: CRL-1740™). The cell line was grown and maintained in vitro with Roswell Park Memorial Institute (RPMI) 1640 medium (Gibco™, Thermo Fisher Scientific, Waltham, MA, USA) supplemented with 10% fetal bovine serum (FBS) and 1% penicillin (100 U/mL)–streptomycin (100 µg/mL).

Cell Viability assays: To determine the effect of test compounds on the cellular activity of LNCaP and NCI H295R cells, a 3-(4,5-Dimethylthiazol-2-yl)-2,5-Diphenyltetrazolium Bromide (MTT)-based cell viability assay was performed. For the NCI-H295R cell assays, in a 96-well plate, about 30,000 cells per well were seeded with complete medium. The next day, the medium was replaced with fresh medium and 10 µM of test compounds were added. DMSO (less than 1% v/v) was used as a vehicle control. Abiraterone was used as a positive control. In total, 0.5mg/mL MTT reagent was added to the culture medium for another 4 h. After the incubation, the medium was entirely replaced with DMSO to dissolve the formazan crystals. After 20 min, absorbance was measured at 570nm (SpectraMax M2, Bucher Biotec, Basel, Switzerland). Percent viability was calculated with respect to the mean value of control samples.

The prostate cancer LNCAP cells were seeded in 96-well culture plates at a density of 0.5×10^4 cells per well and grown overnight at normoxic conditions with 5% CO_2, temperature at 37 °C, and humidity at 90%. After 24 h, the medium was changed, and dilutions of the drugs were added to the medium and the cells were incubated for another 24h or 48 h. After the 24 h or 48 h incubation of cells with the drugs, 20 µL of sterile filtered 5 mg/mL MTT in PBS solvent was added into each well, and the incubation was continued for another 2 h. After the incubation with MTT, the culture medium in each well was replaced with 200 µL of DMSO, and the plate was incubated for 20 min in the dark. The absorbances of the solution in each well were then measured at 570 nm. The percentage cell viability was calculated as previously described [15].

CYP17A1 and CYP21A2 Enzyme activity assay: According to our previously established protocols [15], NCI H295R cells were seeded overnight in a 12-well plate at a cell density of 0.5×10^6 cells per well. Overall, 10 µM of test compounds were added to respective wells containing fresh medium and were incubated for 4 h. Abiraterone and DMSO were used as the reference and control, respectively. To determine CYP17A1 hydroxylase activity, cells were treated with the substrate, [^{14}C]-Progesterone, at a concentration of 10,000 cpm/1 µM per well [23]. Trilostane was added prior to the addition of test compounds in order to block 3β-hydroxysteroid dehydrogenase activity [24]. Radiolabeled steroids were extracted from the media with ethyl acetate and isooctane (1:1 v/v) and separated through Thin Layer Chromatography (TLC) on a silica-gel-coated aluminum plate (Supelco® Analytics, Sigma Aldrich Chemie GmbH, Darmstadt, Germany). TLC spots were exposed to a phosphor screen and detected via autoradiography using Typhoon™ FLA-7000 PhosphorImager (GE Healthcare, Uppsala, Sweden). Radioactivity was quantified using ImageQuant™ TL analysis software (GE Healthcare Europe GmbH, Freiburg, Germany). Enzyme activity was calculated as a percentage of radioactivity incorporated into the product with respect to the total radioactivity. Similarly, CYP21A2 activity was evaluated using [^{3}H]-17α-Hydroxyprogesterone (~30,000 cpm/1 µM per well) as the substrate [25].

Using similar treatment conditions, [21-^{3}H]-17α-Hydroxypregnenolone (50,000 cpm/1 µM per well) was used as a substrate to analyze CYP17A1 lyase activity. Tritiated water release assays were performed to measure DHEA production [26]. Steroids in the media were precipitated using 5% activated charcoal/0.5% dextran solution. The enzyme activity was estimated with reference to the water-soluble tritiated by-product formed in an equimolar ratio with the corresponding steroid product. The radioactivity in the aqueous phase was measured via Liquid Scintillation counting (MicroBeta2® Plate Counter, PerkinElmer Inc. Waltham, MA, USA). The percent inhibition was calculated with respect to the control [27].

Steroid profiling using mass spectrometry: Steroid profiling in NCI H295R cells was performed using a liquid chromatography high-resolution mass spectrometry (LC-HRMS) method as previously described and validated with 1 µM of the unlabeled substrate added to the cell culture [28–30]. Steroids from 500 µL cell media, plus 38 µL of a mixture of internal standards (at 3.8 nM each), were extracted using solid-phase extraction with an OasisPrime HLB 96-well plate. Samples were resuspended in 100 µL 33% methanol in water and 20 µL injected into the LC-HRMS instrument (Vanquish UHPLC coupled to a QExactive Orbitrap Plus, from Thermo Fisher Scientific) using an Acquity UPLC HSS T3 column (Waters, Milford, MA, USA). Data from the mass spectrometer were processed using TraceFinder 4.0 (Thermo Fisher Scientific, Waltham, MA, USA).

AKR1C3 inhibitor screening: AKR1C3 expression and purification were performed as previously described [31]. Briefly, the bacteria cells were grown in YT2X media that was supplemented with ampicillin, and, at OD 600 nm = 0.6, the expression was induced by IPTG 0.5 mM for 2 h. The bacteria were then centrifuged and lysed with four freeze–thaw cycles in the presence of lysozyme and protease inhibitors. The lysate was centrifuged for 30 min at 13,000× g and the supernatant was collected. AKR1C3 was affinity purified via an N-terminal GST-tag on glutathione (GT) sepharose (GE-Healthcare) and cleaved by thrombin, according to the manufacturer's protocol.

The inhibition assays were performed on purified recombinant enzyme, as previously described [31]. Briefly, the enzymatic reaction was fluorometrically (exc/em; 340 nm/460 nm) monitored by the measurement of NADPH production on the Ensight plate reader (Perkin Elmer, Waltham, MA, USA) at 37 °C. The assay mixture, which contained 100 mM phosphate buffer pH 7, 200 µM $NADP^+$, S-tetralol (in ETOH), inhibitor (in DMSO), and purified enzyme (1 µM), was added to a 96-well plate at a final volume of 200 µL. The S-tetralol concentration was 160 µM, in accordance with the Km described for AKR1C3 under the same experimental conditions. The solvent added to the reaction mixture did not exceed 10% of the final concentration. Percentage inhibition with respect

to the controls that contained the same amount of solvent, without the inhibitor, was calculated from the initial velocities, which were obtained via the linear regression of the progress curve at different inhibitor concentrations. The results are expressed as the mean value ± standard error (SE) of at least three experiments, each carried out in triplicate.

Statistical analysis: Calculations were performed using Microsoft Excel and GraphPad Prism 3.0 (Graph Pad Software, Inc. San Diego, CA, USA). Data are represented as the mean of triplicate values. Dunnett's multiple comparison ANOVA test was performed to determine the significant difference between the mean values of samples and the control. Error bars denote standard deviation from respective mean values. Significant p values were set as * $p < 0.05$ and ** $p < 0.01$, *** $p < 0.001$.

2.5. Computational Chemistry

The experimentally determined structure of CYP17A1 complexed with galeterone (PDB 3SWZ) was used as a target for the docking studies due to the structural similarity between galeterone and the compounds reported in this paper [32]. The protein was prepared using the Protein Preparation Wizard in Maestro (v. 11.1) [33]. The Protein Preparation Wizard optimizes the hydrogen-bonding network at pH 7.0 and performs a short restrained protein minimization using the OPLS-2005 force field [34]. The ligands were prepared by the LigPrep module in Maestro [33]. Docking was performed with GOLD (Genetic Optimisation for Ligand Docking) version 5.6 [35]. The binding site was defined to be within 15 Å around the Fe atom in the heme group. Ligands were docked 10 times with the default option slow genetic algorithm, and with the heme-modified ChemScore as scoring function [36]. The sulfoxides may exist in two enantiomeric forms with an R- or S-configuration at the sulfur atom, and, accordingly, both stereoisomers were docked to CYP17A1.

3. Results and Discussion

3.1. Chemistry

In our previous work, we synthesized non-steroidal ligands of CYP17A1 which could only bind to the heme via the nitrogen atom [37]. Here, we were interested in using sulfur-based moieties in order to discern if they could constitute a viable binding group. Thus, we envisioned using sulfides and sulfoxides for this purpose. Two different positions of these groups were explored to allow better accommodation of the ligand in the CYP17A1 active site. Two categories of compounds were prepared: benzimidazole derivatives with the possibility of a well-established sp^2 nitrogen–heme interaction (**3a**–**b** and **4a**–**b**), and indole derivatives which can potentially interact only with their sulfur groups (**3c**–**d** and **4c**–**d**).

The synthesis started from 4-(1*H*-benzo[*d*]imidazol-1-yl)aniline (**1a**) or 4-(1H-indol-1-yl)aniline (**1b**) which were coupled with commercially available 3-bromothioanisole **2a** and 4-bromothioanisole **2b** via a Buchwald–Hartwig reaction, obtaining sulfides **3a**–**d** (Scheme 1). The reaction was carried out using third-generation (G3) Buchwald precatalysts. They are soluble in common organic solvents, and are also air, moisture, and thermally stable, making them convenient sources of the active catalyst [38]. Required anilines **1a** and **1b** were prepared according to our previously published method [39]. Briefly, indole or imidazole were first reacted with 1-fluoro-4-nitrobenze in the presence of potassium phosphate and then catalytically reduced with hydrogen over palladium. Subsequent oxidation with hydrogen peroxide afforded sulfoxide analogues **4a**–**d** [40]. This reaction was characterized by a very rapid progress and was completed in just a few minutes. Obtained sulfoxides displayed a characteristic downfield shift of the S(O)-methyl group in 1H NMR and 13C NMR (Supplementary Information).

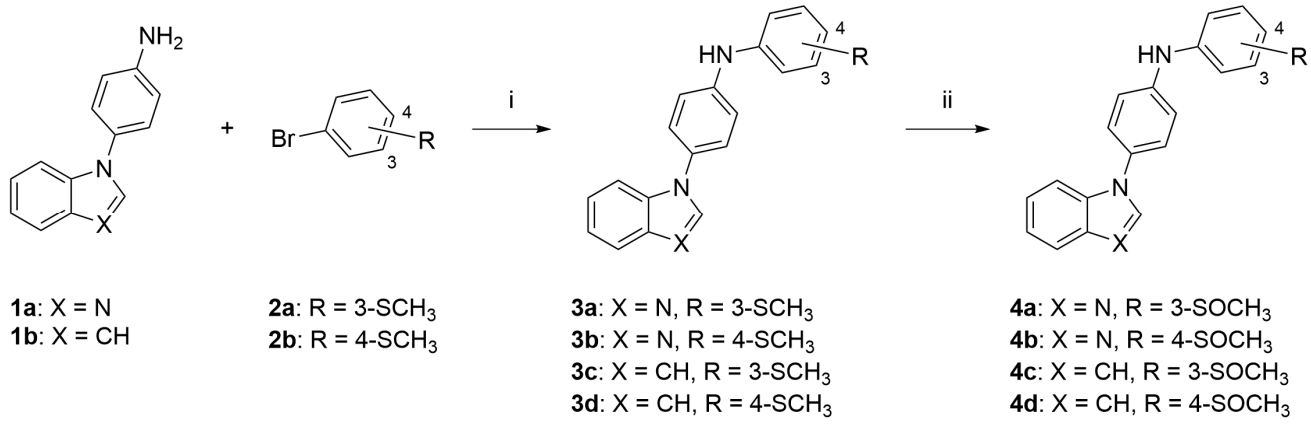

1a: X = N
1b: X = CH

2a: R = 3-SCH_3
2b: R = 4-SCH_3

3a: X = N, R = 3-SCH_3
3b: X = N, R = 4-SCH_3
3c: X = CH, R = 3-SCH_3
3d: X = CH, R = 4-SCH_3

4a: X = N, R = 3-$SOCH_3$
4b: X = N, R = 4-$SOCH_3$
4c: X = CH, R = 3-$SOCH_3$
4d: X = CH, R = 4-$SOCH_3$

Scheme 1. Synthesis of the final compounds **3a**–**d** and **4a**–**d**. Reagents and conditions: (**i**) t-BuXPhos G3, t-BuXPhos, t-BuONa, t-BuOH or THF, 100 °C, MW; (**ii**) H_2O_2, phenol, 40 °C.

3.2. CYP17A1 Inhibition

The initial screening of compounds showed marked inhibition of CYP17A1 hydroxylase activity. The four most potent compounds demonstrating more than 50% inhibition at a concentration of 10 μM were **3a**, **3b**, **4a**, and **4c** with remaining enzymatic activities of 23%, 31%, 35%, and 27% of the control, respectively (Figure 3A). All of them were less potent than the abiraterone used as a reference. Regarding the lyase reaction, only compound **3a** was able demonstrate an inhibitory activity higher than 50% (33% of the remaining enzymatic activity, Figure 3B). None of the compounds showed selective inhibition of CYP17A1 lyase activity. We noticed that the -meta substitution provided more active compounds compared to the ones with sulfur groups in the -para position. Contrary to this observation, we were not able to capture a clear trend when analyzing the influence of the remaining two variables: benzimidazole vs. indole moiety and sulfide vs. sulfoxide. However, it appears that benzimidazole is preferred as evidenced by **3a**, **3b**, and **4a**. Those compounds can theoretically bind to the heme via either the sp^2 nitrogen atom or sulfur atom. This possibility does not exist for compound **4c**, which can only bind via its sulfoxide group. Still, this compound showed nearly the same level of potency as **3a**, while **4b**, which retains benzimidazole, was the least potent among the whole set. Because our tested compounds were generally less potent than the compounds they were based on, it can be concluded that the presence of the nitrogen atom seems to be superior to the sulfur atom [37].

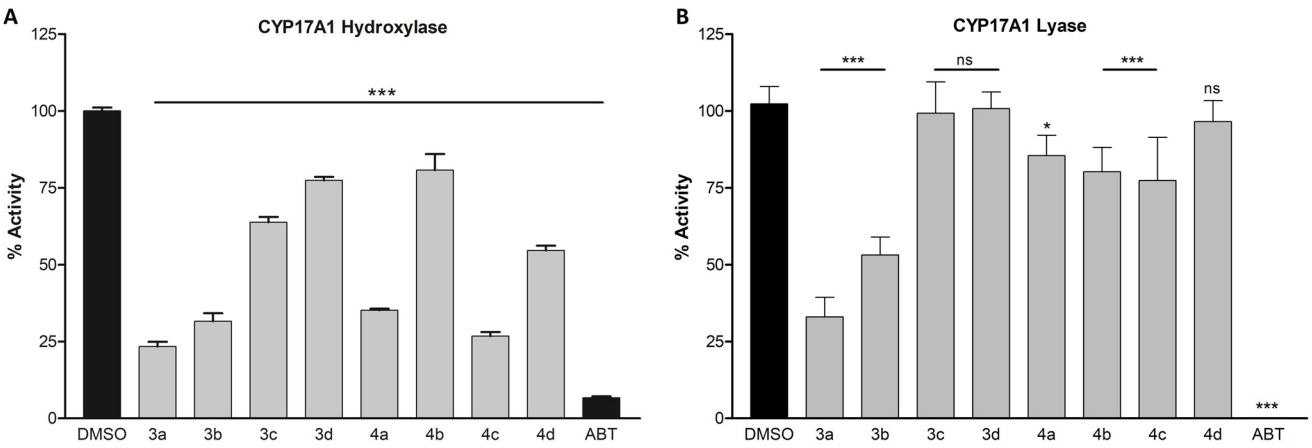

Figure 3. Inhibition of CYP17A1 hydroxylase activity (**A**) and lyase activity (**B**). Compounds were screened at 10 μM in the NCI H295R cell line. Inhibition is presented as the remaining enzymatic activity after the treatment with the tested compounds. Error bars denote standard deviation from

respective mean values. Significant p values were set as ns not significant, * $p < 0.05$, *** $p < 0.001$. DMSO, dimethyl sulfoxide; ABT, abiraterone.

3.3. Possible Binding Modes

Although the compounds bind to CYP17A1 in a similar way, adopting a conformation bending over Helix I with the benzimidazole or indole moiety facing the heme group and the sulfur part occupying a cavity formed by Helices F, G, and I (Figure 4), they also display some characteristic differences.

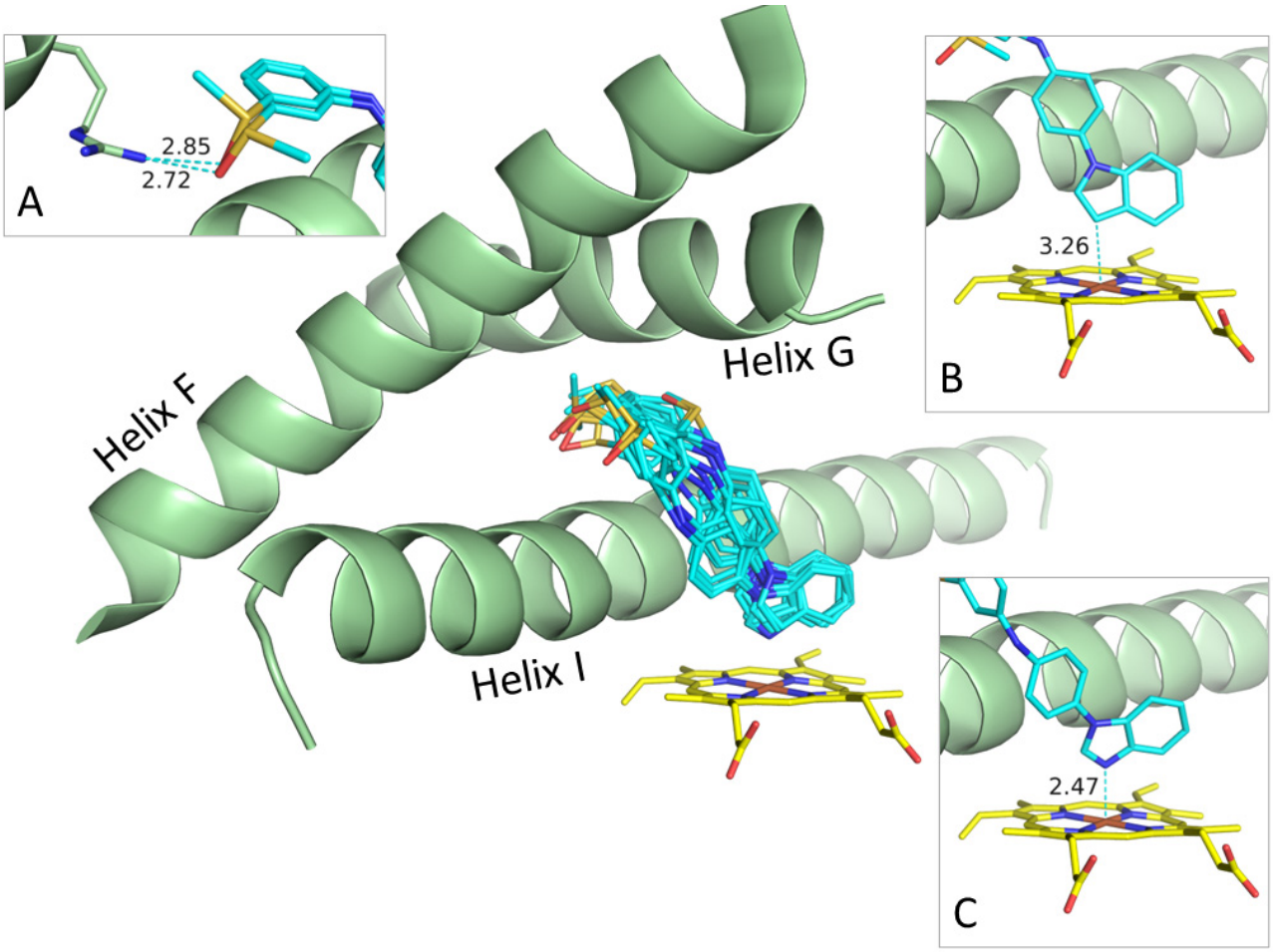

Figure 4. Preferred binding mode determined by docking of all the compounds. Inserts showing examples on protein–ligand contacts: (**A**) Hydrogen bonds between sulfoxide group of R- and S-forms of **4c** and Arg239. (**B**) Binding of indole moiety of R-form of **4c** to Fe atom in heme group. (**C**) Binding of benzimidazole moiety of S-form of **4a** to iron atom in heme group. Helices F, G, and I of CYP17A1 shown as green cartoons; heme groups and ligands shown as stick models using standard type-coloring except for carbons in heme and ligands colored yellow and cyan, respectively.

For benzimidazoles **3a**, **3b**, **4a**, and **4b**, the lone pair on the N3 coordinates to the iron atom in the heme group with a Fe-N3 distance between 2.2 and 2.5 Å, which is a typical distance for the binding of nitrogen-containing heteroaromatic to heme groups (Figure 4C) [32]. The indoles, **3c**, **3d**, **4c**,and **4d** do not coordinate to the heme group, but, nevertheless, the indole moiety faces the heme group with a Fe-C3 distance between 2.7 Å and 3.5 Å (Figure 4B).

As already mentioned, all the molecules bent over Helix I with the para-substituted benzene ring oriented flat against Helix I. The sulfide or sulfoxide parts of the molecules are placed in a primary hydrophobic cavity formed by Tyr201, Asn202, and Ile205 in Helix

F and Arg239 in Helix G. The only specific contact between this part of the ligands and CYP17A1 is a hydrogen bond between Arg239 and the sulfoxide oxygen atom at 2.5–3.0 Å (Figure 4A).

The binding modes generated by docking suggest that the benzimidazole ring system is a better iron coordinator than the sulfoxide moiety, but it may also reflect or be influenced by the overall shape of these structurally similar ligands favoring this binding mode. We see a few examples among the poses on an inverted binding mode with the benzimidazole moiety facing Arg239, and, thereby, placing the benzene-sulfoxide part of the ligands roughly parallel to the heme group without any specific contacts to the iron atom.

3.4. Docking

The docking scores, which may reflect the experimental binding energies, are listed in Table 1. The benzimidazoles, **3a**, **3b**, **4a**, and **4b**, are predicted to bind better than their corresponding indoles, **3c**, **3d**, **4c**, and **4d**, with score difference of 1-4 probably due to the favorable Fe-N coordination. This calculation would corroborate the apparent better performance of the benzimidazole compounds in CYP assays. In addition to this likely significant trend in binding, we also observe some minor differences. For **3a**/**4a**, **3b**/**4b**, and **3c**/**4c**, the sulfoxides bind better than the sulfides, but for **3d**/**4d** the sulfide binds better than the sulfoxides. For the meta-substituted sulfoxides **4a** and **4c**, the *S*-enantiomer binds better than the *R*-enantiomer, whereas it is the opposite for the para-substituted sulfoxides **4b** and **4d**.

Table 1. Key binding data for best poses derived from GOLD docking. [a] Docking score for the best binding pose, except for *S*-**4d** where values are from third best pose at 0.7 above best pose. [b] Difference between best poses of the *R*- and *S*-enantiomers of the sulfoxides. [c] Distance between the iron in the heme group and the N3/C3 in the benzimidazole/indole moiety. [d] Atom/atom group in the N3/C3 position in the benzimidazole/indole moiety.

Compound	Docking Score [a]	R/S Difference [b]	Fe-X3 Distance [c] [A]	X3 [d]
3a	47.0		2.3	N
3b	45.9		2.5	N
3c	43.4		3.2	CH
3d	44.0		3.3	CH
R-**4a**	47.9		2.4	N
S-**4a**	49.9	−2.1	2.5	N
R-**4b**	47.8		2.5	N
S-**4b**	46.4	1.4	2.2	N
R-**4c**	45.3		3.4	CH
S-**4c**	46.2	−0.9	3.3	CH
R-**4d**	44.1		2.7	CH
S-**4d**	43.4	0.7	3.5	CH

Nevertheless, we observe that, except for **4b**, the best inhibitors of the CYP17A1 hydroxylase reaction **3a**, **3b**, **4a**, and **4c** also have higher docking scores than the less efficient CYP17A1 hydroxylase inhibitors **3c**, **3d**, and **4d** (Figure 3).

3.5. CYP21A2, CYP3A4, and POR Inhibition

CYP21A2 is an enzyme catalyzing the transformation of progesterone and 17α-hydroxy progesterone into mineralocorticoids and glucocorticoids, respectively (Figure 1). It is often an off-target for many CYP17A1 inhibitors due to the high structural similarity between the two enzymes [41]. To test the compounds' selectivity, we measured CYP21A2 activity after treatment with our compounds at 10 µM. The activity was reduced to 31%, 43%, 41%, 26%, and 49% in the presence of compounds **3a**, **3b**, **4a**, **4c**, and **4d**, respectively (Figure 5A). Although the effects were not as pronounced as with abiraterone, it was nevertheless comparable to the effects observed in CYP17A1 inhibition.

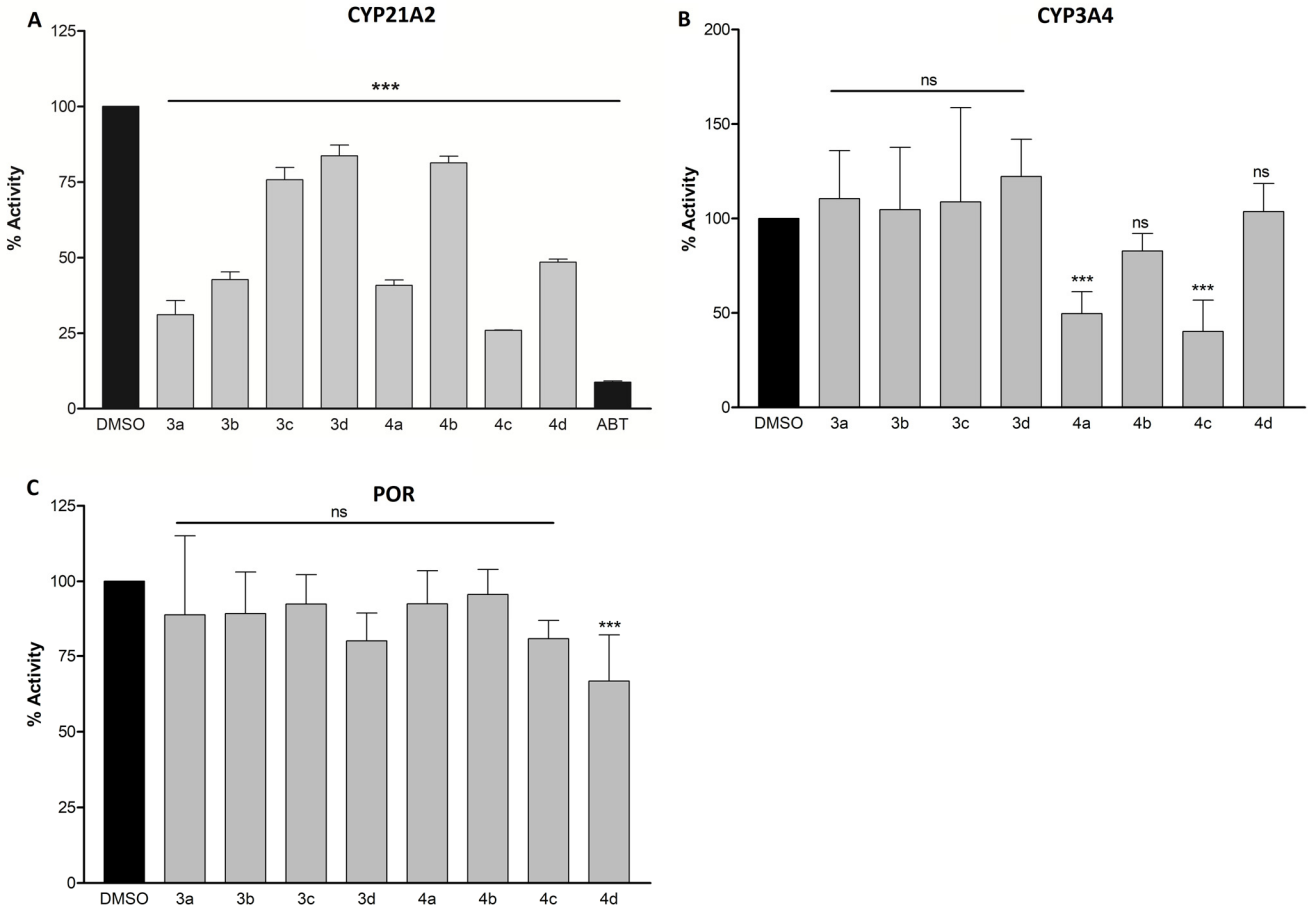

Figure 5. Inhibition of CYP21A2 (**A**), CYP3A4 (**B**), and POR (**C**). NCI H295R cells were used for CYP21A2 inhibition and purified proteins for CYP3A4 and POR inhibition. The concentration of the compounds was 10 μM in all assays. Inhibition is presented as the remaining enzymatic activity after the treatment with the tested compounds. Significant p values were set as ns not significant, *** $p < 0.001$. DMSO, dimethyl sulfoxide; ABT, abiraterone.

CYP3A4 belongs to the CYP3A subfamily of enzymes that is responsible for the metabolism of around 30% of clinically used drugs [42]. Interactions with this enzyme leading to its inhibition or induction can result in serious drug interactions; therefore, the influence of drug candidates on these enzymes should always be investigated. Only compounds **4a** and **4c** demonstrated inhibitory activity greater than 50%, with the remaining enzymatic activity being 50% and 40%, respectively, as compared to the control (Figure 5B). Compound **3a**, which was the most potent CYP17A1 inhibitor, had little influence on CYP3A4, thereby demonstrating selectivity for CYP17A1.

Cytochrome P450 oxidoreductase (POR) plays a major role in the metabolism of drugs and steroids. All microsomal P450s depend on POR for the supply of electrons for their catalytic activities. Therefore, the disruption of POR may effectively lead to disabling CYP enzymes [43]. An interaction between POR and the compounds was investigated using resazurin, a synthetic redox substrate of POR. No significant difference in reduction of resazurin was observed in the presence of a 10 μM concentration of compounds with respect to the control (Figure 5C). Limiting the activity towards CYP3A4 and POR becomes a crucial factor in developing the compounds for targeted CYP17A1 inhibition, owing to their vast role in drug metabolism and redox reactions in the cell.

3.6. AKR1C3 Inhibition

AKR1C3 is an important enzyme in the androgen steroidogenic pathway [9,10]. AKR1C3 facilitates the conversion of the weak androgens—androstenedione and 5α-androstanedione—to the more active androgens, T and DHT, respectively. Its activation contributes to CRPC drug resistance in patients treated with both abiraterone and enzalutamide through increasing intracrine androgen synthesis and enhancing androgen signaling. The overexpression of *AKR1C3* in abiraterone-resistant cells suggested that its concomitant blockade might yield therapeutic response in tumors resistant to abiraterone or other CYP17A1 inhibitors [11,12]. It has been shown that the treatment of abiraterone-resistant cells with an AKR1C3 inhibitor, like indomethacin, overcomes resistance and enhances abiraterone therapy both in vitro and in vivo by reducing the levels of intracrine androgens and diminishing AR transcriptional activity [11]. The surmountable effect of combined treatment with inhibitors of AKR1C3 and abiraterone has been also observed [44,45]. Thus, the possibility of dual CYP17A1/AKR1C3 inhibition was investigated with the aim to pave the way for the future development of more potent dual inhibitors.

The indole scaffold of indomethacin is also present in ASP9521 [46], a potent AKR1C3 inhibitor that was in a phase 1 clinical trial for CRPC (May 2011, NCT01352208, discontinued) and seems to be a crucial molecular moiety for establishing effective interactions with the active site of AKR1C3 [47]. With the aim of investigating whether the indole and benzimidazole moieties present in our studied compounds could provide the ability to inhibit the AKR1C3 enzyme resulting in synergistic multi-target properties, we tested compounds **3a**–**3d** and **4a**–**4d** on the recombinant purified AKR1C3 enzyme by measuring S-tetralol oxidation in the presence of $NADP^+$ (Figure 6).

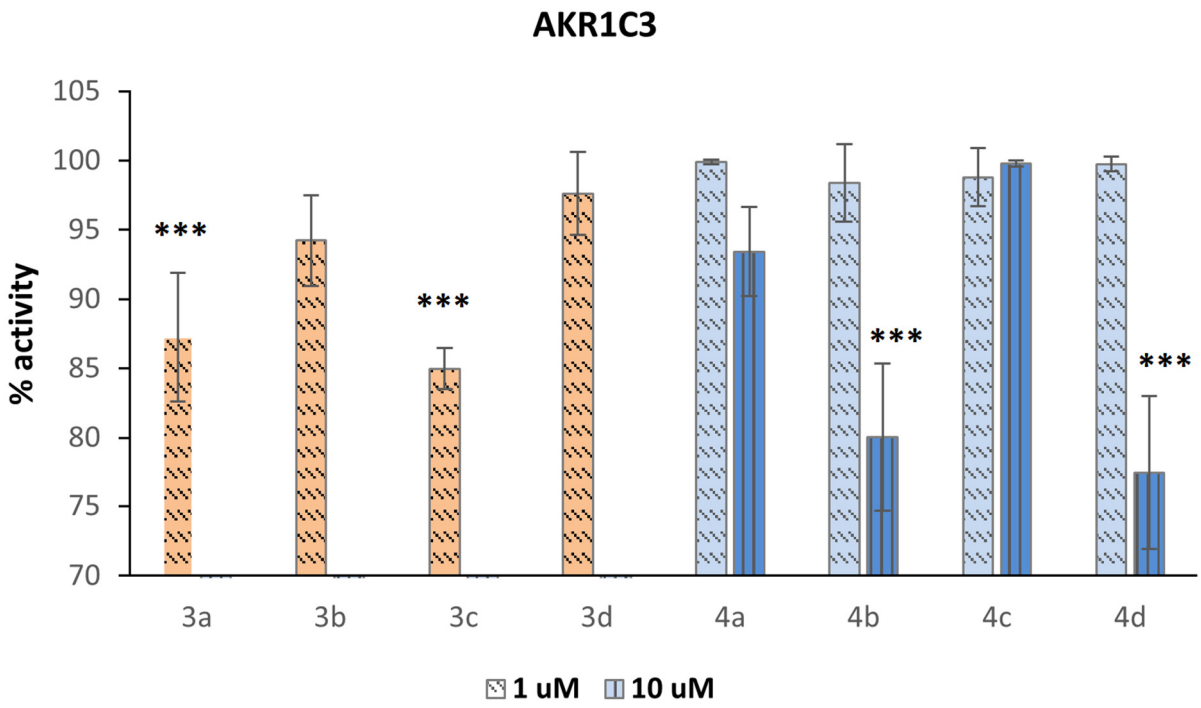

Figure 6. Inhibition of AKR1C3 represented as the remaining enzyme activity after the treatment with compounds. Compounds **3a**–**3d** were only tested at 1 μM concentration because they showed a strong interference fluorescent signal when tested at 10 μM concentration in the enzymatic assay. Significant *p* values were set as, *** $p < 0.001$.

Compounds **3a**–**3d** were only tested at 1 μM because they were very fluorescent at 10 μM in the enzymatic assay. Except for compound **4c**, which displayed no activity even at 10 μM, all the compounds showed weak inhibitory activity. The most active compounds were **3a** and **3c**, demonstrating that the thioether functionality is beneficial for activity,

in particular when present in the meta position. If sulfide is oxidized to sulfoxide, the activity decreases, as demonstrated by **4a** versus **3a** and **4c** versus **3c**. If the thioether group is inserted in the para position, the oxidation is not detrimental to the inhibitor activity because the corresponding sulfoxides show residual inhibitory activity when tested at 10 μM. The presence of a heterocyclic ring containing a sp^2-hybridized nitrogen atom is not essential because benzimidazoles **3a**, **3b**, **4a**, and **4b** show similar activity to their corresponding indoles **3c**, **3d**, **4c**, and **4d**, respectively.

3.7. Steroid Profiling

The overall effect of the compounds on hormone levels in NCI H295R cells was measured using LC-MS (Figure 7). The results correlate with enzyme assays performed using specific radiolabeled substrates. The accumulation of progesterone, comparable to abiraterone, was noted after treatment with **3a**. This might be attributed to the inhibition of CYP17A1 in the hydroxylase reaction and CYP21A2 for which progesterone is a substrate. However, compound **4c**, demonstrating a similar level of potency towards CYP17A1 and CYP21A2, was able to decrease the level of progesterone, which would be preferable in an ideal CYP17A1 inhibitor. Elevated progesterone levels have been shown to activate the proliferation of cancer cells and have oncogenic properties [48]. Notably, both compounds were less potent in both of the CYP assays compared to abiraterone. This suggest that additional mechanisms might be operational. The compounds had varying effects on the levels of glucocorticoids compared to abiraterone, but, overall, the impact was less pronounced.

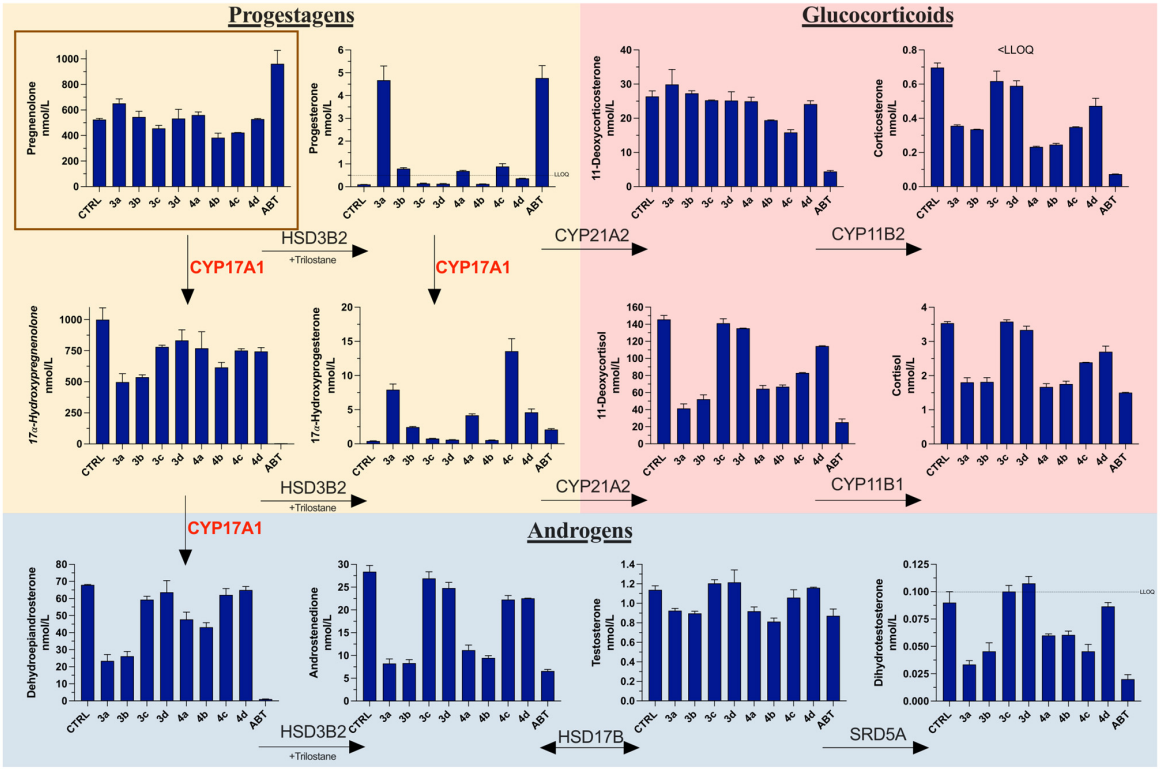

Figure 7. Influence of the tested compounds on steroid metabolic pathways in NCI-H295R cells. Steroid substrate, pregnenolone (1 μM), boxed in brown. Trilostane added at 2 μM, and all compounds tested at 10 μM. CTRL, control (DMSO); ABT, abiraterone; LLOQ, lower limit of accurate quantification; HSD3B2, 3β-hydroxysteroid dehydrogenase type 2; CYP21A2, cytochrome P450 21-hydroxylase; CYP11B1, cytochrome P450 11β-hydroxylase; CYP17A1, cytochrome P450 17α-hydroxylase/17,20-lyase; CYP11B2, cytochrome P450 aldosterone synthase; HSD17B, 17β-hydroxysteroid dehydrogenases; SRD5A, 5α-reductases. Values are represented as nmol/L (n = 2; mean ± SD).

This is important because one of the side effects of abiraterone treatment is glucocorticoid imbalance, necessitating the co-administration of prednisone during therapy. Interestingly, compound **3a** was able to decrease the level of DHT close to that observed after abiraterone treatment. Similarly, compounds **3b** and **4c** decreased the DHT levels two-fold compared to the control. This was also observed after abiraterone treatment, which suggests that these compounds might affect the function of 5α-reductase, which is responsible for the conversion of T to DHT. Since DHT levels were measured below the lower limit of quantification and levels of T remained relatively unchanged, it is possible that other enzymes, operating in the "backdoor" pathways where DHT is produced from androstanedione or androstanediol, are affected. The levels of weak androgens such as dehydroepiandrosterone and androstenedione were also diminished by some of the compounds, notably **3a** and **3b**. The overall effect on androgen biosynthesis, especially DHT, suggests that despite the rather weak inhibition of CYP17A1 and AKR1C3 enzymes alone, the observed result might be arising from the combined dual action.

3.8. Antiproliferative Activity

The AR-dependent prostate cancer cells (LNCaP) were used to evaluate the antiproliferative activity in vitro of compounds **3a**–**4b**. Although these cells are androgen sensitive, they exhibit bone metastatic behavior, better mimicking the clinical human disease [49]. After 24 h, all compounds demonstrated a weaker antiproliferative effect when compared to abiraterone (Figure 8). However, after 48 h, compound **4c** had a similar activity to that of abiraterone, decreasing the cell viability below 50%. Compound **3a** was the second most potent compound in this assay, decreasing the cell viability to close to 50%.

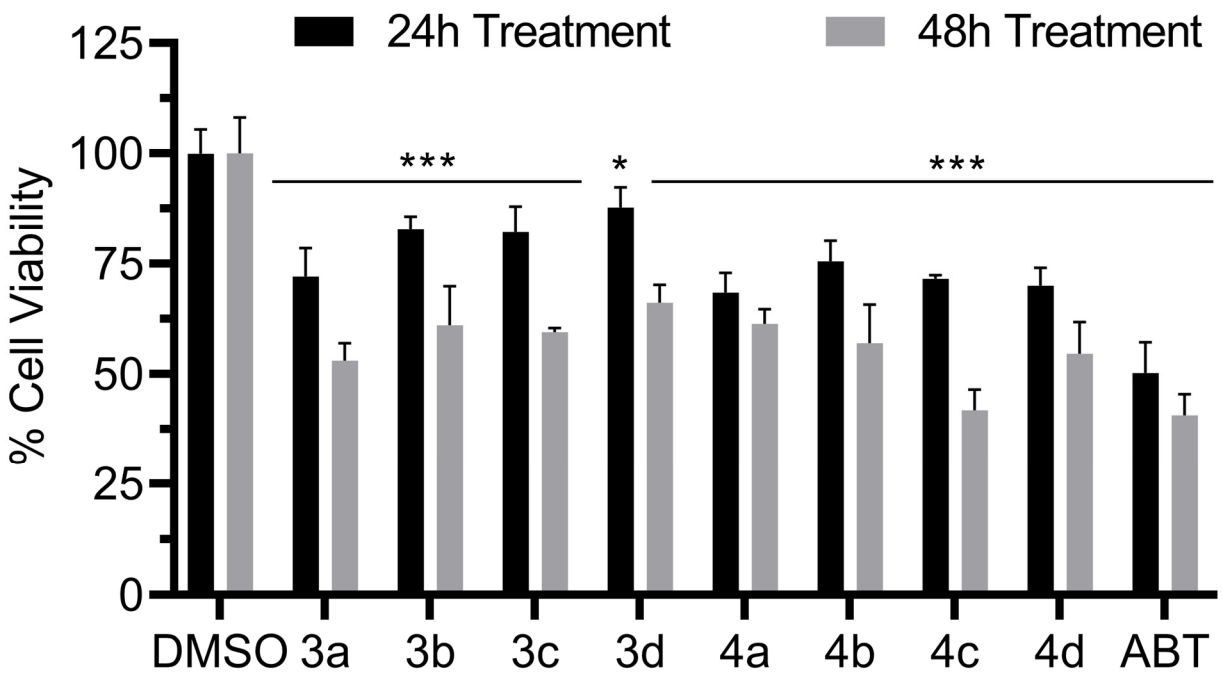

Figure 8. LNCaP cell viability in the presence of compounds **3a**–**d** and **4a**–**d**. Compound concentrations were 10 μM. Significant *p* values were set as * $p < 0.05$, *** $p < 0.001$.

4. Conclusions

The aim of our study was twofold. The main aim was to explore the effect of CYP17A1 inhibition by compounds endowed with the sulfur moiety, and, as a secondary aim, we were interested in examining whether the dual inhibition of CYP17A1 and AKR1C3 can result in an enhanced effect on steroid hormone production. The most potent compound **3a** displayed marked inhibitory activity towards CYP17A1. **3a** also demonstrated varying degrees of inhibition against CYP21A2, CYP3A4, and POR enzymes, highlighting its

potential for selective inhibition. Our limited SAR analysis suggests that the meta position of sulfur groups and the presence of benzimidazole are advantageous for the observed activity. This latter observation suggests that the presence of a nitrogen atom might be superior to a sulfur atom in inhibiting CYP17A1. Through molecular docking, we inferred that the benzimidazole ring system might serve as a better iron coordinator than the sulfur-based moiety. However, it is important to add that only limited functionalities were tested, and other motifs might offer better inhibitory profiles.

The compounds' impact on hormone levels in NCI H295R cells was apparently stronger than what could be expected based on separate enzymatic assays alone. Our compounds did not perform particularly potently in those assays. The investigation of the potential dual inhibition of CYP17A1 and AKR1C3 offered preliminary insights, suggesting that these compounds could pave the way for the development of more potent dual inhibitors.

In essence, our findings present a promising starting point for the design of selective CYP17A1 inhibitors and potential dual inhibitors of CYP17A1 and AKR1C3. Future work will focus on refining these ideas to enhance potency and selectivity, thereby laying the ground for potential therapeutic application in hormone-related diseases, such as PCa or polycystic ovary syndrome (PCOS).

Supplementary Materials: The following supporting information can be downloaded at: https://www.mdpi.com/article/10.3390/biom13091349/s1, File S1: NMR, IR spectra and HPLC traces.

Author Contributions: Conceptualization, T.M.W.; synthesis, T.M.W., I.M. and P.N.; CYP17A1 assays, K.S.; cell viability, K.S., J.Y. and S.T.; AKR1C3 assays, S.O.-B.; steroid profiling, T.D.T. and C.D.V.; CYP3A4 and POR assays, M.N.R.V.; CYP21A2 assays, A.M.; molecular modeling, F.S.J.; writing—original draft preparation, T.M.W.; writing—review and editing, T.M.W., S.O.-B., T.D.T., C.D.V., F.S.J., A.V.P., A.C.P., M.L.L., D.B. and F.B.; project administration T.M.W. All authors have read and agreed to the published version of the manuscript.

Funding: T.M.W. research is funded by the Narodowe Centrum Nauki grant Sonata 2020/39/D/NZ7/00572. A.V.P. acknowledges SWISS NATIONAL SCIENCE FOUNDATION, grant number 310030M_204518 and CANCER RESEARCH SWITZERLAND grant number KFS-5557-02-2022. J.Y., M.N.R.V., and K.S. are funded by the SWISS GOVERNMENT EXCELLENCE SCHOLARSHIP (ESKAS) grant numbers 2022.0470, 2020.0557, and 2019.0385. T.d.T. is funded by the Marie Skłodowska-Curie Individual Fellowship (#101023999). I.M., S.O.B., M.L.L., and D.B. acknowledge Fondazione CRT (grant OLIS_CRT_22_01) and A.C.P. acknowledges the University of Torino (grant PIPA_GFI_22_01_F).

Institutional Review Board Statement: Not Applicable.

Informed Consent Statement: Not Applicable.

Data Availability Statement: Raw NMR data will be deposited in https://repod.icm.edu.pl/ (accessed on 30 August 2023).

Conflicts of Interest: The authors declare no conflict of interest.

References

1. Siegel, R.L.; Miller, K.D.; Wagle, N.S.; Jemal, A. Cancer statistics, 2023. *CA A Cancer J. Clin.* **2023**, *73*, 17–48. [CrossRef] [PubMed]
2. Muniyan, S.; Li, B.; Batra, S.K. Editorial: Metastatic Castration Resistant Prostate Cancer: Prognosis and Treatment. *Front. Oncol.* **2022**, *12*, 913630. [CrossRef] [PubMed]
3. Culig, Z.; Santer, F.R. Androgen receptor signaling in prostate cancer. *Cancer Metastasis Rev.* **2014**, *33*, 413–427. [CrossRef] [PubMed]
4. Yin, L.; Hu, Q. CYP17 inhibitors—Abiraterone, C17,20-lyase inhibitors and multi-targeting agents. *Nat. Rev. Urol.* **2014**, *11*, 32–42. [CrossRef]
5. Wróbel, T.M.; Jørgensen, F.S.; Pandey, A.V.; Grudzińska, A.; Sharma, K.; Yakubu, J.; Björkling, F. Non-steroidal CYP17A1 Inhibitors: Discovery and Assessment. *J. Med. Chem.* **2023**, *66*, 6542–6566. [CrossRef]
6. Maity, S.N.; Titus, M.A.; Gyftaki, R.; Wu, G.; Lu, J.-F.; Ramachandran, S.; Li-Ning-Tapia, E.M.; Logothetis, C.J.; Araujo, J.C.; Efstathiou, E. Targeting of CYP17A1 Lyase by VT-464 Inhibits Adrenal and Intratumoral Androgen Biosynthesis and Tumor Growth of Castration Resistant Prostate Cancer. *Sci. Rep.* **2016**, *6*, 35354. [CrossRef]

7. Hara, T.; Kouno, J.; Kaku, T.; Takeuchi, T.; Kusaka, M.; Tasaka, A.; Yamaoka, M. Effect of a novel 17,20-lyase inhibitor, orteronel (TAK-700), on androgen synthesis in male rats. *J. Steroid Biochem. Mol. Biol.* **2013**, *134*, 80–91. [CrossRef]
8. Fizazi, K.; Jones, R.; Oudard, S.; Efstathiou, E.; Saad, F.; de Wit, R.; De Bono, J.; Cruz, F.M.; Fountzilas, G.; Ulys, A.; et al. Phase III, Randomized, Double-Blind, Multicenter Trial Comparing Orteronel (TAK-700) Plus Prednisone with Placebo Plus Prednisone in Patients with Metastatic Castration-Resistant Prostate Cancer That Has Progressed During or after Docetaxel-Based Therapy: ELM-PC 5. *J. Clin. Oncol.* **2015**, *33*, 723–731. [CrossRef]
9. Liu, Y.; He, S.; Chen, Y.; Liu, Y.; Feng, F.; Liu, W.; Guo, Q.; Zhao, L.; Sun, H. Overview of AKR1C3: Inhibitor Achievements and Disease Insights. *J. Med. Chem.* **2020**, *63*, 11305–11329. [CrossRef]
10. Shiota, M.; Endo, S.; Blas, L.; Fujimoto, N.; Eto, M. Steroidogenesis in castration-resistant prostate cancer. *Urol. Oncol.* **2022**, *41*, 240–251. [CrossRef]
11. Liu, C.; Armstrong, C.M.; Lou, W.; Lombard, A.; Evans, C.P.; Gao, A.C. Inhibition of AKR1C3 Activation Overcomes Resistance to Abiraterone in Advanced Prostate Cancer. *Mol. Cancer Ther.* **2017**, *16*, 35–44. [CrossRef] [PubMed]
12. Penning, T.M.; Jonnalagadda, S.; Trippier, P.C.; Rižner, T.L. Aldo-Keto Reductases and Cancer Drug Resistance. *Pharmacol. Rev.* **2021**, *73*, 1150–1171. [CrossRef]
13. Bonomo, S.; Hansen, C.H.; Petrunak, E.M.; Scott, E.E.; Styrishave, B.; Jørgensen, F.S.; Olsen, L. Promising Tools in Prostate Cancer Research: Selective Non-Steroidal Cytochrome P450 17A1 Inhibitors. *Sci. Rep.* **2016**, *6*, 29468. [CrossRef] [PubMed]
14. Leach, A.G.; Kidley, N.J. Quantitatively Interpreted Enhanced Inhibition of Cytochrome P450s by Heteroaromatic Rings Containing Nitrogen. *J. Chem. Inf. Model.* **2011**, *51*, 1048–1063. [CrossRef]
15. Castaño, P.R.; Parween, S.; Pandey, A.V. Bioactivity of Curcumin on the Cytochrome P450 Enzymes of the Steroidogenic Pathway. *Int. J. Mol. Sci.* **2019**, *20*, 4606. [CrossRef] [PubMed]
16. Kimura, K.-i.; Itakura, Y.; Goto, R.; Tojima, M.; Egawa, N.; Yoshihama, M. Inhibition of 17α-Hydroxylase/C17,20-Lyase (CYP17) from Rat Testis by Green Tea Catechins and Black Tea Theaflavins. *Biosci. Biotechnol. Biochem.* **2007**, *71*, 2325–2328. [CrossRef]
17. Frydenvang, K.; Verkade-Vreeker, M.C.A.; Dohmen, F.; Commandeur, J.N.M.; Rafiq, M.; Mirza, O.; Jorgensen, F.S.; Geerke, D.P. Structural analysis of Cytochrome P450 BM3 mutant M11 in complex with dithiothreitol. *PLoS ONE* **2019**, *14*, e0217292. [CrossRef]
18. Doukov, T.; Li, H.; Sharma, A.; Martell, J.D.; Soltis, S.M.; Silverman, R.B.; Poulos, T.L. Temperature-dependent spin crossover in neuronal nitric oxide synthase bound with the heme-coordinating thioether inhibitors. *J. Am. Chem. Soc.* **2011**, *133*, 8326–8334. [CrossRef]
19. Martell, J.D.; Li, H.; Doukov, T.; Martasek, P.; Roman, L.J.; Soltis, M.; Poulos, T.L.; Silverman, R.B. Heme-coordinating inhibitors of neuronal nitric oxide synthase. Iron-thioether coordination is stabilized by hydrophobic contacts without increased inhibitor potency. *J. Am. Chem. Soc.* **2010**, *132*, 798–806. [CrossRef]
20. Jarman, M.; John Smith, H.; Nicholls, P.J.; Simons, C. Inhibitors of enzymes of androgen biosynthesis: Cytochrome P45017α and 5α-steroid reductase. *Nat. Prod. Rep.* **1998**, *15*, 495–512. [CrossRef]
21. Gazdar, A.F.; Oie, H.K.; Shackleton, C.H.; Chen, T.R.; Triche, T.J.; Myers, C.E.; Chrousos, G.P.; Brennan, M.F.; Stein, C.A.; La Rocca, R.V. Establishment and Characterization of a Human Adrenocortical Carcinoma Cell Line That Expresses Multiple Pathways of Steroid Biosynthesis1. *Cancer Res.* **1990**, *50*, 5488–5496. [PubMed]
22. Kurlbaum, M.; Sbiera, S.; Kendl, S.; Martin Fassnacht, M.; Kroiss, M. Steroidogenesis in the NCI-H295 Cell Line Model is Strongly Affected By Culture Conditions and Substrain. *Exp. Clin. Endocrinol. Diabetes* **2020**, *128*, 672–680. [CrossRef] [PubMed]
23. Yoshimoto, F.K.; Auchus, R.J. The diverse chemistry of cytochrome P450 17A1 (P450c17, CYP17A1). *J. Steroid Biochem. Mol. Biol.* **2015**, *151*, 52–65. [CrossRef]
24. Potts, G.O.; Creange, J.E.; Harding, H.R.; Schane, H.P. Trilostane, an orally active inhibitor of steroid biosynthesis. *Steroids* **1978**, *32*, 257–267. [CrossRef] [PubMed]
25. Malikova, J.; Brixius-Anderko, S.; Udhane, S.S.; Parween, S.; Dick, B.; Bernhardt, R.; Pandey, A.V. CYP17A1 inhibitor abiraterone, an anti-prostate cancer drug, also inhibits the 21-hydroxylase activity of CYP21A2. *J. Steroid Biochem. Mol. Biol.* **2017**, *174*, 192–200. [CrossRef] [PubMed]
26. Morán, F.M.; VandeVoort, C.A.; Overstreet, J.W.; Lasley, B.L.; Conley, A.J. Molecular Target of Endocrine Disruption in Human Luteinizing Granulosa Cells by 2,3,7,8-Tetrachlorodibenzo-p-Dioxin: Inhibition of Estradiol Secretion Due to Decreased 17α-Hydroxylase/17,20-Lyase Cytochrome P450 Expression. *Endocrinology* **2003**, *144*, 467–473. [CrossRef] [PubMed]
27. McManus, J.M.; Bohn, K.; Alyamani, M.; Chung, Y.-M.; Klein, E.A.; Sharifi, N. Rapid and structure-specific cellular uptake of selected steroids. *PLoS ONE* **2019**, *14*, e0224081. [CrossRef]
28. Ahmed, K.E.M.; Frøysa, H.G.; Karlsen, O.A.; Sagen, J.V.; Mellgren, G.; Verhaegen, S.; Ropstad, E.; Goksøyr, A.; Kellmann, R. LC-MS/MS based profiling and dynamic modelling of the steroidogenesis pathway in adrenocarcinoma H295R cells. *Toxicol. Vitro* **2018**, *52*, 332–341. [CrossRef] [PubMed]
29. Wudy, S.A.; Schuler, G.; Sánchez-Guijo, A.; Hartmann, M.F. The art of measuring steroids: Principles and practice of current hormonal steroid analysis. *J. Steroid Biochem. Mol. Biol.* **2018**, *179*, 88–103. [CrossRef]
30. Andrieu, T.; du Toit, T.; Vogt, B.; Mueller, M.D.; Groessl, M. Parallel targeted and non-targeted quantitative analysis of steroids in human serum and peritoneal fluid by liquid chromatography high-resolution mass spectrometry. *Anal. Bioanal. Chem.* **2022**, *414*, 7461–7472. [CrossRef]

31. Pippione, A.C.; Giraudo, A.; Bonanni, D.; Carnovale, I.M.; Marini, E.; Cena, C.; Costale, A.; Zonari, D.; Pors, K.; Sadiq, M.; et al. Hydroxytriazole derivatives as potent and selective aldo-keto reductase 1C3 (AKR1C3) inhibitors discovered by bioisosteric scaffold hopping approach. *Eur. J. Med. Chem.* **2017**, *139*, 936–946. [CrossRef] [PubMed]
32. DeVore, N.M.; Scott, E.E. Structures of cytochrome P450 17A1 with prostate cancer drugs abiraterone and TOK-001. *Nature* **2012**, *482*, 116–119. [CrossRef] [PubMed]
33. Sastry, G.M.; Adzhigirey, M.; Day, T.; Annabhimoju, R.; Sherman, W. Protein and ligand preparation: Parameters, protocols, and influence on virtual screening enrichments. *J. Comput.-Aided Mol. Des.* **2013**, *27*, 221–234. [CrossRef] [PubMed]
34. Banks, J.L.; Beard, H.S.; Cao, Y.; Cho, A.E.; Damm, W.; Farid, R.; Felts, A.K.; Halgren, T.A.; Mainz, D.T.; Maple, J.R.; et al. Integrated Modeling Program, Applied Chemical Theory (IMPACT). *J. Comput. Chem.* **2005**, *26*, 1752–1780. [CrossRef]
35. Jones, G.; Willett, P.; Glen, R.C.; Leach, A.R.; Taylor, R. Development and validation of a genetic algorithm for flexible docking. *J. Mol. Biol.* **1997**, *267*, 727–748. [CrossRef]
36. Kirton, S.B.; Murray, C.W.; Verdonk, M.L.; Taylor, R.D. Prediction of binding modes for ligands in the cytochromes P450 and other heme-containing proteins. *Proteins* **2005**, *58*, 836–844. [CrossRef] [PubMed]
37. Wróbel, T.M.; Rogova, O.; Andersen, K.L.; Yadav, R.; Brixius-Anderko, S.; Scott, E.E.; Olsen, L.; Jørgensen, F.S.; Björkling, F. Discovery of Novel Non-Steroidal Cytochrome P450 17A1 Inhibitors as Potential Prostate Cancer Agents. *Int. J. Mol. Sci.* **2020**, *21*, 4868. [CrossRef]
38. Ruiz-Castillo, P.; Buchwald, S.L. Applications of Palladium-Catalyzed C–N Cross-Coupling Reactions. *Chem. Rev.* **2016**, *116*, 12564–12649. [CrossRef]
39. Wróbel, T.M.; Rogova, O.; Sharma, K.; Rojas Velazquez, M.N.; Pandey, A.V.; Jørgensen, F.S.; Arendrup, F.S.; Andersen, K.L.; Björkling, F. Synthesis and Structure-Activity Relationships of Novel Non-Steroidal CYP17A1 Inhibitors as Potential Prostate Cancer Agents. *Biomolecules* **2022**, *12*, 165. [CrossRef]
40. Xu, W.L.; Li, Y.Z.; Zhang, Q.S.; Zhu, H.S. A Selective, Convenient, and Efficient Conversion of Sulfides to Sulfoxides. *Synthesis* **2004**, *2004*, 227–232. [CrossRef]
41. Fehl, C.; Vogt, C.D.; Yadav, R.; Li, K.; Scott, E.E.; Aubé, J. Structure-Based Design of Inhibitors with Improved Selectivity for Steroidogenic Cytochrome P450 17A1 over Cytochrome P450 21A2. *J. Med. Chem.* **2018**, *61*, 4946–4960. [CrossRef] [PubMed]
42. Zanger, U.M.; Schwab, M. Cytochrome P450 enzymes in drug metabolism: Regulation of gene expression, enzyme activities, and impact of genetic variation. *Pharmacol. Ther.* **2013**, *138*, 103–141. [CrossRef] [PubMed]
43. Pandey, A.V.; Flück, C.E. NADPH P450 oxidoreductase: Structure, function, and pathology of diseases. *Pharmacol. Ther.* **2013**, *138*, 229–254. [CrossRef] [PubMed]
44. Pippione, A.C.; Carnovale, I.M.; Bonanni, D.; Sini, M.; Goyal, P.; Marini, E.; Pors, K.; Adinolfi, S.; Zonari, D.; Festuccia, C.; et al. Potent and selective aldo-keto reductase 1C3 (AKR1C3) inhibitors based on the benzoisoxazole moiety: Application of a bioisosteric scaffold hopping approach to flufenamic acid. *Eur. J. Med. Chem.* **2018**, *150*, 930–945. [CrossRef]
45. Pippione, A.C.; Kilic-Kurt, Z.; Kovachka, S.; Sainas, S.; Rolando, B.; Denasio, E.; Pors, K.; Adinolfi, S.; Zonari, D.; Bagnati, R.; et al. New aldo-keto reductase 1C3 (AKR1C3) inhibitors based on the hydroxytriazole scaffold. *Eur. J. Med. Chem.* **2022**, *237*, 114366. [CrossRef]
46. Kikuchi, A.; Furutani, T.; Azami, H.; Watanabe, K.; Niimi, T.; Kamiyama, Y.; Kuromitsu, S.; Baskin-Bey, E.; Heeringa, M.; Ouatas, T.; et al. In vitro and in vivo characterisation of ASP9521: A novel, selective, orally bioavailable inhibitor of 17β-hydroxysteroid dehydrogenase type 5 (17βHSD5; AKR1C3). *Investig. New Drugs* **2014**, *32*, 860–870. [CrossRef]
47. Sun, M.; Zhou, Y.; Zhuo, X.; Wang, S.; Jiang, S.; Peng, Z.; Kang, K.; Zheng, X.; Sun, M. Design, Synthesis and Cytotoxicity Evaluation of Novel Indole Derivatives Containing Benzoic Acid Group as Potential AKR1C3 Inhibitors. *Chem. Biodivers.* **2020**, *17*, e2000519. [CrossRef]
48. Hou, Z.; Huang, S.; Mei, Z.; Chen, L.; Guo, J.; Gao, Y.; Zhuang, Q.; Zhang, X.; Tan, Q.; Yang, T.; et al. Inhibiting 3βHSD1 to eliminate the oncogenic effects of progesterone in prostate cancer. *Cell Rep. Med.* **2022**, *3*, 100561. [CrossRef]
49. Sobel, R.E.; Sadar, M.D. Cell Lines Used in Prostate Cancer Research: A Compendium of Old and New Lines—Part 1. *J. Urol.* **2005**, *173*, 342–359. [CrossRef]

Chapter 2

Endocrine Disrupting Chemical as structural cues for the development of inhibitors of CYP17A1 activity

Section C: Essential oil components may act as antiandrogen compounds in prostate cancer by inhibition of steroidogenic cytochrome P450 activities.

Status: Submitted, preprint available

My Contributions in the paper:

Original draft was prepared by me under the guidance of co-author, Amit V Pandey.
Following sections were contributed by other co-authors:
Section 2 (Materials and Methods): Molecular Docking analysis, Steroid profiling.
Section 3 (Results): Docking with CYP17A1 and CYP19A1

Concept and Methodology was shared between me and co-authors, Angelo Lanzilotto and Amit V Pandey

In vitro experiments:

- Maintenance of cell culture: NCI H295R cell line and LNCaP cell line
- Cell-based enzyme assays - CYP17A1 17α-Hydroxylase activity, CYP17A1 17,20 Lyase activity and CYP19A1 activity in microsomal preparations
- Treatment of cells and preparation of media for steroid profiling by LC/MS
- Cell viability assays

Figures:

- Figure 1: An overview of biological activities of essential oil components
- Figure 2: Androgen production in humans
- Figure 3: Prostate cancer cells are driven by the binding Androgens to the Androgen Receptor 105 (AR).
- Figure 7: Assay of CYP17A1 17α-hydroxylase activity.
- Figure 8: Effect of essential oil compounds of CYP17A1 17,20 lyase activity.
- Figure 9: Effects of essential oil components on CYP19A1 activity
- Figure 10: Effect of essential oil components on LNCaP cell proliferation.
- Figure 11: Steroid profiling using LC-MS/MS.
- Figure 12: Different approaches to target androgen production for prostate cancer 417 treatment.

Statistical analysis for enzyme assays and generating graphs.

Essential Oil Components May Act as Antiandrogen Compounds in Prostate Cancer by Inhibition of Steroidogenic Cytochrome P450 Activities

Katyayani Sharma , Angelo Lanzilotto , Jibira Yakubu , Søren Therkelsen , Clarissa Daniela Voegel , Therina Du Toit , Flemming Steen Jørgensen , Amit V. Pandey *

Posted Date: 1 November 2023

doi: 10.20944/preprints202311.0063.v1

Keywords: EDCs; Prostate cancer; CYP17A1; steroidogenesis; DHEA; anti cancer drugs

Article

Essential Oil Components May Act as Antiandrogen Compounds in Prostate Cancer by Inhibition of Steroidogenic Cytochrome P450 Activities

Katyayani Sharma [1,2,3], Angelo Lanzilotto [1,2], Jibira Yakubu [1,2,3], Søren Therkelsen [1,2,4], Clarissa Daniela Vöegel [2,5], Therina Du Toit [1,2,5], Flemming Steen Jørgensen [4], Amit V. Pandey [1,2,*]

[1] Department of Pediatrics, Division of Endocrinology, Diabetology and Metabolism, University Children's Hospital, Inselspital, University of Bern, 3010 Bern, Switzerland; katyayani.sharma@unibe.ch (K.S.); angelolanzilotto@gmail.com (A.L.); jibira.yakubu@unibe.ch (J.Y.); therina.dutoit@unibe.ch (T.d.T.); amit.pandey@unibe.ch (A.V.P.)
[2] Translational Hormone Research Program, Department of Biomedical Research, University of Bern, 3010 Bern, Switzerland; clarissa.voegel@insel.ch (C.V.)
[3] Graduate School for Cellular and Biomedical Sciences, University of Bern, 3012 Bern, Switzerland
[4] Department of Drug Design and Pharmacology University of Copenhagen, 2100 Copenhagen, Denmark; fsx728@alumni.ku.dk (S.T.); fsj@sund.ku.dk (F.S.J.)
[5] Department of Nephrology and Hypertension, University Hospital Inselspital, University of Bern, 3010 Bern, Switzerland
* Correspondence: amit.pandey@unibe.ch ; Tel.: +41-31-632-9637

Abstract: Endocrine-disrupting chemicals (EDCs) may impact the development of Prostate Cancer (PCa) by altering the steroid metabolism. Although their exact mechanism of action in controlling tumor growth is not known, EDCs may inhibit steroidogenic enzymes such as Cytochrome P450 c17 (CYP17A1) or aromatase (CYP19A1) involved in the production of Androgens or Estrogens. High levels of circulating androgens are linked to PCa in men and Polycystic Ovary Syndrome (PCOS) in women. Essential Oils or their metabolites (EOs) like lavender oil and tea tree oil have been reported to act as potential EDCs and contribute towards sex steroid imbalance in case of prepubertal gynecomastia in boys and premature thelarche in girls due to the regular exposure to lavender-based fragrances among Hispanic population. We screened a range of EO components to determine their effects on CYP17A1 and CYP19A1 Computational docking was performed to predict the binding of EOs with CYP17A1 and CYP19A1 and functional assays were done using the radiolabeled substrates or Liquid Chromatography high-resolution Mass Spectrometry and cell viability assays were carried out in LNCaP cells. Many of the tested compounds bind close to the active site of CYP17A1, and (+)-Cedrol had the best binding with CYP17A1 and CYP19A1. Eucalyptol, Dihydro-β-Ionone & (-)-α-pinene showed 20% to 40% inhibition of dehydroepiandrosterone production; and some compounds also effected CYP19A1. Extensive use of these EOs in various beauty and hygiene products is common, but only a limited knowledge about their potential detrimental side effects exists. Our results suggest that prolonged exposure to some of these essential oils may result in steroid imbalances. On the other hand, due to their effect on lowering androgen output, ability to bind at the active site of steroidogenic cytochrome P450s, these compounds may provide design ideas for the novel compounds against hyperandrogenic disorders such as PCa and PCOS.

Keywords: EDCs; Prostate cancer; CYP17A1; steroidogenesis; DHEA; anti cancer drugs

1. Introduction

Essential Oils (EOs) are a complex mixture of volatile compounds extracted from aromatic plant tissues with a characteristic "essence" or smell [1]. Pure extracts of EOs are obtained through different

Preprints (www.preprints.org) | NOT PEER-REVIEWED | Posted: 1 November 2023 doi:10.20944/preprints202311.0063.v1

methods such as steam distillation, solvent extraction, and hydro distillation [2]. The chemical composition of EOs can vary depending on the origin and species of the plant, climate, and extraction method [3]. Two major constituents of EOs are terpenes and terpenoids [4]; some examples of terpenes found in EOs are cineol (eucalyptol), linalool, pinene, limonene, thujene, bisabolene, caryophyllene, p-cymene, camphor, neral, menthol, and geraniolwhile aromatic compounds consist of carvacrol, thymol, cinnamaldehyde, eugenol, and estragole [5]. Owing to their charestric fragrance, EOs are extensively used in many cosmetics and hygiene products [6,7]. Due to their anti-microbial, antibiotic, antiviral, antioxidant, and anti-inflammatory properties, they have been part of traditional therapies and herbal medicines [8–10] (Figure 1). Being "natural" in origin, EOs are often considered as safer substitutes of chemical drugs that may have adverse side effects [11]. However, in addition to their therapeutic role, EOs might function as potential Endocrine Disrupting Chemicals (EDCs).

EDCs are chemical substances that can alter endocrine function by interfering with steroid metabolism resulting in hormonal imbalance in the body. Abnormal levels of steroids, especially sex steroids, can cause detrimental effects on sexual development and possess an increased risk of infertility [12], though the exact mechanism of action of EDCs is not fully known. Clinical case reports have linked prepubertal gynecomastia in boys and premature thelarche in girls to prolonged use of lavender and tea tree oil-based fragrant products which resolved upon cessation of the products. Moreover, studies in human breast cancer cell lines showed estrogenic and anti-androgenic activity of some EOs [8,13].

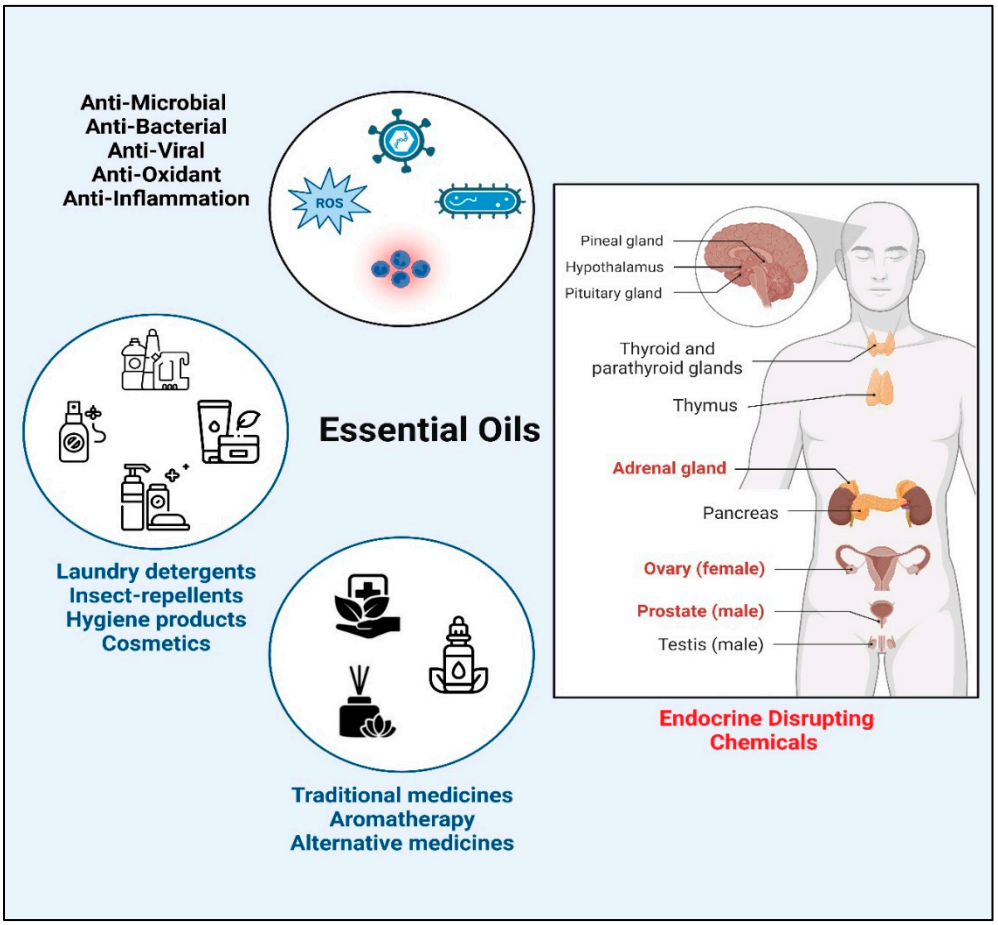

Figure 1. An overview of biological activities of essential oil components.

In humans, androgens are primarily produced in the male testis, female ovaries, and adrenal glands (Figure 2). Androgens control male sexual traits and development as well as influence female sexual behavior. The zona reticularis of the adrenal cortex produces dehydroepiandrosterone (DHEA) and its sulfate DHEA(S). DHEA acts as a precursor to produce androgens (testosterone and androstenedione). The first rate-limiting step in the biosynthesis of all steroid hormones is the

Preprints (www.preprints.org) | NOT PEER-REVIEWED | Posted: 1 November 2023 doi:10.20944/preprints202311.0063.v1

cleavage of the cholesterol side chain by the mitochondrial P450 enzyme CYP11A1 system (CYP11A1-FDX-FDXR) also called P450scc, to convert cholesterol into pregnenolone (Preg) [14]. Further in multi-enzymatic steps, Preg is converted into mineralocorticoids, glucocorticoids, and androgens.

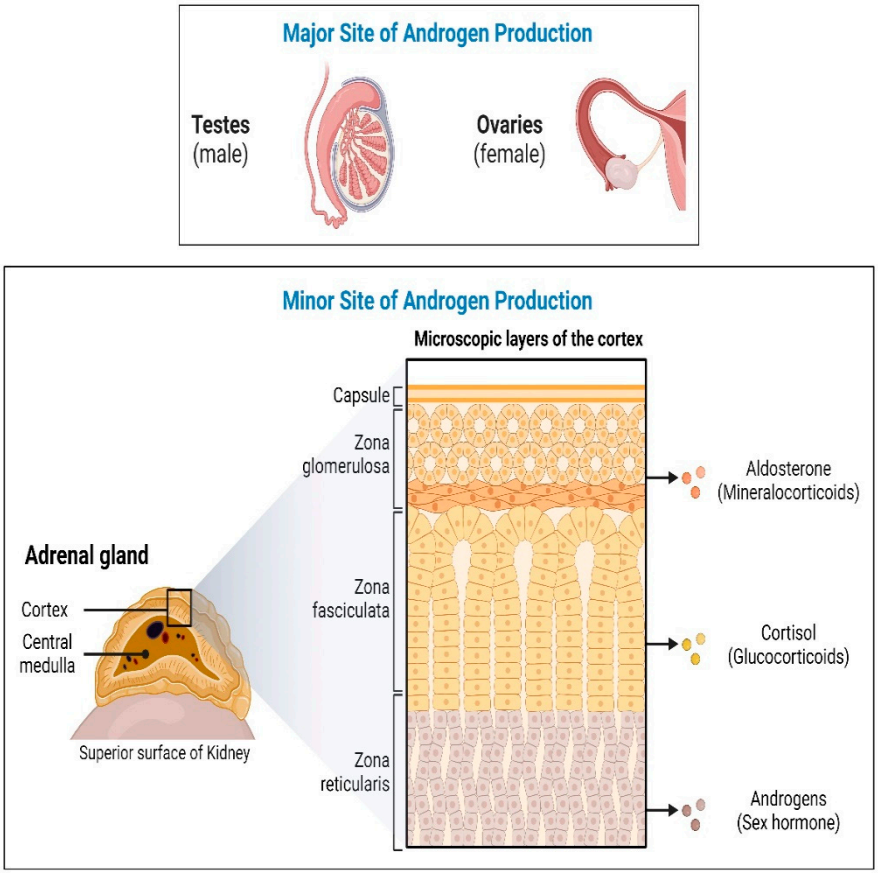

Figure 2. Androgen production in humans. In humans, androgens are mainly produced in the adrenal glands, male testis and female ovaries. Sexual traits and development as well as influence on female sexual behavior may be regulated by androgens. Androgen precursors, dehydroepiandrosterone (DHEA) and its sulfate DHEA(S) are produced in the zona reticularis of the adrenal cortex which are then converted into active androgens by the action of a series of steroid metabolizing enzymes.

The enzyme P450c17 (CYP17A1, Cytochrome P450 17alpha-monooxygenase), encoded by *CYP17A1* gene [15,16] is an essential enzyme that plays a vital role in adrenal androgen production [16,17]. The CYP17A1 localized in the endoplasmic reticulum can catalyze both 17α-hydroxylase and 17,20 lyase reactions [18]. This characteristic dual activity is conferred through post-translational regulation of CYP17A1 protein. Especially, the 17, 20 lyase activity of CYP17A1 is supported by at least three factors. First, the amount of P450 Oxidoreductase (POR) for electron transfer [19,20], second, the presence of allosteric activator microsomal Cytochrome B5 (CYB5) [21,22], and third, the phosphorylation of the CYP17A1 protein at serine/threonine residues [22–26]. Understanding the regulatory mechanisms of 17,20 lyase activity is important for the understanding of hyperandrogenic disorders such as premature, exaggerated adrenarche, PCa, and PCOS [27,28].

Epidemiological studies suggest that EDCs may function as hormone mimics and bind to nuclear receptors to elicit altered expression of genes involved in the development and progression of Prostate Cancer (PCa) [29] (Figure 3). Prostate tumor cells are driven by Androgens binding to the intracellular Androgen Receptor (AR). The AR acts as a transcriptional activator for the expression of genes responsible for the growth and survival of the tumor [30]. These studies suggest that the possible role of EOs could be either in direct inhibition or co-activation of certain steroidogenic enzymes or in the regulation of gene expression of these enzymes resulting in abnormal androgen

Preprints (www.preprints.org) | NOT PEER-REVIEWED | Posted: 1 November 2023 doi:10.20944/preprints202311.0063.v1

levels in the body. High levels of circulating androgens are linked to both PCa and Polycystic Ovary Syndrome (PCOS) [31]. The anti-androgenic property of EOs could be exploited to target androgen production in the treatment of PCa and PCOS.

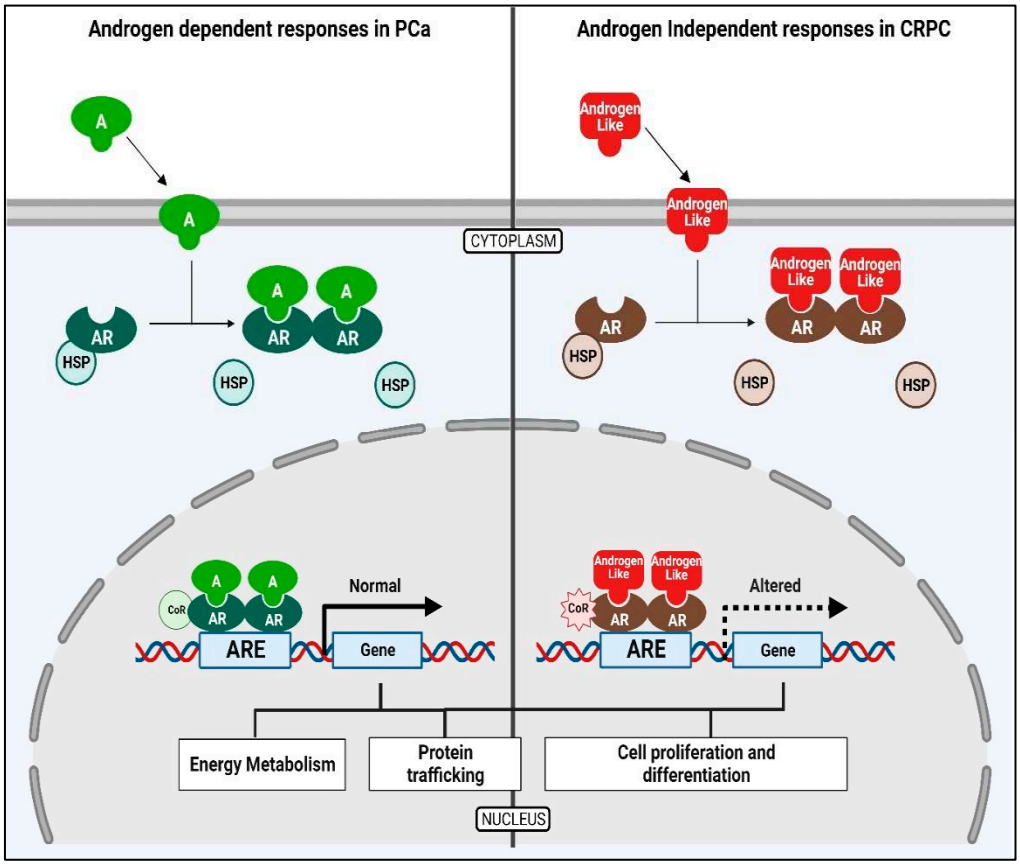

Figure 3. Prostate cancer cells are driven by the binding Androgens to the Androgen Receptor (AR). The AR then acts as a transcriptional activator for the expression of genes that are responsible for the growth and progression of the prostate cancer cells.

Considering the potential role of essential oils as EDCs, we explored the potential of several common essential oil components on human steroid metabolizing enzymes CYP17A1 and CYP19A1 for potential effects on androgen and estrogen production in humans and as potential structural leads for design of novel chemicals targeting these enzymes in hormone dependent cancers. We docked 53 terpene compounds that are naturally present in essential oils, into the structures of steroid-metabolizing enzymes CYP17A1 and CYP19A1 in order to estimate binding affinity and possible binding modes and sites to identify possible endocrine disrupting properties of these compounds.

2. Materials and Methods

Terpenes: The terpenes used in the experiments cannot be called essential oils, as they do not exist as mixtures of compounds but are commercially available as single chemical entities (sometimes multiple isomers coexist because the separation process can bring purity only to a certain point). The terpenes we sourced are of mixed natural/synthetic origin depending on which provided higher purity. Their isolation usually consisted of an essential oil first collected through steam distillation or alcoholic extraction of the dry plant/flower mass, and then fractional distillation to collect the main components.

All terpenes were sourced from Sigma Aldrich, unless otherwise indicated, and the (individual product purity was between 90-99%) product codes were: (-)-α-Pinene (305715, (purity 99%), (+)-α-Pinene (268070, purity 99%), α-Ionone (I12409, purity 90%), Benzaldehyde (B1334, purity 99%), p-Anisaldehyde (A88107, purity 98%), 1,4-Cineole (W365820, purity 95%), Isoamyl acetate (W205532,

 doi:10.20944/preprints202311.0063.v1

purity 97%), Octyl acetate (W280607, purity 98%), Benzyl acetate (B15805, purity 99%), Propyl acetate (133108, purity 99%), β-Pinene (402753, purity 99%), Bisabolene (Alfa Aesar, A18724, mixture of isomers), (−)-α-Bisabolol (14462, purity 93%), 3-Carene (115576, purity 90%), (S)-(+) Carvone (435759, purity 96%), (+)-Cedrol (22135, purity 99%, sum of enantiomers), Cinnamyl alcohol (108197, purity 98%), p-Cymene (C121452, purity 99%), Dihydrocarvone (218286, purity 98%, mixture of isomers), Dihydro-β-ionone (W362603, purity 90%), Eucalyptol (C80601, purity 99%), Farnesol (W247804, purity 95%, mixture of isomers), Geraniol (163333, purity 98%), Methyl anthranilate (W268208, purity 98%), (R)-(+)-Limonene (183164, purity 98%), (+-)-Citronellal (27470, purity 95%), (R)-(-) Carvone (124931, purity 98%), (1R)-(-) Myrtenal (218243, purity 98%), Nerol (268909, purity 97%), Ocimene (W353977, purity 90%, mixture of isomers), (S)-(-)-Limonene (218367, purity 96%), Carvacrol (282197, purity 98%), (+)-Sabinene (W530597, purity 75%), (S)-(-) Perillyl alcohol (218391, purity 96%), Estragole (A29208, purity 98%), (-)-α-Terpineol (W304522, purity 96%), Terpinolene (W304603, purity 95%), Thymol (T0501, purity 98%), Vanillin (V1104, purity 99%), Methyl salicylate (M6752, purity 99%), α-Terpinyl acetate (W304799, purity 95%), α-Phelladrene (W285611, purity 85%), γ-Terpinene (223190, purity 97%).

Molecular Docking Analysis: In a first attempt, 53 terpene compounds were docked into CYP17A1 and CYP19A1 using AutoDock VINA [32,33]. Ligands co-crystallized with the PDB structures [34] in PDB IDs 4NKZ [35] and 3S79 [36–38] (CYP17A1 and CYP19A1, respectively) were removed, and the remaining protein structures were used for docking. Three-dimensional structures of the ligands were extracted from PubChem and prepared for docking using the LigPrep [39] function within Maestro [Schrödinger Release 2022-3: Maestro, Schrödinger, LLC, NY, 2021], removing possible salts and ensuring generation of possible ionization and tautomeric states at pH=7±1 using the Epik [40] setting. Prior to docking the compounds were subjected to a short energy minimization. As reference compounds, abiraterone and 17α-hydroxypregnenolone were docked into CYP17A1 as well and androstenedione into CYP19A1 and compared with known structures of CYP17A1 [35,41,42] and CYP19A1 [36–38,43]. This yielded a global docking simulation including the whole protein structure. For each ligand, 25 docking runs were performed. The results were subjected to a cluster analysis with each cluster differing at least 5Å heavy atom RMSD, representing different possible sites and modes of binding.

In a further refinement of this process, the compounds were docked into not only CYP17A and CYP19A1, but also to CYP11A1 and CYP21A2 with GLIDE [v 5.8, Schrödinger, LLC, NY, 2021] using both the SP and XP scoring functions [44,45]. Subsequently, the best scoring poses for each compound for each enzyme and for each scoring function were extracted and analyzed and heat maps produced (cf. Figure 4).

Chemicals: Trilostane was obtained from the extraction of commercially available tablets as Modrenal® (Bioenvision, NY, USA). Abiraterone acetate was purchased from MedChemExpress®, Lucerna Chem AG (Lucerne, Switzerland). Commercially available drug, Anastrazole was purchased from AstraZeneca. Radiolabeled substrates, Progesterone [4-^{14}C] (SA 55mCi/mmol; Conc. 0.1mCi/mL); 17α-Hydroxypregnenolone [21-^{3}H] (SA 15Ci/mmol; Conc. 1mCi/mL) and Androstenedione [1β-^{3}H(N)] (SA 24 Ci/mmol; Conc. 1mCi/mL) were obtained from American Radiolabeled Chemicals Inc. (St. Louis, MO, USA). Non-radiolabeled standard substrates, Pregnenolone; Progesterone; 17α-Hydroxypregnenolone; 3-(4,5-Dimethyl-2-thiazolyl)-2,5-diphenyl-2H-tetrazolium bromide (MTT); Resazurin sodium salt; Dimethyl sulfoxide (DMSO) and Dextran were purchased from Sigma-Aldrich® (St. Louis, MO, USA). NADPH tetrasodium salt and Organic solvents such as Isooctane, Ethyl acetate, and Chloroform/Trichloromethane were acquired from Carl Roth® GmbH + Co. KG (Karlsruhe, Germany). Activated Charcoal was obtained from Merck AG (Darmstadt, Germany).

Cell line and culture: The current standard model system to study molecular and biochemical mechanisms of steroidogenesis is the NCI H295R cell line [46,47]. These cells express genes from all three zones of the adrenal cortex, providing an excellent system that closely reflects human adrenal physiology [14]. The human adrenocortical carcinoma cell line NCI H295R was obtained from the American Type Culture Collection (ATCC® CRL2128™), Manassas, VA, USA [46,47]. Cells between

 doi:10.20944/preprints202311.0063.v1

passages 12-24 were cultivated in DMEM/Ham's F-12 medium (1:1 Mix) supplemented with L-glutamine and 15 mM HEPES (Gibco™, Thermo Fisher Scientific, Waltham, MA, USA) along with 5% Nu-Serum I; 0.1% insulin, transferrin, selenium in form of ITS Premix (Corning™, Manassas, VA, USA); 1% Penicillin-Streptomycin (Gibco™, Thermo Fisher Scientific, Waltham, MA, USA) at 37°C in a humid atmosphere with a constant supply of 5% carbon dioxide to maintain the physiological pH. Human prostate cancer cell line, derived from metastatic site, left supraclavicular lymph node, LNCaP clone FGC (ATCC® CRL1740™) was cultured in RPMI-1640 Medium containing 2mM L-glutamine with 10mM HEPES, 1mM Sodium pyruvate, 10% Fetal Bovine Serum and 1% Penicillin-Streptomycin as supplements (Gibco™, Thermo Fisher Scientific, Waltham, MA, USA). For experiments, cells with passage numbers 12-30 were used as previously described [48].

Cell Viability Assays: To determine the effect of test compounds on the cellular activity of human adrenal NCI H295R cells, MTT-based cell viability assay was performed [49,50]. In a 96-well plate, about 30,000 cells per well were seeded with complete medium. After 24 hours, the medium was replaced with fresh medium and 10μM of test compounds were added. DMSO (less than 1% v/v) was used as vehicle control. 10μM Abiraterone was used as a positive control [51,52]. 0.5mg/mL MTT reagent was added to the culture medium for another 4 hours. After the incubation, the medium was entirely replaced with DMSO to dissolve the formazan crystals. After 20 minutes, absorbance was measured at 570nm (SpectraMax M2, Bucher Biotec, Basel Switzerland). Percent viability is calculated with respect to the mean value of control samples.

For prostate cancer LNCaP cells, Resazurin-based Alamar blue assay was performed to evaluate the cell toxicity [49,50]. Cells seeded at a cell density of 10,000 cells per well were treated with test compounds and the controls for 24 and 48 hours. After incubation, 0.05mg/mL Resazurin in Phosphate buffer was added. Cells were incubated for another 4 hours in dark at 37°C. Fluorescence was measured at an excitation wavelength of 550nm and an emission wavelength of 590nm. Percent viability is calculated with respect to the mean value of control samples (DMSO).

CYP17A1 enzyme assays: The CYP17A1 enzyme assays were carried out according to well-established protocols [52,53] in our laboratory. The NCI H295R cells were seeded overnight in a 12-well plate at a cell density of 0.5 X 10^6 cells per well. Next day, 10μM of test compounds were added to respective wells containing fresh medium and incubated for 4 hours. Abiraterone and DMSO were used as reference and control respectively. To determine CYP17A1 hydroxylase activity, cells were treated with the [^{14}C]-Progesterone at a concentration of 10,000cpm/1μM per well [22–24,54]. Trilostane was added prior to the addition of test compounds and the substrate to block 3β-hydroxysteroid dehydrogenase activity [55]. Radiolabeled steroids were extracted from the media with help of Ethyl acetate and Isooctane (1:1 v/v) and separated through Thin Layer Chromatography (TLC) on a Silica gel coated aluminum plate (Supelco® Analytics, Sigma Aldrich Chemie GmbH, Germany) [56]. TLC spots were exposed to a phosphor screen and detected by autoradiography using Typhoon™ FLA-7000 PhosphorImager (GE Healthcare, Uppsala, Sweden). Radioactivity was quantified using ImageQuant™ TL analysis software (GE Healthcare Europe GmbH, Freiburg, Germany). Enzyme activity was calculated as a percentage of radioactivity incorporated into the product with respect to the total radioactivity.

Using similar treatment conditions, [21-^{3}H]-17α-Hydroxypregnenolone (50,000cpm/1uM per well) was used as a substrate to analyze CYP17A1 Lyase activity . NCI H295R cells were treated with test compounds for 24hours before the addition of the substrate and Trilostane. Tritiated water release assay was performed [57] by measuring the conversion of 17OH-Preg into DHEA. Steroids in the media were precipitated using 5% activated charcoal/0.5% dextran solution. The enzyme activity was estimated with reference to the water-soluble tritiated by-product formed in an equimolar ratio with the corresponding DHEA. The radioactivity in the aqueous phase was measured by Liquid Scintillation counting (MicroBeta2® Plate Counter, PerkinElmer Inc. Waltham, MA, USA). The percent inhibition was calculated with respect to the control [58].

Steroid Profiling: For steroid analysis, NCI H295R cells were treated in a similar way except that 1μM of the unlabeled substrate, Pregnenolone, was used instead of radiolabeled substrates for 4 hours. Steroids were measured by a liquid chromatography high-resolution mass spectrometry (LC-

 doi:10.20944/preprints202311.0063.v1

HRMS) method as previously described and validated [59]. Briefly, steroids were extracted from 500 µL cell media aliquots, plus 38 µL of a mixture of internal standards (at 3.8 nM each), using solid-phase extraction with an OasisPrime HLB 96-well plate. Samples were resuspended in 100 µL 33% methanol and 20 µL injected into the LC-HRMS instrument (Vanquish UHPLC coupled to a Q Exactive Orbitrap Plus, from Thermo Fisher Scientific) using an Acquity UPLC HSS T3 column (from Waters). Data from the mass spectrometer was processed using TraceFinder 4.0 (from Thermo Fisher). The lower limit of quantification (LOQ) for pregnenolone was 0.77 nmol/L, for DHEA it was 0.85 nmol/L, for DHEA-S it was 6.25 nmol/L and for 17OHP5 (quantified relative to the calibration of progesterone using a calculated response factor) it was 20 nmol/L.

Aromatase (CYP19A1) Assay: Estrogens are synthesized from androgens through the action of the enzyme, Cytochrome P450c19a1 (CYP19A1, Aromatase) [60]. We used 40 µg of microsomal fraction from placental JEG-3 (Human Choriocarcinoma; ATCC® HTB36™) cells in 100mM potassium phosphate buffer (pH 7.4) containing 100mM NaCl in a reaction mixture of 200 µL to carry out Aromatase enzyme activity assay. For determining the impact on aromatase activity, 10 µM of test compounds, DMSO as a negative Control, and Anastrozole (a known CYP19A1 inhibitor) as positive control were added to the reaction mixture. Tritium-labelled Androstenedione (~30,000 cpm/µL/50nM) was used as the substrate to monitor the enzyme activity. The chemical reaction was initiated by the addition of reduced Nicotinamide adenine dinucleotide phosphate (NADPH) followed by incubation at 37°C with constant shaking for 1 hour. The reaction was stopped by the addition of Charcoal/Dextran solution. Enzyme activity was measured using a Tritiated water release assay as described earlier [53,61].

Statistical analysis: Calculations were done with Microsoft Excel and GraphPad Prism 3.0 (Graph Pad Software, Inc. San Diego, CA, USA). Data are represented as the mean of triplicate values from a single experiment or three independent sets of experiments. Dunnett's multiple comparison ANOVA test was performed to determine the significant difference between the mean values of samples and the control. Error bars exhibit standard deviation from respective mean values. Significant p values were set as $*p < 0.05$ and $**p < 0.01$, $***p < 0.001$.

3. Results

Docking with CYP17A1 and CYP19A1 - We performed computational docking and binding analysis of essential oil compounds against the three-dimensional crystal structures of multiple steroid metabolizing cytochrome P450 enzymes including CYP11A1, CYP17A1, CYP19A1 and CYP21A2.

Preprints (www.preprints.org) | NOT PEER-REVIEWED | Posted: 1 November 2023 doi:10.20944/preprints202311.0063.v1

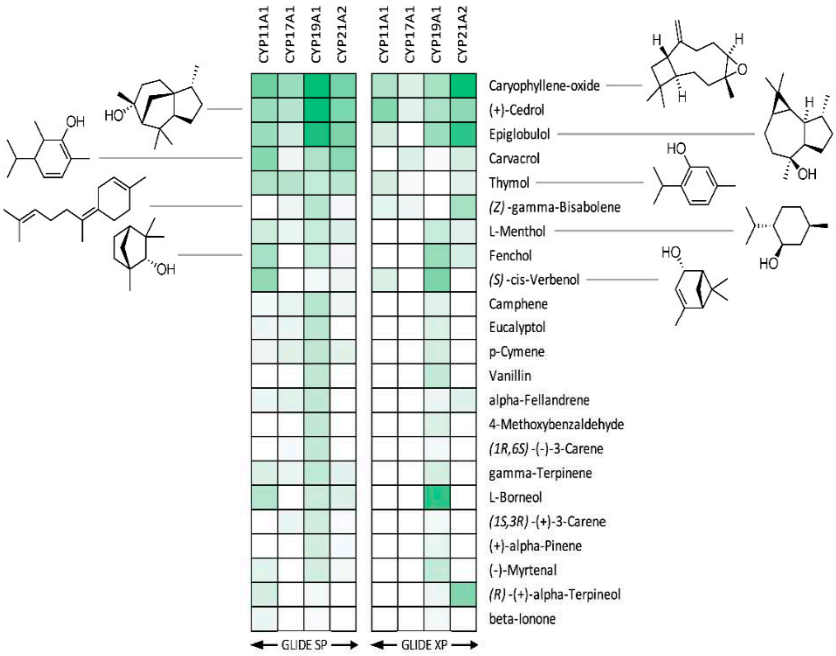

Figure 4. Heat maps of binding poses obtained after docking of terpenes from essential oils into steroid metabolizing CYP enzymes. Binding energies vary from -8.2 kcal/mol for the best binding poses (corresponding to dark green boxes) to -3.3 kcal/mol for the poorest binding poses (white boxes).

Best binders were clustered into groups based on binding to multiple enzymes and subjected to detailed binding analysis. While we observed no significant selectivity (Figure 4), we identified the generally potential best binders for these CYP enzymes and made a preliminary look at the binding mode of the best poses. The conclusion is that a small number of compounds (Caryophyllene oxide, (+)-Cedrol and Epiglobulol), seems to bind reasonably well to the CYPs primarily by hydrophobic interactions. The compounds bind in the active sites of both CYP17A1 and CYP19A1 without coordinating directly to the Fe atom in the heme group (Figure 5). Docking studies revealed that (+)-Cedrol was among the best binding compounds to both CYP17A1 and CYP19A1 (Figure 6). Experimental results provided some context to the computational studies. Though it didn't inhibit CYP17A1 activity, it caused 30% inhibition of CYP19A1 activity. Dihydro-β-Ionone showed 30% inhibition of both CYP17A1 and CYP19A1 activities. Eucalyptol and (-)-α-pinene showed 20% to 40% inhibition of CYP17A1. Although the inhibition was weaker than the reference compounds, it could be an inspiration for design of novel inhibitors, since the top scoring poses are rather globular compounds filling the cavity above the heme group in the CYPs.

Preprints (www.preprints.org) | NOT PEER-REVIEWED | Posted: 1 November 2023 doi:10.20944/preprints202311.0063.v1

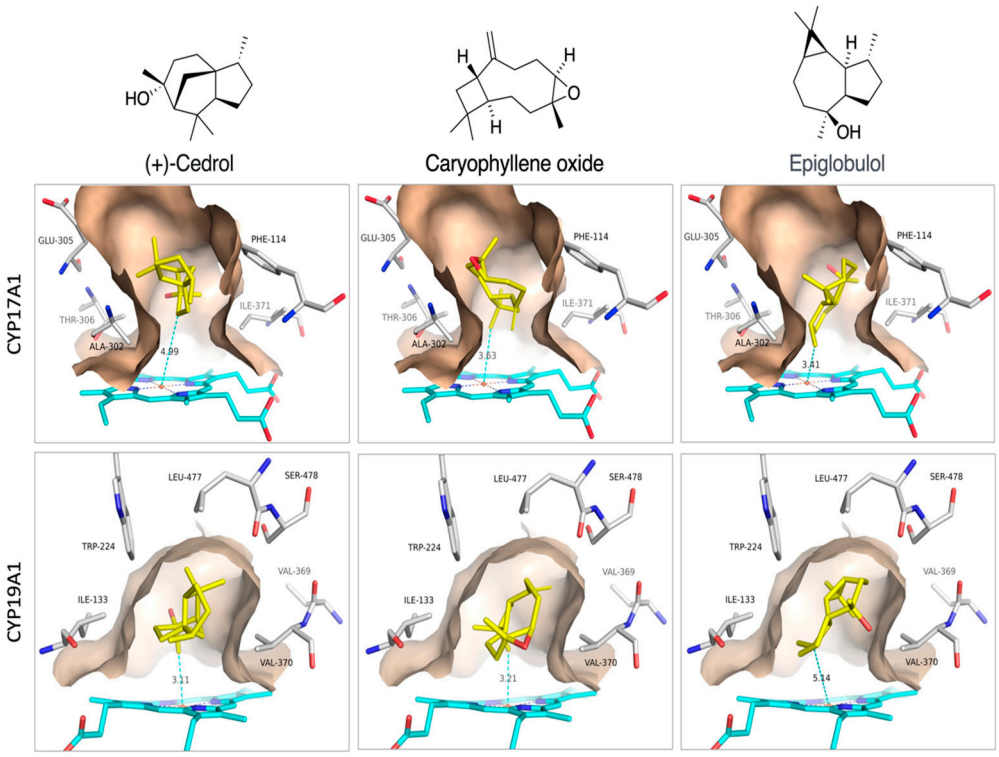

Figure 5. Proposed binding modes of (+)-Cedrol, Caryophyllene oxide and Epiglobulol to CYP17A1 and CYP19A1.

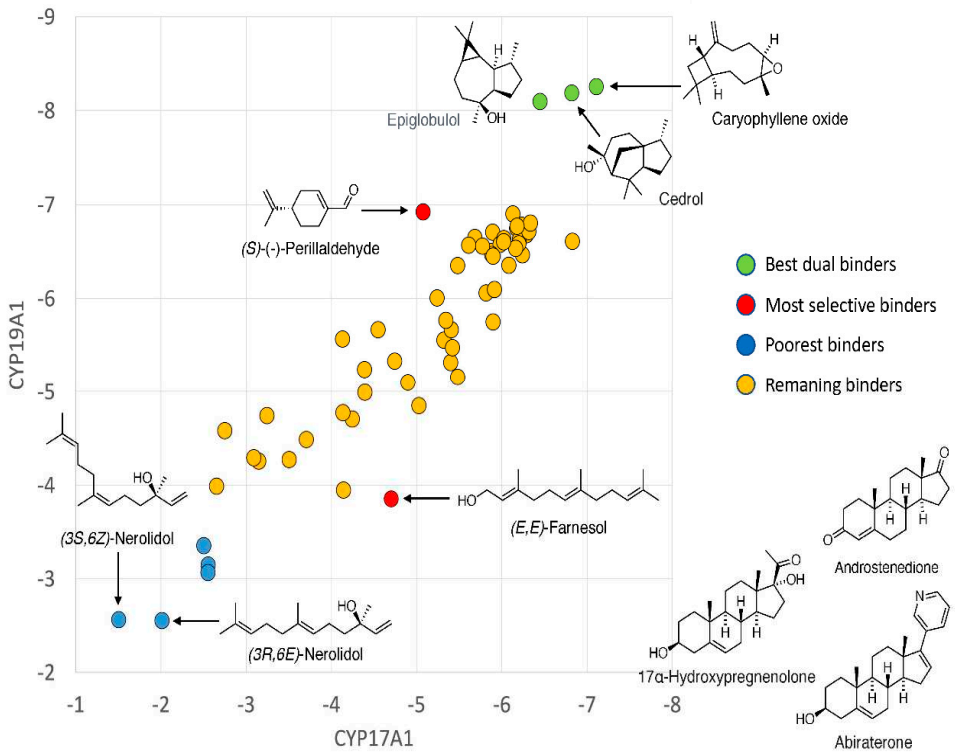

Figure 6. CYP17A1/CYP19A1 selectivity. Plot of binding energies to CYP17A1 and CYP19A1, respectively. Known substrates/inhibitors of CYP17A1 and CYP19A1 were used as controls.

Preprints (www.preprints.org) | NOT PEER-REVIEWED | Posted: 1 November 2023 doi:10.20944/preprints202311.0063.v1

Effect on CYP17A1 Activity – Studies in human cell lines [8,13] have shown that Lavender oil (LO) and Tea tree oil (TTO) act as hormone mimics for Estrogen receptors (ER) and antagonists for AR. Moreover, LO and TTO impacted the ER and AR-mediated regulation of several endogenous genes. Owing to these different mechanisms of action by LO and TTO, we screened several EO components including the ones found in TTO and LO. In the initial screening of 50 test compounds against CYP17A1 hydroxylase activity, we found no significant effect in NCI H295R cells treated with 10 μM of compounds for 4 hours (Figure 7).

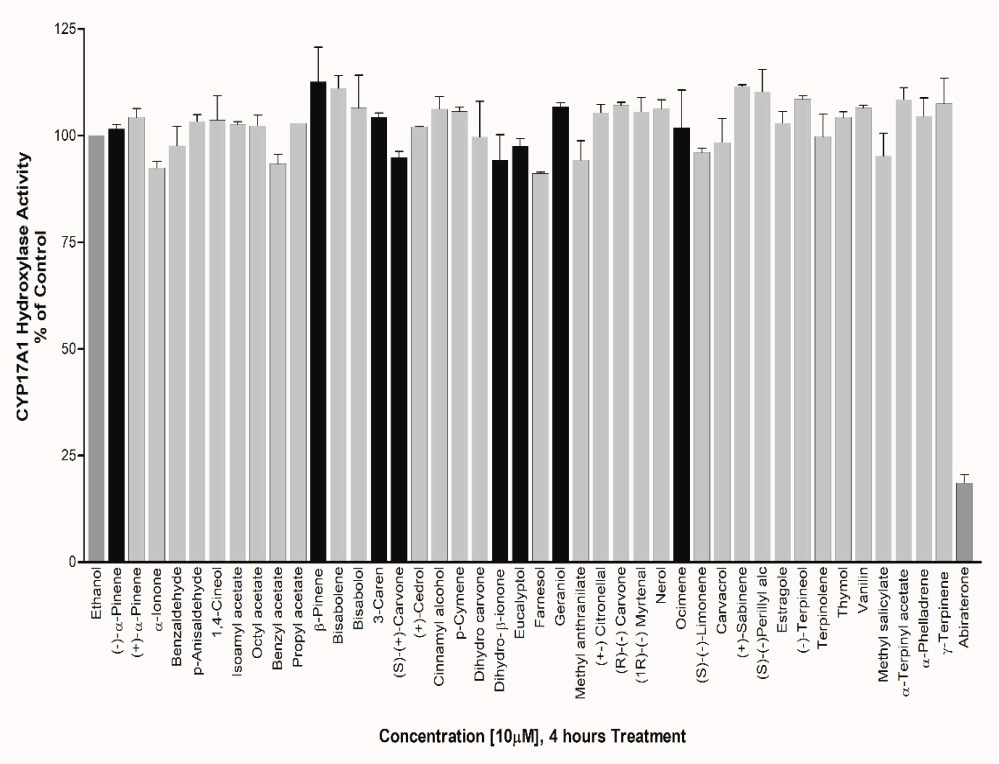

Figure 7. Assay of CYP17A1 17-hydroxylase activity. Essential oil compounds were tested for effects on CYP17A1 17-hydroxylase activity using radiolabelled progesterone as substrate and conversion to 17-hydroxy progesterone was monitored using autoradiography of steroids after separation by TLC. Effects were calculated as percentage of control.

However, EOs such as Eucalyptol, Geraniol, (S)-(+) Carvone, 3-Caren, Ocimene, β-Pinene, (-)-α-Pinene, Dihydro-β-ionone showed about 13%, 13%, 15.2%, 16%, 18%, 19%, 20% and 31% inhibition in CYP17A1 Lyase activity respectively. The effect of EOs towards an exclusive inhibition of CYP17A1 lyase activity makes them good candidates to study further as basic structural leads for designing more potent inhibitors (Figure 8).

Effect on CYP19A1 Activity – EOs exhibiting significant effect on CYP17A1 activity and those predicted to be estrogenic in nature in some literatures were selected for screening of CYP19A1 activity. Bisabolol, Cedrol, Dihydro-β-ionone, (R)-(+)-Limonene, (-)-Terpineol, and α-Terpinyl acetate showed significant inhibition of aromatase at about 22%, 29%, 33%, 26%, 27%, and 29% respectively (Figure 9). Dihydro-β-ionone was found to be the most effective inhibitor of both CYP17A1 Lyase activity and CYP19A1 activity.

Effect on Prostate Cancer Cell Viability – (-)-α-Pinene, Dihydro-β-ionone, Eucalyptol were also found to be causing cell toxicity in the prostate cancer cell line, LNCaP cells. All of these compounds showed an increased potency for cell growth inhibition with increasing treatment durations. Up to 50% reduction in cell viability was observed when the cells were treated with these EOs for 48 hours. Cedrol which showed maximum inhibition of CYP19A1 activity was also found to be reducing the cell viability of LNCaP cells. However, since a direct effect on CYP17A1 activity was not observed by cedrol, a different mechanism may be involved in toxicity towards LNCaP cells (Figure 10).

Preprints (www.preprints.org) | NOT PEER-REVIEWED | Posted: 1 November 2023 doi:10.20944/preprints202311.0063.v1

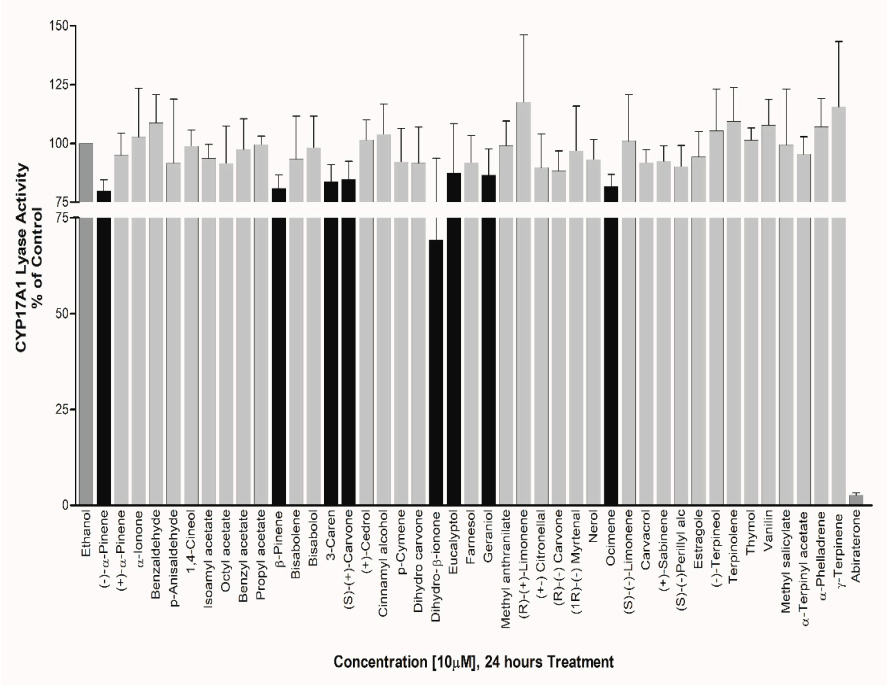

Figure 8. Effect of essential oil compounds of CYP17A1 17,20 lyase activity. Compounds were tested for effects on CYP17A1 17,20 lyase activity using radiolabeled 17OH-Pregnenolone as substrate and conversion to DHEA was monitored using scintillation counting. Effects were calculated as percentage of control.

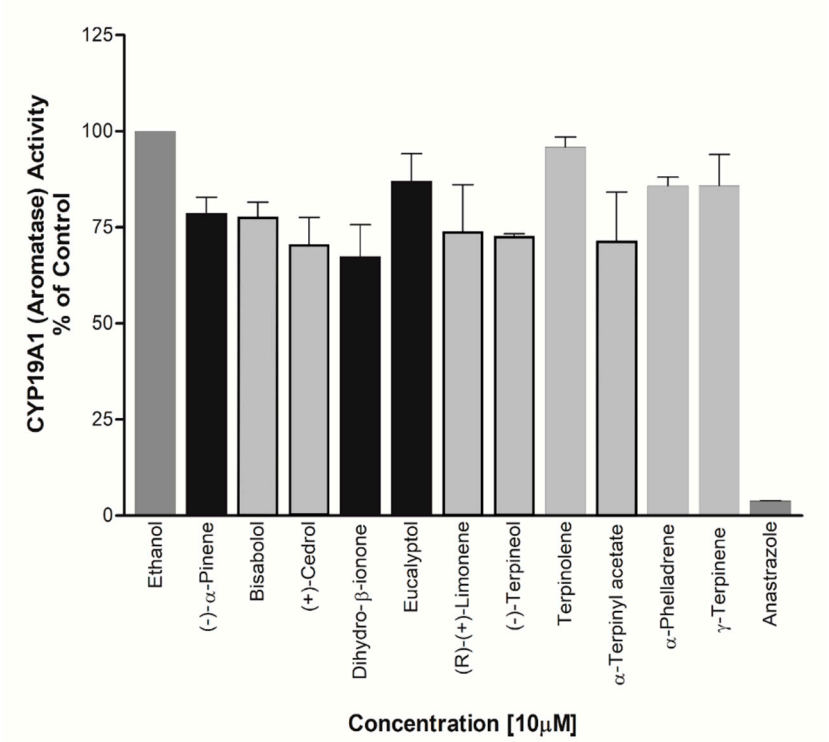

Figure 9. Effects of essential oil components on CYP19A1 activity. Essential oil components were tested against CYP19A1 activity using microsomes prepared from placental JEG-3 cells. Radiolabeled androstenedione was used as substrate and conversion to estrone was monitored by water release assay. A known CYP19A1 inhibitor anastrazole was used as positive control.

Preprints (www.preprints.org) | NOT PEER-REVIEWED | Posted: 1 November 2023 doi:10.20944/preprints202311.0063.v1

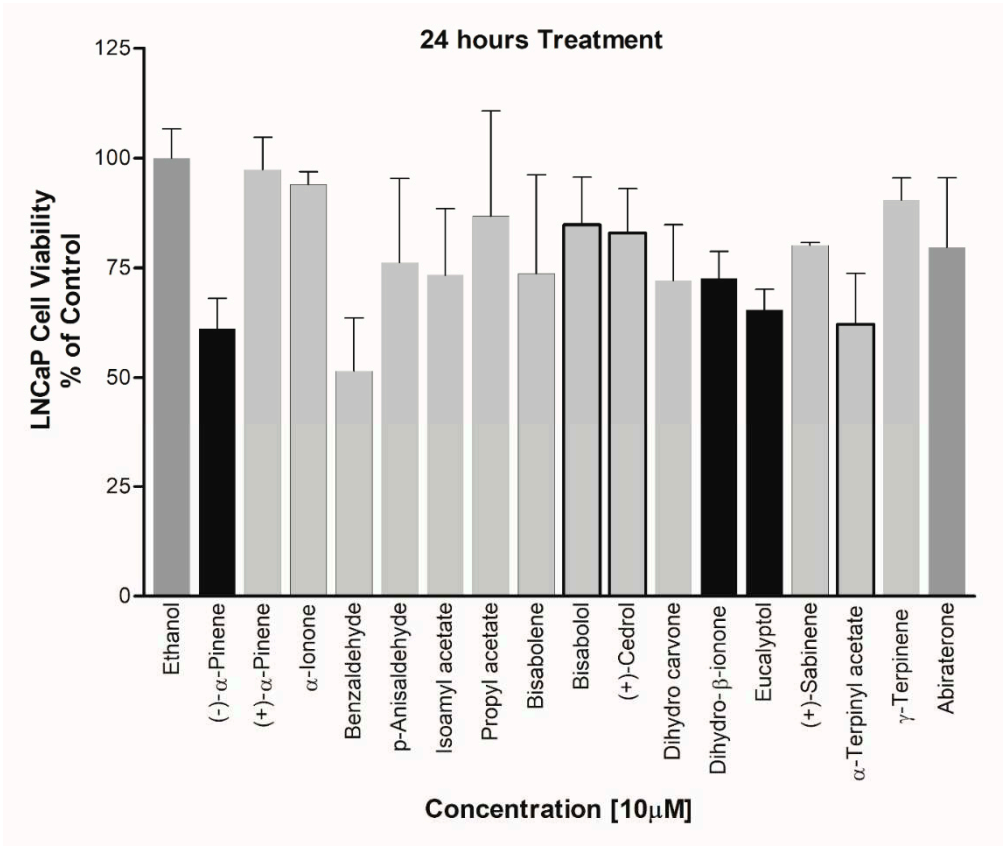

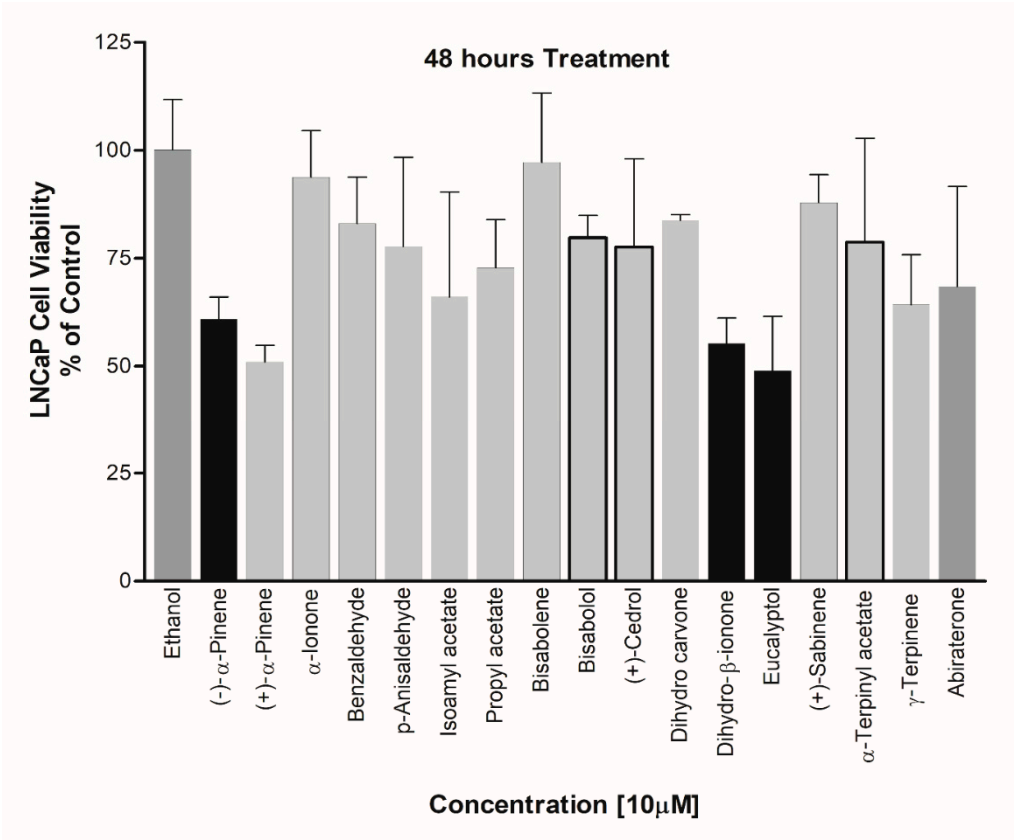

Figure 10. Effect of essential oil components on LnCaP cell proliferation. Essential oil compounds were checked for effect on proliferation of androgen dependent prostate cancer cell line, LnCaP cells. Cell viability was determined after 24h and 48h treatment with selected compounds that showed inhibitory effects in CYP17A1 or CYP19A1 assays.

Preprints (www.preprints.org) | NOT PEER-REVIEWED | Posted: 1 November 2023 doi:10.20944/preprints202311.0063.v1

Steroid analysis by LC-MS/MS

Individual steroid levels were normalized to the amount of Pregnenolone (P5). P5 was the starting steroid substrate to profile all the steroids in the biosynthetic pathway. The addition of dihydro-β-ionone to adrenal cells did not alter the levels of 17OHP5 or DHEA, however DHEA-S levels appeared lower (about 8%) compared to the control. The addition of Eucalyptol reduced DHEA levels (about 13%), 1.2-fold (approaching significance at p=0.0574), also with lower DHEA-S levels compared to the control (Figure 11).

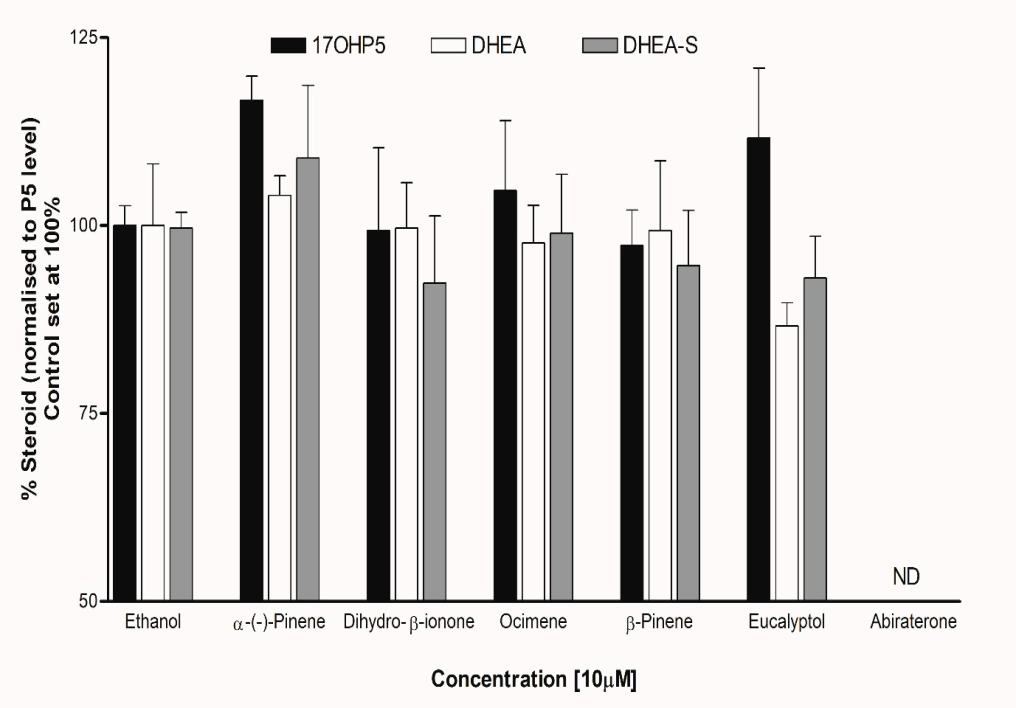

Figure 11. Steroid profiling using LC-MS/MS. Effect of essential oil components was tested for overall effects on steroid profiles of human adrenal NCI-H295R cells. Cells were treated with different compounds and steroid metabolites were analyzed by LC-MS/MS. Results shown are normalized against pregnenolone.

4. Discussion

Essential oils are highly concentrated plant extracts that are routinely used in in wellness, beauty, and cleaning products. However, since EOs are not pharmaceutical products, they are not regulated and therefore, their safety profiles are a topic of concern due to potential adverse reactions associated with their use. The safety of essential oils may also depend on individual metabolic profiles. In the past, few studies have been performed about the effect of EOs on cytochrome P450 enzymes that are involved in drug and xenobiotic metabolism [62]. Spicakova et. al. have studied the effect of sesquiterpenes beta-caryophyllene oxide and trans-nerolidol by docking into CYP3A4 and checking the results by functional assays of enzyme activity [63,64]. Beta-caryophyllene oxide binds to CYP3A4 close to the heme without coordinating to the Fe atom and also showed a waek inhibition of CYP3A4 activity. Similarly a waek inhibition of CYP2C8, CYP2C9 and CYP2C19 was observed for cedrene, cedrol and thujopsene, but cedrol showed strong inhibition of CYP3A4 and CYP2B6 [65].

The steroidogenesis, leading to developmental and reproductive changes as well as impact on immunological and neurological changes linked to steroid hormones. Here we have investigated the impact of several essential oil components on steroid production mediated by CYP17A1 and CYP19A1, two key enzymes involved in regulation of androgen and estrogen in human. While essential oils offer potential benefits, their use should be approached with caution due to potential safety issues and hormonal imbalances. It is crucial to conduct thorough research and consult healthcare professionals before incorporating essential oils into daily routines.

Preprints (www.preprints.org) | NOT PEER-REVIEWED | Posted: 1 November 2023 doi:10.20944/preprints202311.0063.v1

On the other hand, anti-androgen properties of essential oil compounds may offer structural leads for the design of novel drugs targeting steroid hormone production in metabolic disorders dependent on steroid hormones, including prostate cancer, breast cancer and poly cystic ovary syndrome.

Currently, the classical methods employed in the treatment of PCa include Androgen Deprivation Therapy using CYP17A1 inhibitors and/or blocking AR binding to its ligand using AR antagonists [66,67] (Figure 12). CYP17A1 targeted drugs have been developed over the years for the treatment of PCa as well as Castration Resistance Prostate Cancer (CRPC) [68]. Therefore, CYP17A1 has emerged as an attractive target for the design of inhibitors to use as drugs against prostate cancer [69]. From a non-selective Cytochrome P450 inhibitor, Ketoconazole, first-generation CYP17A1 targeted drugs such as Abiraterone and Orteronel (TAK700) to the most recent compounds with better selectivity towards 17,20 Lyase activity like Galeterone (TOK-001) and VT464, there is a continuous search for more efficient and potent inhibitors to overcome the challenges due to their adverse side-effects [70–78]. For instance, in addition to CYP17A1, Abiraterone also targets cytochrome P450 21-hydroxylase (CYP21A2) activity, which is essential for aldosterone and cortisol production [79,80]. As a result, suboptimal levels of cortisol due to inhibition of CYP21A1 leads to the requirement of glucocorticoid co-therapy in these patients [81]. However, most treatments have only a small effect in improving PCa patient survival. Next-generation drugs like Galeterone acts as both an AR antagonist and a CYP17A1 inhibitor. However, in metastasized PCa conditions such as CRPC, the tumor cells develop mechanisms to evade androgen dependency for their growth and survival. These mechanisms include the expression of AR variants which bind to androgen precursors of adrenal origin and *de novo* intra-tumoral androgen production [82,83]. Current strategies for the development of drugs focus on designing inhibitors with the ability to modulate the elevated levels of circulating androgens as well as steroids derived from alternative pathways in the case of androgen independent PCa without disturbing the cortisol metabolism [84,85]. Therefore, in the search for novel inhibitors of CYP17A1 with improved target specificity and reduced off-target effects, EOs could be utilized as chemical leads for the designing novel drugs against PCa and PCOS.

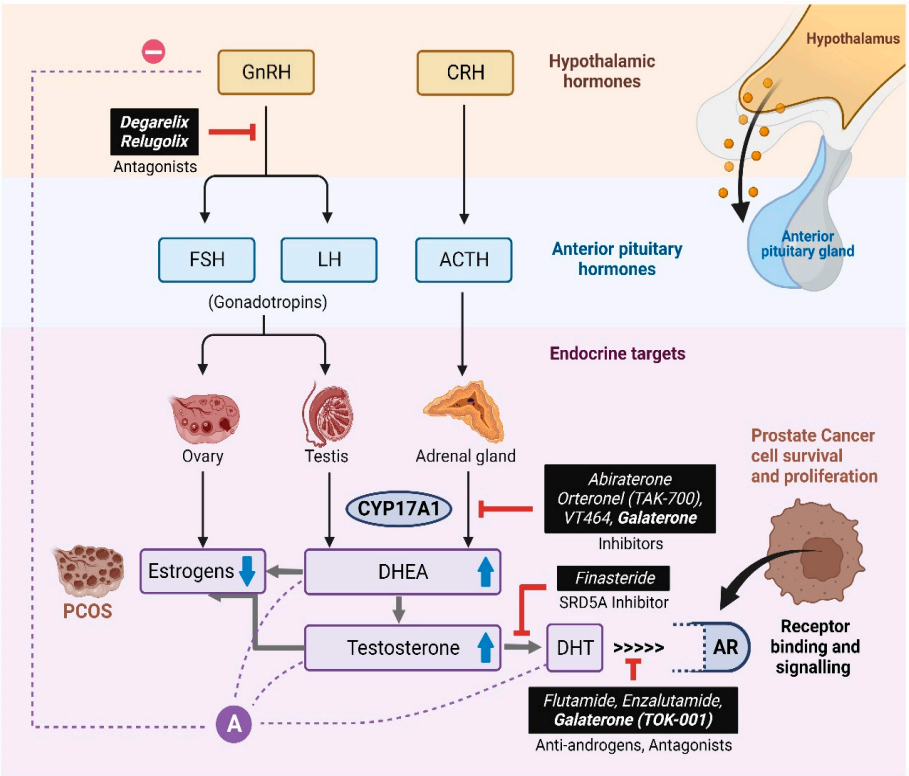

Figure 12. Different approaches to target androgen production for prostate cancer treatment.

Supplementary Materials: The following supporting information can be downloaded at the website of this paper posted on Preprints.org. File S1:. List of compounds used in this study.

Author Contributions: Conceptualization, A.V.P., A.L.; K.S.; CYP17A1 assays, K.S.; cell viability, K.S., J.Y., and S.T.; steroid profiling, T.d.T. and C.D.V.; molecular modeling, S.T. and F.S.J.; writing—original draft preparation, KS and AVP.; writing—review and editing, T.d.T., C.D.V., F.S.J., A.V.P., project administration AVP. All authors have read and agreed to the published version of the manuscript.

Funding: A.V.P. acknowledges CANCER RESEARCH SWITZERLAND grant number KFS-5557-02-2022 and SWISS NATIONAL SCIENCE FOUNDATION, grant number 310030M_204518. J.Y., and K.S. are funded by the SWISS GOVERNMENT EXCELLENCE SCHOLARSHIP (ESKAS) grant numbers 2022.0470, and 2019.0385. T.d.T. is funded by the Marie Skłodowska-Curie Individual Fellowship (#101023999).

Institutional Review Board Statement: Not applicable.

Informed Consent Statement: Not applicable.

Data Availability Statement: Data are available in manuscript text or in supplementary materials.

Conflicts of Interest: The authors declare no conflicts of interest.

References

1. Mendonca, A.; Jackson-Davis, A.; Moutiq, R.; Thomas-Popo, E., Chapter 14 - Use of Natural Antimicrobials of Plant Origin to Improve the Microbiological Safety of Foods. In *Food and Feed Safety Systems and Analysis*, Ricke, S. C.; Atungulu, G. G.; Rainwater, C. E.; Park, S. H., Eds. Academic Press: 2018; pp 249-272.
2. Cimino, C.; Maurel, O. M.; Musumeci, T.; Bonaccorso, A.; Drago, F.; Souto, E. M. B.; Pignatello, R.; Carbone, C., Essential Oils: Pharmaceutical Applications and Encapsulation Strategies into Lipid-Based Delivery Systems. *Pharmaceutics* **2021,** 13, (3), 327.
3. de Groot, A. C.; Schmidt, E., Essential Oils, Part I: Introduction. *Dermatitis* **2016,** 27, (2), 39-42.
4. Bakkali, F.; Averbeck, S.; Averbeck, D.; Idaomar, M., Biological effects of essential oils – A review. *Food and Chemical Toxicology* **2008,** 46, (2), 446-475.
5. Paco, N., Terpenes in Essential Oils: Bioactivity and Applications. In *Terpenes and Terpenoids*, Shagufta, P.; Areej Mohammad, A.-T., Eds. IntechOpen: Rijeka, 2020; p Ch. 2.
6. Sharmeen, J. B.; Mahomoodally, F. M.; Zengin, G.; Maggi, F., Essential Oils as Natural Sources of Fragrance Compounds for Cosmetics and Cosmeceuticals. *Molecules* **2021,** 26, (3), 666.
7. de Groot, A. C.; Schmidt, E., Essential Oils, Part III: Chemical Composition. *Dermatitis* **2016,** 27, (4), 161-9.
8. Ramsey, J. T.; Shropshire, B. C.; Nagy, T. R.; Chambers, K. D.; Li, Y.; Korach, K. S., Essential Oils and Health. *Yale J Biol Med* **2020,** 93, (2), 291-305.
9. Ali, B.; Al-Wabel, N. A.; Shams, S.; Ahamad, A.; Khan, S. A.; Anwar, F., Essential oils used in aromatherapy: A systemic review. *Asian Pacific Journal of Tropical Biomedicine* **2015,** 5, (8), 601-611.
10. Burt, S., Essential oils: their antibacterial properties and potential applications in foods—a review. *International Journal of Food Microbiology* **2004,** 94, (3), 223-253.
11. Mittal, P. R.; Rana, A.; Jaitak, V., Essential Oils: An Impending Substitute of Synthetic Antimicrobial Agents to Overcome Antimicrobial Resistance. *Current Drug Targets* **2019,** 20, (6), 605-624.
12. Yilmaz, B.; Terekeci, H.; Sandal, S.; Kelestimur, F., Endocrine disrupting chemicals: exposure, effects on human health, mechanism of action, models for testing and strategies for prevention. *Reviews in Endocrine and Metabolic Disorders* **2020,** 21, (1), 127-147.
13. Henley, D. V.; Lipson, N.; Korach, K. S.; Bloch, C. A., Prepubertal gynecomastia linked to lavender and tea tree oils. *N Engl J Med* **2007,** 356, (5), 479-85.
14. Miller, W. L.; Auchus, R. J., The molecular biology, biochemistry, and physiology of human steroidogenesis and its disorders. *Endocr Rev* **2011,** 32, (1), 81-151.
15. Matteson, K. J.; Picado-Leonard, J.; Chung, B. C.; Mohandas, T. K.; Miller, W. L., Assignment of the gene for adrenal P450c17 (steroid 17 alpha-hydroxylase/17,20 lyase) to human chromosome 10. *J Clin Endocrinol Metab* **1986,** 63, (3), 789-91.
16. Chung, B. C.; Picado-Leonard, J.; Haniu, M.; Bienkowski, M.; Hall, P. F.; Shively, J. E.; Miller, W. L., Cytochrome P450c17 (steroid 17 alpha-hydroxylase/17,20 lyase): cloning of human adrenal and testis cDNAs indicates the same gene is expressed in both tissues. *Proc Natl Acad Sci U S A* **1987,** 84, (2), 407-11.

17. Pallan, P. S.; Nagy, L. D.; Lei, L.; Gonzalez, E.; Kramlinger, V. M.; Azumaya, C. M.; Wawrzak, Z.; Waterman, M. R.; Guengerich, F. P.; Egli, M., Structural and kinetic basis of steroid 17alpha,20-lyase activity in teleost fish cytochrome P450 17A1 and its absence in cytochrome P450 17A2. *J Biol Chem* **2015,** 290, (6), 3248-68.
18. Zuber, M. X.; Simpson, E. R.; Waterman, M. R., Expression of bovine 17 alpha-hydroxylase cytochrome P-450 cDNA in nonsteroidogenic (COS 1) cells. *Science* **1986,** 234, (4781), 1258-61.
19. Yanagibashi, K.; Hall, P. F., Role of electron transport in the regulation of the lyase activity of C21 side-chain cleavage P-450 from porcine adrenal and testicular microsomes. *J Biol Chem* **1986,** 261, (18), 8429-33.
20. Pandey, A. V.; Flück, C. E., NADPH P450 oxidoreductase: structure, function, and pathology of diseases. *Pharmacol Ther* **2013,** 138, (2), 229-54.
21. Auchus, R. J.; Lee, T. C.; Miller, W. L., Cytochrome b5 augments the 17,20-lyase activity of human P450c17 without direct electron transfer. *J Biol Chem* **1998,** 273, (6), 3158-3165.
22. Pandey, A. V.; Miller, W. L., Regulation of 17,20 lyase activity by cytochrome b5 and by serine phosphorylation of P450c17. *J Biol Chem* **2005,** 280, (14), 13265-71.
23. Zhang, L. H.; Rodriguez, H.; Ohno, S.; Miller, W. L., Serine phosphorylation of human P450c17 increases 17,20-lyase activity: implications for adrenarche and the polycystic ovary syndrome. *Proc Natl Acad Sci U S A* **1995,** 92, (23), 10619-23.
24. Pandey, A. V.; Mellon, S. H.; Miller, W. L., Protein phosphatase 2A and phosphoprotein SET regulate androgen production by P450c17. *J Biol Chem* **2003,** 278, (5), 2837-44.
25. Kempna, P.; Hirsch, A.; Hofer, G.; Mullis, P. E.; Fluck, C. E., Impact of differential P450c17 phosphorylation by cAMP stimulation and by starvation conditions on enzyme activities and androgen production in NCI-H295R cells. *Endocrinology* **2010,** 151, (8), 3686-96.
26. Wang, Y. H.; Tee, M. K.; Miller, W. L., Human cytochrome p450c17: single step purification and phosphorylation of serine 258 by protein kinase a. *Endocrinology* **2010,** 151, (4), 1677-84.
27. Miller, W. L.; Tee, M. K., The post-translational regulation of 17,20 lyase activity. *Mol Cell Endocrinol* **2015,** 408, 99-106.
28. Tee, M. K.; Miller, W. L., Phosphorylation of human cytochrome P450c17 by p38alpha selectively increases 17,20 lyase activity and androgen biosynthesis. *J Biol Chem* **2013,** 288, (33), 23903-13.
29. Prins, G. S., Endocrine disruptors and prostate cancer risk. *Endocr Relat Cancer* **2008,** 15, (3), 649-56.
30. Tan, M. H. E.; Li, J.; Xu, H. E.; Melcher, K.; Yong, E.-l., Androgen receptor: structure, role in prostate cancer and drug discovery. *Acta Pharmacologica Sinica* **2015,** 36, (1), 3-23.
31. Liu, W.-J.; Zhao, G.; Zhang, C.-Y.; Yang, C.-Q.; Zeng, X.-B.; Li, J.; Zhu, K.; Zhao, S.-Q.; Lu, H.-M.; Yin, D.-C.; Lin, S.-X., Comparison of the roles of estrogens and androgens in breast cancer and prostate cancer. *Journal of Cellular Biochemistry* **2020,** 121, (4), 2756-2769.
32. Trott, O.; Olson, A. J., AutoDock Vina: improving the speed and accuracy of docking with a new scoring function, efficient optimization, and multithreading. *J Comput Chem* **2010,** 31, (2), 455-61.
33. Eberhardt, J.; Santos-Martins, D.; Tillack, A. F.; Forli, S., AutoDock Vina 1.2.0: New Docking Methods, Expanded Force Field, and Python Bindings. *J Chem Inf Model* **2021,** 61, (8), 3891-3898.
34. Berman, H. M.; Westbrook, J.; Feng, Z.; Gilliland, G.; Bhat, T. N.; Weissig, H.; Shindyalov, I. N.; Bourne, P. E., The Protein Data Bank. *Nucleic Acids Res* **2000,** 28, (1), 235-42.
35. Petrunak, E. M.; DeVore, N. M.; Porubsky, P. R.; Scott, E. E., Structures of human steroidogenic cytochrome P450 17A1 with substrates. *J Biol Chem* **2014,** 289, (47), 32952-64.
36. Ghosh, D.; Griswold, J.; Erman, M.; Pangborn, W., X-ray structure of human aromatase reveals an androgen-specific active site. *J Steroid Biochem Mol Biol* **2010,** 118, (4-5), 197-202.
37. Lo, J.; Di Nardo, G.; Griswold, J.; Egbuta, C.; Jiang, W.; Gilardi, G.; Ghosh, D., Structural basis for the functional roles of critical residues in human cytochrome p450 aromatase. *Biochemistry* **2013,** 52, (34), 5821-9.
38. Ghosh, D.; Griswold, J.; Erman, M.; Pangborn, W., Structural basis for androgen specificity and oestrogen synthesis in human aromatase. *Nature* **2009,** 457, (7226), 219-23.
39. Sastry, G. M.; Adzhigirey, M.; Day, T.; Annabhimoju, R.; Sherman, W., Protein and ligand preparation: parameters, protocols, and influence on virtual screening enrichments. *J Comput Aided Mol Des* **2013,** 27, (3), 221-34.
40. Shelley, J. C.; Cholleti, A.; Frye, L. L.; Greenwood, J. R.; Timlin, M. R.; Uchimaya, M., Epik: a software program for pK(a) prediction and protonation state generation for drug-like molecules. *J Comput Aided Mol Des* **2007,** 21, (12), 681-91.

41. DeVore, N. M.; Scott, E. E., Structures of cytochrome P450 17A1 with prostate cancer drugs abiraterone and TOK-001. *Nature* **2012,** 482, (7383), 116-9.
42. Yadav, R.; Petrunak, E. M.; Estrada, D. F.; Scott, E. E., Structural insights into the function of steroidogenic cytochrome P450 17A1. *Mol Cell Endocrinol* **2017,** 441, 68-75.
43. Ghosh, D.; Egbuta, C.; Lo, J., Testosterone complex and non-steroidal ligands of human aromatase. *J Steroid Biochem Mol Biol* **2018,** 181, 11-19.
44. Friesner, R. A.; Murphy, R. B.; Repasky, M. P.; Frye, L. L.; Greenwood, J. R.; Halgren, T. A.; Sanschagrin, P. C.; Mainz, D. T., Extra Precision Glide: Docking and Scoring Incorporating a Model of Hydrophobic Enclosure for Protein−Ligand Complexes. *Journal of Medicinal Chemistry* **2006,** 49, (21), 6177-6196.
45. Halgren, T. A.; Murphy, R. B.; Friesner, R. A.; Beard, H. S.; Frye, L. L.; Pollard, W. T.; Banks, J. L., Glide: A New Approach for Rapid, Accurate Docking and Scoring. 2. Enrichment Factors in Database Screening. *Journal of Medicinal Chemistry* **2004,** 47, (7), 1750-1759.
46. Rainey, W. E.; Saner, K.; Schimmer, B. P., Adrenocortical cell lines. *Molecular and Cellular Endocrinology* **2004,** 228, (1), 23-38.
47. Gazdar, A. F.; Oie, H. K.; Shackleton, C. H.; Chen, T. R.; Triche, T. J.; Myers, C. E.; Chrousos, G. P.; Brennan, M. F.; Stein, C. A.; La Rocca, R. V., Establishment and characterization of a human adrenocortical carcinoma cell line that expresses multiple pathways of steroid biosynthesis. *Cancer Res* **1990,** 50, (17), 5488-96.
48. Wu, X.; Gong, S.; Roy-Burman, P.; Lee, P.; Culig, Z., Current mouse and cell models in prostate cancer research. *Endocr Relat Cancer* **2013,** 20, (4), R155-70.
49. Riss, T. L.; Moravec, R. A.; Niles, A. L.; Duellman, S.; Benink, H. A.; Worzella, T. J.; Minor, L., Cell Viability Assays. In *Assay Guidance Manual*, Markossian, S.; Grossman, A.; Brimacombe, K.; Arkin, M.; Auld, D.; Austin, C.; Baell, J.; Chung, T. D. Y.; Coussens, N. P.; Dahlin, J. L.; Devanarayan, V.; Foley, T. L.; Glicksman, M.; Gorshkov, K.; Haas, J. V.; Hall, M. D.; Hoare, S.; Inglese, J.; Iversen, P. W.; Kales, S. C.; Lal-Nag, M.; Li, Z.; McGee, J.; McManus, O.; Riss, T.; Saradjian, P.; Sittampalam, G. S.; Tarselli, M.; Trask, O. J., Jr.; Wang, Y.; Weidner, J. R.; Wildey, M. J.; Wilson, K.; Xia, M.; Xu, X., Eds. Eli Lilly & Company and the National Center for Advancing Translational Sciences: Bethesda (MD), 2004.
50. Kamiloglu, S.; Sari, G.; Ozdal, T.; Capanoglu, E., Guidelines for cell viability assays. *Food Frontiers* **2020,** 1, (3), 332-349.
51. Potter, G. A.; Barrie, S. E.; Jarman, M.; Rowlands, M. G., Novel Steroidal Inhibitors of Human Cytochrome P45017.alpha.-Hydroxylase-C17,20-lyase): Potential Agents for the Treatment of Prostatic Cancer. *Journal of Medicinal Chemistry* **1995,** 38, (13), 2463-2471.
52. Udhane, S. S.; Dick, B.; Hu, Q.; Hartmann, R. W.; Pandey, A. V., Specificity of anti-prostate cancer CYP17A1 inhibitors on androgen biosynthesis. *Biochemical and Biophysical Research Communications* **2016,** 477, (4), 1005-1010.
53. Castaño, P. R.; Parween, S.; Pandey, A. V., Bioactivity of Curcumin on the Cytochrome P450 Enzymes of the Steroidogenic Pathway. In *International Journal of Molecular Sciences*, 2019; Vol. 20.
54. Staels, B.; Hum, D. W.; Miller, W. L., Regulation of steroidogenesis in NCI-H295 cells: a cellular model of the human fetal adrenal. *Mol Endocrinol* **1993,** 7, (3), 423-33.
55. Potts, G. O.; Creange, J. E.; Harding, H. R.; Schane, H. P., Trilostane, an orally active inhibitor of steroid biosynthesis. *Steroids* **1978,** 32, (2), 257-267.
56. Brown, J. W.; Fishman, L. M., Biosynthesis and metabolism of steroid hormones by human adrenal carcinomas. *Braz J Med Biol Res* **2000,** 33, (10), 1235-44.
57. Morán, F. M.; VandeVoort, C. A.; Overstreet, J. W.; Lasley, B. L.; Conley, A. J., Molecular Target of Endocrine Disruption in Human Luteinizing Granulosa Cells by 2,3,7,8-Tetrachlorodibenzo-p-Dioxin: Inhibition of Estradiol Secretion Due to Decreased 17α-Hydroxylase/17,20-Lyase Cytochrome P450 Expression. *Endocrinology* **2003,** 144, (2), 467-473.
58. McManus, J. M.; Bohn, K.; Alyamani, M.; Chung, Y. M.; Klein, E. A.; Sharifi, N., Rapid and structure-specific cellular uptake of selected steroids. *PLoS One* **2019,** 14, (10), e0224081.
59. Andrieu, T.; du Toit, T.; Vogt, B.; Mueller, M. D.; Groessl, M., Parallel targeted and non-targeted quantitative analysis of steroids in human serum and peritoneal fluid by liquid chromatography high-resolution mass spectrometry. *Anal Bioanal Chem* **2022,** 414, (25), 7461-7472.
60. Siiteri, P. K.; Thompson, E. A., Studies of human placental aromatase. *Journal of Steroid Biochemistry* **1975,** 6, (3), 317-322.
61. Lephart, E. D.; Simpson, E. R., Assay of aromatase activity. *Methods Enzymol* **1991,** 206, 477-83.

62. Zehetner, P.; Höferl, M.; Buchbauer, G., Essential oil components and cytochrome P450 enzymes: a review. *Flavour and Fragrance Journal* **2019,** 34, (4), 223-240.
63. Nguyen, L. T.; Myslivečková, Z.; Szotáková, B.; Špičáková, A.; Lněničková, K.; Ambrož, M.; Kubíček, V.; Krasulová, K.; Anzenbacher, P.; Skálová, L., The inhibitory effects of β-caryophyllene, β-caryophyllene oxide and α-humulene on the activities of the main drug-metabolizing enzymes in rat and human liver in vitro. *Chem-Biol Interact* **2017,** 278, 123-128.
64. Špičáková, A.; Bazgier, V.; Skálová, L.; Otyepka, M.; Anzenbacher, P., beta-caryophyllene oxide and trans-nerolidol affect enzyme activity of CYP3A4 - in vitro and in silico studies. *Physiological research* **2019,** 68, (Suppl 1), S51-s58.
65. Jeong, H.-U.; Kwon, S.-S.; Kong, T. Y.; Kim, J. H.; Lee, H. S., Inhibitory Effects of Cedrol, β-Cedrene, and Thujopsene on Cytochrome P450 Enzyme Activities in Human Liver Microsomes. *Journal of Toxicology and Environmental Health, Part A* **2014,** 77, (22-24), 1522-1532.
66. Stein, M. N.; Patel, N.; Bershadskiy, A.; Sokoloff, A.; Singer, E. A., Androgen synthesis inhibitors in the treatment of castration-resistant prostate cancer. *Asian Journal of Andrology* **2014,** 16, (3).
67. Norris, J. D.; Ellison, S. J.; Baker, J. G.; Stagg, D. B.; Wardell, S. E.; Park, S.; Alley, H. M.; Baldi, R. M.; Yllanes, A.; Andreano, K. J.; Stice, J. P.; Lawrence, S. A.; Eisner, J. R.; Price, D. K.; Moore, W. R.; Figg, W. D.; McDonnell, D. P., Androgen receptor antagonism drives cytochrome P450 17A1 inhibitor efficacy in prostate cancer. *J Clin Invest* **2017,** 127, (6), 2326-2338.
68. Bird, I. M.; Abbott, D. H., The hunt for a selective 17,20 lyase inhibitor; learning lessons from nature. *The Journal of Steroid Biochemistry and Molecular Biology* **2016,** 163, 136-146.
69. Wróbel, T. M.; Jørgensen, F. S.; Pandey, A. V.; Grudzińska, A.; Sharma, K.; Yakubu, J.; Björkling, F., Non-steroidal CYP17A1 Inhibitors: Discovery and Assessment. *Journal of Medicinal Chemistry* **2023,** 66, (10), 6542-6566.
70. van der Pas, R.; Hofland, L. J.; Hofland, J.; Taylor, A. E.; Arlt, W.; Steenbergen, J.; van Koetsveld, P. M.; de Herder, W. W.; de Jong, F. H.; Feelders, R. A., Fluconazole inhibits human adrenocortical steroidogenesis in vitro. *J Endocrinol* **2012,** 215, (3), 403-12.
71. Attard, G.; Reid, A. H. M.; Yap, T. A.; Raynaud, F.; Dowsett, M.; Settatree, S.; Barrett, M.; Parker, C.; Martins, V.; Folkerd, E.; Clark, J.; Cooper, C. S.; Kaye, S. B.; Dearnaley, D.; Lee, G.; de Bono, J. S., Phase I Clinical Trial of a Selective Inhibitor of CYP17, Abiraterone Acetate, Confirms That Castration-Resistant Prostate Cancer Commonly Remains Hormone Driven. *Journal of Clinical Oncology* **2008,** 26, (28), 4563-4571.
72. Yamaoka, M.; Hara, T.; Hitaka, T.; Kaku, T.; Takeuchi, T.; Takahashi, J.; Asahi, S.; Miki, H.; Tasaka, A.; Kusaka, M., Orteronel (TAK-700), a novel non-steroidal 17,20-lyase inhibitor: Effects on steroid synthesis in human and monkey adrenal cells and serum steroid levels in cynomolgus monkeys. *The Journal of Steroid Biochemistry and Molecular Biology* **2012,** 129, (3), 115-128.
73. Njar, V. C. O.; Brodie, A. M. H., Discovery and Development of Galeterone (TOK-001 or VN/124-1) for the Treatment of All Stages of Prostate Cancer. *Journal of Medicinal Chemistry* **2015,** 58, (5), 2077-2087.
74. Yin, L.; Hu, Q., CYP17 inhibitors—abiraterone, C17,20-lyase inhibitors and multi-targeting agents. *Nature Reviews Urology* **2014,** 11, (1), 32-42.
75. Bonomo, S.; Hansen, C. H.; Petrunak, E. M.; Scott, E. E.; Styrishave, B.; Jorgensen, F. S.; Olsen, L., Promising Tools in Prostate Cancer Research: Selective Non-Steroidal Cytochrome P450 17A1 Inhibitors. *Sci Rep* **2016,** 6, 29468.
76. Larsen, M.; Hansen, C. H.; Rasmussen, T. B.; Islin, J.; Styrishave, B.; Olsen, L.; Jorgensen, F. S., Structure-based optimisation of non-steroidal cytochrome P450 17A1 inhibitors. *Chemical communications* **2017,** 53, (21), 3118-3121.
77. Wrobel, T. M.; Rogova, O.; Andersen, K. L.; Yadav, R.; Brixius-Anderko, S.; Scott, E. E.; Olsen, L.; Jorgensen, F. S.; Bjorkling, F., Discovery of Novel Non-Steroidal Cytochrome P450 17A1 Inhibitors as Potential Prostate Cancer Agents. *Int J Mol Sci* **2020,** 21, (14).
78. Wrobel, T. M.; Rogova, O.; Sharma, K.; Rojas Velazquez, M. N.; Pandey, A. V.; Jorgensen, F. S.; Arendrup, F. S.; Andersen, K. L.; Bjorkling, F., Synthesis and Structure-Activity Relationships of Novel Non-Steroidal CYP17A1 Inhibitors as Potential Prostate Cancer Agents. *Biomolecules* **2022,** 12, (2).
79. Malikova, J.; Brixius-Anderko, S.; Udhane, S. S.; Parween, S.; Dick, B.; Bernhardt, R.; Pandey, A. V., CYP17A1 inhibitor abiraterone, an anti-prostate cancer drug, also inhibits the 21-hydroxylase activity of CYP21A2. *The Journal of Steroid Biochemistry and Molecular Biology* **2017,** 174, 192-200.

80. Vogt, C. D.; Bart, A. G.; Yadav, R.; Scott, E. E.; Aubé, J., Effects of fluorine substitution on substrate conversion by cytochromes P450 17A1 and 21A2. **2021,** 19, (35), 7664-7669.
81. Richards, J.; Lim, A. C.; Hay, C. W.; Taylor, A. E.; Wingate, A.; Nowakowska, K.; Pezaro, C.; Carreira, S.; Goodall, J.; Arlt, W.; McEwan, I. J.; de Bono, J. S.; Attard, G., Interactions of Abiraterone, Eplerenone, and Prednisolone with Wild-type and Mutant Androgen Receptor: A Rationale for Increasing Abiraterone Exposure or Combining with MDV3100. *Cancer Research* **2012,** 72, (9), 2176-2182.
82. Montgomery, R. B.; Mostaghel, E. A.; Vessella, R.; Hess, D. L.; Kalhorn, T. F.; Higano, C. S.; True, L. D.; Nelson, P. S., Maintenance of Intratumoral Androgens in Metastatic Prostate Cancer: A Mechanism for Castration-Resistant Tumor Growth. *Cancer Research* **2008,** 68, (11), 4447-4454.
83. Barnard, M.; Mostaghel, E. A.; Auchus, R. J.; Storbeck, K.-H., The role of adrenal derived androgens in castration resistant prostate cancer. *The Journal of Steroid Biochemistry and Molecular Biology* **2020,** 197, 105506.
84. Bambury, R. M.; Rathkopf, D. E., Novel and next-generation androgen receptor–directed therapies for prostate cancer: Beyond abiraterone and enzalutamide. *Urologic Oncology: Seminars and Original Investigations* **2016,** 34, (8), 348-355.
85. Yin, L.; Hu, Q.; Hartmann, R. W., Recent Progress in Pharmaceutical Therapies for Castration-Resistant Prostate Cancer. In *International Journal of Molecular Sciences*, 2013; Vol. 14, pp 13958-13978.

Section D: Effect of crude extracts from plant tissue of Ghost pepper and Vietnamese coriander on CYP17A1 activity.

Background: Extracts from medicinal plants are used extensively in traditional medicines from India and China. Anti-pyretic drug, Aspirin and anti-malarial drug, Quinine has shown that traditional medicines can be the source for development of modern therapeutics (Greenwood, 1992; Mahdi et al., 2006). As already seen in case of endocrine disrupting chemicals, naturally occurring complex biochemicals can act as hormone mimics to regulate endocrine function. However, there is little known information about traditional medicines despite being in use from ancient time. Ghost Pepper (GP) is cultivated as a hybrid of Capsicum chinense and Capsicum frutescens L. belonging to family of Solanaceae. Typically grown in the northeast region of India it is considered one of the hottest peppers in the world. It has been reported that it possesses anti-inflammatory, antioxidant and antimicrobial properties. Capsaicinoids, including capsaicin, are the major bioactive components in GP (Culver et al., 2021; Govindarajan & Sathyanarayana, 1991). Capsaicin showed anti-cancer property via inhibition of CYP2E1. This suggests a possible interaction of capsaicin-like structure with other CYP enzymes with an additional cytotoxic effect on cancer cells (Bley et al., 2012; Oyagbemi et al., 2010).

On the other hand, essential oils extracted from Vietnamese coriander (VC), Persicaria odorata have shown anti-bacterial activity. Belonging to family Polygonaceae, VC contains essential oils, flavonoids, polyphenols and monoterpenoids (Řebíčková et al., 2020). Extracts derived from VC showed cytotoxic effect on lymphoma, leukaemia, oral, lung, breast, colon, and liver cancer cells. These effects were mediated through regulation of proteins involved in cell proliferation, migration, apoptosis, and angiogenesis. Notable proteins affected include cyclin-D, cyclooxygenase 2 (COX-2), matrix metalloproteinase-9 (MMP-9), and vascular endothelial growth factor A (VEGF-A) (Devi Khwairakpam et al., 2019; Khuayjarernpanishk et al., 2022). These instances provide enough reasons to find the effect of essential oils derived from GP and VC on any aspect of PCa growth and progression as well as androgen production since androgens govern the cellular processes of PCa cells. GP and VC are common ingredients found in a number of south-east Asian cuisines. Their anti-cancerous property has already been in use in traditional medicines. Therefore, it becomes essential to determine their possible effects in human physiology and pathology.

The detailed description of the materials and methods is given in Section 3.

Crude extracts of Ghost Pepper (S1) & Vietnamese coriander (S2) were prepared using the methanol extraction method (Larson et al., 2016). Cell viability assays were performed in the Prostate cancer cell line, LNCaP to determine the effect of EOs in tumor growth using resazurin based assay. MTT assay was carried out in NCI H295R cells to validate that the inhibition of CYP17A1 activity was not due to any kind of cell toxicity. For cell based CYP17A1 enzyme assay, the protocol is the same as previous with the respective radiolabeled substrate. For the whole steroid profile, Liquid Chromatography high-resolution Mass Spectrometry assays were performed in adrenal cells.

Results: Preliminary data shows that at concentration of 50 µg/mL and 100 µg/mL, a severe reduction in CYP17A1 Hydroxylase activity was observed. In case of S1, the inhibition was similar to the levels of Abiraterone (***Figure 5***). However, higher doses of these extracts were found to be toxic to the NCI H295R cells. Therefore, for determination of CYP17A1 lyase activity through LC-MS/MS, we treated the cells with lower concentration of extracts (50 µg/mL) to eliminate any discrepancies in the enzyme activity due to cell toxicity.

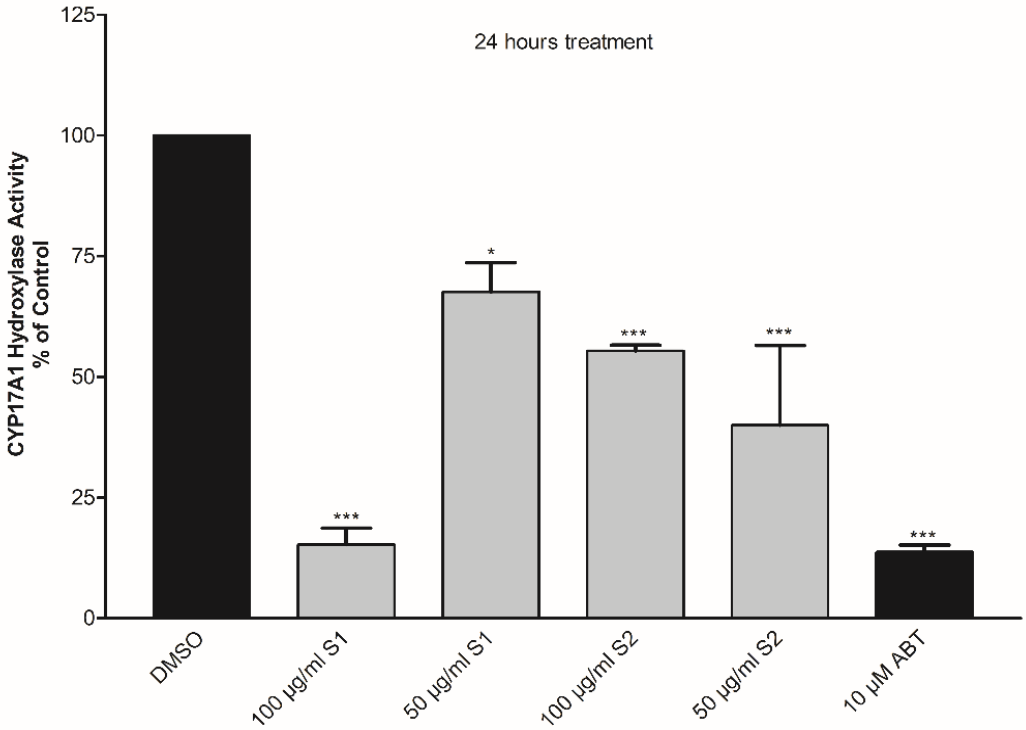

Figure 5 *Inhibition of CYP17A1 Hydroxylase activity by test compounds for 24 hours in NCI H295R cells. Abiraterone (ABT) was used as a positive control. Trilostane (HSD3β inhibitor) was used to block the further conversion of obtained products. P values: *p<0.5, ***p<0.001 calculated with respect to Control (DMSO)*

Reduction in both 17α-hydroxy pregnenolone and DHEA levels in comparison to control was higher in case of S1 than S2. Also, S2 showed little effect on the CYP17A1 lyase activity as indicated in *(**Figure 6***). Whereas, in case of S1, only 50% of 17α-hydroxy pregnenolone was able to convert to DHEA.

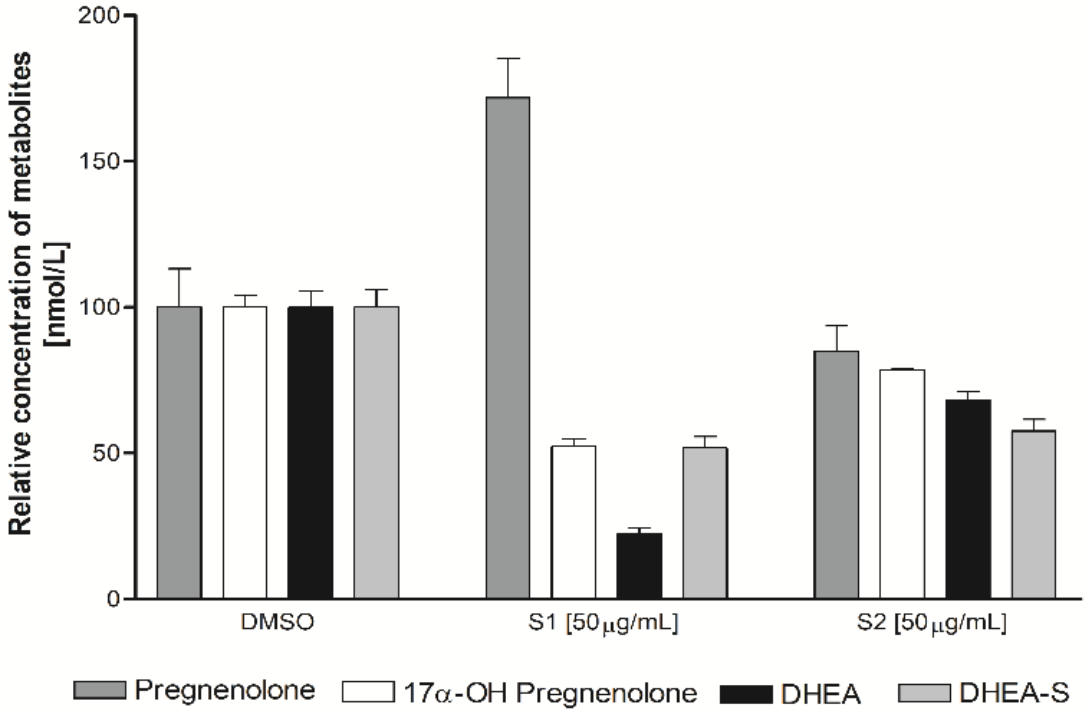

***Figure 6**: Steroid profile by LC-MS in cells treated with 50µg/mL extracts for 24 hours. P values were determined through two-way ANOVA and the respective values were calculated with corresponding control values (P<0.0001)*

In addition, to determine the potential of these extracts to affect cellular growth of Prostate cells, cell viability assays were performed in LNCaP cells. Although significant toxicity was observed only at higher concentration of the extracts. But if the cells are exposed to longer incubation time, increased toxicity will be observed even at lower concentrations (***Figure 7***)

Discussion: The preliminary results indicate the potential of these extracts in the inhibition of CYP17A1 activity. The results also indicate towards selectivity of S1 in the inhibition of CYP17A1 lyase activity. Cellular toxicity towards LNCaP cells can be utilized in reduction of overall prostate tumor if developed further. Since these plants are part local food belonging to specific geographical area, their consumption can contribute to exogenous factors affecting overall androgen levels. Thus, they might also possess endocrine disrupting properties similar to essential oils. Characterization of the bioactive components in the extracts that are causing these effects can help us to assess the potential risks or benefits associated with the use of these medicinal plants.

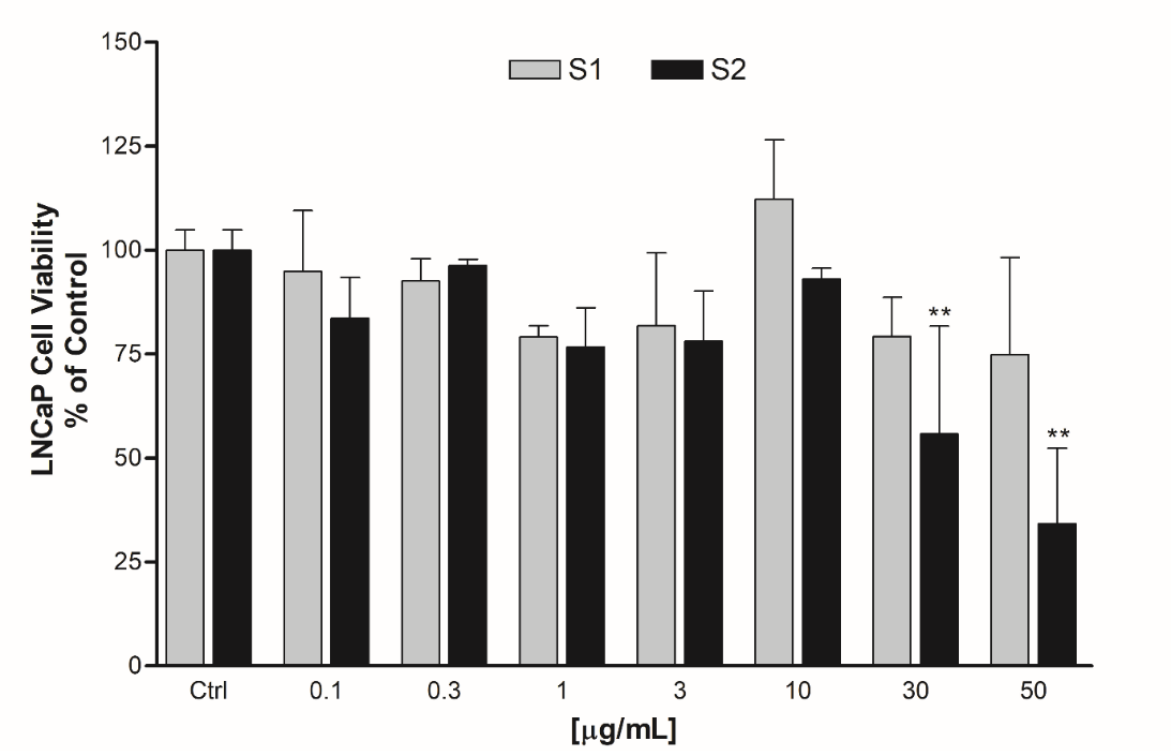

***Figure 7**: Cell viability assay performed in LNCaP cells to determine the effect of increasing concentration of the extracts on tumor growth for a duration of 24 hours. (**p<0.01)*

Outlook: We plan to collect information about the composition of the plant extracts including the determination of major essential oil components. Purified compounds from these plants will be tested for CYP17A1 inhibition. Additionally other CYP enzyme activity will be assessed to find any cross reactivity. Effect of common drugs metabolizing CYPs in the xenobiotic transformation of the active components will also be evaluated. Computational docking would help predict exactly which component or combination of components would be better for efficient and selective inhibition of lyase activity to design novel drugs. Finally, the identified components could be designed as nanoparticles for efficient drug delivery in adrenal cell lines to achieve actual physiological dose.

AIM: To identify novel pathways involved in the regulation of CYP17A1 through post-translational mechanisms.

Chapter 3

Study the role of specific Kinases and Phosphatases involved in the regulation of CYP17A1 lyase activity.

Section E: Effect of selected kinases and phosphatases in the regulation of CYP17A1 activity

Background: Multiple genomic and transcriptomic studies have identified differentially expressed genes in PCa and PCOS. A transcriptomic study in our lab identified differential expression of protein kinases and phosphatases that were linked to changes in androgen production in human adrenal cells. Protein kinases like p38α, ROCK1 (Rho associated kinase) and protein phosphatase, PP2A have been reported to be involved in the signaling cascade leading to phosphorylation of CYP17A1 (Miller et al., 1997; A. V. Pandey et al., 2003; Pandey & Miller, 2005a). These might in turn be regulated by other protein kinases and phosphatases constituting a possible signaling cascade which have been partially known and predicted by Tee et al (Tee & Miller, 2013). Based on this, we selected few protein kinases and phosphatases overexpressed as cDNA plasmid in NCI H295R cells and monitored the change in CYP17A1 activity in preliminary experiments.

The detailed description of the materials and methods is given in Section 3.

Transient transfection in NCI H295R cells were performed to overexpress selected kinases and phosphatases from transcriptomic analysis. CYP17A1 lyase assay was performed at 24hours, 48 hours and 72hours post transfection with help of tritiated water release assay. Stable cell lines were generated expressing following kinases and phosphatases using COS-1 cell line.

- **PPP2R2C** (Protein Phosphatase 2 regulatory subunit B gamma)
- **PPP1CB** (Protein Phosphatase 1 catalytic subunit beta)
- **PPP2CA** (Protein Phosphatase 2 catalytic subunit alpha)
- **DUSP6** (Dual Specificity Phosphatase 6)
- **GSK3A** (Glycogen Synthase Kinase 3 alpha)
- **MAPK14** (Mitogen-Activated protein Kinase 14)
- **DUSP10** (Dual Specificity Phosphatase 10)

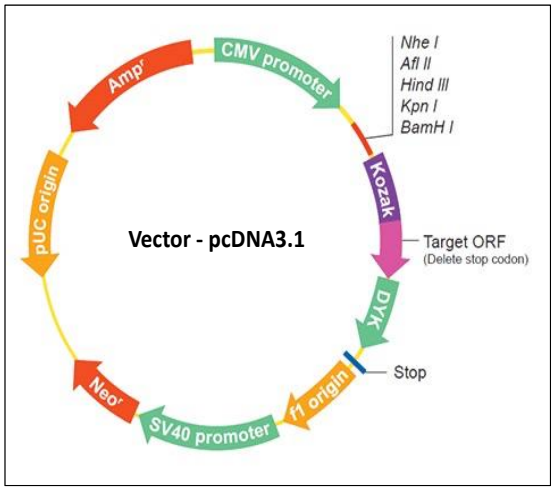

Figure 8: Gene Map of pcDNA 3.1 plasmid (GenScript) used in transfection experiments.

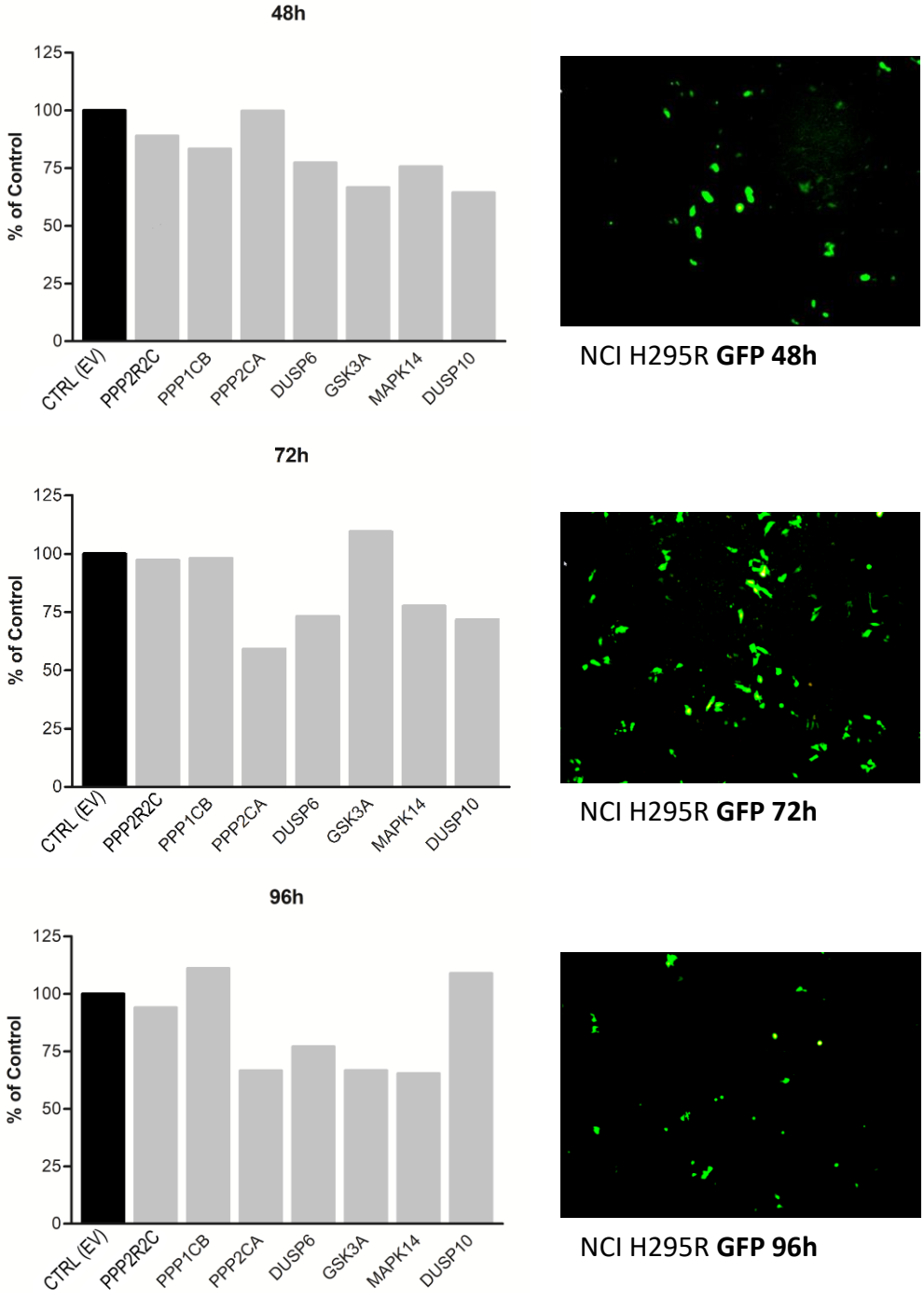

***Figure 9**: Inhibition of CYP17A1 Lyase activity in transiently transfected NCI H295R cells with plasmids of Kinases and Phosphatases at 48, 72 and 96 hours. For detection of effective transfection level, cells transfected with eGFP plasmid were used as control and monitored using fluorescent microscopy.*

Results: A significant decrease in DHEA production was observed in cells overexpressing protein phosphatase (PPP) 2CA, glycogen synthase kinase 3 (GSK3) and dual specificity phosphatase 6 and 10 (DUSP6/10). However, there was no change in the activity in presence of PPP1CB and PPP2R2C (***Figure 9***). Moreover, the change in CYP17A1 activity was affected by the duration and levels of transfection with respective plasmids. The presence of a phosphorylated form of a protein depends on the ratio and action of protein kinases and phosphatases present in the cytoplasm of the cell. Therefore, a variation in the levels of CYP17A1 lyase activity was observed. This was also the reason to monitor the enzyme activity through Tritiated water release assay for the lyase activity. The stable cell lines generated need to be further validated to confirm the presence of required protein. The cell lines will be used to isolate microsomal and cytoplasmic fractions for cleaner systems to analyze the interaction of protein kinases and phosphatases with CYP17A1.

Section F: Effect of PLK1 in the regulation of CYP17A1 activity.

Background: Small molecules available through OpnMe program initiated by Boehringer Ingelheim (BI), Inc provides pre-clinical compounds for scientific collaborations. Some of these are already in clinical trial stage and have been well characterized as molecules targeting key regulatory mechanisms linked to cancer cell development and progression including certain protein kinases. Details regarding in vitro and in vivo studies are also available from BI. Compounds seems to be targeting mechanisms related to PCa, PCOS or overall steroid biosynthesis were screened for possible CYP17A1 inhibition (***Table 1***). Among them, BI-2536, a selective inhibitor of PLK1 was found to affect CYP17A1 activity. Literature search revealed that PLK1 plays a crucial role in activating the cyclin B1/CDK1 complex involved in early events of mitosis (Steegmaier et al., 2007). Since these proteins belong to kinase family, there is a possibility that a number of proteins activated through phosphorylation can be regulated by PLK1. PLK1 have shown to be effective in several cancer cell lines as well as mouse xenograft models (Steegmaier et al., 2007). Moreover, PLK1 was found to be overexpressed in PCa. Although the mechanism of action of PLK1 is not fully understood. PLK1 has been implicated to be involved in PI3K–AKT–mTOR pathway and AR signaling (Zhang et al., 2014). Synergistic effect of abiraterone and PLK1 inhibitor in disruption of mitosis have been reported in PCa cells with partial information about the possible mechanisms (Patterson et al., 2023). Therefore, it becomes essential to study the role of PLK1 regulation through different signaling pathways and CYP17A1 regulation can be one such target.

Label	ID no.	Function
A+	BI 3802	BCL6::Co-repressor inhibitor which induces efficacious BCL6 protein degradation
A-	BI 5273	Negative control of 3802
B	BI 2536	**selective PLK1 inhibitor**
C+	BI 1347	CDK8/cyclinC inhibition
C-	BI 1374	Negative control of 1347
D+	BI 653048	Glucocorticoid Receptor Agonist
D-	BI 3047	Negative control of 653048

***Table 1**: Small molecule inhibitors from Boehringer Ingelheim. Selective PLK1 inhibitor, BI 2536 were used to test CYP17A1 activity in NCI H295R cell line.*

The detailed description of the materials and methods is given in Section 3.

Cells were treated with different concentrations of PLK1 inhibitor, BI2536 for 4 hours. CYP17A1 activity was determined using radiolabeled substrate [^{3}H]-Preg. Steroids were separated through TLC and the radiolabeled spots were analyzed through autoradiography. For CYP17A1 lyase activity, tritiated water release assay was performed as described earlier. Transfection with siRNA for PLK1 was done using Lipofectamine 2000 reagent. Universal scrambled siRNA (20 µM), from Integrated DNA Technology, LubioScience, GmbH) was used as negative control and TYE-563 fluorescent was used as positive control for knockdown experiments. 3 unique 27mer siRNA duplexes (2 nmol each) was used for PLK1 knockdown and collectively referred as siPLK1. The duplexes are available as PLK1 Human siRNA Oligo Duplex (ID 5347, UniProt P53350) from OriGene^{TM}. For our experiments, siRNA PLK1 was a kind gift from Prof. Dr. Ren Wang Peng (Associate Professor, Division of General Thoracic Surgery, Inselspital, Bern University Hospital, Department of Biomedical Research (DBMR), University of Bern). All the siRNAs were resuspended in the resuspension buffer provided by the manufacturer.

Results: An inhibitor of polo like kinase 1 (PLK1) specifically altered the lyase activity of CYP17A1. Preliminary experiments to determine both CYP17A1 hydroxylase and lyase activity showed that BI-2536 selectively inhibits the lyase activity. Moreover, the effect was observed in a dose dependent manner with maximum inhibition at 1 nM ($p<0.05$) for 4 hours ***(Figure 10***).

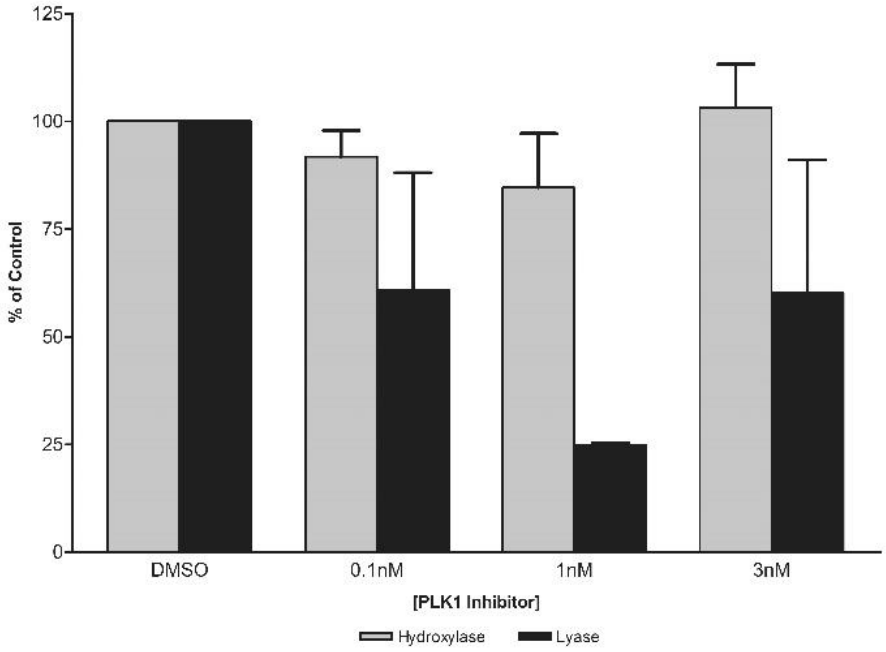

Figure 10: *Inhibition of CYP17A1 activity by PLK1 inhibitor. Preliminary data shows that BI-2536 is selective towards CYP17A1 lyase activity that the 17α-hydroxylase activity.*

Tritiated water release assay for the direct measurement of the lyase activity showed inhibition comparable to the levels caused by Abiraterone at 10 µM concentration. for a treatment of duration of 3 hours (***Figure 11***). However, this effect was not observed for longer treatment duration suggesting that the phosphorylation state of the CYP17A1 changes with time and so does the lyase activity. Optimal treatment duration for measurement should be within 1 hour for minimum detection.

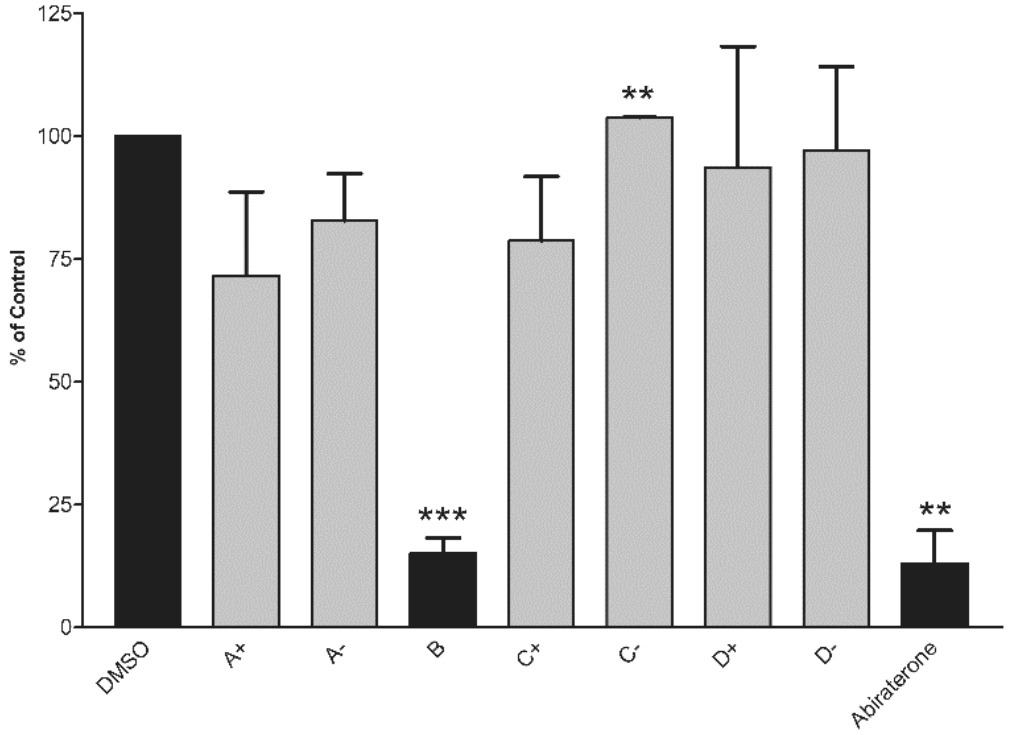

Figure 11*: Inhibition of CYP17A1 Lyase activity by test compounds at 10 µM concentration for 3h in NCI H295R cells. (**p<0.01, ***p<0.001). For description of labels, refer to* ***Table 1****.*

We transfected the cells with siPLK1 for complete loss of PLK1 which is more potent than inhibition by BI-2536. After 72 hours post transfection a 50% reduction in CYP17A1 lyase activity was observed. This suggests that knockdown of PLK1 activity drives the dynamics of cell towards unphosphorylated states resulting in disruption of lyase activity (***Figure 12***)

Additionally, BI-2536 showed cytotoxic effects in prostate cancer cells, LNCaP in a dose-dependent manner with IC50 of about 11.6 µM. At same concentration, PLK1 inhibitor showed higher toxicity than Abiraterone for 24 hours of treatment (***Figure 13***)

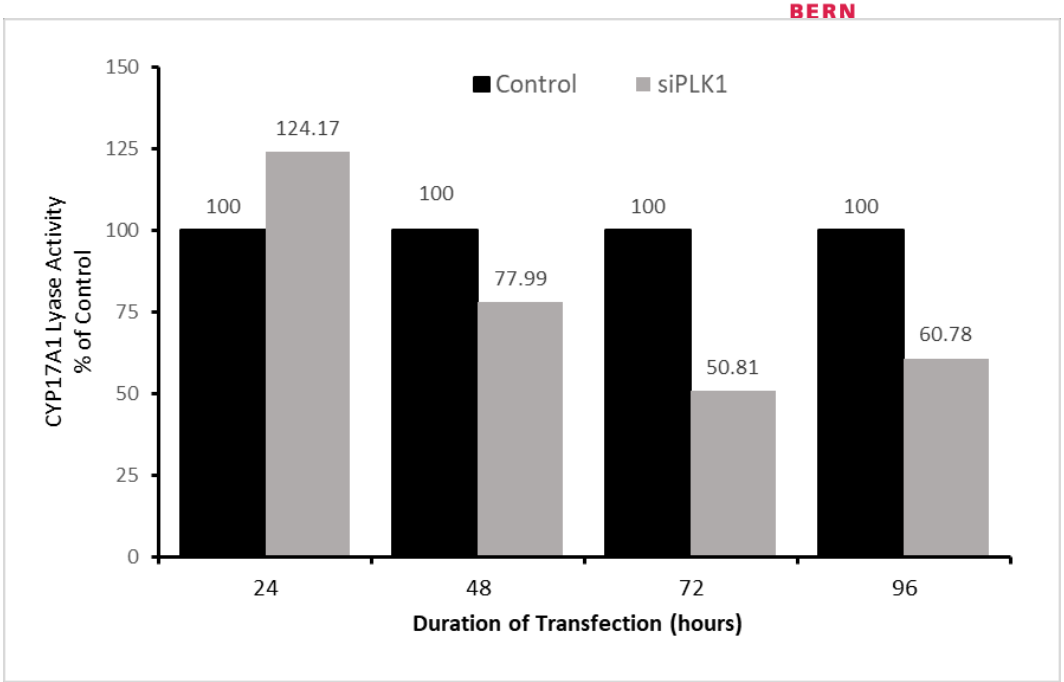

***Figure 12**: PLK1 knock-down in NCI H295R cells transfected with siPLK1 using Lipofectamine 2000 reagent. About 50% reduction in CYP17A1 lyase activity was observed at 72 hours post transfection.*

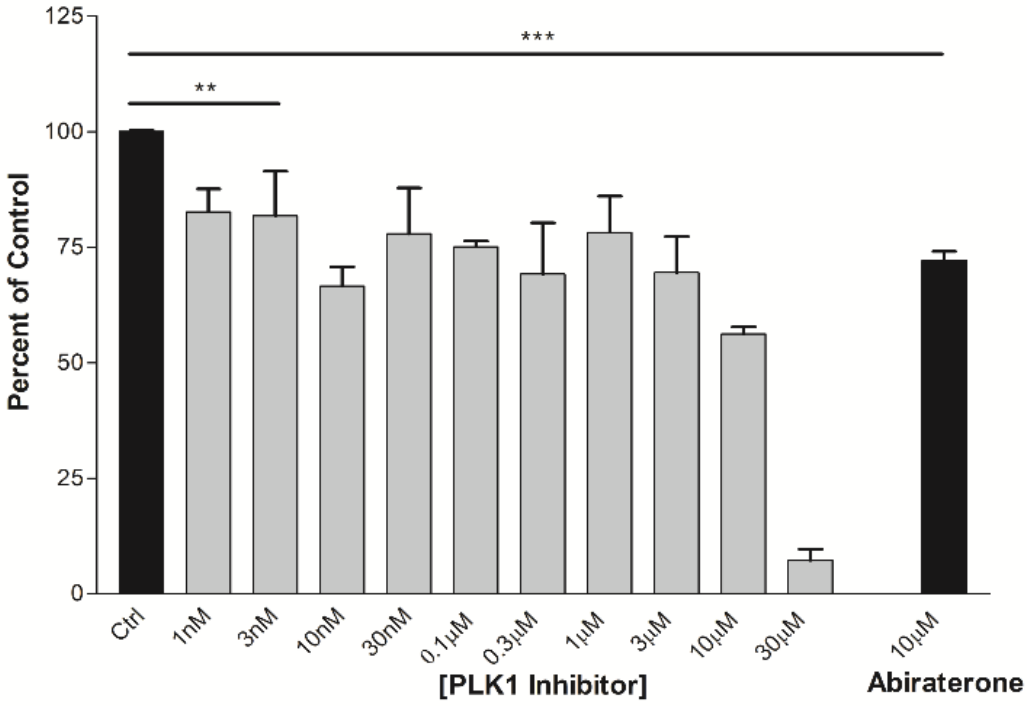

Figure continued in next page.

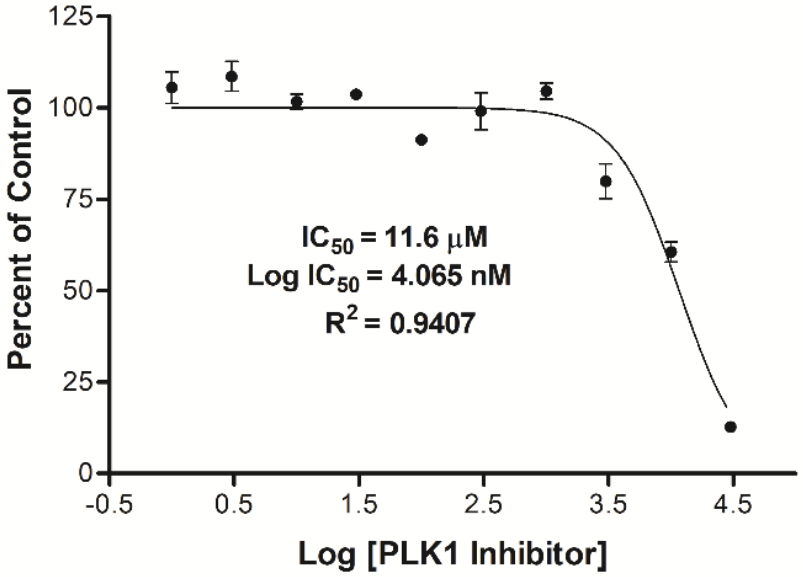

***Figure 13**: PLK1 inhibits cellular growth of LNCaP cells in a dose-dependent manner with an IC50 at 11.6 µM. Data is represented as mean of triplicates. Data reveals that PLK1 plays an important role in the regulation of tumor growth in prostate cancer.*

Chapter 3 Discussion: Although we observed changes in CYP17A1 lyase activity in the NCI H295R cells overexpressing selected protein kinases and phosphatases. The variability in the level of enzyme activity hints to the fact that the dynamic state of phosphorylation and dephosphorylation within the cells makes it difficult to catch the exact time of action of the proteins. The assays used in the experiments were required to be incubated with radiolabeled substrate for at least 1 hour for the detection of signals. Therefore, effect of phosphorylation on enzyme activity showed great variability and few inconsistencies in the measurements. The change in the lyase activity of CYP17A1 shows a dependence on the expression of different kinases and phosphatases. We showed that signaling events can regulate CYP17A1 lyase activity either directly or indirectly through protein-protein interactions.

Moreover, the role of PLK1 in the signaling cascade provides us with insight into broader range of protein kinases and phosphatases involved in phosphorylation of CYP17A1. It also opens the prospective role of different mechanisms for the regulation of CYP17A1 enzyme activity as well as steroidogenesis. Given the fact that PLK1 also inhibits the growth of prostate cancer cells like LNCaP, it can be further developed into drugs having dual mode of action. The protein-protein interaction pathway from the STRING database reveals that there is an indirect interaction of PLK1, PPP2CA and ROCK1, which can be corelated to the protein involved in the signaling cascade predicted earlier in the regulation of CYP17A1 lyase activity through phosphorylation (***Figure 14***) (Tee & Miller, 2013). Therefore, there could be either a

direct or indirect interaction between these proteins to bring about CYP17A1 regulation through phosphorylation.

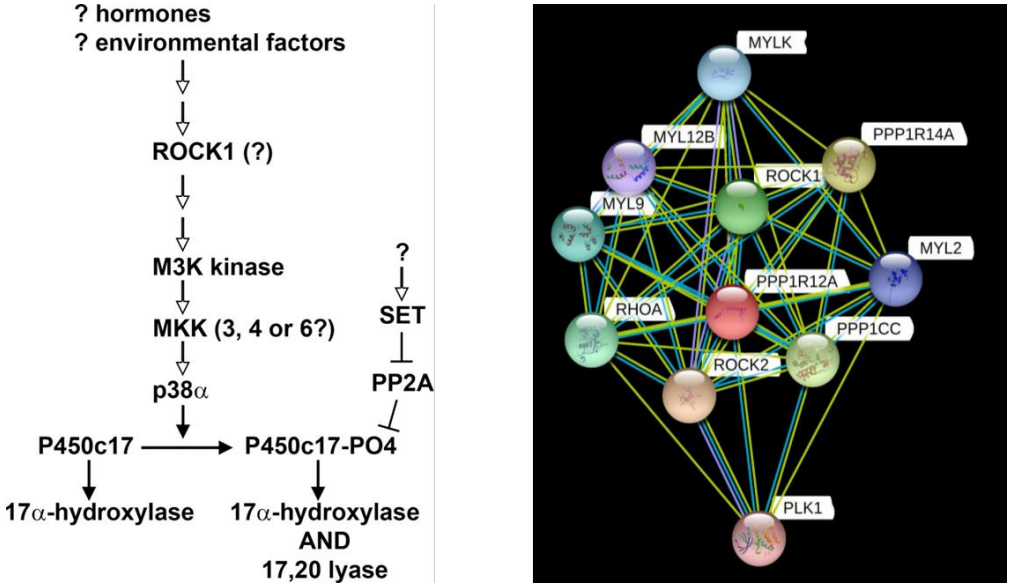

***Figure 14**: Left – Signaling pathway involving different protein kinases and phosphatases in post translational regulation of CYP17A1 as predicted by (Tee & Miller, 2013). Right - Studies in human adrenal cell line and STRING database search have suggested novel proteins that can be the missing links in the predicted pathway.*

Chapter-3-Outlook- An overall steroid profile will be done in cells expressing these kinases and phosphatases to monitor any changes in activity of other CYPs. Total protein estimation and Western blot analysis will be performed to confirm the presence of a protein of interest in the stable cell lines. Microsomes and cytoplasm will be isolated from these stable cell lines to perform functional assays for CYP17A1 activity. Compounds initially screened for CYP17A1 inhibition will be further analyzed for any effect on other CYP enzymes in the steroidogenic pathway. Potential effect of PLK1 inhibition in different prostate cancer cell lines can provide broad idea about possible role of PLK1. PLK1 is overexpressed in PCa and causes altered gene expression of the AR as well as genes involved in de novo steroidogenesis affecting both androgen-dependent and androgen-independent PCa (CRPC). Since drugs against PLK1 are already used for treatment of number of cancers (Zhang et al., 2015). It becomes essential to identify every aspect of PLK1 in cellular process including phosphorylation of CYP17A1. Regulation of CYP17A1 activity by different kinases and phosphatases will provide better design ideas to look for specific inhibitors of CYP17A1 lyase activity since an increase in lyase activity is observed with phosphorylation of Cytochrome P450 c17. In vitro studies with stable cell lines will help us to understand whether these kinases or phosphatases are directly or indirectly involved in the signaling cascade for the regulation of CYP17A1 activity.

GENERAL DISCUSSION

Current therapeutic strategies used in the treatment of PCa ranges from targeting regulatory pathways involved in gene expression to direct inhibition of key enzymes responsible for androgen production. Although blocking or downregulating AR seems to be a good strategy to prevent prostate tumor growth and progression. In more severe forms of PCa like CRPC, adaptation of androgen independent mechanisms by the tumor cells pushes for alternative approaches. It has been observed that somehow the androgen levels are compensated to keep feeding the cancer cells even in loss of androgen dependency. The only enzyme that acts as qualitative controller of androgen production is CYP17A1. Therefore, CYP17A1 inhibitors have been the center of drug development against PCa. With the emergence of drugs like Abiraterone, potent inhibition of CYP17A1 activity has been achieved but the associated selectivity and cross-reactivity issues are not resolved yet (Malikova et al., 2017) . A major disadvantage of synthetic drugs designed for CYP17A1 inhibition is their structural similarity with the native substrates of CYP enzymes. This results in metabolic transformation of the inhibitor into ligands that can be recognized by AR making it futile in androgen deprivation therapies. Therefore, designing and synthesis of non-steroidal inhibitors is required to overcome these challenges (Wróbel et al., 2023). Availability of crystal structure of CYP17A1 protein and its interaction with natural substrates, synthetic analogues or known inhibitors has provided critical information that can be utilized in designing better drug candidates. The work presented in this thesis deals with the potential of several drug candidates developed over a period of time to selectively target CYP17A1 lyase activity (Wróbel et al., 2020).

An effective drug should be comparatively simple and cost-effective to produce with increased disease specificity. A descriptive information about characteristics like absorption, distribution, metabolism, excretion, and toxicity (ADMET) is required before subjecting it to clinical trial (Doogue & Polasek, 2013). If not scientific, reports of natural products being used in the treatment of several diseases including chronic disorders in traditional settings are well documented. Unlike synthetic libraries, this provides us with some basic knowledge of possible use of natural products for development of therapeutics. However, the transition from plant to product is a challenging process and particularly complex when the active component is an extract or mixture rather than an isolated compound. Once a reliable compound has been identified, validation of cellular targets and mechanisms of action becomes essential. In vitro and in vivo studies are one of the first steps in the process of drug development. Further advancement requires new tools including methods that compare phenotypic or gene expression profiles induced by a small molecule with those induced by known compounds or chemical enhancer/suppressor screens. The development of in silico tools for "docking" small molecules with protein structures help in narrowing down

appropriate candidates for in vitro testing. Advancements in such techniques help greatly in the ongoing interdisciplinary research efforts essential for realizing the pharmaceutical potential of traditional therapeutics (Corson & Crews, 2007).

Post-translational regulation of CYP17A1 through phosphorylation can also be a selective target for inhibition of lyase activity. The regulatory proteins involved in the signaling cascade leading to phosphorylation of CYP17A1 during lyase activity is not fully known. Therefore, strategies to develop drug candidates targeting this aspect of CYP17A1 activity not only provides better selectivity but also help in identification of novel proteins in the signaling. Our current work identified the possible role of PLK1 in the regulation of CYP17A1 activity. PLK1 is already involved in regulation of proteins involved in mitosis and the overexpression of PLK1 in PCa cells is linked to decreased AR activity (Zhang et al., 2015). Therefore, exploring multiple mechanisms involving PLK1 in overall prostate tumor progression holds a great potential to understand the switch from androgen dependent to androgen independent PCa. Moreover, the Ser/Thr phosphorylation sites within the proteins have not been identified so far. There is a possibility of variants existing in these sites which could cause aberration in gene and protein function. Nevertheless, identification of proteins involved in the regulation of CYP function can provide information about the factors related to tissue specific development and differentiation of gonads.

Interaction of CYP17A1 with its substrate, different small molecule drugs and regulatory proteins has a combinatorial effect on its enzyme activity. These factors contribute to the dual function of the enzyme and production of androgen precursor. Machine learning approach is a useful tool to design non-steroidal inhibitors of CYP17A1 and to modify structures derived from natural products. Identification of novel mechanism as well as partially predicted pathways in the regulation of CYP17A1 helps us to have a comprehensive knowledge about the full potential of CYP17A1 inhibitors. Lastly, given the important role of androgens in PCa, PCOS and other hyperandrogenic disorders, information about developing therapeutics should be applicable to the clinical settings.

References

References

Abdel-Khalik, J., Björklund, E., & Hansen, M. (2013). Development of a solid phase extraction method for the simultaneous determination of steroid hormones in H295R cell line using liquid chromatography–tandem mass spectrometry. *Journal of Chromatography B*, *935*, 61-69. https://doi.org/https://doi.org/10.1016/j.jchromb.2013.07.013

Abidi, A. (2013). Cabazitaxel: A novel taxane for metastatic castration-resistant prostate cancer-current implications and future prospects. *Journal of Pharmacology and Pharmacotherapeutics*, *4*(4), 230-237. https://doi.org/10.4103/0976-500x.119704

Agrawal, N., Dasaradhi, P. V., Mohmmed, A., Malhotra, P., Bhatnagar, R. K., & Mukherjee, S. K. (2003). RNA interference: biology, mechanism, and applications. *Microbiol Mol Biol Rev*, *67*(4), 657-685. https://doi.org/10.1128/mmbr.67.4.657-685.2003

Ahmed, K. E. M., Frøysa, H. G., Karlsen, O. A., Sagen, J. V., Mellgren, G., Verhaegen, S., Ropstad, E., Goksøyr, A., & Kellmann, R. (2018). LC-MS/MS based profiling and dynamic modelling of the steroidogenesis pathway in adrenocarcinoma H295R cells. *Toxicology in Vitro*, *52*, 332-341. https://doi.org/https://doi.org/10.1016/j.tiv.2018.07.002

Ahmed, K. E. M., Frøysa, H. G., Karlsen, O. A., Sagen, J. V., Mellgren, G., Verhaegen, S., Ropstad, E., Goksøyr, A., & Kellmann, R. (2018). LC-MS/MS based profiling and dynamic modelling of the steroidogenesis pathway in adrenocarcinoma H295R cells. *Toxicol In Vitro*, *52*, 332-341. https://doi.org/10.1016/j.tiv.2018.07.002

Albany, C., Alva, A. S., Aparicio, A. M., Singal, R., Yellapragada, S., Sonpavde, G., & Hahn, N. M. (2011). Epigenetics in prostate cancer. *Prostate Cancer*, *2011*, 580318. https://doi.org/10.1155/2011/580318

Andersen, C. Y., & Ezcurra, D. (2014). Human steroidogenesis: implications for controlled ovarian stimulation with exogenous gonadotropins. *Reproductive Biology and Endocrinology*, *12*(1), 128. https://doi.org/10.1186/1477-7827-12-128

Attard, G., Reid, A. H., Auchus, R. J., Hughes, B. A., Cassidy, A. M., Thompson, E., Oommen, N. B., Folkerd, E., Dowsett, M., Arlt, W., & de Bono, J. S. (2012). Clinical and biochemical consequences of CYP17A1 inhibition with abiraterone given with and without exogenous glucocorticoids in castrate men with advanced prostate cancer. *J Clin Endocrinol Metab*, *97*(2), 507-516. https://doi.org/10.1210/jc.2011-2189

Attard, G., Reid, A. H., Yap, T. A., Raynaud, F., Dowsett, M., Settatree, S., Barrett, M., Parker, C., Martins, V., Folkerd, E., Clark, J., Cooper, C. S., Kaye, S. B., Dearnaley, D., Lee, G., & de Bono, J. S. (2008). Phase I clinical trial of a selective inhibitor of CYP17, abiraterone acetate, confirms that castration-resistant prostate cancer commonly remains hormone driven [Clinical Trial, Phase I

Research Support, Non-U.S. Gov't]. *J Clin Oncol*, *26*(28), 4563-4571. https://doi.org/10.1200/JCO.2007.15.9749

Azad, A. A., Volik, S. V., Wyatt, A. W., Haegert, A., Le Bihan, S., Bell, R. H., Anderson, S. A., McConeghy, B., Shukin, R., Bazov, J., Youngren, J., Paris, P., Thomas, G., Small, E. J.,

Wang, Y., Gleave, M. E., Collins, C. C., & Chi, K. N. (2015). Androgen Receptor Gene Aberrations in Circulating Cell-Free DNA: Biomarkers of Therapeutic Resistance in Castration-Resistant Prostate Cancer. *Clin Cancer Res*, *21*(10), 2315-2324. https://doi.org/10.1158/1078-0432.Ccr-14-2666

Baston, E., & Leroux, F. R. (2007). Inhibitors of steroidal cytochrome p450 enzymes as targets for drug development. *Recent patents on anti-cancer drug discovery*, *2*(1), 31-58.

Bernhardt, R., & Neunzig, J. (2021). Underestimated reactions and regulation patterns of adrenal cytochromes P450. *Molecular and Cellular Endocrinology*, *530*, 111237. https://doi.org/https://doi.org/10.1016/j.mce.2021.111237

Bertani, G. (1951). Studies on lysogenesis. I. The mode of phage liberation by lysogenic Escherichia coli. *J Bacteriol*, *62*(3), 293-300. https://doi.org/10.1128/jb.62.3.293-300.1951

Bilusic, M., Madan, R. A., & Gulley, J. L. (2017). Immunotherapy of Prostate Cancer: Facts and Hopes. *Clinical Cancer Research*, *23*(22), 6764-6770. https://doi.org/10.1158/1078-0432.Ccr-17-0019

Bird, I. M., & Abbott, D. H. (2016). The hunt for a selective 17,20 lyase inhibitor; learning lessons from nature. *J Steroid Biochem Mol Biol*, *163*, 136-146. https://doi.org/10.1016/j.jsbmb.2016.04.021

Bird, I. M., Hanley, N. A., Word, R. A., Mathis, J. M., McCarthy, J. L., Mason, J. I., & Rainey, W. E. (1993). Human NCI-H295 adrenocortical carcinoma cells: a model for angiotensin-II-responsive aldosterone secretion. *Endocrinology*, *133*(4), 1555-1561. https://doi.org/10.1210/endo.133.4.8404594

Birnboim, H. C., & Doly, J. (1979). A rapid alkaline extraction procedure for screening recombinant plasmid DNA. *Nucleic Acids Res*, *7*(6), 1513-1523. https://doi.org/10.1093/nar/7.6.1513

Bley, K., Boorman, G., Mohammad, B., McKenzie, D., & Babbar, S. (2012). A comprehensive review of the carcinogenic and anticarcinogenic potential of capsaicin. *Toxicol Pathol*, *40*(6), 847-873. https://doi.org/10.1177/0192623312444471

Bluemn, E. G., & Nelson, P. S. (2012). The androgen/androgen receptor axis in prostate cancer. *Current Opinion in Oncology*, *24*(3), 251-257. https://doi.org/10.1097/CCO.0b013e32835105b3

Brown, J. W., & Fishman, L. M. (2000). Biosynthesis and metabolism of steroid hormones by human adrenal carcinomas. *Braz J Med Biol Res*, *33*(10), 1235-1244. https://doi.org/10.1590/s0100-879x2000001000014

Budäus, L., Bolla, M., Bossi, A., Cozzarini, C., Crook, J., Widmark, A., & Wiegel, T. (2012). Functional Outcomes and Complications Following Radiation Therapy for Prostate Cancer: A Critical Analysis of the Literature. *European Urology*, *61*(1), 112-127. https://doi.org/https://doi.org/10.1016/j.eururo.2011.09.027

Bylsma, L. C., & Alexander, D. D. (2015). A review and meta-analysis of prospective studies of red and processed meat, meat cooking methods, heme iron, heterocyclic amines and prostate cancer. *Nutr J*, *14*, 125. https://doi.org/10.1186/s12937-015-0111-3

Cai, C., Chen, S., Ng, P., Bubley, G. J., Nelson, P. S., Mostaghel, E. A., Marck, B., Matsumoto, A. M., Simon, N. I., Wang, H., Chen, S., & Balk, S. P. (2011). Intratumoral de novo steroid

synthesis activates androgen receptor in castration-resistant prostate cancer and is upregulated by treatment with CYP17A1 inhibitors. *Cancer Res*, *71*(20), 6503-6513. https://doi.org/10.1158/0008-5472.Can-11-0532

Carey, A. H., Waterworth, D., Patel, K., White, D., Little, J., Novelli, P., Franks, S., & Williamson, R. (1994). Polycystic ovaries and premature male pattern baldness are associated with one allele of the steroid metabolism gene CYP17. *Human molecular genetics*, *3*(10), 1873-1876.

Castaño, P. R., Parween, S., & Pandey, A. V. (2019). Bioactivity of Curcumin on the Cytochrome P450 Enzymes of the Steroidogenic Pathway. *International Journal of Molecular Sciences*, *20*(18), 4606. https://www.mdpi.com/1422-0067/20/18/4606

Castillejos-Molina, R. A., & Gabilondo-Navarro, F. B. (2016). Prostate cancer. *Salud Publica Mex*, *58*(2), 279-284. https://doi.org/10.21149/spm.v58i2.7797

Chang, K. H., Li, R., Kuri, B., Lotan, Y., Roehrborn, C. G., Liu, J., Vessella, R., Nelson, P. S., Kapur, P., Guo, X., Mirzaei, H., Auchus, R. J., & Sharifi, N. (2013). A gain-of-function mutation in DHT synthesis in castration-resistant prostate cancer. *Cell*, *154*(5), 1074-1084. https://doi.org/10.1016/j.cell.2013.07.029

Chapter 4 Radio-thin-layer chromatography. (1978). In T. R. Roberts (Ed.), *Journal of Chromatography Library* (Vol. 14, pp. 45-83). Elsevier. https://doi.org/https://doi.org/10.1016/S0301-4770(08)60932-X

Chen, C., & Okayama, H. (1987). High-efficiency transformation of mammalian cells by plasmid DNA. *Mol Cell Biol*, *7*(8), 2745-2752. https://doi.org/10.1128/mcb.7.8.2745-2752.1987

Cheng, L., Montironi, R., Bostwick, D. G., Lopez-Beltran, A., & Berney, D. M. (2012). Staging of prostate cancer. *Histopathology*, *60*(1), 87-117. https://doi.org/10.1111/j.1365-2559.2011.04025.x

Corson, T. W., & Crews, C. M. (2007). Molecular Understanding and Modern Application of Traditional Medicines: Triumphs and Trials. *Cell*, *130*(5), 769-774. https://doi.org/https://doi.org/10.1016/j.cell.2007.08.021

Cui, J., Shen, Y., & Li, R. (2013). Estrogen synthesis and signaling pathways during aging: from periphery to brain. *Trends Mol Med*, *19*(3), 197-209. https://doi.org/10.1016/j.molmed.2012.12.007

Culver, K. D., Allen, J. L., Shaw, L. N., & Hicks, L. M. (2021). Too Hot to Handle: Antibacterial Peptides Identified in Ghost Pepper. *Journal of Natural Products*, *84*(8), 2200-2208. https://doi.org/10.1021/acs.jnatprod.1c00281

Cutler, G. B., Jr., Glenn, M., Bush, M., Hodgen, G. D., Graham, C. E., & Loriaux, D. L. (1978). Adrenarche: a survey of rodents, domestic animals, and primates. *Endocrinology*, *103*(6), 2112-2118. https://doi.org/10.1210/endo-103-6-2112

Dai, C., Dehm, S. M., & Sharifi, N. (2023). Targeting the Androgen Signaling Axis in Prostate Cancer. *J Clin Oncol*, Jco2300433. https://doi.org/10.1200/jco.23.00433

Dasgupta, S., Srinidhi, S., & Vishwanatha, J. K. (2012). Oncogenic activation in prostate cancer progression and metastasis: Molecular insights and future challenges. *J Carcinog*, *11*, 4. https://doi.org/10.4103/1477-3163.93001

Deng, X., He, G., Liu, J., Luo, F., Peng, X., Tang, S., Gao, Z., Lin, Q., Keller, J. M., Yang, T., & Keller, E. T. (2014). Recent advances in bone-targeted therapies of metastatic prostate cancer. *Cancer Treatment Reviews*, *40*(6), 730-738. https://doi.org/https://doi.org/10.1016/j.ctrv.2014.04.003

Denmeade, S. R., & Isaacs, J. T. (2002). A history of prostate cancer treatment. *Nat Rev Cancer*, *2*(5), 389-396. https://doi.org/10.1038/nrc801

Descotes, J. L. (2019). Diagnosis of prostate cancer. *Asian J Urol*, *6*(2), 129-136. https://doi.org/10.1016/j.ajur.2018.11.007

Devi Khwairakpam, A., Monisha, J., Roy, N. K., Bordoloi, D., Padmavathi, G., Banik, K., Khatoon, E., & Kunnumakkara, A. B. (2019). Vietnamese coriander inhibits cell proliferation, survival and migration via suppression of Akt/mTOR pathway in oral squamous cell carcinoma. *J Basic Clin Physiol Pharmacol*, *31*(3). https://doi.org/10.1515/jbcpp-2019-0162

Doogue, M. P., & Polasek, T. M. (2013). The ABCD of clinical pharmacokinetics. *Ther Adv Drug Saf*, *4*(1), 5-7. https://doi.org/10.1177/2042098612469335

Elbashir, S. M., Harborth, J., Lendeckel, W., Yalcin, A., Weber, K., & Tuschl, T. (2001). Duplexes of 21-nucleotide RNAs mediate RNA interference in cultured mammalian cells. *Nature*, *411*(6836), 494-498. https://doi.org/10.1038/35078107

Epstein, J. I., Egevad, L., Amin, M. B., Delahunt, B., Srigley, J. R., & Humphrey, P. A. (2016). The 2014 International Society of Urological Pathology (ISUP) Consensus Conference on Gleason Grading of Prostatic Carcinoma: Definition of Grading Patterns and Proposal for a New Grading System. *Am J Surg Pathol*, *40*(2), 244-252. https://doi.org/10.1097/pas.0000000000000530

Essah, P. A., Wickham, E. P., Nunley, J. R., & Nestler, J. E. (2006). Dermatology of androgen-related disorders. *Clinics in Dermatology*, *24*(4), 289-298. https://doi.org/10.1016/j.clindermatol.2006.04.004

Ewing, C. M., Ray, A. M., Lange, E. M., Zuhlke, K. A., Robbins, C. M., Tembe, W. D., Wiley, K. E., Isaacs, S. D., Johng, D., Wang, Y., Bizon, C., Yan, G., Gielzak, M., Partin, A. W., Shanmugam, V., Izatt, T., Sinari, S., Craig, D. W., Zheng, S. L., . . . Cooney, K. A. (2012). Germline mutations in HOXB13 and prostate-cancer risk. *N Engl J Med*, *366*(2), 141-149. https://doi.org/10.1056/NEJMoa1110000

Fagète, S., Steimer, C., & Girod, P.-A. (2019). Comparing two automated high throughput viable-cell counting systems for cell culture applications. *Journal of Biotechnology*, *305*, 23-26. https://doi.org/https://doi.org/10.1016/j.jbiotec.2019.08.014

Fay, E. K., & Graff, J. N. (2020). Immunotherapy in Prostate Cancer. *Cancers*, *12*(7), 1752. https://www.mdpi.com/2072-6694/12/7/1752

Fernández-Cancio, M., Camats, N., Flück, C. E., Zalewski, A., Dick, B., Frey, B. M., Monné, R., Torán, N., Audí, L., & Pandey, A. V. (2018). Mechanism of the Dual Activities of Human CYP17A1 and Binding to Anti-Prostate Cancer Drug Abiraterone Revealed by a Novel V366M Mutation Causing 17,20 Lyase Deficiency. *Pharmaceuticals*, *11*(2), 37. https://www.mdpi.com/1424-8247/11/2/37

Ferrís, I. T. J., Berbel-Tornero, O., Garcia, I. C. J., López-Andreu, J. A., Sobrino-Najul, E., & Ortega-García, J. A. (2011). [Non dietetic environmental risk factors in prostate

cancer]. *Actas Urol Esp*, *35*(5), 289-295. https://doi.org/10.1016/j.acuro.2010.12.010 (Factores de riesgo ambientales no dietéticos en el cáncer de próstata.)

Flück, C. E., & Miller, W. L. (2004). GATA-4 and GATA-6 modulate tissue-specific transcription of the human gene for P450c17 by direct interaction with Sp1. *Mol Endocrinol*, *18*(5), 1144-1157. https://doi.org/10.1210/me.2003-0342

Flück, C. E., Tajima, T., Pandey, A. V., Arlt, W., Okuhara, K., Verge, C. F., Jabs, E. W., Mendonça, B. B., Fujieda, K., & Miller, W. L. (2004). Mutant P450 oxidoreductase causes disordered steroidogenesis with and without Antley-Bixler syndrome. *Nature Genetics*, *36*(3), 228-230. https://doi.org/10.1038/ng1300

Fujita, K., & Nonomura, N. (2019). Role of Androgen Receptor in Prostate Cancer: A Review. *World J Mens Health*, *37*(3), 288-295. https://doi.org/10.5534/wjmh.180040

Gal, M., & Orly, J. (2014). Selective inhibition of steroidogenic enzymes by ketoconazole in rat ovary cells. *Clin Med Insights Reprod Health*, *8*, 15-22. https://doi.org/10.4137/cmrh.S14036

Gann, P. H. (2002). Risk factors for prostate cancer. *Rev Urol*, *4 Suppl 5*(Suppl 5), S3-s10.

Gazdar, A. F., Oie, H. K., Shackleton, C. H., Chen, T. R., Triche, T. J., Myers, C. E., Chrousos, G. P., Brennan, M. F., Stein, C. A., & La Rocca, R. V. (1990). Establishment and characterization of a human adrenocortical carcinoma cell line that expresses multiple pathways of steroid biosynthesis. *Cancer Res*, *50*(17), 5488-5496.

Ghadimi, M., & Sapra, A. (2023). Magnetic Resonance Imaging Contraindications. In *StatPearls*. StatPearls Publishing

Copyright © 2023, StatPearls Publishing LLC.

Ghasemi, M., Turnbull, T., Sebastian, S., & Kempson, I. (2021). The MTT Assay: Utility, Limitations, Pitfalls, and Interpretation in Bulk and Single-Cell Analysis. *Int J Mol Sci*, *22*(23). https://doi.org/10.3390/ijms222312827

Giwercman, A., & Giwercman, Y. L. (2000). Epidemiology of male reproductive disorders. In K. R. Feingold, B. Anawalt, M. R. Blackman, A. Boyce, G. Chrousos, E. Corpas, W. W. de Herder, K. Dhatariya, K. Dungan, J. Hofland, S. Kalra, G. Kaltsas, N. Kapoor, C. Koch, P. Kopp, M. Korbonits, C. S. Kovacs, W. Kuohung, B. Laferrère, M. Levy, E. A. McGee, R. McLachlan, M. New, J. Purnell, R. Sahay, A. S. Shah, F. Singer, M. A. Sperling, C. A. Stratakis, D. L. Trence, & D. P. Wilson (Eds.), *Endotext*. MDText.com, Inc.

Copyright © 2000-2023, MDText.com, Inc.

Gordetsky, J., & Epstein, J. (2016). Grading of prostatic adenocarcinoma: current state and prognostic implications. *Diagn Pathol*, *11*, 25. https://doi.org/10.1186/s13000-016-0478-2

Govindarajan, V. S., & Sathyanarayana, M. N. (1991). Capsicum--production, technology, chemistry, and quality. Part V. Impact on physiology, pharmacology, nutrition, and metabolism; structure, pungency, pain, and desensitization sequences. *Crit Rev Food Sci Nutr*, *29*(6), 435-474. https://doi.org/10.1080/10408399109527536

Gowtham Kumar, G., Paul, S. F. D., Molia, C., Manickavasagam, M., Ramya, R., Usha Rani, G., Ganesan, N., & Andrea Mary, F. (2022). The association between CYP17A1, CYP19A1, and HSD17B1 gene polymorphisms of estrogen synthesis pathway and ovarian

cancer predisposition. *Meta Gene*, *31*, 100985. https://doi.org/https://doi.org/10.1016/j.mgene.2021.100985

Greenwood, D. (1992). The quinine connection. *Journal of Antimicrobial Chemotherapy*, *30*(4), 417-427. https://doi.org/10.1093/jac/30.4.417

Guengerich, F. P. (2018). Mechanisms of Cytochrome P450-Catalyzed Oxidations. *ACS Catal*, *8*(12), 10964-10976. https://doi.org/10.1021/acscatal.8b03401

Gurel, B., Ali, T. Z., Montgomery, E. A., Begum, S., Hicks, J., Goggins, M., Eberhart, C. G., Clark, D. P., Bieberich, C. J., Epstein, J. I., & De Marzo, A. M. (2010). NKX3.1 as a marker of prostatic origin in metastatic tumors. *Am J Surg Pathol*, *34*(8), 1097-1105. https://doi.org/10.1097/PAS.0b013e3181e6cbf3

Hamilton, W., Sharp, D. J., Peters, T. J., & Round, A. P. (2006). Clinical features of prostate cancer before diagnosis: a population-based, case-control study. *Br J Gen Pract*, *56*(531), 756-762.

Hancock, J. F. (1992). COS Cell Expression. *Methods Mol Biol*, *8*, 153-158. https://doi.org/10.1385/0-89603-191-8:153

Hankey, B. F., Feuer, E. J., Clegg, L. X., Hayes, R. B., Legler, J. M., Prorok, P. C., Ries, L. A., Merrill, R. M., & Kaplan, R. S. (1999). Cancer surveillance series: interpreting trends in prostate cancer--part I: Evidence of the effects of screening in recent prostate cancer incidence, mortality, and survival rates. *J Natl Cancer Inst*, *91*(12), 1017-1024. https://doi.org/10.1093/jnci/91.12.1017

Hanley, N. A., Rainey, W. E., Wilson, D. I., Ball, S. G., & Parker, K. L. (2001). Expression profiles of SF-1, DAX1, and CYP17 in the human fetal adrenal gland: potential interactions in gene regulation. *Mol Endocrinol*, *15*(1), 57-68. https://doi.org/10.1210/mend.15.1.0585

Harris, W. P., Mostaghel, E. A., Nelson, P. S., & Montgomery, B. (2009). Androgen deprivation therapy: progress in understanding mechanisms of resistance and optimizing androgen depletion. *Nature clinical practice. Urology*, *6*(2), 76-85. https://doi.org/10.1038/ncpuro1296

Hellerstedt, B. A., & Pienta, K. J. (2002). The current state of hormonal therapy for prostate cancer. *CA Cancer J Clin*, *52*(3), 154-179. https://doi.org/10.3322/canjclin.52.3.154

HERBERT, V., LAU, K.-S., GOTTLIEB, C. W., & BLEICHER, S. J. (1965). Coated Charcoal Immunoassay of Insulin. *The Journal of Clinical Endocrinology & Metabolism*, *25*(10), 1375-1384. https://doi.org/10.1210/jcem-25-10-1375

Hornsby, P. J., & McAllister, J. M. (1991). Culturing steroidogenic cells. *Methods Enzymol*, *206*, 371-380. https://doi.org/10.1016/0076-6879(91)06107-e

Horoszewicz, J. S., Leong, S. S., Chu, T. M., Wajsman, Z. L., Friedman, M., Papsidero, L., Kim, U., Chai, L. S., Kakati, S., Arya, S. K., & Sandberg, A. A. (1980). The LNCaP cell line--a new model for studies on human prostatic carcinoma. *Prog Clin Biol Res*, *37*, 115-132.

Huang, N., Pandey, A. V., Agrawal, V., Reardon, W., Lapunzina, P. D., Mowat, D., Jabs, E. W., Van Vliet, G., Sack, J., Flück, C. E., & Miller, W. L. (2005). Diversity and function of mutations in p450 oxidoreductase in patients with Antley-Bixler syndrome and disordered steroidogenesis. *Am J Hum Genet*, *76*(5), 729-749. https://doi.org/10.1086/429417

Huggins, C., & Hodges, C. V. (1972). Studies on prostatic cancer. I. The effect of castration, of estrogen and androgen injection on serum phosphatases in metastatic carcinoma of the prostate. *CA Cancer J Clin*, *22*(4), 232-240. https://doi.org/10.3322/canjclin.22.4.232

Hyun, J. S. (2012). Prostate cancer and sexual function. *World J Mens Health*, *30*(2), 99-107. https://doi.org/10.5534/wjmh.2012.30.2.99

İnce Ergüç, E., Özcan Sezer, S., & Gürer Orhan, H. (2022). Advantages and Disadvantages of Two In Vitro Assays in Evaluating Aromatase Activity: "A Cell-Based and a Cell-Free Assay". *Turk J Pharm Sci*, *19*(6), 626-629. https://doi.org/10.4274/tjps.galenos.2021.85530

Jang, T. H., Park, S. C., Yang, J. H., Kim, J. Y., Seok, J. H., Park, U. S., Choi, C. W., Lee, S. R., & Han, J. (2017). Cryopreservation and its clinical applications. *Integr Med Res*, *6*(1), 12-18. https://doi.org/10.1016/j.imr.2016.12.001

Kamiloglu, S., Sari, G., Ozdal, T., & Capanoglu, E. (2020). Guidelines for cell viability assays [https://doi.org/10.1002/fft2.44]. *Food Frontiers*, *1*(3), 332-349. https://doi.org/https://doi.org/10.1002/fft2.44

Kandel, S. E., & Lampe, J. N. (2014). Role of protein-protein interactions in cytochrome P450-mediated drug metabolism and toxicity. *Chem Res Toxicol*, *27*(9), 1474-1486. https://doi.org/10.1021/tx500203s

Karlsson, Q., Brook, M. N., Dadaev, T., Wakerell, S., Saunders, E. J., Muir, K., Neal, D. E., Giles, G. G., MacInnis, R. J., Thibodeau, S. N., McDonnell, S. K., Cannon-Albright, L., Teixeira, M. R., Paulo, P., Cardoso, M., Huff, C., Li, D., Yao, Y., Scheet, P., . . . Kote-Jarai, Z. (2021). Rare Germline Variants in ATM Predispose to Prostate Cancer: A PRACTICAL Consortium Study. *Eur Urol Oncol*, *4*(4), 570-579. https://doi.org/10.1016/j.euo.2020.12.001

Katagiri, M., Kagawa, N., & Waterman, M. R. (1995). The Role of Cytochrome b5 in the Biosynthesis of Androgens by Human P450c17. *Archives of Biochemistry and Biophysics*, *317*(2), 343-347. https://doi.org/https://doi.org/10.1006/abbi.1995.1173

Kempná, P., Hirsch, A., Hofer, G., Mullis, P. E., & Flück, C. E. (2010). Impact of differential P450c17 phosphorylation by cAMP stimulation and by starvation conditions on enzyme activities and androgen production in NCI-H295R cells. *Endocrinology*, *151*(8), 3686-3696. https://doi.org/10.1210/en.2010-0093

Kempná, P., Hirsch, A., Hofer, G., Mullis, P. E., & Flück, C. E. (2010). Impact of Differential P450c17 Phosphorylation by cAMP Stimulation and by Starvation Conditions on Enzyme Activities and Androgen Production in NCI-H295R Cells. *Endocrinology*, *151*(8), 3686-3696. https://doi.org/10.1210/en.2010-0093

Kempná, P., Marti, N., Udhane, S., & Flück, C. E. (2015). Regulation of androgen biosynthesis - A short review and preliminary results from the hyperandrogenic starvation NCI-H295R cell model. *Mol Cell Endocrinol*, *408*, 124-132. https://doi.org/10.1016/j.mce.2014.12.015

Khuayjarernpanishk, T., Sookying, S., Duangjai, A., Saokaew, S., Sanbua, A., Bunteong, O., Rungruangsri, N., Suepsai, W., Sodsai, P., Soylaiad, J., Nacharoen, V., Noidamnoen, S., & Phisalprapa, P. (2022). Anticancer Activities of Polygonum odoratum Lour.: A

Systematic Review. *Front Pharmacol*, *13*, 875016. https://doi.org/10.3389/fphar.2022.875016

Kim, K., & Kim, J. S. (2017). Intervention for patient reported urinary symptoms in prostate cancer survivors: Systematic review. *J Cancer Surviv*, *11*(5), 643-654. https://doi.org/10.1007/s11764-017-0637-9

Kluth, L. A., Shariat, S. F., Kratzik, C., Tagawa, S., Sonpavde, G., Rieken, M., Scherr, D. S., & Pummer, K. (2014). The hypothalamic-pituitary-gonadal axis and prostate cancer: implications for androgen deprivation therapy. *World J Urol*, *32*(3), 669-676. https://doi.org/10.1007/s00345-013-1157-5

Kok, R. C., Timmerman, M. A., Wolffenbuttel, K. P., Drop, S. L., & de Jong, F. H. (2010). Isolated 17,20-lyase deficiency due to the cytochrome b5 mutation W27X. *J Clin Endocrinol Metab*, *95*(3), 994-999. https://doi.org/10.1210/jc.2008-1745

Korpimäki, T., Kurittu, J., & Karp, M. (2003). Surprisingly fast disappearance of beta-lactam selection pressure in cultivation as detected with novel biosensing approaches. *J Microbiol Methods*, *53*(1), 37-42. https://doi.org/10.1016/s0167-7012(02)00213-0

Kurlbaum, M., Sbiera, S., Kendl, S., Martin Fassnacht, M., & Kroiss, M. (2020). Steroidogenesis in the NCI-H295 Cell Line Model is Strongly Affected By Culture Conditions and Substrain. *Exp Clin Endocrinol Diabetes*, *128*(10), 672-680. https://doi.org/10.1055/a-1105-6332

Kwizera, R., Akampurira, A., Kandole, T. K., Nabaggala, M. S., Williams, D. A., Kambugu, A., Meya, D. B., Rhein, J., & Boulware, D. R. (2018). Evaluation of trypan blue stain in the TC20 automated cell counter as a point-of-care for the enumeration of viable cryptococcal cells in cerebrospinal fluid. *Med Mycol*, *56*(5), 559-564. https://doi.org/10.1093/mmy/myx076

Larson, E. C., Pond, C. D., Rai, P. P., Matainaho, T. K., Piskaut, P., Franklin, M. R., & Barrows, L. R. (2016). Traditional Preparations and Methanol Extracts of Medicinal Plants from Papua New Guinea Exhibit Similar Cytochrome P450 Inhibition. *Evid Based Complement Alternat Med*, *2016*, 7869710. https://doi.org/10.1155/2016/7869710

Larsson, P., Engqvist, H., Biermann, J., Werner Rönnerman, E., Forssell-Aronsson, E., Kovács, A., Karlsson, P., Helou, K., & Parris, T. Z. (2020). Optimization of cell viability assays to improve replicability and reproducibility of cancer drug sensitivity screens. *Sci Rep*, *10*(1), 5798. https://doi.org/10.1038/s41598-020-62848-5

Leblans, P., Vandenbroucke, D., & Willems, P. (2011). Storage Phosphors for Medical Imaging. *Materials (Basel)*, *4*(6), 1034-1086. https://doi.org/10.3390/ma4061034

Lepor, H. (2005). A review of surgical techniques for radical prostatectomy. *Rev Urol*, *7 Suppl 2*(Suppl 2), S11-17.

Leslie, S. W., Soon-Sutton, T. L., R, I. A., Sajjad, H., & Siref, L. E. (2023). Prostate Cancer. In *StatPearls*. StatPearls Publishing

Copyright © 2023, StatPearls Publishing LLC.

Lytton, B. (2001). Prostate cancer: a brief history and the discovery of hormonal ablation treatment. *J Urol*, *165*(6 Pt 1), 1859-1862.

MacGrogan, D., & Bookstein, R. (1997). Tumour suppressor genes in prostate cancer. *Semin Cancer Biol*, *8*(1), 11-19. https://doi.org/10.1006/scbi.1997.0048

Mahdi, J. G., Mahdi, A. J., Mahdi, A. J., & Bowen, I. D. (2006). The historical analysis of aspirin discovery, its relation to the willow tree and antiproliferative and anticancer potential. *Cell Proliferation*, *39*(2), 147-155. https://doi.org/https://doi.org/10.1111/j.1365-2184.2006.00377.x

Malikova, J., Brixius-Anderko, S., Udhane, S. S., Parween, S., Dick, B., Bernhardt, R., & Pandey, A. V. (2017). CYP17A1 inhibitor abiraterone, an anti-prostate cancer drug, also inhibits the 21-hydroxylase activity of CYP21A2. *The Journal of Steroid Biochemistry and Molecular Biology*, *174*, 192-200. https://doi.org/https://doi.org/10.1016/j.jsbmb.2017.09.007

Malke, H. (1990). J. SAMBROCK, E. F. FRITSCH and T. MANIATIS, Molecular Cloning, A Laboratory Manual (Second Edition), Volumes 1, 2 and 3. 1625 S., zahlreiche Abb. und Tab. Cold Spring Harbor 1989. Cold Spring Harbor Laboratory Press. $ 115.00. ISBN: 0-87969-309-6. *Journal of Basic Microbiology*, *30*(8), 623-623. https://doi.org/https://doi.org/10.1002/jobm.3620300824

Marston, A. (2011). Thin-layer chromatography with biological detection in phytochemistry. *J Chromatogr A*, *1218*(19), 2676-2683. https://doi.org/10.1016/j.chroma.2010.12.068

Martin, N. E., & D'Amico, A. V. (2014). Progress and controversies: Radiation therapy for prostate cancer. *CA: A Cancer Journal for Clinicians*, *64*(6), 389-407. https://doi.org/https://doi.org/10.3322/caac.21250

Martinez-Arguelles, D. B., & Papadopoulos, V. (2010). Epigenetic regulation of the expression of genes involved in steroid hormone biosynthesis and action. *Steroids*, *75*(7), 467-476. https://doi.org/10.1016/j.steroids.2010.02.004

Mateo, J., Boysen, G., Barbieri, C. E., Bryant, H. E., Castro, E., Nelson, P. S., Olmos, D., Pritchard, C. C., Rubin, M. A., & de Bono, J. S. (2017). DNA Repair in Prostate Cancer: Biology and Clinical Implications. *European Urology*, *71*(3), 417-425. https://doi.org/https://doi.org/10.1016/j.eururo.2016.08.037

Maxwell, K. N., Cheng, H. H., Powers, J., Gulati, R., Ledet, E. M., Morrison, C., Le, A., Hausler, R., Stopfer, J., Hyman, S., Kohlmann, W., Naumer, A., Vagher, J., Greenberg, S. E., Naylor, L., Laurino, M., Konnick, E. Q., Shirts, B. H., AlDubayan, S. H., . . . Pritchard, C. C. (2022). Inherited TP53 Variants and Risk of Prostate Cancer. *Eur Urol*, *81*(3), 243-250. https://doi.org/10.1016/j.eururo.2021.10.036

Melau, C., Riis, M. L., Nielsen, J. E., Perlman, S., Lundvall, L., Thuesen, L. L., Hare, K. J., Hammerum, M. S., Mitchell, R. T., Frederiksen, H., Juul, A., & Jørgensen, A. (2021). The effects of selected inhibitors on human fetal adrenal steroidogenesis differs under basal and ACTH-stimulated conditions. *BMC Medicine*, *19*(1), 204. https://doi.org/10.1186/s12916-021-02080-8

Meyer, M. S., Penney, K. L., Stark, J. R., Schumacher, F. R., Sesso, H. D., Loda, M., Fiorentino, M., Finn, S., Flavin, R. J., Kurth, T., Price, A. L., Giovannucci, E. L., Fall, K., Stampfer, M. J., Ma, J., & Mucci, L. A. (2010). Genetic variation in RNASEL associated with prostate cancer risk and progression. *Carcinogenesis*, *31*(9), 1597-1603. https://doi.org/10.1093/carcin/bgq132

Miller, W. L. (2009). Androgen synthesis in adrenarche. *Reviews in Endocrine and Metabolic Disorders*, *10*(1), 3-17. https://doi.org/10.1007/s11154-008-9102-4

Miller, W. L., & Auchus, R. J. (2011). The Molecular Biology, Biochemistry, and Physiology of Human Steroidogenesis and Its Disorders. *Endocrine Reviews*, *32*(1), 81-151. https://doi.org/10.1210/er.2010-0013

Miller, W. L., Auchus, R. J., & Geller, D. H. (1997). The regulation of 17,20 lyase activity. *Steroids*, *62*(1), 133-142. https://doi.org/https://doi.org/10.1016/S0039-128X(96)00172-9

Montgomery, R. B., Mostaghel, E. A., Vessella, R., Hess, D. L., Kalhorn, T. F., Higano, C. S., True, L. D., & Nelson, P. S. (2008). Maintenance of Intratumoral Androgens in Metastatic Prostate Cancer: A Mechanism for Castration-Resistant Tumor Growth. *Cancer Research*, *68*(11), 4447. https://doi.org/10.1158/0008-5472.can-08-0249

Montgomery, R. B., Mostaghel, E. A., Vessella, R., Hess, D. L., Kalhorn, T. F., Higano, C. S., True, L. D., & Nelson, P. S. (2008). Maintenance of intratumoral androgens in metastatic prostate cancer: a mechanism for castration-resistant tumor growth. *Cancer Res*, *68*(11), 4447-4454. https://doi.org/10.1158/0008-5472.Can-08-0249

Morán, F. M., VandeVoort, C. A., Overstreet, J. W., Lasley, B. L., & Conley, A. J. (2003). Molecular Target of Endocrine Disruption in Human Luteinizing Granulosa Cells by 2,3,7,8-Tetrachlorodibenzo-p-Dioxin: Inhibition of Estradiol Secretion Due to Decreased 17α-Hydroxylase/17,20-Lyase Cytochrome P450 Expression. *Endocrinology*, *144*(2), 467-473. https://doi.org/10.1210/en.2002-220813

Mosmann, T. (1983). Rapid colorimetric assay for cellular growth and survival: application to proliferation and cytotoxicity assays. *J Immunol Methods*, *65*(1-2), 55-63. https://doi.org/10.1016/0022-1759(83)90303-4

Mountjoy, K. G., Bird, I. M., Rainey, W. E., & Cone, R. D. (1994). ACTH induces up-regulation of ACTH receptor mRNA in mouse and human adrenocortical cell lines. *Mol Cell Endocrinol*, *99*(1), R17-20. https://doi.org/10.1016/0303-7207(94)90160-0

Mustafa, M., Salih, A., Illzam, E., Sharifa, A., Suleiman, M., & Hussain, S. (2016). Prostate cancer: pathophysiology, diagnosis, and prognosis. *IOSR Journal of Dental and Medical Sciences*, *15*(6), 04-11.

Njar, V. C. O., & Brodie, A. M. H. (2015). Discovery and Development of Galeterone (TOK-001 or VN/124-1) for the Treatment of All Stages of Prostate Cancer. *Journal of Medicinal Chemistry*, *58*(5), 2077-2087. https://doi.org/10.1021/jm501239f

Nyberg, T., Frost, D., Barrowdale, D., Evans, D. G., Bancroft, E., Adlard, J., Ahmed, M., Barwell, J., Brady, A. F., Brewer, C., Cook, J., Davidson, R., Donaldson, A., Eason, J., Gregory, H., Henderson, A., Izatt, L., Kennedy, M. J., Miller, C., . . . Antoniou, A. C. (2020). Prostate Cancer Risks for Male BRCA1 and BRCA2 Mutation Carriers: A Prospective Cohort Study. *Eur Urol*, *77*(1), 24-35. https://doi.org/10.1016/j.eururo.2019.08.025

O'Brien, M. F., Galvin, D. J., & Mulhall, J. P. (2009). The Contribution of Irish Urology to Clinical Practice. *Urology*, *74*(5), 972-978. https://doi.org/https://doi.org/10.1016/j.urology.2009.05.019

Okada, K., Laudenbach, I., & Schroeder, F. H. (1976). Human prostatic epithelial cells in culture: clonal selection and androgen dependence of cell line EB 33. *J Urol*, *115*(2), 164-167. https://doi.org/10.1016/s0022-5347(17)59116-8

Okoye, E., & Saikali, S. W. (2023). Orchiectomy. In *StatPearls*. StatPearls Publishing Copyright © 2023, StatPearls Publishing LLC.

Owen, L. J., & Keevil, B. G. (2012). Testosterone measurement by liquid chromatography tandem mass spectrometry: the importance of internal standard choice. *Ann Clin Biochem*, *49*(Pt 6), 600-602. https://doi.org/10.1258/acb.2012.012037

Oyagbemi, A. A., Saba, A. B., & Azeez, O. I. (2010). Capsaicin: a novel chemopreventive molecule and its underlying molecular mechanisms of action. *Indian J Cancer*, *47*(1), 53-58. https://doi.org/10.4103/0019-509x.58860

Ozbay, T., Rowan, A., Leon, A., Patel, P., & Sewer, M. B. (2006). Cyclic adenosine 5'-monophosphate-dependent sphingosine-1-phosphate biosynthesis induces human CYP17 gene transcription by activating cleavage of sterol regulatory element binding protein 1. *Endocrinology*, *147*(3), 1427-1437. https://doi.org/10.1210/en.2005-1091

Pandey, A. V., Mellon, S. H., & Miller, W. L. (2003). Protein Phosphatase 2A and Phosphoprotein SET Regulate Androgen Production by P450c17. *Journal of Biological Chemistry*, *278*(5), 2837-2844. https://doi.org/10.1074/jbc.M209527200

Pandey, A. V., Mellon, S. H., & Miller, W. L. (2003). Protein phosphatase 2A and phosphoprotein SET regulate androgen production by P450c17. *J Biol Chem*, *278*(5), 2837-2844. https://doi.org/10.1074/jbc.M209527200

Pandey, A. V., & Miller, W. L. (2005a). Regulation of 17,20 Lyase Activity by Cytochrome b5 and by Serine Phosphorylation of P450c17*. *Journal of Biological Chemistry*, *280*(14), 13265-13271. https://doi.org/https://doi.org/10.1074/jbc.M414673200

Pandey, A. V., & Miller, W. L. (2005b). Regulation of 17,20 Lyase Activity by Cytochromeb5and by Serine Phosphorylation of P450c17. *Journal of Biological Chemistry*, *280*(14), 13265-13271. https://doi.org/10.1074/jbc.M414673200

Patterson, J. C., Varkaris, A., Croucher, P. J. P., Ridinger, M., Dalrymple, S., Nouri, M., Xie, F., Varmeh, S., Jonas, O., Whitman, M. A., Chen, S., Rashed, S., Makusha, L., Luo, J., Isaacs, J. T., Erlander, M. G., Einstein, D. J., Balk, S. P., & Yaffe, M. B. (2023). Plk1 Inhibitors and Abiraterone Synergistically Disrupt Mitosis and Kill Cancer Cells of Disparate Origin Independently of Androgen Receptor Signaling. *Cancer Res*, *83*(2), 219-238. https://doi.org/10.1158/0008-5472.Can-22-1533

Qiu, X., Boufaied, N., Hallal, T., Feit, A., de Polo, A., Luoma, A. M., Alahmadi, W., Larocque, J., Zadra, G., Xie, Y., Gu, S., Tang, Q., Zhang, Y., Syamala, S., Seo, J.-H., Bell, C., O'Connor, E., Liu, Y., Schaeffer, E. M., . . . Labbé, D. P. (2022). MYC drives aggressive prostate cancer by disrupting transcriptional pause release at androgen receptor targets. *Nature Communications*, *13*(1), 2559. https://doi.org/10.1038/s41467-022-30257-z

Rainey, W. E., Bird, I. M., Sawetawan, C., Hanley, N. A., McCarthy, J. L., McGee, E. A., Wester, R., & Mason, J. I. (1993). Regulation of human adrenal carcinoma cell (NCI-H295) production of C19 steroids. *J Clin Endocrinol Metab*, *77*(3), 731-737. https://doi.org/10.1210/jcem.77.3.8396576

Ramsey, J. T., Li, Y., Arao, Y., Naidu, A., Coons, L. A., Diaz, A., & Korach, K. S. (2019). Lavender Products Associated With Premature Thelarche and Prepubertal Gynecomastia: Case Reports and Endocrine-Disrupting Chemical Activities. *J Clin Endocrinol Metab*, *104*(11), 5393-5405. https://doi.org/10.1210/jc.2018-01880

Ramsey, J. T., Shropshire, B. C., Nagy, T. R., Chambers, K. D., Li, Y., & Korach, K. S. (2020). Essential Oils and Health. *Yale J Biol Med*, *93*(2), 291-305.

Rawla, P. (2019). Epidemiology of Prostate Cancer. *World J Oncol*, *10*(2), 63-89. https://doi.org/10.14740/wjon1191

Řebíčková, K., Bajer, T., Šilha, D., Houdková, M., Ventura, K., & Bajerová, P. (2020). Chemical Composition and Determination of the Antibacterial Activity of Essential Oils in Liquid and Vapor Phases Extracted from Two Different Southeast Asian Herbs—Houttuynia cordata (Saururaceae) and Persicaria odorata (Polygonaceae). *Molecules*, *25*(10), 2432. https://www.mdpi.com/1420-3049/25/10/2432

Reed, K. C., & Ohno, S. (1976). Kinetic properties of human placental aromatase. Application of an assay measuring 3H2O release from 1beta,2beta-3H-androgens. *J Biol Chem*, *251*(6), 1625-1631.

Reynolds, A. R., & Kyprianou, N. (2006). Growth factor signalling in prostatic growth: significance in tumour development and therapeutic targeting. *Br J Pharmacol*, *147 Suppl 2*(Suppl 2), S144-152. https://doi.org/10.1038/sj.bjp.0706635

Riss, T. L., Moravec, R. A., Niles, A. L., Duellman, S., Benink, H. A., Worzella, T. J., & Minor, L. (2004). Cell Viability Assays. In S. Markossian, A. Grossman, K. Brimacombe, M. Arkin, D. Auld, C. Austin, J. Baell, T. D. Y. Chung, N. P. Coussens, J. L. Dahlin, V. Devanarayan, T. L. Foley, M. Glicksman, K. Gorshkov, J. V. Haas, M. D. Hall, S. Hoare, J. Inglese, P. W. Iversen, S. C. Kales, M. Lal-Nag, Z. Li, J. McGee, O. McManus, T. Riss, P. Saradjian, G. S. Sittampalam, M. Tarselli, O. J. Trask, Jr., Y. Wang, J. R. Weidner, M. J. Wildey, K. Wilson, M. Xia, & X. Xu (Eds.), *Assay Guidance Manual*. Eli Lilly & Company and the National Center for Advancing Translational Sciences.

Romijn, J. C., Verkoelen, C. F., & Schroeder, F. H. (1988). Application of the MTT assay to human prostate cancer cell lines in vitro: Establishment of test conditions and assessment of hormone-stimulated growth and drug-induced cytostatic and cytotoxic effects. *The Prostate*, *12*(1), 99-110. https://doi.org/https://doi.org/10.1002/pros.2990120112

Ruggiero, C., & Lalli, E. (2016). Impact of ACTH Signaling on Transcriptional Regulation of Steroidogenic Genes. *Front Endocrinol (Lausanne)*, *7*, 24. https://doi.org/10.3389/fendo.2016.00024

Santiago, M., & Strobel, S. (2013). Thin layer chromatography. *Methods Enzymol*, *533*, 303-324. https://doi.org/10.1016/b978-0-12-420067-8.00024-6

Schally, A. V., Kastin, A. J., & Arimura, A. (1971). Hypothalamic follicle-stimulating hormone (FSH) and luteinizing hormone (LH)-regulating hormone: structure, physiology, and clinical studies. *Fertil Steril*, *22*(11), 703-721.

Seidenfeld, J., Samson, D. J., Hasselblad, V., Aronson, N., Albertsen, P. C., Bennett, C. L., & Wilt, T. J. (2000). Single-therapy androgen suppression in men with advanced prostate cancer: a systematic review and meta-analysis. *Ann Intern Med*, *132*(7), 566-577. https://doi.org/10.7326/0003-4819-132-7-200004040-00009

Sewer, M. B., & Jagarlapudi, S. (2009). Complex assembly on the human CYP17 promoter. *Mol Cell Endocrinol*, *300*(1-2), 109-114. https://doi.org/10.1016/j.mce.2008.10.006

Shackleton, C. H. L., Kletke, C., Wudy, S., & Pratt, J. H. (1990). Dehydroepiandrosterone sulfate quantification in serum using high-performance liquid chromatography/ mass spectrometry and a deuterated internal standard: a technique suitable for routine use or as a reference method. *Steroids*, *55*(10), 472-478. https://doi.org/https://doi.org/10.1016/0039-128X(90)90016-5

Shapira, J., & Perkins, W. H. (1960). Liquid scintillation counting of aqueous solutions of carbon-14 and tritium. *Science*, *131*(3398), 414-415. https://doi.org/10.1126/science.131.3398.414

Shariat, S. F., & Roehrborn, C. G. (2008). Using biopsy to detect prostate cancer. *Rev Urol*, *10*(4), 262-280.

Shen, S., & Strobel, H. W. (1993). Role of lysine and arginine residues of cytochrome P450 in the interaction between cytochrome P4502B1 and NADPH-cytochrome P450 reductase. *Arch Biochem Biophys*, *304*(1), 257-265. https://doi.org/10.1006/abbi.1993.1347

Shimizu, T., Tateishi, T., Hatano, M., & Fujii-Kuriyama, Y. (1991). Probing the role of lysines and arginines in the catalytic function of cytochrome P450d by site-directed mutagenesis. Interaction with NADPH-cytochrome P450 reductase. *J Biol Chem*, *266*(6), 3372-3375.

Silvestre, C. I. C., Santos, J. L. M., Lima, J. L. F. C., & Zagatto, E. A. G. (2009). Liquid–liquid extraction in flow analysis: A critical review. *Analytica Chimica Acta*, *652*(1), 54-65. https://doi.org/https://doi.org/10.1016/j.aca.2009.05.042

Simard, J., Ricketts, M. L., Gingras, S., Soucy, P., Feltus, F. A., & Melner, M. H. (2005). Molecular biology of the 3beta-hydroxysteroid dehydrogenase/delta5-delta4 isomerase gene family. *Endocr Rev*, *26*(4), 525-582. https://doi.org/10.1210/er.2002-0050

Sjöblom, L., Saramäki, O., Annala, M., Leinonen, K., Nättinen, J., Tolonen, T., Wahlfors, T., Nykter, M., Bova, G. S., Schleutker, J., Tammela, T. L., Lilja, H., & Visakorpi, T. (2016). Microseminoprotein-Beta Expression in Different Stages of Prostate Cancer. *PLoS One*, *11*(3), e0150241. https://doi.org/10.1371/journal.pone.0150241

Smail, P. J., Faiman, C., Hobson, W. C., Fuller, G. B., & Winter, J. S. (1982). Further studies on adrenarche in nonhuman primates. *Endocrinology*, *111*(3), 844-848. https://doi.org/10.1210/endo-111-3-844

Soldin, S. J., & Soldin, O. P. (2009). Steroid Hormone Analysis by Tandem Mass Spectrometry. *Clinical Chemistry*, *55*(6), 1061-1066. https://doi.org/10.1373/clinchem.2007.100008

Southern, P. J., & Berg, P. (1982). Transformation of mammalian cells to antibiotic resistance with a bacterial gene under control of the SV40 early region promoter. *J Mol Appl Genet*, *1*(4), 327-341.

Staels, B., Hum, D. W., & Miller, W. L. (1993). Regulation of steroidogenesis in NCI-H295 cells: a cellular model of the human fetal adrenal. *Mol Endocrinol*, *7*(3), 423-433. https://doi.org/10.1210/mend.7.3.8387159

Steegmaier, M., Hoffmann, M., Baum, A., Lénárt, P., Petronczki, M., Krssák, M., Gürtler, U., Garin-Chesa, P., Lieb, S., Quant, J., Grauert, M., Adolf, G. R., Kraut, N., Peters, J. M., & Rettig, W. J. (2007). BI 2536, a potent and selective inhibitor of polo-like kinase 1,

inhibits tumor growth in vivo. *Curr Biol*, *17*(4), 316-322. https://doi.org/10.1016/j.cub.2006.12.037

Stein, M. N., Patel, N., Bershadskiy, A., Sokoloff, A., & Singer, E. A. (2014). Androgen synthesis inhibitors in the treatment of castration-resistant prostate cancer. *Asian J Androl*, *16*(3), 387-400. https://doi.org/10.4103/1008-682x.129133

Stenman, U. H., Leinonen, J., Zhang, W. M., & Finne, P. (1999). Prostate-specific antigen. *Semin Cancer Biol*, *9*(2), 83-93. https://doi.org/10.1006/scbi.1998.0086

Storbeck, K.-H., Swart, A. C., Goosen, P., & Swart, P. (2013). Cytochrome b5: Novel roles in steroidogenesis. *Molecular and Cellular Endocrinology*, *371*(1-2), 87-99. https://doi.org/10.1016/j.mce.2012.11.020

Streicher, J., Meyerson, B. L., Karivedu, V., & Sidana, A. (2019). A review of optimal prostate biopsy: indications and techniques. *Ther Adv Urol*, *11*, 1756287219870074. https://doi.org/10.1177/1756287219870074

Sun, T., Zhao, Y., Mangelsdorf, D. J., & Simpson, E. R. (1998). Characterization of a region upstream of exon I.1 of the human CYP19 (aromatase) gene that mediates regulation by retinoids in human choriocarcinoma cells. *Endocrinology*, *139*(4), 1684-1691. https://doi.org/10.1210/endo.139.4.5959

Taitt, H. E. (2018). Global Trends and Prostate Cancer: A Review of Incidence, Detection, and Mortality as Influenced by Race, Ethnicity, and Geographic Location. *Am J Mens Health*, *12*(6), 1807-1823. https://doi.org/10.1177/1557988318798279

Tan, M. H. E., Li, J., Xu, H. E., Melcher, K., & Yong, E.-l. (2015). Androgen receptor: structure, role in prostate cancer and drug discovery. *Acta Pharmacologica Sinica*, *36*(1), 3-23. https://doi.org/10.1038/aps.2014.18

Tee, M. K., Dong, Q., & Miller, W. L. (2008). Pathways leading to phosphorylation of p450c17 and to the posttranslational regulation of androgen biosynthesis. *Endocrinology*, *149*(5), 2667-2677. https://doi.org/10.1210/en.2007-1527

Tee, M. K., & Miller, W. L. (2013). Phosphorylation of human cytochrome P450c17 by p38α selectively increases 17,20 lyase activity and androgen biosynthesis. *J Biol Chem*, *288*(33), 23903-23913. https://doi.org/10.1074/jbc.M113.460048

Telloni, S. M. (2017). Tumor Staging and Grading: A Primer. *Methods Mol Biol*, *1606*, 1-17. https://doi.org/10.1007/978-1-4939-6990-6_1

Thomason, L. C., Sawitzke, J. A., Li, X., Costantino, N., & Court, D. L. (2014). Recombineering: genetic engineering in bacteria using homologous recombination. *Curr Protoc Mol Biol*, *106*, 1.16.11-11.16.39. https://doi.org/10.1002/0471142727.mb0116s106

Thompson, E. A., & Siiteri, P. K. (1974). The Involvement of Human Placental Microsomal Cytochrome P-450 in Aromatization. *Journal of Biological Chemistry*, *249*(17), 5373-5378. https://doi.org/https://doi.org/10.1016/S0021-9258(20)79736-X

Udhane, S. S., Dick, B., Hu, Q., Hartmann, R. W., & Pandey, A. V. (2016). Specificity of anti-prostate cancer CYP17A1 inhibitors on androgen biosynthesis. *Biochemical and Biophysical Research Communications*, *477*(4), 1005-1010. https://doi.org/https://doi.org/10.1016/j.bbrc.2016.07.019

van Steenbrugge, G. J., Groen, M., van Dongen, J. W., Bolt, J., van der Korput, H., Trapman, J., Hasenson, M., & Horoszewicz, J. (1989). The human prostatic carcinoma cell line

LNCaP and its derivatives. An overview. *Urol Res*, *17*(2), 71-77. https://doi.org/10.1007/bf00262024

Walsh, P. C., Lepor, H., & Eggleston, J. C. (1983). Radical prostatectomy with preservation of sexual function: anatomical and pathological considerations. *Prostate*, *4*(5), 473-485. https://doi.org/10.1002/pros.2990040506

Wang, L., McDonnell, S. K., Elkins, D. A., Slager, S. L., Christensen, E., Marks, A. F., Cunningham, J. M., Peterson, B. J., Jacobsen, S. J., Cerhan, J. R., Blute, M. L., Schaid, D. J., & Thibodeau, S. N. (2001). Role of HPC2/ELAC2 in hereditary prostate cancer. *Cancer Res*, *61*(17), 6494-6499.

Wiegman, T., Woldring, M. G., & Pratt, J. J. (1975). A new cocktail for liquid scintillation counting of aqueous radioimmunoassay-samples. *Clinica Chimica Acta*, *59*(3), 347-356. https://doi.org/https://doi.org/10.1016/0009-8981(75)90010-8

Wróbel, T. M., Jørgensen, F. S., Pandey, A. V., Grudzińska, A., Sharma, K., Yakubu, J., & Björkling, F. (2023). Non-steroidal CYP17A1 Inhibitors: Discovery and Assessment. *Journal of Medicinal Chemistry*, *66*(10), 6542-6566. https://doi.org/10.1021/acs.jmedchem.3c00442

Wróbel, T. M., Rogova, O., Andersen, K. L., Yadav, R., Brixius-Anderko, S., Scott, E. E., Olsen, L., Jørgensen, F. S., & Björkling, F. (2020). Discovery of Novel Non-Steroidal Cytochrome P450 17A1 Inhibitors as Potential Prostate Cancer Agents. *Int J Mol Sci*, *21*(14). https://doi.org/10.3390/ijms21144868

Wu, X., Gong, S., Roy-Burman, P., Lee, P., & Culig, Z. (2013). Current mouse and cell models in prostate cancer research. *Endocrine-Related Cancer*, *20*(4), R155-R170. https://doi.org/10.1530/erc-12-0285

Wudy, S. A., Schuler, G., Sánchez-Guijo, A., & Hartmann, M. F. (2018). The art of measuring steroids: Principles and practice of current hormonal steroid analysis. *The Journal of Steroid Biochemistry and Molecular Biology*, *179*, 88-103. https://doi.org/https://doi.org/10.1016/j.jsbmb.2017.09.003

Yamaoka, M., Hara, T., Hitaka, T., Kaku, T., Takeuchi, T., Takahashi, J., Asahi, S., Miki, H., Tasaka, A., & Kusaka, M. (2012). Orteronel (TAK-700), a novel non-steroidal 17,20-lyase inhibitor: effects on steroid synthesis in human and monkey adrenal cells and serum steroid levels in cynomolgus monkeys. *J Steroid Biochem Mol Biol*, *129*(3-5), 115-128. https://doi.org/10.1016/j.jsbmb.2012.01.001

Yin, H. H., Simonov, A. N., Holien, J. K., Yeung, J. C. I., Nguyen, A. D., Corbin, C. J., Zheng, J., Kuznetsov, V. L., Auchus, R. J., Conley, A. J., Bond, A. M., Parker, M. W., Rodgers, R. J., & Martin, L. L. (2015). Mechanistic Scrutiny Identifies a Kinetic Role for Cytochrome b5 Regulation of Human Cytochrome P450c17 (CYP17A1, P450 17A1). *Plos One*, *10*(11), e0141252. https://doi.org/10.1371/journal.pone.0141252

Yin, L., & Hu, Q. (2014). CYP17 inhibitors--abiraterone, C17,20-lyase inhibitors and multi-targeting agents. *Nat Rev Urol*, *11*(1), 32-42. https://doi.org/10.1038/nrurol.2013.274

Yoshimoto, F. K., & Auchus, R. J. (2015). The diverse chemistry of cytochrome P450 17A1 (P450c17, CYP17A1). *J Steroid Biochem Mol Biol*, *151*, 52-65. https://doi.org/10.1016/j.jsbmb.2014.11.026

Zeegers, M. P., Jellema, A., & Ostrer, H. (2003). Empiric risk of prostate carcinoma for relatives of patients with prostate carcinoma: a meta-analysis. *Cancer*, *97*(8), 1894-1903. https://doi.org/10.1002/cncr.11262

Zhang, L. H., Rodriguez, H., Ohno, S., & Miller, W. L. (1995). Serine phosphorylation of human P450c17 increases 17,20-lyase activity: implications for adrenarche and the polycystic ovary syndrome. *Proc Natl Acad Sci U S A*, *92*(23), 10619-10623. https://doi.org/10.1073/pnas.92.23.10619

Zhang, Z., Chen, L., Wang, H., Ahmad, N., & Liu, X. (2015). Inhibition of Plk1 represses androgen signaling pathway in castration-resistant prostate cancer. *Cell Cycle*, *14*(13), 2142-2148. https://doi.org/10.1080/15384101.2015.1041689

Zhang, Z., Hou, X., Shao, C., Li, J., Cheng, J. X., Kuang, S., Ahmad, N., Ratliff, T., & Liu, X. (2014). Plk1 inhibition enhances the efficacy of androgen signaling blockade in castration-resistant prostate cancer. *Cancer Res*, *74*(22), 6635-6647. https://doi.org/10.1158/0008-5472.Can-14-1916

Zhu, Y., Liu, C., Nadiminty, N., Lou, W., Tummala, R., Evans, C. P., & Gao, A. C. (2013). Inhibition of ABCB1 expression overcomes acquired docetaxel resistance in prostate cancer. *Mol Cancer Ther*, *12*(9), 1829-1836. https://doi.org/10.1158/1535-7163.Mct-13-0208

Zuber, M. X., Simpson, E. R., & Waterman, M. R. (1986). Expression of bovine 17 alpha-hydroxylase cytochrome P-450 cDNA in nonsteroidogenic (COS 1) cells. *Science*, *234*(4781), 1258. https://doi.org/10.1126/science.3535074

UNIVERSITÄT BERN

List of Publications

- **Sharma, K**., Lanzilotto, A., Yakubu, J., Therkelsen, S., Vöegel, C.D., Du Toit, T., Jørgensen, F.S., Pandey, A.V. Essential oil terpenes may inhibit steroidogenic cytochrome P450 activities. bioRxiv 2023.10.31.564977; doi: https://doi.org/10.1101/2023.10.31.564977 (Published as preprint, Manuscript submitted for publication)
- Wróbel, T.M.; **Sharma, K**.; Mannella, I.; Oliaro-Bosso, S.; Nieckarz, P.; Du Toit, T.; Voegel, C.D.; Rojas Velazquez, M.N.; Yakubu, J.; Matveeva, A.; et al. Exploring the Potential of Sulfur Moieties in Compounds Inhibiting Steroidogenesis. Biomolecules 2023, 13, 1349. https://doi.org/10.3390/biom13091349
- Wróbel, T. M., Jørgensen, F. S., Pandey, A. V., Grudzińska, A., **Sharma, K.**, Yakubu, J., & Björkling, F. (**2023**). Non-steroidal CYP17A1 Inhibitors: Discovery and Assessment. Journal of medicinal chemistry, 66(10), 6542–6566. https://doi.org/10.1021/acs.jmedchem.3c00442
- Wróbel, T.M.; Rogova, O.; **Sharma, K**.; Rojas Velazquez, M.N.; Pandey, A.V.; Jørgensen, F.S.; Arendrup, F.S.; Andersen, K.L.; Björkling, F. Synthesis and Structure–Activity Relationships of Novel Non-Steroidal CYP17A1 Inhibitors as Potential Prostate Cancer Agents. *Biomolecules* **2022**, *12*, 165. https://doi.org/10.3390/biom12020165
- Humbert, M., Seiler, K., Mosimann, S., Rentsch, V., **Sharma, K**., Pandey, A. V., McKenna, S. L., & Tschan, M. P. (**2021**). Reducing FASN expression sensitizes acute myeloid leukemia cells to differentiation therapy. Cell death and differentiation, 28(8), 2465–2481. https://doi.org/10.1038/s41418-021-00768-1

Appendix I

Journal of Medicinal Chemistry

pubs.acs.org/jmc

Perspective

Non-steroidal CYP17A1 Inhibitors: Discovery and Assessment

Tomasz M. Wróbel,* Flemming Steen Jørgensen, Amit V. Pandey, Angelika Grudzińska, Katyayani Sharma, Jibira Yakubu, and Fredrik Björkling

Cite This: *J. Med. Chem.* 2023, 66, 6542−6566

Read Online

ACCESS | Metrics & More | Article Recommendations | Supporting Information

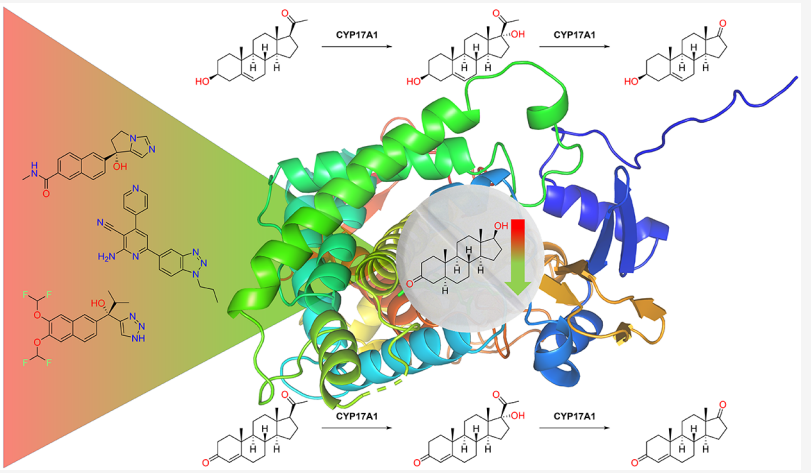

ABSTRACT: CYP17A1 is an enzyme that plays a major role in steroidogenesis and is critically involved in the biosynthesis of steroid hormones. Therefore, it remains an attractive target in several serious hormone-dependent cancer diseases, such as prostate cancer and breast cancer. The medicinal chemistry community has been committed to the discovery and development of CYP17A1 inhibitors for many years, particularly for the treatment of castration-resistant prostate cancer. The current Perspective reflects upon the discovery and evaluation of non-steroidal CYP17A1 inhibitors from a medicinal chemistry angle. Emphasis is placed on the structural aspects of the target, key learnings from the presented chemotypes, and design guidelines for future inhibitors.

1. INTRODUCTION

Cytochrome P450 17A1 (CYP17A1) is a membrane-bound dual-function monooxygenase belonging to the CYP 450 superfamily of enzymes. In humans, these proteins oxidize steroids, fatty acids, and xenobiotics and are crucial in steroid hormone biosynthesis and breakdown. Physiologically, CYP17A1 has an important role in the maturation and sex differentiation process, and the enzyme is found in the testes, adrenal glands, and ovaries. Furthermore, it contributes to the pathogenesis of diseases such as prostate cancer, polycystic ovary syndrome, and breast cancer.[1,2] In view of this, extensive interest and effort have been put into the discovery of compounds that regulate the activity of CYP17A1, with one of the specific aims to find drugs useful in the treatment of castration-resistant prostate cancer.

CYP17A1 is encoded by a single gene on chromosome 10q24.3 and catalyzes two successive reactions, 17α-hydroxylation and 17,20-lyase transformation.[3] The activity of CYP17A1 depends on redox interaction with P450 reductase (POR) and, in the case of the 17,20-lyase reaction, also cytochrome b5 (cyt b_5).[4−6]

The lack of CYP17A1 activity results in a redirection of the synthesis towards the competing formation of aldosterone. The 17α-hydroxylase reaction hydroxylates both pregnenolone and progesterone at C17 to provide 17α-hydroxypregnenolone (17OH-Preg) and 17α-hydroxyprogesterone (17OH-Prog), respectively (Figure 1).[2,7,8] Ultimately, the 17,20-lyase reaction breaks the bond between C17 and C20, transforming 17OH-Preg into dehydroepiandrosterone (DHEA) and 17OH-Prog into androstenedione. However, the direct conversion of 17OH-Prog to androstenedione is inefficient in humans, and androstenedione is formed primarily from the transformation of DHEA.[9] 17OH-Prog is converted mainly to glucocorticoids, including cortisol.

Received: March 12, 2023
Published: May 16, 2023

https://doi.org/10.1021/acs.jmedchem.3c00442
J. Med. Chem. 2023, 66, 6542−6566

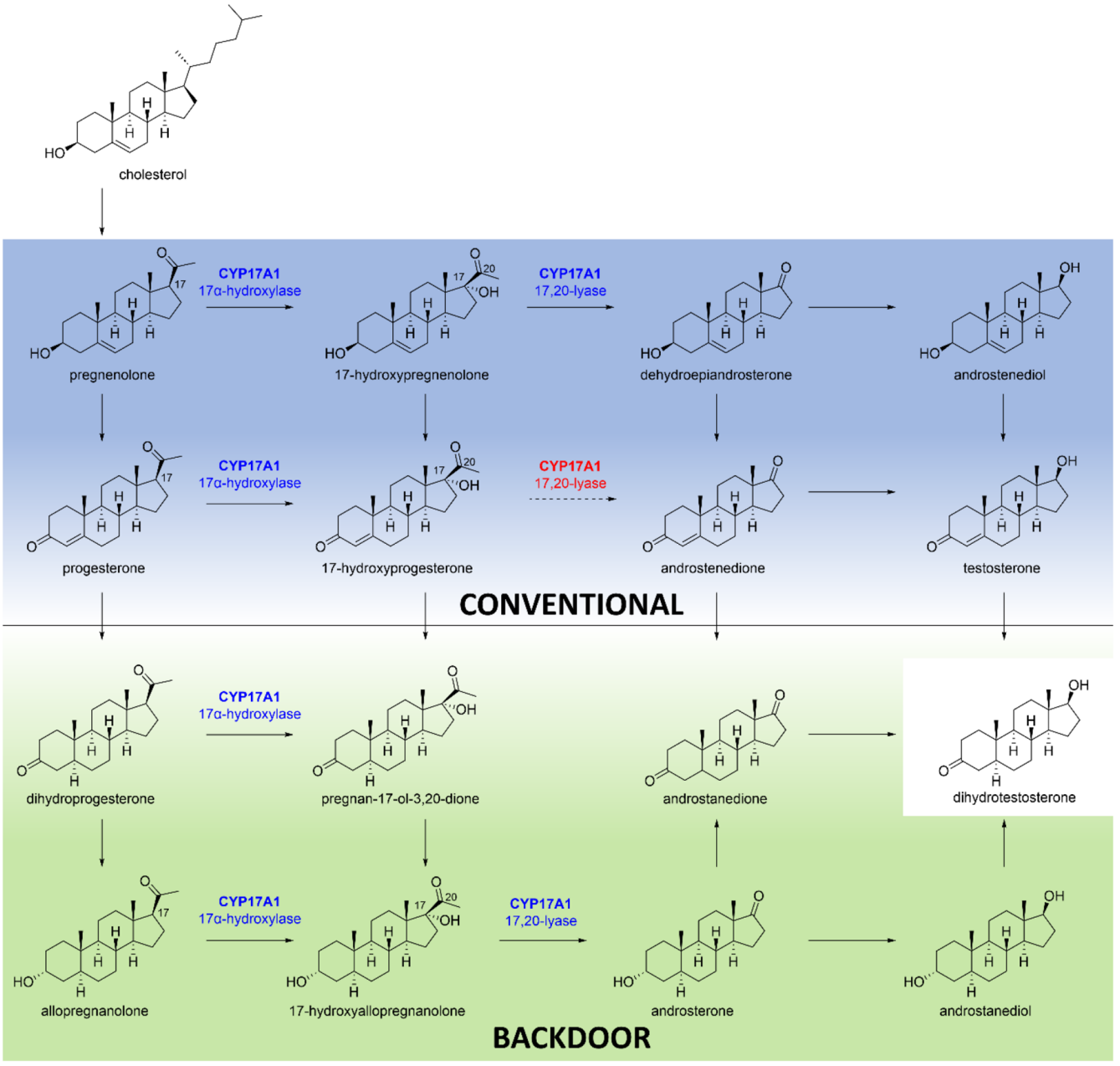

Figure 1. Androgenesis leading to the most potent androgen, dihydrotestosterone (DHT). "Conventional" and "backdoor" pathways are indicated with different color backgrounds. Red color represents inefficient catalysis in humans. Only transformations where CYP17A1 participates are labeled; other enzymes are omitted for clarity.

Subsequently, DHEA and androstenedione are further transformed into testosterone, which is then converted to dihydrotestosterone (DHT). Androstenedione and testosterone also serve as substrates for estrogens. Besides the "conventional" pathway described above there is also the "backdoor" pathway, where a major androgen is an androsterone derived from 17-hydroxyallopregnanolone via the very efficient CYP17A1 17,20-lyase reaction.[10−12] This pathway takes a detour around DHEA and androstenedione to produce DHT.[13,14]

The subtle differences between different CYPs and the preferred selectivity for the inhibition of the CYP17A1 lyase-catalyzed transformation have been addressed in structural and computational chemistry studies. Results of these investigations and compounds with increased selectivity have recently been reported which provide a promise for the next generations of CYP17A1 inhibitors.

To date, abiraterone acetate is the only CYP17A1 inhibitor approved for use in patients. This pioneering compound contains a steroidal scaffold similar to the endogenous CYP17A1 substrates. However, this drug is far from perfect. Side effects of abiraterone include vomiting, swelling, low potassium levels, high blood pressure, high glucose levels, joint pain, and diarrhea. In addition, adrenal insufficiency, liver failure, heart failure, arrhythmia, atrial fibrillation, and tachycardia are also possible side effects of abiraterone. These side effects stem largely from abiraterone promiscuity. At the molecular level, abiraterone is a potent inhibitor of CYP21A2 as well as CYP1A2, CYP2D6, CYP3A4, CYP2C8, and CYP2C9.[15,16] CYP21A2 is responsible for production of glucocorticoids from progesterone

https://doi.org/10.1021/acs.jmedchem.3c00442
J. Med. Chem. 2023, 66, 6542−6566

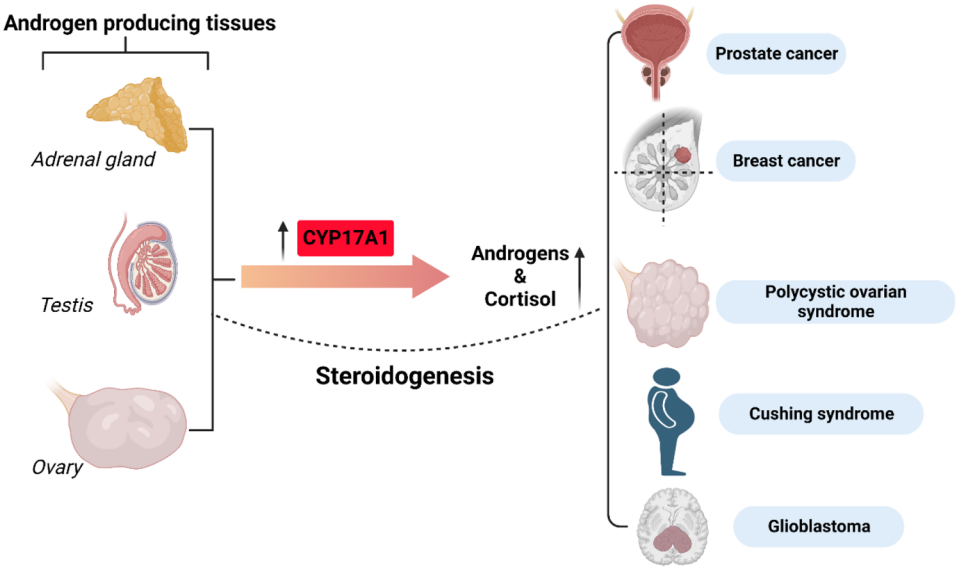

Figure 2. Summary of overexpression of CYP17A1 and activation in the production of steroid hormones linked to human diseases. Created with BioRender.com.

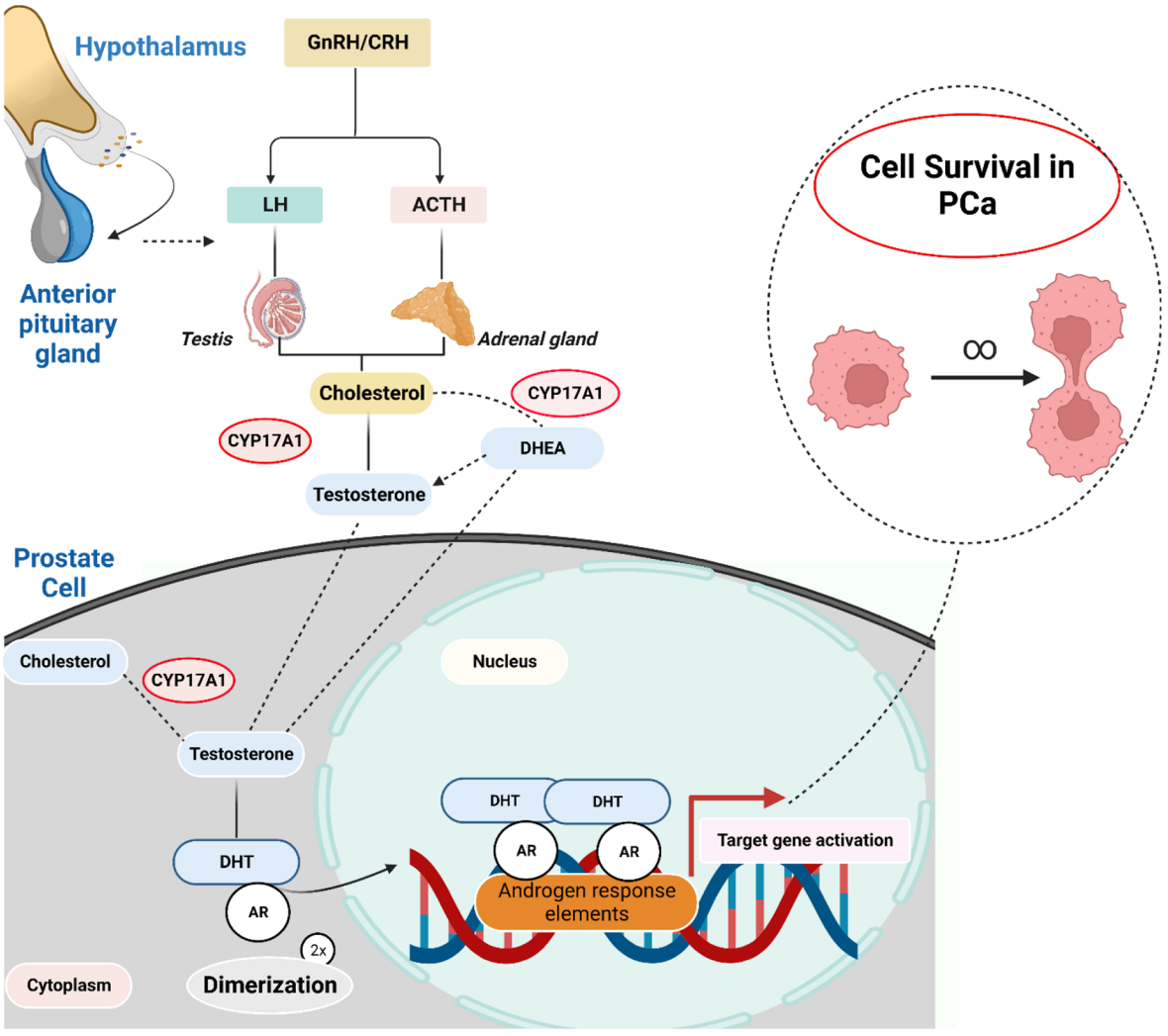

Figure 3. Androgen-dependent pathway in prostate cancer. The androgen receptor (AR, a hormone nuclear receptor) translocates into the nucleus upon activation by DHT as a homodimer and facilitates cell survival through the transcription of androgenic genes. Created with BioRender.com.

https://doi.org/10.1021/acs.jmedchem.3c00442
J. Med. Chem. 2023, 66, 6542−6566

Table 1. List of Experimentally Determined Structures of Human CYP17A1 from the Protein Data Bank

PDB	Ligand	Resolution [Å]	Notes	Year	Ref
3RUK	abiraterone	2.6		2012	38
3SWZ	galeterone	2.4		2012	38
4NKV	abiraterone	2.6	A105L mutant	2014	42
4NKW	pregnenolone	2.5	A105L mutant	2014	42
4NKX	progesterone	2.8	A105L mutant	2014	42
4NKY	17α-hydroxyprogesterone	2.6	A105L mutant	2014	42
4NKZ	17α-hydroxypregnenolone	3.0	A105L mutant	2014	42
5IRQ	(±)-orteronel	2.2		2017	44
5IRV	VT-464	3.1		2017	44
5UYS	3α-OH-5α-abiraterone analog	2.4		2018	
6CHI	abiraterone C6 amide	2.7		2018	43
6CIR	abiraterone C6 oxime	2.6		2018	43
6CIZ	abiraterone C6 nitrile	2.6		2018	43
6WR0	3-keto-Δ4-abiraterone analog	2.7		2021	
6WR1	abiraterone	1.9	N52Y mutant	2021	
6WW0	3-keto-5α-abiraterone analog	2.0		2021	

and 17OH-Prog. To overcome the major side effect of steroid imbalance, abiraterone is now prescribed with corticosteroids like prednisone. In addition, abiraterone can be metabolized by HSD3B1 and 5α-reductase into 3-keto-5α-abiraterone that is capable of activating androgen receptor (AR), leading to the proliferation of cancer cells, undermining the therapeutic effects of abiraterone. Therefore, non-steroidal drugs that cannot be metabolized into androgens would be better candidates for androgen deprivation therapy (ADT), especially in individuals with higher expression or hyperactive variants of HSD3B1.[17] The structural similarity of abiraterone to the substrates of other cytochrome P450 enzymes involved in steroidogenesis is one of the concerns with respect to selectivity and thus tentative side effects. Published work, covered herein, aims for novel non-steroidal compounds which may lead to both increased selectivity towards the CYP17A1 over other CYPs as well as inhibition of the CYP17A1 lyase activity versus the hydroxylase activity catalyzed by the same enzyme.

In this Perspective, we cover literature, from the earliest reports up to date, for compounds aimed to interact with and inhibit the CYP17A1 enzyme as a guide for further discovery and development of novel and important drugs in the field.

2. ROLE OF CYP17A1 IN DISEASES

Due to its central role in regulation of steroids, changes in activities of CYP17A1 due to mutations or regulatory aspects may lead to multiple human disorders. Some of the human disorders linked to CYP17A1 are prostate cancer, polycystic ovary syndrome, breast cancer, Cushing's syndrome, and glioblastoma (Figure 2). Additionally, links to many other disease conditions including hypertension, heart disease, Alzheimer's disease, and leiomyoma have also been reported.[18−20]

2.1. Prostate Cancer. The major androgens implicated in the normal functioning of the prostate gland include DHEA, androstenedione, testosterone, and DHT. DHT is biologically the most active—it stimulates growth and maintains the morphology of the prostatic cells through interaction with the androgen receptor.[21]

Androgens and their androgen receptors are considered key factors in the development of prostate cancer.[22] This is confirmed by the positive response of patients to ADT. While initially the therapy brings the desired results, over time cancer cells acquire the ability to synthesize androgens *de novo*, and prostate cancer transforms into castration-resistant prostate cancer (CRPC).[23] In this stage the hormone-dependent proliferation of the cells results from the great turnover of adrenal androgen precursors to testosterone, which is further reduced to DHT. CRPC is characterized by increased production of adrenal and intratumoral androgens, mutations, and increased expression of AR (Figure 3). Metastatic prostate cancer is manifested by a re-elevation of the prostate-specific antigen (PSA) marker despite the deficit of androgens and clinical deterioration.[24] In the case of CRPC, a promising therapy is the use of inhibitors of the CYP17A1 enzyme, which is essential for the synthesis of androgens, by all routes of synthesis. So far, the only drug in use that represents this mechanism is abiraterone acetate. In 2011, it was approved by the FDA for the treatment of CRPC.

2.2. Breast Cancer. The transcription of genes that drive breast cancer is stimulated by estrogen-dependent signaling. It is believed that in some cases the androgen receptor replaces this signaling. Moreover, as shown by the androgen synthesis pathway, CYP17A1 indirectly plays a role in the synthesis of estrogens, the excessive signaling of which is associated with tumor development. Androgen receptor overexpression has been noted in some breast cancers.[25] It was shown that the reduction of androgen levels was associated with the clinical improvement of patients.[26] Inhibition of CYP17A1 appears to be a valid approach in the treatment of breast cancer.[27]

2.3. Polycystic Ovary Syndrome. Androgen excess is one of the clinical features of polycystic ovary syndrome (PCOS) and affects the development of the disease. CYP17A1 has been associated with PCOS and male pattern baldness.[28] CYP17A1 is highly expressed in PCOS. In a study of Japanese women, age of menarche was significantly lower for women showing higher activities of CYP17A1.[29] The excessive activation of PI3K/AKT signals occurring in the disease can lead to the excess of androgens and ovarian dysfunction.[1,30]

2.4. Cushing's Syndrome. As CYP17A1 also regulates the synthesis of glucocorticoids, overexpression of the enzyme causes an overproduction of cortisol, an excess of which causes metabolic changes leading to Cushing's syndrome. This is manifested by bone loss, high blood pressure, and type 2 diabetes. Inhibition of CYP17A1 lowers both androgen and

https://doi.org/10.1021/acs.jmedchem.3c00442
J. Med. Chem. 2023, 66, 6542−6566

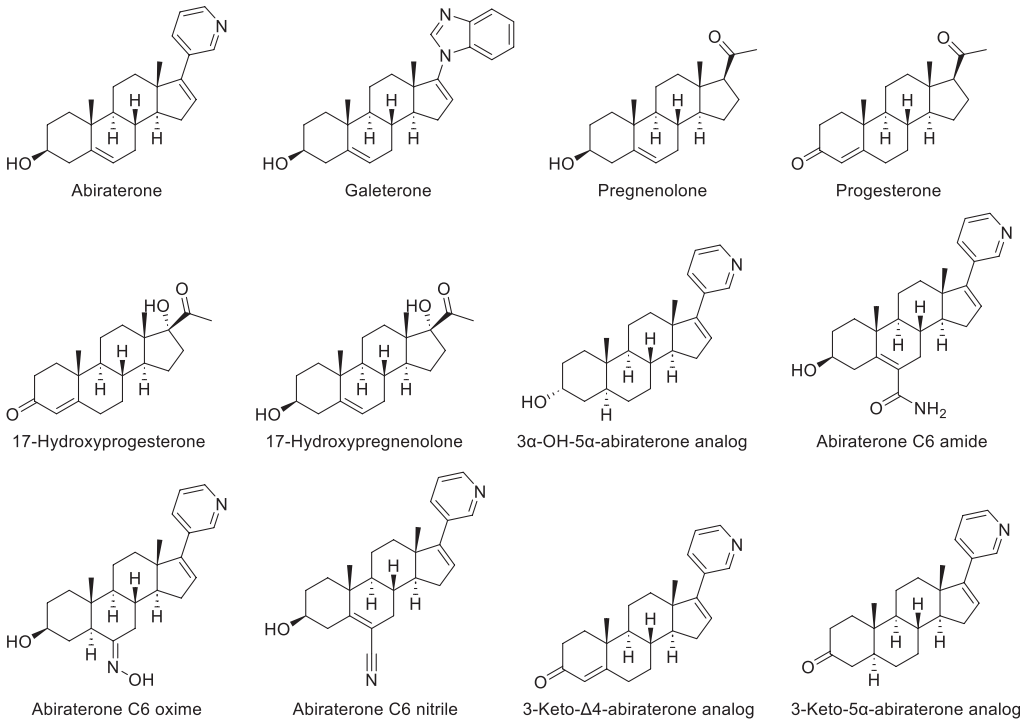

Figure 4. Structures of CYP17A1 steroidal ligands from the Protein Data Bank.

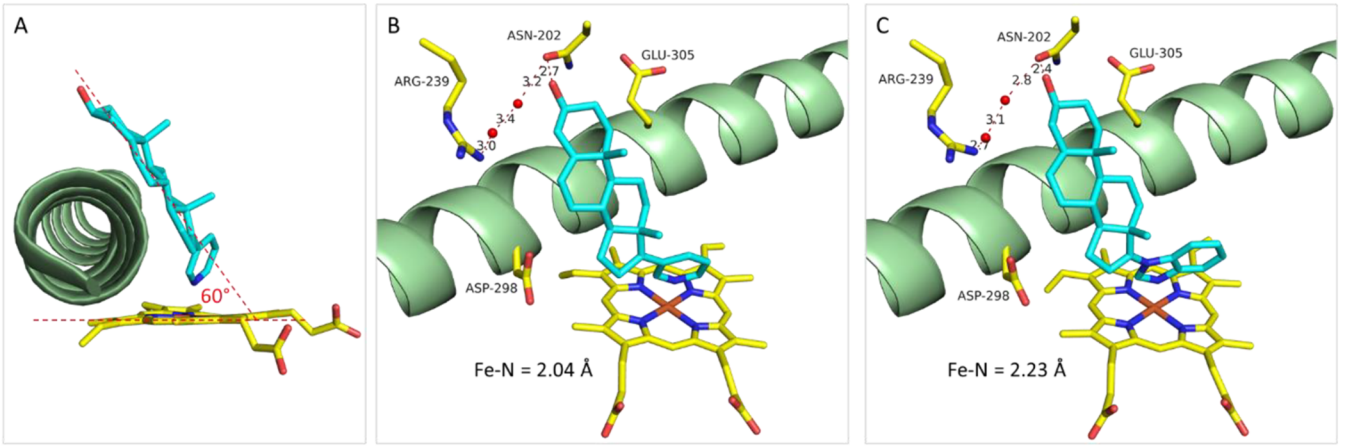

Figure 5. Binding modes of abiraterone (A, B) and galeterone (C) to CYP17A1 (PDB IDs: 3RUK and 3SWZ, respectively). For CYP17A1 the heme group and key residues are displayed as stick models and helix I as a green cartoon. Carbon, oxygen, nitrogen, and iron atoms are colored yellow, red, blue, and orange, respectively.

cortisol levels, which is a promising handle in the development of a treatment for the disease.[31]

2.5. Glioblastoma. It has been reported that CYP17A1 is overexpressed in some forms of glioblastoma. DHEA plays a significant role here, as it protects cancer cells against apoptosis by reducing the effectiveness of chemotherapy. Inhibition of CYP17A1 results in the inhibition of DHEA production, which may be helpful.[32] Following these assumptions, the effect of abiraterone on glioblastoma was investigated. Cellular assays and *in vivo* studies in mice models showed an inhibitory effect of the tested compounds.[33]

3. STRUCTURAL ASPECTS

3.1. CYP17A1 Structure. Initially, structural information was based on homology modeling,[34,35] docking of natural substrates or synthetic analogues, and pharmacophore models.[36,37] At present, a total of 16 structures of human CYP17A1 complexes are available from the Protein Data Bank (Table 1; for ligand structures see Figure 4 and Figure 19, below), comprising three different types of ligands (10 steroidal and 2 non-steroidal inhibitors and 4 substrates), each with their characteristic binding mode.

In 2012, the first crystal structures of CYP17A1 with abiraterone (PDB ID: 3RUK) and galeterone (PDB ID: 3SWZ) were published.[38] Both structures show the enzyme-folding characteristic of CYP450 enzymes. The ligands assume a similar position to each other and, as previously predicted, interact with the heme iron through the sp^2-hybridized nitrogen atom of pyridine or benzimidazole, creating a coordination bond. The steroid nuclei form an angle of 60° above the plane of the heme group, taking a position opposite the Helix I (Figure 5A). The 3β-OH group interacts with N202 in Helix F. The

https://doi.org/10.1021/acs.jmedchem.3c00442
J. Med. Chem. 2023, 66, 6542−6566

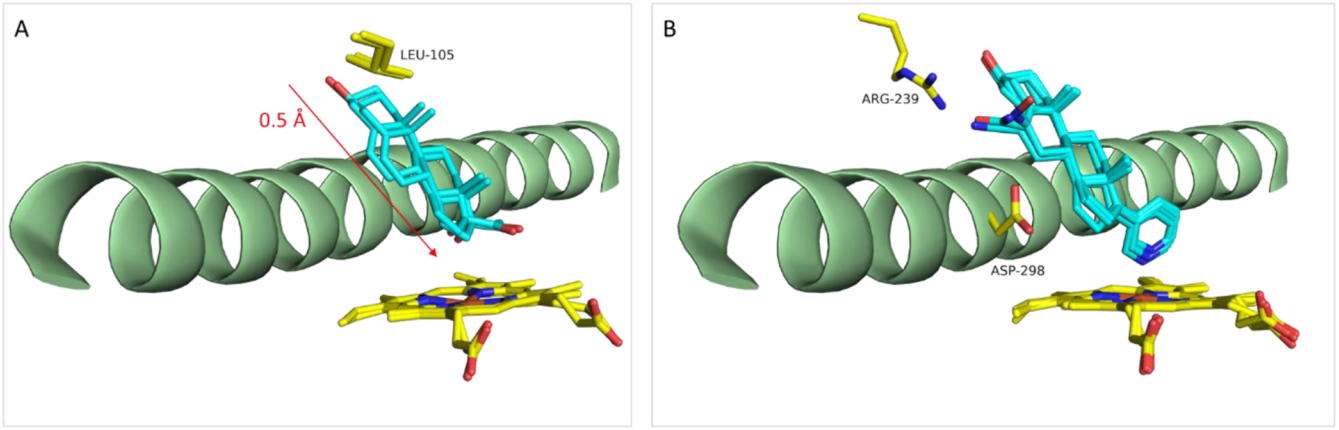

Figure 6. Two different binding modes of 17α-hydroxypregnenolone (A) and binding mode of the abiraterone analogs with C6 substituents (B) to CYP17A1. Color coding as in Figure 5.

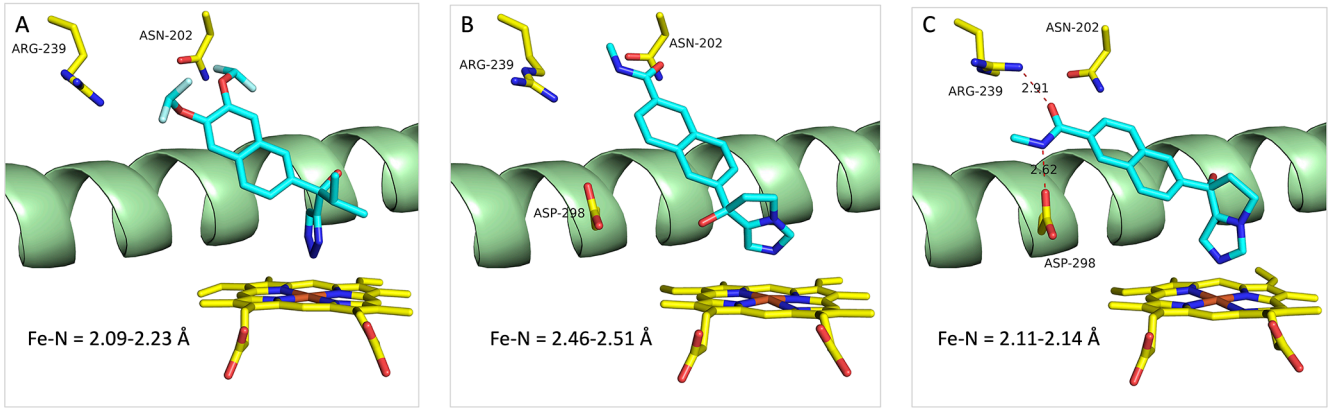

Figure 7. Binding mode of the non-steroidal inhibitors (*S*)-seviteronel (A) (PDB ID: 5IRV), (*R*)-orteronel (B), and (*S*)-orteronel (C) (PDB ID: 5IRQ) to CYP17A1. Color coding as in Figure 5.

alpha surface of the steroid moiety is unsubstituted and flattens with respect to Helix I. This mode of binding differs from steroid binding in other cytochrome P450 enzymes. The C18 and C19 methyl groups are located between the B′ helix, the B4 loop, and the loop behind Helix F. Only three side chains of the ventricular wall are within 4 Å of either C18 or C19. The remaining wall of the pocket is filled with the hydrophobic side chains of A105, S106, A113, F114, I206, L209, V236, and V482.[38,39]

CYP17A1 has a hydrogen bond network at the top of the active site that interacts with abiraterone and galeterone, respectively. Residues N202 and R239 are forming hydrogen bonds, either directly or via water molecules, to the 3-OH group (Figure 5B,C).[38] Two additional polar residues, E305 and D298, are also present in the active site. These residues do not interact with abiraterone or galeterone but are obvious targets for the design of non-steroidal inhibitors. These initial structures confirmed the expected interaction with the Fe in the heme group but also revealed important hydrogen-bonding and steric protein−ligand interactions, which have formed the basis for numerous theoretical studies on the mechanism of hydroxylase and lyase catalysis,[40] recognition, and binding.[41]

The structures of the A105L mutant of CYP17A1 with a series of natural substrates for the 17α-hydroxylation and 17,20-lyase reactions (PDB IDs: 4NKV, 4NKW, 4NKX, 4NKY, 4NKZ) were published in 2014.[42] The idea behind the A105L mutant was to modify the active site to resemble the 17,20-lyase reaction. The binding modes of the two 17α-hydroxylation substrates, pregnenolone and progesterone, and the two 17,20-lyase substrates, 17OH-Prog and 17OH-Preg, are nearly identical, but 17OH-Preg displayed two different binding modes in the crystal, one similar to the other substrates and one shifted 0.5 Å closer to the heme group (Figure 6A).[42] The latter enabled the authors to explain the regioselectivity and substrate selectivity of the 17α-hydroxylation and 17,20-lyase reactions. Although these studies revealed important information on the mechanisms, it remains to be proven if the small structural differences imposed by the A105L mutation reflect the presence of the 17,20-lyase active-site conformation.

To improve the selectivity for CYP17A1 relative to CYP21A2, several abiraterone analogs were prepared with hydrogen-bonding substituents in the C6 position.[43] The structures of three of the compounds (C6 nitrile, amide, and oxime, Table 1) revealed that the C6 substituent indeed was positioned between the two polar residues, R239 and D298 (Figure 6B). Experimental and computational studies showed that the increased CYP17A1 selectivity primarily was due to a reduced affinity for CYP21A2.[43]

The RMSD values based on the Cα atoms between the original abiraterone structure (PDB ID: 3RUK) and the other CYP17A1 structures in Table 1 are 0.33 ± 0.03 Å. This indicates that the CYP17A1 active site can accommodate structurally

https://doi.org/10.1021/acs.jmedchem.3c00442
J. Med. Chem. 2023, 66, 6542−6566

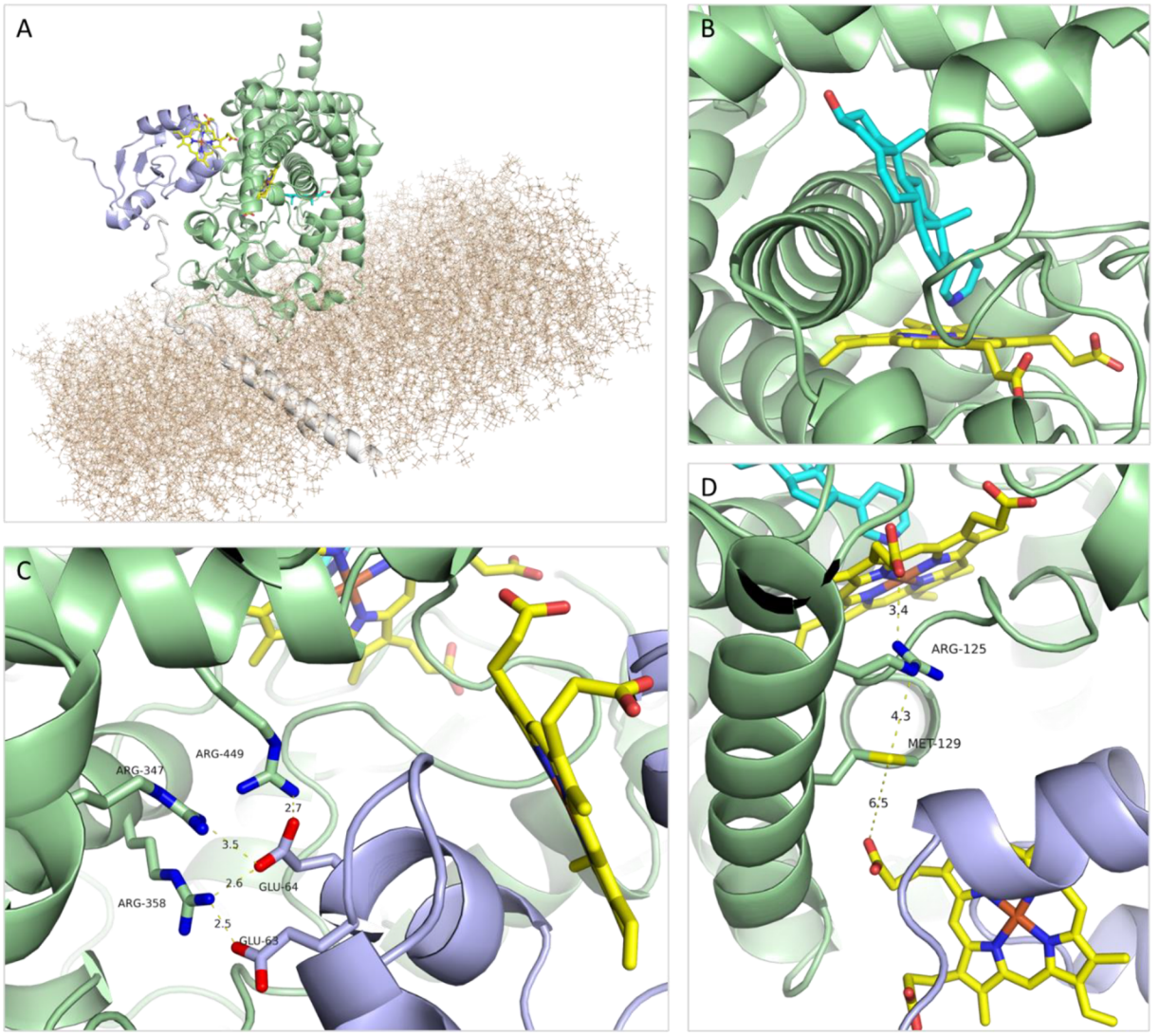

Figure 8. Three-dimensional model of the CYP17A1-cyt b_5 complex anchored in the membrane. CYP17A1 green, cyt b_5 blue, membrane beige, and anchoring helices and additional residues required for the AlphaFold modeling white (A). Close-up of abiraterone binding to the Fe atom in the heme group in the CYP17A1 active site (B). Key residues involved in the CYP17A1-cyt b_5 binding (C). Residues proposed to be involved in the electron transfer from cyt b_5 to CYP17A1 (D). Color coding as in Figure 5. For a movie illustrating the 3D relationships of the structure and interactions, see the SI.

different ligands by changes in side-chain orientations without affecting the overall fold.

It is worth mentioning that only two structures of CYP17A1 complexes with non-steroidal inhibitors, (±)-orteronel (TAK-700) and (*S*)-seviteronel (VT-464) (PDB IDs: 5IRQ and 5IRV respectively), have been published.[44] Both compounds contain a naphthalene moiety substituted in the 2 position with a nitrogen-containing ring system. (*R*)-Orteronel and (*S*)-seviteronel bind "steroid-like" with the naphthalene ring occupying the same space in the CYP17A1 active site as the steroid part of the previously discussed steroidal inhibitors and the sp^2-hybridized nitrogen atom in the substituent coordinating to the Fe atom in the heme group (Figure 7A and Figure 7B). Contrary to (*R*)-orteronel, binding of (*S*)-orteronel is tilted, enabling the substituent in the 6 position to form hydrogen bonds with R239 and D298 (Figure 7C). The Fe−N distance in (*R*)-orteronel is also substantial longer (2.5 Å) than the corresponding distances in (*S*)-orteronel and (*S*)-seviteronel (2.1 Å). An additional interesting feature with the orteronel structures, and to some extent also the seviteronel structures, is the presence of a peripheral binding site formed by different conformation of the loop between helix F and helix G. The function of this primarily hydrophobic site remains to be explored.[44] The orteronel and seviteronel structures are interesting, as they may provide ideas for further optimization of lyase-selective non-steroidal inhibitors. The CYP17A1 structure, function, and therapeutic potential have also been reviewed.[45,46]

Considerable knowledge about the structure of CYP17A1 has also been derived from studying the clinical mutations typically found in patients with 17α-hydroxylase deficiency. Mutations R96W, R125Q, H373D/N, and R440H/C disrupt heme binding, resulting in a loss of enzyme activity. 17,20-Lyase activity is inhibited by mutations E305G, R347H/C, R358Q, and R449A.[47−50]

3.2. CYP17A1 Allosteric Site. The presence and utilization of an allosteric site in CYP17A1 is still a question for debate. It represents an until now not fully explored possibility for

https://doi.org/10.1021/acs.jmedchem.3c00442
J. Med. Chem. 2023, 66, 6542−6566

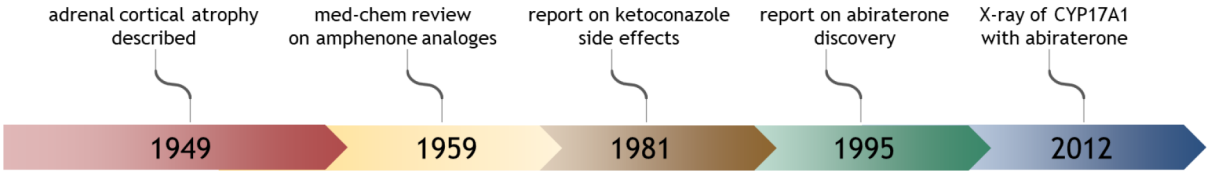

Figure 9. Timeline with milestones in CYP17A1 inhibitors discovery.

controlling the CYP17A1-mediated reactions. Potentially it opens the opportunity for imposing a conformational change of the CYP17A1 enzyme towards a lyase-relevant conformation, which would form the basis for the structure-based design of more lyase-selective CYP17A1 inhibitors.

Allosteric sites have been identified in other CYPs. Most of the studies have focused on CYP3A4, and it is proven without a doubt that this drug-metabolizing CYP contains an allosteric site. The structure showing that the fluorescent agent, fluorol, acts as an allosteric ligand and binds to a high-affinity binding site located in the substrate channel in CYP3A4 has recently been published.[51]

It has been known for many years that the 17,20-lyase activity of CYP17A1 relative to the 17α-hydroxylase activity can be stimulated by phosphorylation or by binding of cyt b_5.[52] Two mechanisms for the cyt b_5 interaction with CYP17A1 have been proposed. Cyt b_5 could either be responsible for supplying the second electron necessary to complete the catalytic cycle or be an allosteric modulator imposing a conformational change in CYP17A1.[53] Indeed, cyt b_5 is an electron donor, but it has been shown that the stimulation of CYP17A1 is an allosteric effect.[54,55] Line broadening of the signals from certain residues in CYP17A1 was observed by means of NMR spectroscopy. This was interpreted as a function of cyt b_5 binding causing a conformational change in CYP17A1. The effect was most pronounced for residues in the distal part of the CYP17A1 active site.[56]

A thermodynamic study of the energetics associated with the interactions between various CYPs and cyt b_5 revealed that the CYP17A1-cyt b_5 was enthalpy driven and that the interactions probably involved electrostatic interactions and formation of salt bridges and/or hydrogen bonds.[57] This is consistent with previous observations that the anionic residues E48 and E49 in cyt b_5 and the cationic residues R347, R358, and R449 in CYP17A1 are involved in the CYP17A1-cyt b_5 interactions.[58,59] NMR studies also revealed that cyt b_5 combined with different substrates may impose different conformational states of the CYP17A1 structure.[60] It is reasonable to assume that the cyt b_5 residues involved in the interaction with CYP17A1 would provide a starting point for the design of peptides and peptidomimetics mimicking the allosteric effect of cyt b_5 on CYP17A1. In a recent study the effect of a hendecapeptide EHPGGEEVLRE, comprising the above-mentioned E48 and E49 residues on CYP17A1, was investigated without obtaining the expected evidence for binding to CYP17A1.[50]

To our knowledge no experimental structure of the CYP17A1-cyt b_5 complex has been reported, but the CYP1A2-cyt b_5 complex has been modeled by computational methods.[61] Figure 8 presents a model of the CYP17A1-cyt b_5 complex constructed by the novel protein structure prediction method AlphaFold2 and subsequently embedded in a membrane analogous to the CYP1A2-cyt b_5 model.[62] We believe that such models may be useful not only to design novel compounds but also to help improve the understanding of other aspects of the enzymatic reactions, like the electron flow from cyt b_5 to the CYP17A1.

4. INHIBITORS

4.1. Brief Historical Overlook. One of the earliest reports goes back to the middle of the 20th century when dichlorodiphenyldichloroethane (DDD, TDE), a metabolite of DDT, was described as causing severe adrenal cortical atrophy in dogs.[63] Since this discovery considerable effort was put into endocrine disruptors. However, no particular focus was placed on the inhibition of androgen production, and only single reports appeared on this topic.[64−69]

At the beginning of 1990 the pace of research into CYP17A1 inhibition picked up with the discovery of abiraterone, reported in 1995. This was fueled by a discovery a decade earlier of ketoconazole causing gynecomastia in men.[70] Closer investigation of the underlying mechanism indicated that inhibition of the 17α-hydroxylation and 17,20-lyase reactions was responsible for this effect.[71] The field gained increased interest when the first X-ray structure of CYP17A1 in complex with an inhibitor was reported in 2012 (Figure 9).[38]

4.2. Non-steroidal Inhibitors of CYP17A1. With a few exceptions, most of the medicinal chemist's efforts rely on mimicking the steroidal scaffold of the natural CYP17A1 substrates (Figure 10). Keeping in mind that the critical moiety

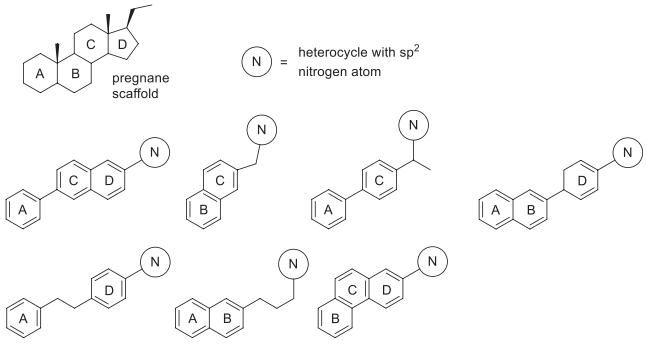

Figure 10. Different strategies aimed at mimicking the steroid scaffold commonly include deletion of one or two rings.

for enzyme inhibition is the lone pair of the sp^2 nitrogen atom which interacts with the heme iron in CYP17A1, many designs emerged where a heterocycle was combined with a steroid mimetic ring system. These heterocycles included predominantly imidazole or pyridine, while other heterocyclic rings were less explored. Although the choice can include virtually any heteroaromatic ring containing nitrogen, imidazole and pyridine offer the most favorable binding energies.[72] This section contains known inhibitors presented as different chemotypes. In some instances the choice is arbitrary as two chemotypes can overlap. It is important to remember that, when comparing IC_{50} values between compounds, care should be taken because these were often measured under different experimental conditions. In

https://doi.org/10.1021/acs.jmedchem.3c00442
J. Med. Chem. 2023, 66, 6542−6566

the case of CYP17A1 inhibition assays, the results are particularly sensitive to the substrate concentration and the ratio of CYP17A1:POR:cyt b_5.[73] In this regard, K_i is usually more informative than IC_{50} and repeated experimentation often reveals, for instance, the lack of initially reported selectivity.[44]

Azobenzene Derivatives. The discovery that bifluranol **1** inhibits CYP17A1 prompted the synthesis of its analogs.[74] Compound **2** showed inhibition of CYP17A1 in the micromolar range (Figure 11). Although **2** achieved favorable selectivity of

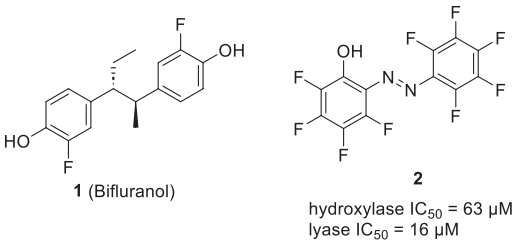

Figure 11. Representative CYP17A1 inhibitors of azobenzene analogs and bifluranol.

hydroxylase vs lyase 1:4, it was noted that the compound was unstable at the pH of the assay, forming dibenzoxadiazepine upon decomposition. Additional testing towards inhibition of 5α-reductase revealed no activity. These studies constitute one of the first attempts to create novel derivatives of a known inhibitor of CYP17A1.

Acetic Acid Derivatives. A set of acetic acid esters was designed as inhibitors of aromatase.[75] However, during testing these compounds showed significant CYP17A1 inhibition. Various alcohols were used for esterification, and closer analysis revealed improved potency with esters of bulkier alcohols (Figure 12). (+)-Isopinocampheol generated the most potent ester, **3**, while its enantiomer was less potent by an order of magnitude, showcasing the important role of stereochemistry. Unfortunately, these compounds, being esters, suffered from hydrolytic susceptibility. Also, the compounds displayed poor selectivity between hydroxylase and lyase inhibition. The problem of metabolic stability was addressed in the analogs with alkylated α carbons.[76] Introduction of an alkyl group significantly increased resistance to esterases in rat liver microsomal preparations, with two groups being more effective than one regardless of their size. It was also noticed that this modification increased selectivity towards CYP17A1. Moreover, replacing the 4-pyridyl group with isomeric 3-pyridyl proved beneficial to the observed potency, as demonstrated by compound **4**. This modification also diminished activity towards aromatase. "Reverse esters", with the reversal of the ester linkage, where the pyridine moiety resides on the alcohol part of the molecule, were designed to explore the effect of chirality adjacent to the pyridyl residue.[77] This was done to circumvent racemization of enantiomers with a benzylic proton at the chiral center. The results showed dramatic differences in the inhibitory activity of monomethylated enantiomers of the 4-pyridyl series, while the enantiomers of the 3-pyridyl series were almost equipotent. The 4-pyridyl series was more potent than the 3-pyridyl in general, culminating in compound **5**, which had the best selectivity between hydroxylase and lyase and towards aromatase (Figure 12). In an attempt to improve the resistance to esterases, several amides analogs were prepared which displayed markedly decreased activity.

Phenyl Derivatives. Phenyl derivatives constitute a case of extreme simplification, where the whole steroidomimetic scaffold has been reduced to just one aromatic ring connected with a carbon linker, varying in length, to a nitrogen-bearing heterocycle (Figure 13). Thus, the initial designs were aimed at exploring the effect of benzene substitution and the length of the linker.[78,79]

It was determined that the presence of a substituent in the phenyl ring was beneficial to the inhibitory activity, as was extension of the linker. No clear structure−activity relationship could be established in relation to the nature of a substituent, although disubstituted compounds were more potent than mono derivatives. However, a trend was observed in relation to the length of the linker showing potency increasing with the linker length, up to 10 carbons. Thus, an increased hydrophobicity led to increased potency.[80] Compounds with the ethyl linker were unstable. Comparison between the incorporation of imidazole and triazole moieties demonstrated the former to be superior. The authors also tested their compounds against hydroxysteroid dehydrogenases and concluded the lack of specificity against these targets. The combination of the extended linker with different halogen atoms attached to the phenyl group was also investigated.[81]

It is noteworthy to add that in the majority of compounds it was possible to achieve a good selectivity profile between hydroxylase and lyase inhibition, as evidenced by compounds **6** to **8** (Figure 13). By adding a bulkier benzenesulfonate group it was possible to obtain compound **9**, which exhibited excellent selectivity of over 100-fold.[82] Additional manipulation of benzenesulfonate moiety by changing the nature of the para-substituent did not improve the selectivity, although it produced compound **10** with enhanced potency.[83]

Stilbene Derivatives. The constrained nature of stilbene offers the possibility of constructing a steroid-mimicking ring system with a fixed geometry. The two geometrical isomers of stilbene (*E* and *Z*) have been used in compounds **11** and **12**. In this case, both the geometry of the double bond and the spacer linking imidazole with the scaffold played important roles in the reported activity (Figure 14). Additionally, compound **12** demonstrated *in vivo* an increased level of testosterone (135% of the control, measured at 5 h after treatment) despite an initial reduction. This was attributed to the cancellation of negative feedback caused by transient suppression of the testosterone levels.[84]

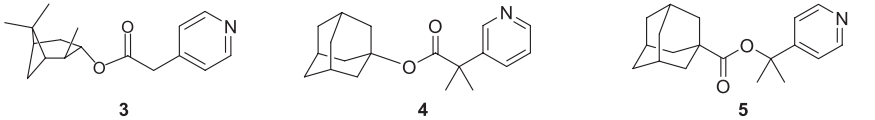

Figure 12. Representative CYP17 inhibitors from the acetic acid ester family.

https://doi.org/10.1021/acs.jmedchem.3c00442
J. Med. Chem. 2023, 66, 6542−6566

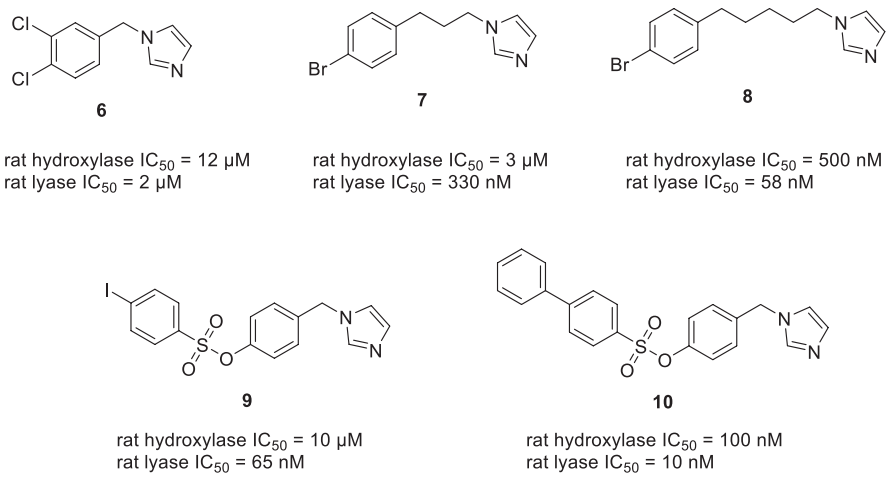

Figure 13. Representative CYP17 inhibitors of the phenyl derivatives group.

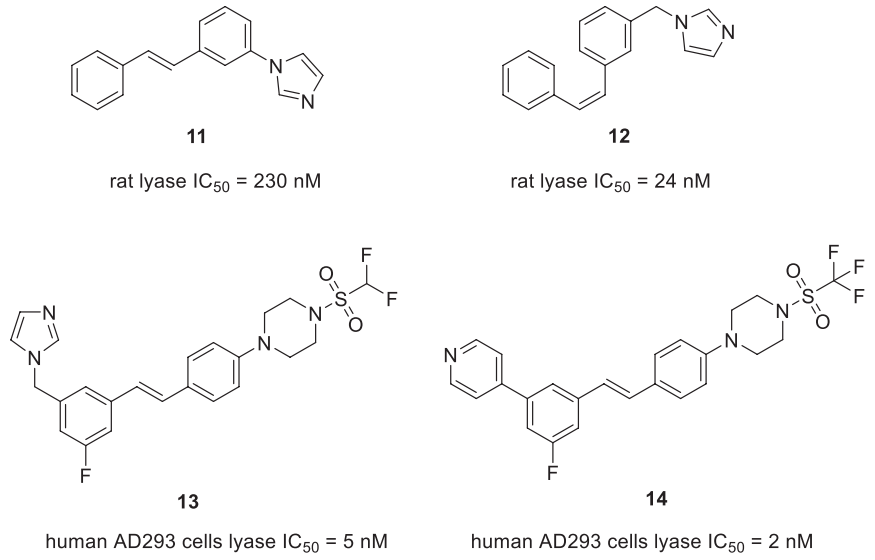

Figure 14. Representative stilbene-based CYP17 inhibitors.

Compounds **13** and **14** were designed as stilbene-based derivatives of ketoconazole in a hope to overcome the synthetic limitation imposed by the complex ketoconazole core, thus enabling straightforward generation of analogs. A comparison between the energy-minimized structures suggested that the key binding components are similarly positioned. This mainly involved overlap of imidazole and pyridine heterocyclic moieties. Incorporation of the pyridine moiety gave more potent compounds in general compared to the imidazole moiety (Figure 14). Compound **14** displayed good selectivity for CYP17A1 against CYP19 (100-fold) and CYP3A4 (1000-fold).[85] It is important to mention that numerous stilbene-based drugs are used in clinical practice. For example, tamoxifen is used to treat estrogen-receptor-positive breast cancer, and clomifene is used to induce ovulation. Both drugs interact with estrogen receptors, which engenders potential off-target liability for this class of compounds. Diethylstilbestrol, once widely used for prostate cancer treatment, no longer enjoys widespread use mainly due to cardiovascular toxicity caused by high doses.[86]

Analogs with a Heterocyclic Core. In search for new inhibitors of CYP steroidogenic enzymes, compounds were designed using 1,2,4-triazole as a core structural element with a pyridine group responsible for interacting with the heme. It was reasoned that the triazole scaffold is a well-tolerated drug component and compared to a benzene core the triazole provides better solubility. Moreover, its basicity is lower than that of imidazole and the resulting geometry would better mimic the A and B rings of the natural substrate. While compound **15** was a nanomolar inhibitor of CYP11B1 and CYP11B2, none of the compounds showed inhibition of CYP17A1, and the structural analysis focused on selectivity between the above-mentioned enzymes (Figure 15).[87]

Compound **16** was designed for CYP11B1 inhibition as a wound healing agent. The compound was tested for selectivity vs CYP17A1 and was found to be a very weak inhibitor (5% at 2 μM) while CYP11B1 was potently inhibited (IC_{50} = 1 nM). No explanation for this selectivity was given based on structural analysis.[88]

Compounds with fragments of N-containing aromatic heterocycles, exhibiting the strongest interaction with the heme, were identified based on the binding energy calculations using density functional theory (DFT) methods. Compounds **17** and **18** were found as a result of this virtual screening. Both compounds displayed potent inhibition of CYP17A1 and good selectivity against CYP3A4, CYP2D6, and CYP21A2.[89] Compound **19** was a result of linking two heterocyclic fragments

https://doi.org/10.1021/acs.jmedchem.3c00442
J. Med. Chem. 2023, 66, 6542−6566

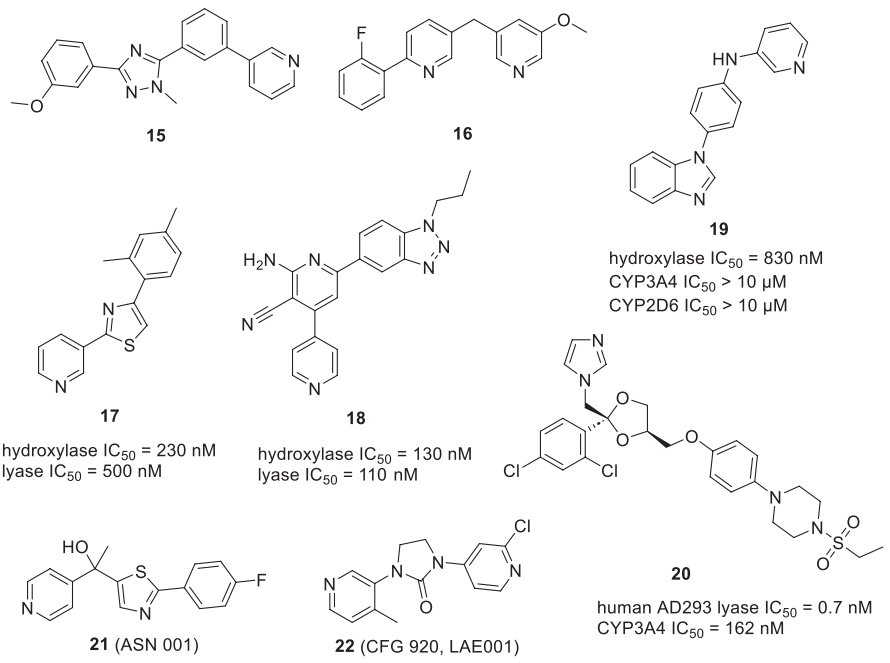

Figure 15. Representative inhibitors with heterocyclic cores.

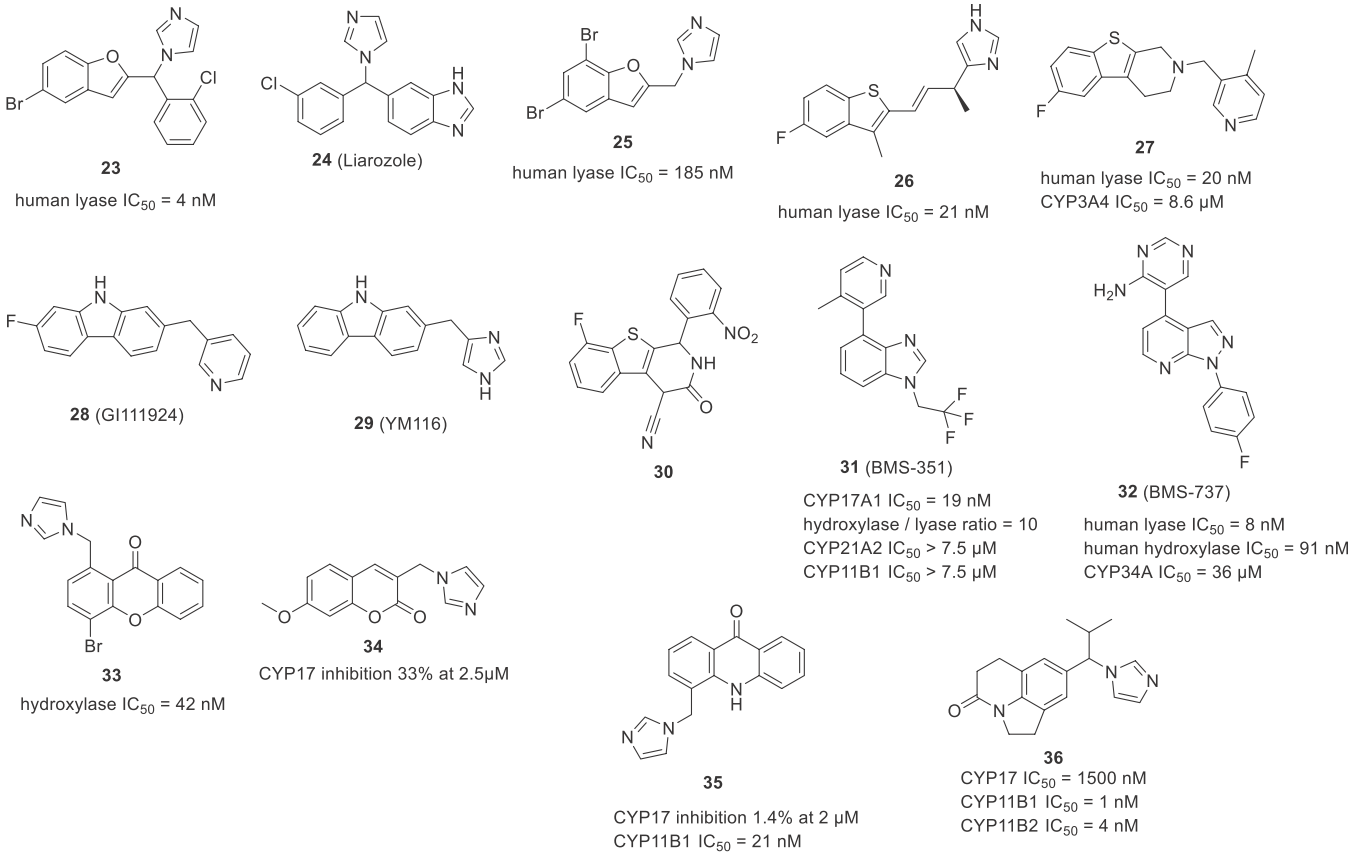

Figure 16. Representative inhibitors with fused 5- and 6-membered heterocyclic cores.

present in abiraterone and galeterone.[90] It displayed good IC_{50} and selectivity vs CYP3A4 and CYP2D6; however, further attempts to optimize this scaffold did not provide more effective compounds.[91]

Compound **20** represents an example of selective optimization of side activities (SOSA). This approach uses old drugs for new pharmacological targets.[92] The obvious benefit would be a molecule with increased probability of having drug-like properties. It was reasoned that ketoconazole with its CYP17A1 "side activity" could be transformed into the entity possessing CYP17A1 as a "main activity" while diminishing other unwanted effects. Replacing the terminal acetyl group with

https://doi.org/10.1021/acs.jmedchem.3c00442
J. Med. Chem. 2023, 66, 6542−6566

the sulfonamide group resulted in increased potency towards CYP17A1 and markedly improved selectivity against CYP3A4 (Figure 15).[93]

Compound **21** (ASN001) was developed by Asana BioSciences as a selective CYP17A1 lyase inhibitor. However, no medicinal chemistry related papers could be found and only pharmacology data is readily available.[94] Similarly, **22** (CFG920, LAE001) was initially developed by Novartis and licensed in 2017 to Laekna Therapeutics as a dual CYP17A1/CYP11B2 inhibitor.

Attempts have been made at producing benzene-fused heterocycles. One of the examples is compound **23**, which was based on **24** (liarozole, R75251), a known inhibitor of several CYP enzymes. This compound replaces the benzimidazole moiety with benzofuran, retaining imidazole and chlorophenyl fragments (Figure 16).[95] Further manipulation of the structure did not increase potency or selectivity, as exemplified by the truncated compound **25**.[96]

As a part of a drug discovery campaign, launched by Takeda, aimed at novel agents for the treatment of prostate cancer, multiple compounds were synthesized and tested. Benzothiophene derivative **26** was identified as a potent inhibitor.[84] Notably this compound reduced testosterone levels in rats to 5% and 2% after 2 h and 5 h, respectively, demonstrating *in vivo* activity. Upon screening in-house compounds and inspecting modeling results, compound **27** was obtained.[97] This compound bears resemblance to **28** (GI111924) and **29** (YM116) developed two decades earlier by GSK and Yamanouchi, respectively.[98] The authors reasoned that the substitution of nitrogen for a sulfur atom in tetrahydro-β-carboline will better accommodate the molecule in the enzyme binding pocket. In addition, introduction of a substituent in the pyridine ring provided a compound with a better fit of this moiety. As a result, **27** proved to be a potent inhibitor with marked selectivity against other CYP isoforms and good *in vivo* activity measured as rat serum testosterone level. Interestingly, based on those findings another group designed and tested benzothiophene analogues, e.g., compound **30**, where an additional phenyl ring bears the nitro group which is claimed to be responsible for the interaction with the heme.[99]

Researchers at Bristol-Myers Squibb found a potent indazole derivative while screening their internal compound collection.[100] They set out to identify a chemotype allowing for continuous CYP17A1 inhibition, reasoning it would be required for efficacy. By changing the indazole scaffold to benzimidazole they were able to identify compound **31** (BMS-351) with potent inhibition of CYP17A1 and enhanced metabolic stability. Moreover, **31** demonstrated higher lyase/hydroxylase selectivity compared to abiraterone, which was attributed to its reversible nature. A superior steroidal profile with >90% decrease in testosterone in cynomolgus monkeys was achieved together with minimal disruption to progesterone and cortisol levels. In further attempts to optimize the desired properties, a wide range of alterations to the scaffold as well as to the heme binding moiety were explored, culminating in compound **32** (BMS-737) with good selectivity against various CYPs and potency and efficacy similar to **31** (Figure 16).[101]

Several fused six-membered heterocyclic compounds were described mainly as CYP19A1 (aromatase) or CYP11B1 and CYP11B2 inhibitors. Most of the reported chromone and xanthone derivatives displayed weak activity towards CYP17A1 with few exceptions, like compound **33**.[102] It is noteworthy to add that the authors used comparative molecular field analysis (CoMFA) to design these compounds. Coumarin derivatives were selective towards CYP19A1 and exhibited only low CYP17A1 inhibition, as exemplified by **34**.[103] In a similar fashion, compounds based on a quinolinone scaffold were weak CYP17A1 inhibitors. Compound **35** was only able to inhibit CYP17A1 by 1.4% at 2 μM, and **36** inhibited CYP17A1 with IC_{50} = 1.5 μM (Figure 16).[104,105] In order to understand the observed selectivity, the authors used sequence alignment between the four CYP enzymes (CYP17A1, CYP19, CYP11B1, and CYP11B2).[104] While not specifically designed to target CYP17A1, these compounds provide useful information on selectivity vs other CYPs.

Diphenylmethane Derivatives. Amphenone (**37**, Figure 17) and its analogs belong to the earliest substances found to inhibit

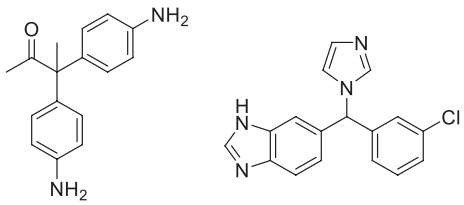

37 (Amphenone) **24** (Liarozole, R75251)

Figure 17. Examples of diphenylmethane analogs.

steroidogenesis.[64] It was tested in humans as a treatment for adrenocortical carcinoma. The effects on androgens were limited with this compound. Higher activity was observed for compound **24** (liarozole, R75251), which was capable of reducing testosterone plasma levels to castrate levels in male dogs.[106] Similar results were obtained in humans.[107] Amphenone did not reach clinical practice while liarozole received orphan drug designation for the treatment of congenital ichthyosis. Liarozole is also capable of CYP26A1 inhibition and has been used as a tool compound.[108]

Biphenyl Derivatives. The biphenyl moiety represents a widely explored possibility to mimic A and C rings of the pregnane scaffold (Figure 10). *In vitro* studies have shown that 3-imidazol-1-yl-methyl-substituted compound **38** and its derivatives are particularly notable (Figure 18).[84,109] However, these compounds lacked sufficient activity *in vivo*. It was assumed that this was related to their fast metabolism.[110] In order to slow down phase 1 metabolism, a series of polyfluorinated compounds was designed.[111] The location of the fluorine atoms turned out to be important because the meta-substituted compound was more resistant to biodegradation than the ortho-substituted one. It has been shown that fluorine in position 3 contributes to both a stronger interaction with the active site and an increase in metabolic stability, consequently increasing the half-life of the compound.[112] Introduction of a fluorine atom is a common strategy employed by medicinal chemists. This can influence the metabolic stability or facilitate cell membrane permeation of a molecule.[113]

Modifications, including introduction of various substituents and structure rigidification, have been carried out to improve activity.[114] It was found that introduction of fluorine into the distal aromatic ring and a methyl group into the methylene bridge connecting the biphenyl moiety and imidazole brought an increase in potency as well as sustained reduced plasma testosterone concentration, as demonstrated by compound **39**. In subsequent years it was determined that the single group on the methylene bridge can be the key to potency and selectivity

https://doi.org/10.1021/acs.jmedchem.3c00442
J. Med. Chem. 2023, 66, 6542−6566

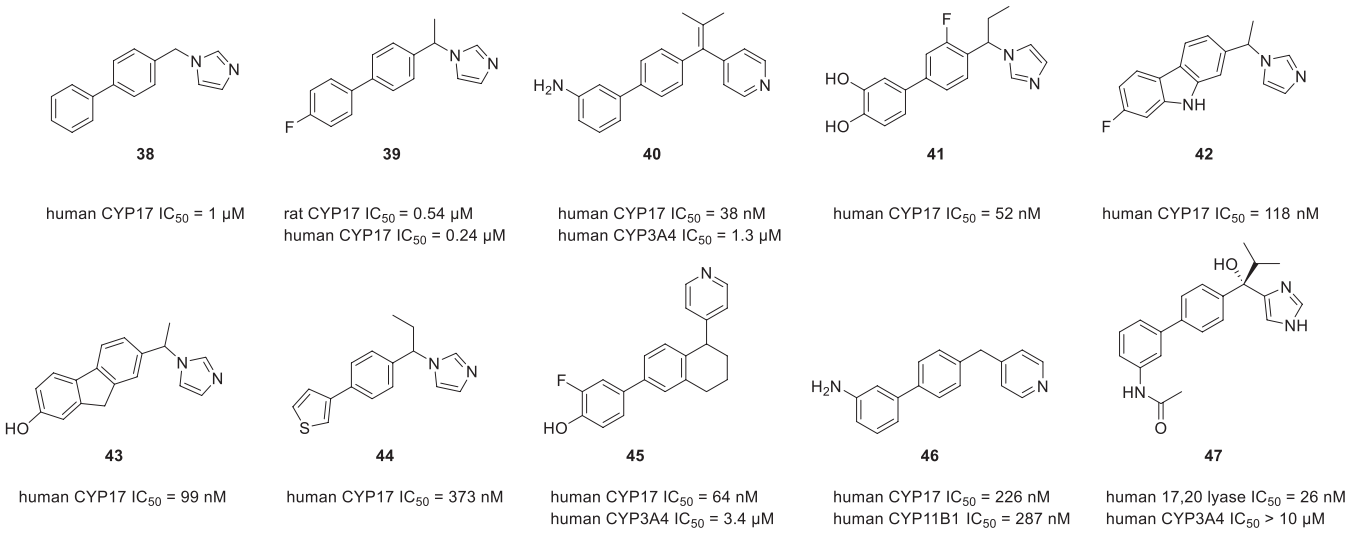

Figure 18. Examples of biphenyl inhibitors.

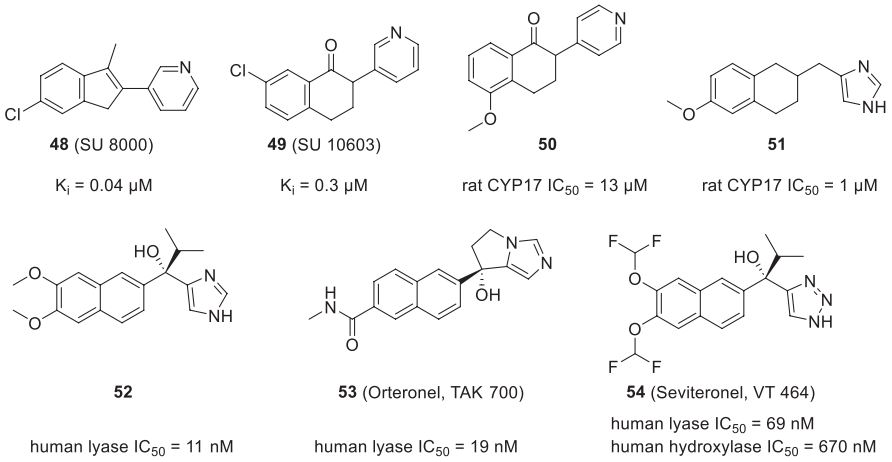

Figure 19. Representatives of naphthalene CYP17A1 inhibitors.

among several CYP enzymes.[115] Compound **40** displayed potent inhibition of CYP17A1. It has also been reported that substitution of the A ring with polar substituents leads to strong inhibitors, represented by compound **41**.[116] Another study showed that the activity of the compounds could also be increased by constraining the molecule in the form of carbazole **42** or fluorene **43**. However, these compounds required further optimization for improved CYP17A1 selectivity.[117]

Another strategy aimed at improving the potency was replacing the A or C aromatic nuclei with different heterocycles. Compound **44** was a potent inhibitor and showed a longer duration of action *in vivo* than the reference abiraterone.[118] Attempts have been made to utilize the ACD and ABD (Figure 10) strategies and annulate A or C rings.[119,120] However, these compounds did not display significant CYP17A1 inhibition. Further studies showed that a potential strategy to improve the activity involved dearomatizing ring D of the ACD system. This led to the potent and selective CYP17A1 inhibitor **45**.[121]

Further modifications of the biaryl compounds led to design of dual inhibitors of CYP17A1 and CYP11B1. The new strategy was to contain elements of the pharmacophores derived from abiraterone as an inhibitor of CYP17A1 and metyrapone as an inhibitor of CYP11B1. A pyridyl group was used in place of an imidazole group, resulting in a dual inhibitor **46**.[122] The importance of the chirality at the linker position was highlighted by compound (−)-**47** which was a very potent CYP17A1 inhibitor and had excellent selectivity for CYP3A4 (>300-fold). The dextrorotatory enantiomer was over 10 times less potent (IC_{50} = 340 nM vs 26 nM). Moreover, the compound displayed a sustained decrease in serum testosterone levels after single oral dosing.[123]

Naphthalenes. Based on two well-known CYP17A1 inhibitors **48** (SU 8000) and **49** (SU 10603), a series of indanes and tetralines were designed, out of which compound **50** was the most potent (Figure 19).[124,125] Further modifications included scaffold hopping, utilizing various heme-binding heterocycles, and modifying the linker between tetraline and heterocyclic moiety into a fused cyclopropane ring or imidazole ring.[126−131] In subsequent research it was determined that the presence of a tetralone oxo group was not essential, but it was beneficial to add a hydrogen bond acceptor, presumably mimicking the natural substrate. Compound **51** showed potent CYP17A1 inhibition and good selectivity.[132] Attempts have been made to introduce an element of unsaturation into the tetralin ring as well as an oxime group into the side chain. These modifications yielded only marginal or no inhibitory properties when tested in human CYP17A1.[133−135]

https://doi.org/10.1021/acs.jmedchem.3c00442
J. Med. Chem. 2023, 66, 6542−6566

Another modification of the naphthalene derivative **51** involved inclusion of a hydroxyl and an isopropyl group at the methylene bridge. This was crucial for limiting the effect of compounds on liver enzymes. However, the best results were achieved by introducing additional methoxy groups in the 6 and 7 positions, which resulted in compound **52**.[136] This compound also proved effective in *in vivo* studies in the monkey model. Subsequent manipulation of the naphthalene substituents resulted in tricyclic derivatives and eventually in (+)-**53** (orteronel, TAK-700).[137,138] Orteronel demonstrated potent reductions in serum testosterone and DHEA concentrations after single oral dosing (1 mg/kg) in cynomolgus monkeys. Selectivity for CYP17 over other CYP enzymes was attributed to the conformational rigidity and low clogP value. Similar to orteronel, another orally active compound, (−)-**54** (seviteronel, VT-464), was designed and proved to be a potent and selective CYP17A1 inhibitor with substantial *in vivo* activity.[139] However, the reported selectivity was not replicated under the very strict conditions.[44] Orteronel and seviteronel represent a handful of non-steroidal inhibitors reaching clinical trials; however, they did not succeed to reach clinical practice.

Natural Products. Natural products represent a unique chemotype because they do not possess a nitrogen atom while the vast majority of the known CYP17A1 inhibitors do. During the screening for CYP17A1 inhibitors, potent activity of methanol extracts from green and black tea was found.[140] These fractions are rich in catechins. Detailed studies on commercially acquired various catechins and theaflavins revealed inhibitory activity surpassing that of ketoconazole. Theaflavin **55** displayed IC_{50} = 25 μM for the lyase reaction (ketoconazole IC_{50} = 35 μM). Similarly, turmeric extract containing curcuminoids was found to inhibit CYP17A1 (Figure 20).[141] Curcumin **56** docked to the 3RUK model showed a

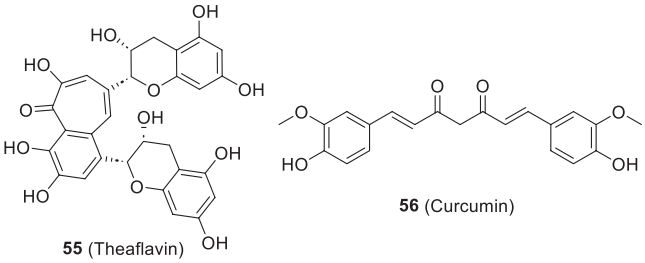

Figure 20. Representative inhibitors belonging to natural compounds.

resemblance to the steroid substrates with phenolic oxygen distanced 2.4 Å from the heme iron. These compounds seem to offer an interesting starting point for further optimization.

5. ASSAYS

5.1. NCI H295R Cell Model. The current standard model system to study molecular and biochemical mechanisms of steroidogenesis is the NCI H295R cell line.[142] This cell line was established from a series of strains of adrenocortical carcinoma tumor cells obtained from a 48-year-old black female exhibiting conditions like acne, facial hirsutism, diarrhea, weight loss, edema, and abnormal menses.[143] The initial cell line, NCI H295, was further developed into the NCI H295R strain having a shorter doubling time, adherent monolayer growth, and retained steroidogenic capacity over subsequent passages. The adrenal gland is a complex system, divided into specific zones of differentially expressed genes involved in the production and regulation of steroids. Cell models arising from animal or human tissues require zone-specific primary regulators to facilitate steroid production, and the steroid profile often changes with successive passaging, response factors, and growth conditions. NCI H295R cells express genes from all three zones of the adrenal cortex, providing an excellent system that closely reflects human adrenal physiology. The available mouse adrenocortical cell line, Y1, produces mainly glucocorticoids and mineralocorticoids and cannot express genes involved in the production of sex steroids, rendering them inefficient to study the production of androgens and CYP17A1 activity.[144] Studies with cDNA isolated from hamster adrenal libraries showed a preference for the Δ4 pathway to produce DHEA like the human adrenal system. Unlike the mouse model, it might serve as a better animal model to study human steroid metabolism.[145] So far, among all these systems, the NCI H295R cell line is the preferred model as it is more convenient, cheaper, and robust to perform enzyme kinetic studies and molecular biology-based assays.

5.2. Enzyme Assays. One of the oldest methods to analyze enzyme activity is the use of colorimetric assays to detect androgens in urine samples.[146] Major disadvantages are the requirement of large sample volumes, lack of specificity, and poor range of detection. The earliest enzyme assays to investigate the production of androgens were performed in microsomes isolated from testicular tissue extracts from guinea pigs which were found to be oxidizing progesterone to testosterone and acetic acid. The products formed were detected using radioactive substrates labeled with carbon-14 or tritium at specific positions.[147] Different isolation and separation techniques were adopted to quantify the steroids present in the reaction mixture, including methods like direct distillation, paper chromatography, or thin-layer chromatography (TLC) using different organic solvent systems as mobile phase.[148,149] These methods, combined with radioimmunoassay (RIA) or protein binding assay, enabled the quantitative detection of steroids with enhanced specificity and sensitivity.[150−152] However, it has a few drawbacks such as the handling of radioactive materials, the requirement of intensive labor work, and cross-reactivity with other steroids resulting in the detection of unwanted steroids in a complex sample.[153] With the development of techniques like normal-phase high-performance liquid chromatography (HPLC), separation and detection of both C19 and C21 steroids became possible and enabled the assay of CYP17A1 activity from both Δ4 (progesterone) and Δ5 (pregnenolone) pathways. Typical chromatographic separation is carried out over a hexane−tetrahydrofuran gradient system with a silica stationary phase. The flow system is coupled to a flow cell radioactivity detector sensitive to tritium. The use of radiolabeled substrates eliminates the need for internal standards and increases the sensitivity for detection.[154,155] Simultaneously, microsomal-like systems containing recombinant and purified CYP17A1 were developed to study the effect of mutant CYP17A1 proteins on enzyme activity and overall steroid metabolism with respect to wild type.[156−158] Combining the advanced techniques of gas chromatography (GC) and HPLC with sophisticated detection systems utilizing mass spectrometry (MS), methods like GC-MS and LC-MS/MS were developed and became widely adopted for performing whole steroid profiling in different biological samples.[159−162] With the advancement leading to decreased sample volume requirements and detection of a range of steroids present at even lower

https://doi.org/10.1021/acs.jmedchem.3c00442
J. Med. Chem. 2023, 66, 6542−6566

concentrations, most of the shortcomings of the previous techniques were resolved. GC/LC-MS/MS has proven to be beneficial to generate steroid profiles from different types of assays as well as diagnostics/patient samples for various clinical diagnoses in a faster and more efficient way.[163−165] Although it has several advantages, it is comparatively expensive and demands highly trained professionals to operate the instruments and analyze the data. This renders it less suitable to perform large-scale drug screening of small molecule inhibitors to target CYP17A1 activity. In this case, the preferred technique is the separation of radiolabeled steroids by TLC and quantification using autoradiography or direct measurement of radioactivity with the help of a liquid scintillation counter.[16,141,166]

6. PERSPECTIVE

6.1. Desired Inhibitory Profile. The CYP17A1 enzyme is a key catalyst involved in steroidogenesis, thus the biosynthesis of steroid hormones in the adrenal glands, gonads, and placenta. CYP17A1 inhibitors can be used to treat a range of medical conditions, including hormonal imbalances or endocrine-dependent cancers. From a drug discovery perspective, the desired inhibitory profile of CYP17A1 inhibitors depends on the specific disease being targeted. For example, in the treatment of prostate cancer, the goal is to reduce androgen synthesis, so a highly specific and potent inhibitor of CYP17A1 would be ideal. On the other hand, in the treatment of congenital adrenal hyperplasia, a less potent inhibitor that does not completely shut down steroidogenesis may be preferred to avoid significant hormonal imbalances. To avoid undesired side effects a high specificity towards the target CYP17A1 cytochrome is important. To address this issue the subtle structural differences in the different CYPs need to be taken into account during the medicinal chemistry optimization. In terms of general side effects that can be tolerated, this will depend on the specific medical condition being targeted. For example, in the treatment of prostate cancer, some of the common side effects associated with CYP17A1 inhibition include hot flashes, osteoporosis, and decreased libido. These side effects may be acceptable, considered the alternative of more severe illness.

6.2. Selectivity against Other CYPs. Whereas potency perhaps has been the driving force in previous drug discovery projects, it is only one of many features to be considered today. Most drugs interact with multiple targets, comprising several anti-targets leading to unwanted effects. To obtain selectivity for the desired target the focus has often been on reducing the effects of the drug-metabolizing CYP1, CYP2, and CYP3 enzymes.

Several of the CYP17A1 inhibitors reported to date also inhibit the drug-metabolizing CYPs, primarily CYP3A4. Due to the promiscuous nature of CYP3A4 it is not straightforward to introduce functionalities to be acceptable for the CYP17A1 enzyme but not for CYP3A4. Nevertheless, several of the previously mentioned non-steroidal CYP17A1 inhibitors are selective against CYP3A4, e.g., the stilbene analog **14** (Figure 14), **17** and **18** identified by virtual screening, **19** identified by combining the heme-binding moiety from abiraterone and galeterone, and the ketoconazole analog **20** (Figure 15).[85,89,90,93] Unfortunately, it is not yet possible to derive some common structural denominator(s) for obtaining selectivity for CYP17A1 against CYP3A4 and the other drug-metabolizing CYPs.

Another important issue is the selectivity for CYP17A1 against CYP19A1 and CYP21A2. The steroidal inhibitors may potentially interact with all three enzymes, although it has been possible to increase CYP17A1 selective inhibition by introducing hydrogen-bonding substituents in the C6 position of abiraterone (Figure 6B).[43] The non-steroidal inhibitor **18** (Figure 15) displayed selectivity against not only CYP3A4 but also CYP21A2, although we at present have not yet identified which of the functional groups are responsible for the observed selectivity.[89]

In a recent report, a summary of the present state-of-the-art in selectivity optimization for various CYP forms was presented.[167] The examples comprise weakening of binding to the heme group, reduction of ligand lipophilicity, and small structural modification.

A CYP index equal to the ring count divided by the lipophilicity (cLogP) has been suggested to be a measure of the conformational rigidity corrected for the effect of lipophilicity.[168] The authors concluded that a CYP index >2 would reduce the risk for getting compounds with submicromolar CYP3A4 binding and that use of the CYP index would increase the possibility for designing heme-binding inhibitors with reduced CYP3A4 binding.

Contrary to the above intuitive approach, a target-specific selectivity has been developed comprising the potency against the target of interest and the potency against other targets called the absolute potency and relative potency, respectively. The most selective compound was then identified by simultaneous optimization of the two potency metrics, yielding a selectivity score for the compound. The potential of this computationally more complex procedure was shown on a dataset comprising 442 kinase targets.[169]

Selectivity is clearly an unsolved issue for CYP17A1 inhibition, with the known selective compounds primarily obtained based on traditional medicinal chemistry experience and/or serendipity. Thus, more knowledge-based quantitative methods are needed to guide future design. We have not yet seen the full potential of novel methods like AI and deep learning applied to the general CYP selectivity problem nor the specific CYP17A1 selectivity problem.[170]

6.3. Selectivity towards Lyase Inhibition. Truly lyase-selective inhibitors would be ideal for an improved cortisol profile in humans. Generally, selectivity is always a vital factor in drug discovery targeting enzyme inhibition. In the case of CYP17A1 it is important to remember that this single enzyme is capable of catalyzing two successive reactions, a hydroxylation and a lyase transformation. The lyase inhibition is preferred over hydroxylase inhibition because this leads to a better control of circulating C19 androgen precursors without decreasing the cortisol levels and elevating ACTH.[171] Both reactions occur in the same active site and therefore it is extremely difficult to design an inhibitor that would selectively block only one reaction. All known inhibitors act by coordinating with the heme iron, therefore by inhibiting hydroxylase reaction they will inherently affect the lyase reaction. However, some insight might be gained from substrate specificity. It is widely known that 17OH-Prog is the poor lyase substrate while 17OH-Preg is the efficient one. A structural explanation has been given pointing to different positions of these two substrates in the active site, where 17OH-Preg is positioned closer to the heme iron without making a hydrogen bond to N202.[42] This offers a potential strategy to design inhibitors with attenuated interactions with N202.[172] Recently, a V362M mutation found at the active site of CYP17A1 was shown to selectively decrease the lyase activity by reducing the binding of 17OH-Preg. Therefore, certain design

https://doi.org/10.1021/acs.jmedchem.3c00442
J. Med. Chem. 2023, 66, 6542−6566

elements could be employed for creating inhibitors that compete with 17OH-Preg for binding to the CYP17A1 active site and may have high specificity for inhibiting the CYP17A1 lyase reaction.[173] Another important aspect of lyase selectivity is associated with cyt b_5. It has been suggested that cyt b_5 binding alters the CYP17A1 conformation to promote the lyase activity.[6] This notion points to disrupting the CYP17A1-cyt b_5 interaction mediated via the ternary CYP17A1-cyt b_5-POR complex or even targeting cytochrome b_5 itself as another potential strategy.[40,50,174] However, conformational changes do not alter the binding of either 17OH-Preg or 17OH-Prog as measured by apparent K_d and binding kinetics.[175] Thus, despite conformational selection appearing to be the dominant mechanism for CYP17A1 binding, structural modifications in ligand design might not easily translate to expected selectivity. Additionally, experimental structural data regarding the ternary CYP17A1-cyt b_5-POR complex is also lacking.

During recent years attention has been brought to a multistep binding of lyase-selective inhibitors to CYP17A1.[73,176] These studies indicate a rapid formation of an initial complex followed by slow conversion into the iron-complexed form. More importantly, this suggests that the formation of the heme iron heterocycle complex is not a prerequisite needed for enzyme inhibition. Consequently, iron-binding moieties may not be necessary structural features. Remembering that essentially all known inhibitors have this feature, this brings about a new generation of inhibitors that do not rely on the necessity to coordinate the heme, thus displaying potentially improved inhibition profiles.

6.4. Exploitation of Atoms Other than Nitrogen to Coordinate the Heme. Nearly all reported CYP17A1 inhibitors, both steroidal and non-steroidal, contain a nitrogen-containing heteroaromatic ring with the nitrogen lone-pair coordinating to the iron atom in the heme group. This bias in design of CYP17A1 inhibitors is probably inspired by the existence of azole-containing antifungals which inhibit the CYP51A1, converting lanosterol to ergosterol.[177] The bias has also been supported by computational studies showing that a variety of nitrogen-containing heterocycles were favorable for binding to the iron in the heme group.[89,178]

The interaction between a ligand with an electron-rich nitrogen and the electron-deficient iron atom in the heme group can be considered as a classical nucleophile−electrophile interaction. The Protein Data Bank contains several examples on other nucleophilic ligands interacting with the iron atom in heme-containing proteins.

In the structure of a bacterial CYP BM3 (CYP102A1) mutant M11, the anionic form of the mercapto group in dithiothreitol coordinates to the heme group with an Fe−S distance of 2.3 Å.[179] Several other examples of CYP structures with sulfur-containing compounds, i.e., primary thiols, coordinating the heme group are known.[179] A handful of thioether-based nitric oxide synthase inhibitors display type II binding to the heme group. X-ray crystallography showed that the sulfur atom in some of these structures coordinated to the iron atom in the heme group with Fe−S distances of ∼2.7 Å.[180,181]

A rather unusual example of a functional group, to our knowledge not present in any drug compounds, is the alkyl isocyanide, where the carbon atom in the isocyanide group is highly nucleophilic. The structure of *n*-butyl isocyanide in complex with sperm whale myoglobin is one of several similar complexes in the Protein Data Bank, and it shows that the isocyanide carbon is located 2.1 Å above the iron atom in the heme group.[182]

Thus, based on the provided examples, we suggest that novel metal-coordinating groups should not be neglected in future design of CYP17A1 inhibitors.[183,184]

6.5. Physicochemical Properties. The physicochemical properties of a compound determine its absorption, distribution, metabolism, and excretion (ADME) profile and thus are vital for the success of any drug candidate. One of the key properties is compound solubility, which heavily influences the ADME profile but is also important for meaningful activities in *in vitro* assays.[185] Factors like temperature, water content, or impurities can have significant impacts on solubility.[186] Visual inspection of published CYP17A1 inhibitor structures suggests that many of these compounds might suffer from poor solubility. Inadequate aqueous solubility can be inferred based on the presence of dominant aromatic fragments with small numbers of polar groups. These structural features were likely put in place due to the hydrophobic nature of the enzyme binding site but also because of the facilitated synthesis. Thus, future design strategies should actively seek a careful balance between maintaining desirable activity and adequate solubility. Non-steroidal inhibitors have an inherent advantage over steroidal compounds in this regard. For instance, abiraterone, the only approved CYP17A1 inhibitor in clinical use, should be taken as a flat dose of 1000 mg administered on an empty stomach.[187] This relatively high dose reflects poor absorption but also a very high fraction of the drug bound to the plasma proteins.[188] The non-steroidal scaffold offers potentially greater flexibility in fine-tuning physicochemical properties.

Besides following the well-established Lipinski rule of five, tentative structural features incorporated in the molecule design can include synthesis of prodrugs, insertion of hydrophilic and ionizable groups, addition and removal of hydrogen-bonding fragments, bioisosteric replacement, and disruption of molecular symmetry and planarity.[189] Reducing the aromatic character of a compound could potentially improve its physicochemical properties, such as solubility. The propensity to design out-of-plane substituents can enhance the compatibility between receptors and ligands. This may facilitate the creation of new protein−ligand interactions that are not attainable with a flat aromatic ring, leading to improved activity and selectivity towards a specific target and minimizing the risk of off-target effects.[190] On the other hand, increased molecular complexity can negatively impact the readiness at which large numbers of analogs can be made.

6.6. Translation of *In Vitro* Effect to *In Vivo*. The translation from *in vitro* activity to *in vivo* efficacy is crucial in any drug discovery project. Many factors, absent in *in vitro* settings, determine the fate of a drug in a living organism. The high attrition rate during the drug development stage is a sobering reminder that a drug candidate can still fail despite high potency and favorable selectivity profile. Little attention is often paid to pharmacokinetics (PK) at the early drug discovery stages, while the focus is on the optimization of ligand−target interactions. The situation is especially common in academic groups. Resources available in industry drug discovery programs often permit extensive PK studies. Assessment of properties such as clearance, half-life, volume of distribution, or maximum concentration can be very costly, especially when undertaken in primate mammals.[101] However, with CYP17A1 inhibitors, efforts should be made to measure *in vivo* testosterone levels as a predictor of potential *in vivo* efficacy. Male Sprague−Dawley rats

https://doi.org/10.1021/acs.jmedchem.3c00442
J. Med. Chem. 2023, 66, 6542−6566

have been successfully used to demonstrate reduction in the plasma testosterone concentration.[132,191] Such determination should ideally include several time points. For instance, testosterone measured after 2 h and 5 h should be diminished, indicating sustained effect.[84] Further *in vivo* assays can include profiling of other steroids. Cortisol level is of high importance because it is often dysregulated. Its imbalance during the abiraterone therapy requires concomitant administration of prednisone. Previously mentioned physicochemical properties play also important role. The most advanced next-generation non-steroidal CYP17A1 inhibitors, such as orteronel and seviteronel, described above, exhibit good bioavailability and general ADME properties in addition to an improved selectivity towards the desired inhibition of the lyase activity of the CYP17A1 enzyme. Both these compounds were taken into clinical development. Unfortunately, orteronel was discontinued after phase III as it failed to extend overall survival rates in the target metastatic, hormone-refractory prostate cancer patient group. Seviteronel is still in clinical development although issues with drug-related tolerability in a phase 2 trial have been reported.

6.7. Emerging Competing Prostate Cancer Therapies. Prostate cancer therapy has been at the forefront of CYP17A1 inhibitor development. Numerous innovative treatment alternatives for prostate cancer have emerged in recent years. Histone deacetylase (HDAC) inhibitors, such as vorinostat, pracinostat, panobinostat, and romidepsin, serve as notable examples. Although all four underwent clinical trials, they ultimately fell short due to a majority of patients experiencing toxicity or disease progression. At present, two critical pieces of information are missing from studies on HDAC inhibitors in cancer: first, the expression profiles of various HDACs in prostate cancer models, and second, the involvement of AR with HDACs in prostate cancer.[192]

Recently, aberrant fatty acid activation of peroxisome proliferator-activated receptors (PPARs) resulting from dysregulated lipid signaling has been implicated as a crucial factor in prostate cancer. Fatty-acid-binding proteins (FABPs), particularly FABP5, facilitate PPAR activation. FABP5 is overexpressed in prostate cancer and is associated with poor patient prognosis and survival.[193] However, the identification of FABP5 as a molecular target for prostate cancer remains in its early stage, with several challenges to overcome, primarily due to the ubiquity of FABP5.

A substantial number of DNA-damage repair (DDR) pathways have been found to be frequently dysregulated in advanced prostate cancer stages. Tumors with compromised ability to repair double-strand DNA breaks via homologous recombination are highly sensitive to the inhibition of poly(ADP) ribose polymerase (PARP) enzyme. Olaparib was the first agent to show benefit in patients with DDR-deficient prostate cancer.[194]

Proteolysis-targeting chimeras (PROTACs) exemplify the therapeutic approach of induced protein degradation. These heterobifunctional molecules create a trimeric complex between a target protein and an E3 ubiquitin ligase, facilitating target ubiquitination and subsequent degradation. AR-targeting PROTACs, notably ARCC-4 (an enzalutamide-based von Hippel−Lindau (VHL)-recruiting AR PROTAC), have been proposed and shown to be superior to enzalutamide.[195] The primary advantages include inducing apoptosis and inhibiting the proliferation of AR-amplified prostate cancer cells, as well as effectively degrading clinically relevant AR mutants associated with antiandrogen therapy. PROTAC-mediated AR degradation could potentially address several AR-dependent drug resistance mechanisms characteristic of castration-resistant prostate cancer.

When comparing these emerging therapies to CYP17A1 inhibition, it is crucial to consider that, at the molecular level, prostate cancer is primarily driven by excessive signaling via the androgenic pathway. While androgenic signaling is considered the primary driver of CRPC, androgen-independent signaling pathways might also contribute to CRPC progression.[196] Nonetheless, as CRPC advances, the concentration of PSA continues to rise. Since PSA is regulated by androgenic signaling, this implies that androgenic signaling remains involved in CRPC progression.[197] Therefore, androgen signaling remains central to prostate cancer pharmacology, leaving CYP17A1 inhibition as an important and attractive strategy.

As the field of prostate cancer therapeutics continues to evolve, it is possible that the ongoing research into the interplay between these pathways may uncover additional synergies and opportunities for combination therapies, further enhancing the effectiveness of cancer treatment.

6.8. Concluding Remarks. In conclusion, there is still a need for improved compounds as potent and selective inhibitors of the steroidogenic CYP17A1 enzyme as a target for treatment of serious hormone-dependent cancer diseases, e.g., prostate cancer. The extensive work in recent years has provided compounds, belonging to the non-steroidal class, with improved activity and selectivity as well as translational properties. However, none of these has yet reached clinical practice. As outlined above, there are key features that still need to be addressed for the next-generation compounds, such as selectivity towards other CYPs, specificity for the CYP17A1 lyase inhibition, and acceptable physicochemical properties. We hope that these issues can be solved with medicinal chemistry efforts towards the optimal compound.

■ ASSOCIATED CONTENT

Supporting Information

The Supporting Information is available free of charge at https://pubs.acs.org/doi/10.1021/acs.jmedchem.3c00442.

Three-dimensional model of CYP17A1-cyt b5 complex anchored in the membrane, available as an animation illustrating the 3D relationships of the structure and interactions (MP4)

■ AUTHOR INFORMATION

Corresponding Author

Tomasz M. Wróbel − *Department of Synthesis and Chemical Technology of Pharmaceutical Substances, Faculty of Pharmacy, Medical University of Lublin, 20093 Lublin, Poland; Department of Drug Design and Pharmacology, Faculty of Health and Medical Sciences, University of Copenhagen, DK-2100 Copenhagen, Denmark;* orcid.org/0000-0002-0313-2522; Phone: +48-81-448-7273; Email: tomasz.wrobel@umlub.pl

Authors

Flemming Steen Jørgensen − *Department of Drug Design and Pharmacology, Faculty of Health and Medical Sciences, University of Copenhagen, DK-2100 Copenhagen, Denmark;* orcid.org/0000-0001-8040-2998

https://doi.org/10.1021/acs.jmedchem.3c00442
J. Med. Chem. 2023, 66, 6542−6566

Amit V. Pandey − *Pediatric Endocrinology, Department of Pediatrics, University Children's Hospital, Inselspital, Bern and Translational Hormone Research Program, Department of Biomedical Research, University of Bern, 3010 Bern, Switzerland*

Angelika Grudzińska − *Department of Synthesis and Chemical Technology of Pharmaceutical Substances, Faculty of Pharmacy, Medical University of Lublin, 20093 Lublin, Poland*

Katyayani Sharma − *Pediatric Endocrinology, Department of Pediatrics, University Children's Hospital, Inselspital, Bern and Translational Hormone Research Program, Department of Biomedical Research, University of Bern, 3010 Bern, Switzerland*

Jibira Yakubu − *Pediatric Endocrinology, Department of Pediatrics, University Children's Hospital, Inselspital, Bern and Translational Hormone Research Program, Department of Biomedical Research, University of Bern, 3010 Bern, Switzerland*

Fredrik Björkling − *Department of Drug Design and Pharmacology, Faculty of Health and Medical Sciences, University of Copenhagen, DK-2100 Copenhagen, Denmark;* orcid.org/0000-0001-7018-8334

Complete contact information is available at: https://pubs.acs.org/10.1021/acs.jmedchem.3c00442

Notes

The authors declare no competing financial interest.

Biographies

Tomasz M. Wróbel received his M.Sc. in pharmacy from the Medical University in Lublin. After a few years working in a community pharmacy in Ireland, he returned to academia to his alma mater, where he obtained his Ph.D. in pharmaceutical sciences in 2014. He completed his postdoctoral training in 2018 at the University of Copenhagen under the supervision of Prof. Fredrik Björkling. He currently holds a position of associate professor at the Medical University of Lublin. His research interests involve non-steroidal CYP17A1 inhibitors and CNS agents.

Flemming Steen Jørgensen is a professor in Computational Chemistry/Molecular Modelling at the Faculty of Health and Medical Sciences, University of Copenhagen (UCPH). He started at the University in 1973, studied chemistry, and got a M.Sc. and subsequently a Ph.D. from UCPH. Initially an organic chemist, he moved during his Ph.D. to work with UV photoelectron spectroscopy. He spent a year at the University of Alberta, Canada, doing X-ray photoelectron spectroscopy and then returned to UCPH for three years doing computational chemistry. In 1984 he moved to the Royal Danish School of Pharmacy (from 2009 part of UCPH) as an associate professor, setting up a molecular graphics and modelling unit, and in 2007 was appointed full professor. His main interests are in the use of computational methods to discover chemical properties and reactions, primarily related to drug compounds and their metabolism.

Amit V. Pandey received his B.Sc. in chemistry and physics (1990) and a M.Sc. in biochemistry (1992) from the University of Lucknow, followed by doctoral studies at the Central Drug Research Institute, Lucknow, India, on cytochrome P450 and heme metabolism. Following postdoctoral research at the University of California San Francisco (UCSF) working on CYP17A1 and androgen regulation with Prof. Walter L Miller, he began his career at the University of Bern in 2005, obtaining his habilitation in endocrinology in 2010. He is currently the head of steroid biochemistry and growth hormone research laboratories at the University Children's Hospital Bern and a professor at the University of Bern, Switzerland. His research focuses on androgen regulation in humans and pharmacogenomics of steroid and drug metabolizing cytochrome P450 enzymes.

Angelika Grudzińska earned her master's degree in pharmacy from the Medical University of Lublin in 2020. She is currently pursuing a Ph.D. under the supervision of Prof. Tomasz M. Wróbel from the Department of Synthesis and Chemical Technology of Pharmaceutical Substances, Medical University of Lublin. Her research is focused on the synthesis of small-molecule non-steroidal CYP17A1 inhibitors.

Katyayani Sharma received her B.Sc. degree in 2016 from the University of Lucknow, India, then obtained a master's degree in biochemistry at the University of Lucknow in 2018, where she received the Prof. P. S. Krishnan gold medal for graduating at the top of her class. She received the prestigious Swiss Government Excellence Scholarship in 2019 for her doctoral studies. Currently, she is a Ph.D. student in biochemistry at the University of Bern, Switzerland, under the supervision of Prof. Amit V. Pandey. Her research activity is focused on the regulation of androgen production in humans by cytochrome P450 CYP17A1 enzyme.

Jibira Yakubu received his B.Sc. degree in herbal medicine (2015) from the Kwame Nkrumah University of Science and Technology, Ghana. He then obtained a M.Phil. degree in pharmacology from the same university in 2019. His master's research project was on the medicinal properties of hydroethanol stem bark extract of *Burkea africana*, a plant used in Ghanian traditional medicine. He received the prestigious Swiss Government Excellence Scholarship in 2022 for his doctoral studies. Currently, he is a Ph.D. student in cell biology at the University of Bern, Switzerland, under the supervision of Prof. Amit V. Pandey. His research activity is focused on targeting hyperandrogenic disorders like prostate cancer and polycystic ovary syndrome by novel synthetic chemicals as well as phytochemicals isolated from medicinal plants.

Fredrik Björkling received his master's degree in chemical engineering from the Royal Institute of Technology in Stockholm, Sweden, in 1980 and Ph.D. from the same institution in 1985. He is a highly experienced medicinal chemist with over 20 years in director level management positions in both pharma and biotech (Novo Nordisk A/S, LEO Pharma, and TopoTarget A/S). He has been involved in drug discovery programs in several therapeutic areas such as cancer, inflammation, infectious diseases, diabetes, and dermatological diseases. Since 2008 he has been associated with the University of Copenhagen as Head of the Department of Medicinal Chemistry, Molecular Drug Research, and Deputy Head of the Department of Drug Design and Pharmacology. He retired in 2022.

■ ACKNOWLEDGMENTS

T.M.W.'s work is funded by the Narodowe Centrum Nauki grant Sonata 16 2020/39/D/NZ7/00572. A.V.P. acknowledges the Swiss National Science Foundation, grant number 310030M_204518, and Cancer Research Switzerland, grant number KFS-5557-02-2022. J.Y. and K.S. are funded by Swiss Government Excellence Scholarships (ESKAS), grant numbers 2022.0470 and 2019.0385.

■ ABBREVIATIONS USED

17OH-Preg, 17α-hydroxypregnenolone; 17OH-Prog, 17α-hydroxyprogesterone; AR, androgen receptor; ADT, androgen deprivation therapy; CoMFA, comparative molecular field analysis; CRPC, castration-resistant prostate cancer; cyt b5, cytochrome b5; CYP17A1, cytochrome P450 17A1; DDR, DNA damage repair; DHEA, dehydroepiandrosterone; DFT,

density functional theory; DHT, dihydrotestosterone; GC, gas chromatography; HDAC, histone deacetylase; HPLC, high-performance liquid chromatography; MS, mass spectrometry; PARP, poly(ADP) ribose polymerase; PPAR, peroxisome proliferator-activated receptor; PK, pharmacokinetics; POR, P450 reductase; PCOS, polycystic ovary syndrome; PROTAC, proteolysis targeting chimera; PSA, prostate-specific antigen; RIA, radioimmunoassay; SOSA, optimization of side activities; TLC, thin-layer chromatography

REFERENCES

(1) Rosenfield, R. L.; Barnes, R. B.; Cara, J. F.; Lucky, A. W. Dysregulation of cytochrome P450c17α as the cause of polycystic ovarian syndrome. *Fertility Sterility* **1990**, *53* (5), 785−791.

(2) Miller, W. L.; Auchus, R. J. The Molecular Biology, Biochemistry, and Physiology of Human Steroidogenesis and Its Disorders. *Endocrine Rev.* **2011**, *32* (1), 81−151.

(3) Fan, Y. S.; Sasi, R.; Lee, C.; Winter, J. S. D.; Waterman, M. R.; Lin, C. C. Localization of the human CYP17 gene (cytochrome P45017α) to 10q24.3 by fluorescence in situ hybridization and simultaneous chromosome banding. *Genomics* **1992**, *14* (4), 1110−1111.

(4) Katagiri, M.; Kagawa, N.; Waterman, M. R. The Role of Cytochrome b5 in the Biosynthesis of Androgens by Human P450c17. *Arch. Biochem. Biophys.* **1995**, *317* (2), 343−347.

(5) Akhtar, M. K.; Kelly, S. L.; Kaderbhai, M. A. Cytochrome b5 modulation of 17α hydroxylase and 17−20 lyase (CYP17) activities in steroidogenesis. *J. Endocrinol.* **2005**, *187* (2), 267−274.

(6) Auchus, R. J.; Lee, T. C.; Miller, W. L. Cytochrome b5 Augments the 17,20-Lyase Activity of Human P450c17 without Direct Electron Transfer. *J. Biol. Chem.* **1998**, *273* (6), 3158−3165.

(7) Yoshimoto, F. K.; Auchus, R. J. The diverse chemistry of cytochrome P450 17A1 (P450c17, CYP17A1). *J. Steroid Biochem. Mol. Biol.* **2015**, *151*, 52−65.

(8) Turcu, A.; Smith, J. M.; Auchus, R.; Rainey, W. E. Adrenal Androgens and Androgen Precursors—Definition, Synthesis, Regulation and Physiologic Actions. *Comprehensive Physiol.* **2014**, 1369−1381.

(9) Mak, P. J.; Duggal, R.; Denisov, I. G.; Gregory, M. C.; Sligar, S. G.; Kincaid, J. R. Human Cytochrome CYP17A1: The Structural Basis for Compromised Lyase Activity with 17-Hydroxyprogesterone. *J. Am. Chem. Soc.* **2018**, *140* (23), 7324−7331.

(10) Miller, W. L.; Auchus, R. J. The "backdoor pathway" of androgen synthesis in human male sexual development. *PLOS Biol.* **2019**, *17* (4), e3000198.

(11) Fiandalo, M. V.; Wilton, J.; Mohler, J. L. Roles for the Backdoor Pathway of Androgen Metabolism in Prostate Cancer Response to Castration and Drug Treatment. *Int. J. Biological Sci.* **2014**, *10* (6), 596−601.

(12) O'Shaughnessy, P. J.; Antignac, J. P.; Le Bizec, B.; Morvan, M.-L.; Svechnikov, K.; Söder, O.; Savchuk, I.; Monteiro, A.; Soffientini, U.; Johnston, Z. C.; Bellingham, M.; Hough, D.; Walker, N.; Filis, P.; Fowler, P. A. Alternative (backdoor) androgen production and masculinization in the human fetus. *PLOS Biol.* **2019**, *17* (2), e3000002.

(13) Wilson, J. D.; Auchus, R. J.; Leihy, M. W.; Guryev, O. L.; Estabrook, R. W.; Osborn, S. M.; Shaw, G.; Renfree, M. B. 5α-Androstane-3α,17β-Diol Is Formed in Tammar Wallaby Pouch Young Testes by a Pathway Involving 5α-Pregnane-3α,17α-Diol-20-One as a Key Intermediate. *Endocrinol.* **2003**, *144* (2), 575−580.

(14) Auchus, R. J. The backdoor pathway to dihydrotestosterone. *Trends in Endocrinol. & Metabolism* **2004**, *15* (9), 432−438.

(15) Malikova, J.; Brixius-Anderko, S.; Udhane, S. S.; Parween, S.; Dick, B.; Bernhardt, R.; Pandey, A. V. CYP17A1 inhibitor abiraterone, an anti-prostate cancer drug, also inhibits the 21-hydroxylase activity of CYP21A2. *J. Steroid Biochem. Mol. Biol.* **2017**, *174*, 192−200.

(16) Udhane, S. S.; Dick, B.; Hu, Q.; Hartmann, R. W.; Pandey, A. V. Specificity of anti-prostate cancer CYP17A1 inhibitors on androgen biosynthesis. *Biochem. Biophys. Res. Commun.* **2016**, *477* (4), 1005−1010.

(17) Alyamani, M.; Emamekhoo, H.; Park, S.; Taylor, J.; Almassi, N.; Upadhyay, S.; Tyler, A.; Berk, M. P.; Hu, B.; Hwang, T. H.; Figg, W. D.; Peer, C. J.; Chien, C.; Koshkin, V. S.; Mendiratta, P.; Grivas, P.; Rini, B.; Garcia, J.; Auchus, R. J.; Sharifi, N. HSD3B1(1245A > C) variant regulates dueling abiraterone metabolite effects in prostate cancer. *J. Clin. Invest.* **2018**, *128* (8), 3333−3340.

(18) Dai, C.-F.; Xie, X.; Yang, Y.-N.; Li, X.-M.; Zheng, Y.-Y.; Fu, Z.-Y.; Liu, F.; Chen, B.-D.; Gai, M.-T.; Ma, Y.-T. Relationship between CYP17A1 genetic polymorphism and coronary artery disease in a Chinese Han population. *Lipids Health Disease* **2015**, *14* (1), 16.

(19) Chace, C.; Pang, D.; Weng, C.; Temkin, A.; Lax, S.; Silverman, W.; Zigman, W.; Ferin, M.; Lee, J. H.; Tycko, B.; Schupf, N. Variants in CYP17 and CYP19 Cytochrome P450 Genes are Associated with Onset of Alzheimer's Disease in Women with Down Syndrome. *J. Alzheimer's Disease* **2012**, *28*, 601−612.

(20) Huang, P.-C.; Li, W.-F.; Liao, P.-C.; Sun, C.-W.; Tsai, E.-M.; Wang, S.-L. Risk for estrogen-dependent diseases in relation to phthalate exposure and polymorphisms of CYP17A1 and estrogen receptor genes. *Environ. Sci. Pollution Res.* **2014**, *21* (24), 13964−13973.

(21) Swerdloff, R. S.; Dudley, R. E.; Page, S. T.; Wang, C.; Salameh, W. A. Dihydrotestosterone: Biochemistry, Physiology, and Clinical Implications of Elevated Blood Levels. *Endocrine Rev.* **2017**, *38* (3), 220−254.

(22) Fujimoto, N. Role of the Androgen-Androgen Receptor Axis in the Treatment Resistance of Advanced Prostate Cancer: From Androgen-Dependent to Castration Resistant and Further. *J. UOEH* **2016**, *38* (2), 129−138.

(23) Cai, C.; Chen, S.; Ng, P.; Bubley, G. J.; Nelson, P. S.; Mostaghel, E. A.; Marck, B.; Matsumoto, A. M.; Simon, N. I.; Wang, H.; Chen, S.; Balk, S. P. Intratumoral De Novo Steroid Synthesis Activates Androgen Receptor in Castration-Resistant Prostate Cancer and Is Upregulated by Treatment with CYP17A1 Inhibitors. *Cancer Res.* **2011**, *71* (20), 6503−6513.

(24) Attard, G.; Parker, C.; Eeles, R. A.; Schröder, F.; Tomlins, S. A.; Tannock, I.; Drake, C. G.; de Bono, J. S. Prostate cancer. *Lancet* **2016**, *387* (10013), 70−82.

(25) De Amicis, F.; Thirugnansampanthan, J.; Cui, Y.; Selever, J.; Beyer, A.; Parra, I.; Weigel, N. L.; Herynk, M. H.; Tsimelzon, A.; Lewis, M. T.; Chamness, G. C.; Hilsenbeck, S. G.; Andò, S.; Fuqua, S. A. W. Androgen receptor overexpression induces tamoxifen resistance in human breast cancer cells. *Breast Cancer Res. Treatment* **2010**, *121* (1), 1−11.

(26) Micheli, A.; Meneghini, E.; Secreto, G.; Berrino, F.; Venturelli, E.; Cavalleri, A.; Camerini, T.; Di Mauro, M. G.; Cavadini, E.; De Palo, G.; Veronesi, U.; Formelli, F. Plasma Testosterone and Prognosis of Postmenopausal Breast Cancer Patients. *J. Clin. Oncol.* **2007**, *25* (19), 2685−2690.

(27) Vera-Badillo, F. E.; Templeton, A. J.; de Gouveia, P.; Diaz-Padilla, I.; Bedard, P. L.; Al-Mubarak, M.; Seruga, B.; Tannock, I. F.; Ocana, A.; Amir, E. Androgen Receptor Expression and Outcomes in Early Breast Cancer: A Systematic Review and Meta-Analysis. *JNCI: J. National Cancer Institute* **2014**, *106* (1), djt319.

(28) Carey, A. H.; Waterworth, D.; Patel, K.; White, D.; Little, J.; Novelli, P.; Franks, S.; Williamson, R. Polycystic ovaries and premature male pattern baldness are associated with one allele of the steroid metabolism gene CYP17. *Hum. Mol. Genet.* **1994**, *3* (10), 1873−1876.

(29) Gorai, I.; Tanaka, K.; Inada, M.; Morinaga, H.; Uchiyama, Y.; Kikuchi, R.; Chaki, O.; Hirahara, F. Estrogen-Metabolizing Gene Polymorphisms, But Not Estrogen Receptor-α Gene Polymorphisms, Are Associated with the Onset of Menarche in Healthy Postmenopausal Japanese Women. *J. Clin. Endocrinol. Metab.* **2003**, *88* (2), 799−803.

(30) Ye, W.; Xie, T.; Song, Y.; Zhou, L. The role of androgen and its related signals in PCOS. *J. Cell. Mol. Med.* **2021**, *25* (4), 1825−1837.

(31) Valassi, E.; Aulinas, A.; Glad, C. A. M.; Johannsson, G.; Ragnarsson, O.; Webb, S. M. A polymorphism in the CYP17A1 gene influences the therapeutic response to steroidogenesis inhibitors in Cushing's syndrome. *Clin. Endocrinol.* **2017**, *87* (5), 433−439.

https://doi.org/10.1021/acs.jmedchem.3c00442
J. Med. Chem. 2023, 66, 6542−6566

(32) Chuang, J. Y.; Lo, W. L.; Ko, C. Y.; Chou, S. Y.; Chen, R. M.; Chang, K. Y.; Hung, J. J.; Su, W. C.; Chang, W. C.; Hsu, T. I. Upregulation of CYP17A1 by Sp1-mediated DNA demethylation confers Temozolomide resistance through DHEA-mediated protection in glioma. *Oncogenesis* **2017**, *6* (5), e339−e339.
(33) Lin, H.-Y.; Ko, C.-Y.; Kao, T.-J.; Yang, W.-B.; Tsai, Y.-T.; Chuang, J.-Y.; Hu, S.-L.; Yang, P.-Y.; Lo, W.-L.; Hsu, T.-I. CYP17A1Maintains the Survival of Glioblastomas by Regulating SAR1-Mediated Endoplasmic Reticulum Health and Redox Homeostasis. *Cancers* **2019**, *11*, 1378.
(34) Laughton, C. A.; Neidle, S.; Zvelebil, M. J. J. M.; Sternberg, M. J. E. A molecular model for the enzyme cytochrome P45017α, a major target for the chemotherapy of prostatic cancer. *Biochem. Biophys. Res. Commun.* **1990**, *171* (3), 1160−1167.
(35) Haider, S. M.; Patel, J. S.; Poojari, C. S.; Neidle, S. Molecular Modeling on Inhibitor Complexes and Active-Site Dynamics of Cytochrome P450 C17, a Target for Prostate Cancer Therapy. *J. Mol. Biol.* **2010**, *400* (5), 1078−1098.
(36) Gianti, E.; Zauhar, R. J. Modeling Androgen Receptor Flexibility: A Binding Mode Hypothesis of CYP17 Inhibitors/Antiandrogens for Prostate Cancer Therapy. *J. Chem. Inf. Model.* **2012**, *52* (10), 2670−2683.
(37) Clement, O. O.; Freeman, C. M.; Hartmann, R. W.; Handratta, V. D.; Vasaitis, T. S.; Brodie, A. M. H.; Njar, V. C. O. Three Dimensional Pharmacophore Modeling of Human CYP17 Inhibitors. Potential Agents for Prostate Cancer Therapy. *J. Med. Chem.* **2003**, *46* (12), 2345−2351.
(38) DeVore, N. M.; Scott, E. E. Structures of cytochrome P450 17A1 with prostate cancer drugs abiraterone and TOK-001. *Nature* **2012**, *482*, 116.
(39) Poulos, T. L.; Johnson, E. F., Structures of Cytochrome P450 Enzymes. In *Cytochrome P450: Structure, Mechanism, and Biochemistry*; Ortiz de Montellano, P. R., Ed.; Springer International Publishing: Cham, 2015; pp 3−32.
(40) Bonomo, S.; Jørgensen, F. S.; Olsen, L. Mechanism of Cytochrome P450 17A1-Catalyzed Hydroxylase and Lyase Reactions. *J. Chem. Inf. Model.* **2017**, *57* (5), 1123−1133.
(41) Xiao, F.; Song, X.; Tian, P.; Gan, M.; Verkhivker, G. M.; Hu, G. Comparative Dynamics and Functional Mechanisms of the CYP17A1 Tunnels Regulated by Ligand Binding. *J. Chem. Inf. Model.* **2020**, *60* (7), 3632−3647.
(42) Petrunak, E. M.; DeVore, N. M.; Porubsky, P. R.; Scott, E. E. Structures of Human Steroidogenic Cytochrome P450 17A1 with Substrates. *J. Biol. Chem.* **2014**, *289* (47), 32952−32964.
(43) Fehl, C.; Vogt, C. D.; Yadav, R.; Li, K.; Scott, E. E.; Aubé, J. Structure-Based Design of Inhibitors with Improved Selectivity for Steroidogenic Cytochrome P450 17A1 over Cytochrome P450 21A2. *J. Med. Chem.* **2018**, *61* (11), 4946−4960.
(44) Petrunak, E. M.; Rogers, S. A.; Aubé, J.; Scott, E. E. Structural and Functional Evaluation of Clinically Relevant Inhibitors of Steroidogenic Cytochrome P450 17A1. *Drug Metab. Dispos.* **2017**, *45* (6), 635−645.
(45) Burris-Hiday, S. D.; Scott, E. E. Steroidogenic cytochrome P450 17A1 structure and function. *Mol. Cell. Endocrinol.* **2021**, *528*, 111261.
(46) Yadav, R.; Petrunak, E. M.; Estrada, D. F.; Scott, E. E. Structural insights into the function of steroidogenic cytochrome P450 17A1. *Mol. Cell. Endocrinol.* **2017**, *441*, 68−75.
(47) Lee-Robichaud, P.; Akhtar, M. E.; Wright, J. N.; Sheikh, Q. I.; Akhtar, M. The cationic charges on Arg347, Arg358 and Arg449 of human cytochrome P450c17 (CYP17) are essential for the enzyme's cytochrome b5-dependent acyl-carbon cleavage activities. *J. Steroid Biochem. Mol. Biol.* **2004**, *92* (3), 119−30.
(48) Tiosano, D.; Knopf, C.; Koren, I.; Levanon, N.; Hartmann, M. F.; Hochberg, Z. e.; Wudy, S. A. Metabolic evidence for impaired 17α-hydroxylase activity in a kindred bearing the E305G mutation for isolate 17,20-lyase activity. *Eur. J. Endocrinol.* **2008**, *158* (3), 385−392.
(49) Gupta, M. K.; Geller, D. H.; Auchus, R. J. Pitfalls in Characterizing P450c17 Mutations Associated with Isolated 17,20-Lyase Deficiency. *J. Clin. Endocrinol. Metabolism* **2001**, *86* (9), 4416−4423.
(50) Kim, D.; Kim, V.; McCarty, K. D.; Guengerich, F. P. Tight binding of cytochrome b_5 to cytochrome P450 17A1 is a critical feature of stimulation of C21 steroid lyase activity and androgen synthesis. *J. Biol. Chem.* **2021**, *296*, 100571.
(51) Sevrioukova, I. F. Crystal Structure of CYP3A4 Complexed with Fluorol Identifies the Substrate Access Channel as a High-Affinity Ligand Binding Site. *Int. J. Mol. Sci.* **2022**, *23*, 12591.
(52) Miller, W. L. Minireview: Regulation of Steroidogenesis by Electron Transfer. *Endocrinology* **2005**, *146* (6), 2544−2550.
(53) Duggal, R.; Liu, Y.; Gregory, M. C.; Denisov, I. G.; Kincaid, J. R.; Sligar, S. G. Evidence that cytochrome b5 acts as a redox donor in CYP17A1 mediated androgen synthesis. *Biochem. Biophys. Res. Commun.* **2016**, *477* (2), 202−208.
(54) Tee, M. K.; Miller, W. L. Phosphorylation of Human Cytochrome P450c17 by p38α Selectively Increases 17,20 Lyase Activity and Androgen Biosynthesis*. *J. Biol. Chem.* **2013**, *288* (33), 23903−23913.
(55) Liu, Y.; Denisov, I. G.; Sligar, S. G.; Kincaid, J. R. Substrate-Specific Allosteric Effects on the Enhancement of CYP17A1 Lyase Efficiency by Cytochrome b5. *J. Am. Chem. Soc.* **2021**, *143* (10), 3729−3733.
(56) Estrada, D. F.; Laurence, J. S.; Scott, E. E. Cytochrome P450 17A1 Interactions with the FMN Domain of Its Reductase as Characterized by NMR*. *J. Biol. Chem.* **2016**, *291* (8), 3990−4003.
(57) Yablokov, E.; Florinskaya, A.; Medvedev, A.; Sergeev, G.; Strushkevich, N.; Luschik, A.; Shkel, T.; Haidukevich, I.; Gilep, A.; Usanov, S.; Ivanov, A. Thermodynamics of interactions between mammalian cytochromes P450 and b5. *Arch. Biochem. Biophys.* **2017**, *619*, 10−15.
(58) Estrada, D. F.; Laurence, J. S.; Scott, E. E. Substrate-modulated Cytochrome P450 17A1 and Cytochrome b5 Interactions Revealed by NMR. *J. Biol. Chem.* **2013**, *288* (23), 17008−17018.
(59) Peng, H.-M.; Liu, J.; Forsberg, S. E.; Tran, H. T.; Anderson, S. M.; Auchus, R. J. Catalytically Relevant Electrostatic Interactions of Cytochrome P450c17 (CYP17A1) and Cytochrome b5. *J. Biol. Chem.* **2014**, *289* (49), 33838−33849.
(60) Estrada, D. F.; Skinner, A. L.; Laurence, J. S.; Scott, E. E. Human Cytochrome P450 17A1 Conformational Selection: Modulation by Ligand and Cytochrome b5. *J. Biol. Chem.* **2014**, *289* (20), 14310−14320.
(61) Jeřábek, P.; Florián, J.; Martínek, V. Membrane-Anchored Cytochrome P450 1A2−Cytochrome b5 Complex Features an X-Shaped Contact between Antiparallel Transmembrane Helices. *Chem. Res. Toxicol.* **2016**, *29* (4), 626−636.
(62) Jumper, J.; Evans, R.; Pritzel, A.; Green, T.; Figurnov, M.; Ronneberger, O.; Tunyasuvunakool, K.; Bates, R.; Žídek, A.; Potapenko, A.; Bridgland, A.; Meyer, C.; Kohl, S. A. A.; Ballard, A. J.; Cowie, A.; Romera-Paredes, B.; Nikolov, S.; Jain, R.; Adler, J.; Back, T.; Petersen, S.; Reiman, D.; Clancy, E.; Zielinski, M.; Steinegger, M.; Pacholska, M.; Berghammer, T.; Bodenstein, S.; Silver, D.; Vinyals, O.; Senior, A. W.; Kavukcuoglu, K.; Kohli, P.; Hassabis, D. Highly accurate protein structure prediction with AlphaFold. *Nature* **2021**, *596* (7873), 583−589.
(63) Nelson, A. A.; Woodard, G. Severe adrenal cortical atrophy (cytotoxic) and hepatic damage produced in dogs by feeding 2,2-bis(parachlorophenyl)-1,1-dichloroethane (DDD or TDE). *Arch. Pathol. (Chic.)* **1949**, *48* (5), 387−94.
(64) Bencze, W. L.; Allen, M. J. Chemistry and Structure-Activity Relationships of Amphenone Analogues. *J. Med. Pharm. Chem.* **1959**, *1* (5), 395−406.
(65) Kahnt, F. W.; Neher, R. On the specific inhibition of adrenal steroid biosynthesis. *Experientia* **1962**, *18* (11), 499−501.
(66) Hall, P. F.; Eik-Nes, K. B.; Samuels, L. T. Influence of an Inhibitor of 17α-Hydroxylation on the Biosynthesis of Testosterone by Testicular Tissue. *Endocrinology* **1963**, *73* (5), 547−553.
(67) Neher, R.; Kahnt, F. W. On the biosynthesis of testicular steroids in vitro and its inhibition. *Experientia* **1965**, *21* (6), 310−312.

https://doi.org/10.1021/acs.jmedchem.3c00442
J. Med. Chem. 2023, 66, 6542−6566

(68) Goldman, A. S. Production of Hypospadias in the Rat by Selective Inhibition of Fetal Testicular 17α-Hydroxylase and C17−20-lyase. *Endocrinology* **1971**, *88* (2), 527−531.
(69) Gower, D. B. Modifiers of steroid-hormone metabolism: a review of their chemistry, biochemistry and clinical applications. *J. Steroid Biochem.* **1974**, *5* (5), 501−523.
(70) DeFelice, R.; Johnson, D. G.; Galgiani, J. N. Gynecomastia with Ketoconazole. *Antimicrob. Agents Chemother.* **1981**, *19* (6), 1073−1074.
(71) Pont, A.; Williams, P. L.; Loose, D. S.; Feldman, D.; Reitz, R. E.; Bochra, C.; Stevens, D. A. Ketoconazole Blocks Adrenal Steroid Synthesis. *Ann. Int. Med.* **1982**, *97* (3), 370−372.
(72) Leach, A. G.; Kidley, N. J. Quantitatively Interpreted Enhanced Inhibition of Cytochrome P450s by Heteroaromatic Rings Containing Nitrogen. *J. Chem. Inf. Model.* **2011**, *51* (5), 1048−1063.
(73) Guengerich, F. P.; McCarty, K. D.; Chapman, J. G.; Tateishi, Y. Stepwise binding of inhibitors to human cytochrome P450 17A1 and rapid kinetics of inhibition of androgen biosynthesis. *J. Biol. Chem.* **2021**, *297* (2), 100969.
(74) Jarman, M.; Barrie, S. E.; Deadman, J. J.; Houghton, J.; McCague, R.; Rowlands, M. G. Hydroxyperfluoroazobenzenes: novel inhibitors of enzymes of androgen biosynthesis. *J. Med. Chem.* **1990**, *33* (9), 2452−2455.
(75) McCague, R.; Rowlands, M. G.; Barrie, S. E.; Houghton, J. Inhibition of enzymes of estrogen and androgen biosynthesis by esters of 4-pyridylacetic acid. *J. Med. Chem.* **1990**, *33* (11), 3050−3055.
(76) Rowlands, M. G.; Barrie, S. E.; Chan, F.; Houghton, J.; Jarman, M.; McCague, R.; Potter, G. A. Esters of 3-Pyridylacetic Acid That Combine Potent Inhibition of 17.alpha.-Hydroxylase/C17,20-Lyase (Cytochrome P45017.alpha.) with Resistance to Esterase Hydrolysis. *J. Med. Chem.* **1995**, *38* (21), 4191−4197.
(77) Chan, F. C. Y.; Potter, G. A.; Barrie, S. E.; Haynes, B. P.; Rowlands, M. G.; Houghton, J.; Jarman, M. 3- and 4-Pyridylalkyl Adamantanecarboxylates: Inhibitors of Human Cytochrome P45017α (17α-Hydroxylase/C17,20-Lyase). Potential Nonsteroidal Agents for the Treatment of Prostatic Cancer. *J. Med. Chem.* **1996**, *39* (17), 3319−3323.
(78) Owen, C. P.; Dhanani, S.; Patel, C. H.; Shahid, I.; Ahmed, S. Synthesis and biochemical evaluation of a range of potent benzyl imidazole-based compounds as potential inhibitors of the enzyme complex 17α-hydroxylase/17,20-lyase (P45017α). *Bioorg. Med. Chem. Lett.* **2006**, *16* (15), 4011−4015.
(79) Patel, C. H.; Dhanani, S.; Owen, C. P.; Ahmed, S. Synthesis, biochemical evaluation and rationalisation of the inhibitory activity of a range of 4-substituted phenyl alkyl imidazole-based inhibitors of the enzyme complex 17α-hydroxylase/17,20-lyase (P45017α). *Bioorg. Med. Chem. Lett.* **2006**, *16* (18), 4752−4756.
(80) Owen, C. P.; Shahid, I.; Olusanjo, M. S.; Patel, C. H.; Dhanani, S.; Ahmed, S. Synthesis, biochemical evaluation and rationalisation of the inhibitory activity of a range of phenyl alkyl imidazole-based compounds as potent inhibitors of the enzyme complex 17α-hydroxylase/17,20-lyase (P45017α). *J. Steroid Biochem. Mol. Biol.* **2008**, *111* (1), 117−127.
(81) Shahid, I.; Patel, C. H.; Dhanani, S.; Owen, C. P.; Ahmed, S. Synthesis, biochemical evaluation of a range of potent 4-substituted phenyl alkyl imidazole-based inhibitors of the enzyme complex 17α-Hydroxylase/17,20-Lyase (P45017α). *J. Steroid Biochem. Mol. Biol.* **2008**, *110* (1), 18−29.
(82) Ahmed, S.; Shahid, I.; Dhanani, S.; Owen, C. P. Synthesis and biochemical evaluation of a range of sulfonated derivatives of 4-hydroxybenzyl imidazole as highly potent inhibitors of rat testicular 17α-hydroxylase/17,20-lyase (P-45017α). *Bioorg. Med. Chem. Lett.* **2009**, *19* (16), 4698−4701.
(83) Owen, C. P.; Shahid, I.; Lee, W.-Y.; Ahmed, S. Synthesis and biochemical evaluation of a range of (4-substituted phenyl)sulfonate derivatives of 4-hydroxybenzyl imidazole-based compounds as potent inhibitors of 17α-hydroxylase/17,20-lyase (P45017α) derived from rat testicular microsomes. *Bioorg. Med. Chem. Lett.* **2010**, *20* (17), 5345−5348.
(84) Matsunaga, N.; Kaku, T.; Itoh, F.; Tanaka, T.; Hara, T.; Miki, H.; Iwasaki, M.; Aono, T.; Yamaoka, M.; Kusaka, M.; Tasaka, A. C17,20-Lyase inhibitors I. Structure-based de novo design and SAR study of C17,20-lyase inhibitors. *Bioorg. Med. Chem.* **2004**, *12* (9), 2251−2273.
(85) Blass, B. E.; Iyer, P.; Abou-Gharbia, M.; Childers, W. E.; Gordon, J. C.; Ramanjulu, M.; Morton, G.; Arumugam, P.; Boruwa, J.; Ellingboe, J.; Mitra, S.; Reddy Nimmareddy, R.; Paliwal, S.; Rajasekhar, J.; Shivakumar, S.; Srivastava, P.; Tangirala, R. S.; Venkataramanaiah, K.; Bobbala, R.; Yanamandra, M.; Krishnakanth Reddy, L. Design and synthesis of functionalized piperazin-1yl-(E)-stilbenes as inhibitors of 17α-hydroxylase-C17,20-lyase (Cyp17). *Bioorg. Med. Chem. Lett.* **2018**, *28* (13), 2270−2274.
(86) Reis, L. O.; Zani, E. L.; García-Perdomo, H. A. Estrogen therapy in patients with prostate cancer: a contemporary systematic review. *Int. Urol. Nephrol.* **2018**, *50* (6), 993−1003.
(87) Al-Soud, Y. A.; Heydel, M.; Hartmann, R. W. Design and synthesis of 1,3,5-trisubstituted 1,2,4-triazoles as CYP enzyme inhibitors. *Tetrahedron Lett.* **2011**, *52* (48), 6372−6375.
(88) Emmerich, J.; van Koppen, C. J.; Burkhart, J. L.; Engeli, R. T.; Hu, Q.; Odermatt, A.; Hartmann, R. W. Accelerated skin wound healing by selective 11β-Hydroxylase (CYP11B1) inhibitors. *Eur. J. Med. Chem.* **2018**, *143*, 591−597.
(89) Bonomo, S.; Hansen, C. H.; Petrunak, E. M.; Scott, E. E.; Styrishave, B.; Jørgensen, F. S.; Olsen, L. Promising Tools in Prostate Cancer Research: Selective Non-Steroidal Cytochrome P450 17A1 Inhibitors. *Sci. Rep.* **2016**, *6*, 29468.
(90) Wróbel, T. M.; Rogova, O.; Andersen, K. L.; Yadav, R.; Brixius-Anderko, S.; Scott, E. E.; Olsen, L.; Jørgensen, F. S.; Björkling, F. Discovery of Novel Non-Steroidal Cytochrome P450 17A1 Inhibitors as Potential Prostate Cancer Agents. *Int. J. Mol. Sci.* **2020**, *21* (14), 4868.
(91) Wróbel, T. M.; Rogova, O.; Sharma, K.; Rojas Velazquez, M. N.; Pandey, A. V.; Jørgensen, F. S.; Arendrup, F. S.; Andersen, K. L.; Björkling, F. Synthesis and Structure-Activity Relationships of Novel Non-Steroidal CYP17A1 Inhibitors as Potential Prostate Cancer Agents. *Biomolecules* **2022**, *12* (2), 165.
(92) Wermuth, C. G. Selective optimization of side activities: the SOSA approach. *Drug Discovery Today* **2006**, *11* (3), 160−164.
(93) Blass, B. E.; Iyer, P.; Abou-Gharbia, M.; Childers, W. E.; Gordon, J. C.; Ramanjulu, M.; Morton, G.; Arumugam, P.; Boruwa, J.; Ellingboe, J.; Mitra, S.; Nimmareddy, R. R.; Paliwal, S.; Rajasekhar, J.; Shivakumar, S.; Srivastava, P.; Tangirala, R. S.; Venkataramanaiah, K.; Yanamandra, M. Design, synthesis, and evaluation of (2S,4R)-Ketoconazole sulfonamide analogs as potential treatments for Metabolic Syndrome. *Bioorg. Med. Chem. Lett.* **2016**, *26* (23), 5825−5829.
(94) Rao, N. S.; Tolcher, A. W.; Papadopoulos, K. P.; Rasco, D. W.; Haas, N. B.; Pantuck, A. J.; Denis, L. J.; Dreicer, R. ASN001, a novel CYP17 lyase inhibitor, in men with metastatic castration-resistant prostate cancer (mCRPC): Safety/tolerability and early activity in a multicenter phase 1/2 trial. *J. Clin. Oncol.* **2016**, *34* (15_suppl), e14129−e14129.
(95) Al-Hamrouni, A. M.; Ahmadi, M.; Nicholls, P. J.; Smith, H. J.; Lombardi, P.; Pestellini, V. 1-[(Benzofuran-2-yl) phenylmethyl] Imidazoles as Inhibitors of 17α-Hydroxylase: 17, 20-lyase (P450 17): Species and Tissue Differences. *Pharmacy Pharmacol. Commun.* **1997**, *3* (5-6), 259−263.
(96) Bahshwan, S. A.; Owen, C. P.; Nicholls, P. J.; Smith, H. J.; Ahmadi, M. Med. Chemistry: Some 1-[(Benzofuran-2-yl)methyl]-imidazoles as Inhibitors of 17α-Hydroxylase:17, 20-lyase (P450 17) and Their Specificity Patterns. *J. Pharm. Pharmacol.* **2011**, *50* (10), 1109−1116.
(97) Wang, M.; Fang, Y.; Gu, S.; Chen, F.; Zhu, Z.; Sun, X.; Zhu, J. Discovery of novel 1,2,3,4-tetrahydrobenzo[4, 5]thieno[2, 3-c]pyridine derivatives as potent and selective CYP17 inhibitors. *Eur. J. Med. Chem.* **2017**, *132*, 157−172.
(98) Ideyama, Y.; Kudoh, M.; Tanimoto, K.; Susaki, Y.; Nanya, T.; Nakahara, T.; Ishikawa, H.; Yoden, T.; Okada, M.; Fujikura, T.; Akaza, H.; Shikama, H. Novel nonsteroidal inhibitor of cytochrome P45017α (17α-hydroxylase/C17−20 lyase), YM116, decreased prostatic weights

https://doi.org/10.1021/acs.jmedchem.3c00442
J. Med. Chem. 2023, 66, 6542−6566

by reducing serum concentrations of testosterone and adrenal androgens in rats. *Prostate* **1998**, *37* (1), 10−18.
(99) Khalil, N. A.; Ahmed, E. M.; Zaher, A. F.; Sobh, E. A.; El-Sebaey, S. A.; El-Zoghbi, M. S. New benzothieno[2,3-c]pyridines as non-steroidal CYP17 inhibitors: design, synthesis, anticancer screening, apoptosis induction, and in silico ADME profile studies. *J. Enzyme Inhibition Med. Chem.* **2021**, *36* (1), 1839−1859.
(100) Huang, A.; Jayaraman, L.; Fura, A.; Vite, G. D.; Trainor, G. L.; Gottardis, M. M.; Spires, T. E.; Spires, V. M.; Rizzo, C. A.; Obermeier, M. T.; Elzinga, P. A.; Todderud, G.; Fan, Y.; Newitt, J. A.; Beyer, S. M.; Zhu, Y.; Warrack, B. M.; Goodenough, A. K.; Tebben, A. J.; Doweyko, A. M.; Gold, D. L.; Balog, A. Discovery of the Selective CYP17A1 Lyase Inhibitor BMS-351 for the Treatment of Prostate Cancer. *ACS Med. Chem. Lett.* **2016**, *7* (1), 40−45.
(101) Padmakar Darne, C.; Velaparthi, U.; Saulnier, M.; Frennesson, D.; Liu, P.; Huang, A.; Tokarski, J.; Fura, A.; Spires, T.; Newitt, J.; Spires, V. M.; Obermeier, M. T.; Elzinga, P. A.; Gottardis, M. M.; Jayaraman, L.; Vite, G. D.; Balog, A. The discovery of BMS-737 as a potent, CYP17 lyase-selective inhibitor for the treatment of castration-resistant prostate cancer. *Bioorg. Med. Chem. Lett.* **2022**, *75*, 128951.
(102) Recanatini, M.; Bisi, A.; Cavalli, A.; Belluti, F.; Gobbi, S.; Rampa, A.; Valenti, P.; Palzer, M.; Palusczak, A.; Hartmann, R. W. A New Class of Nonsteroidal Aromatase Inhibitors: Design and Synthesis of Chromone and Xanthone Derivatives and Inhibition of the P450 Enzymes Aromatase and 17α-Hydroxylase/C17,20-Lyase. *J. Med. Chem.* **2001**, *44* (5), 672−680.
(103) Stefanachi, A.; Favia, A. D.; Nicolotti, O.; Leonetti, F.; Pisani, L.; Catto, M.; Zimmer, C.; Hartmann, R. W.; Carotti, A. Design, Synthesis, and Biological Evaluation of Imidazolyl Derivatives of 4,7-Disubstituted Coumarins as Aromatase Inhibitors Selective over 17-α-Hydroxylase/C17−20 Lyase. *J. Med. Chem.* **2011**, *54* (6), 1613−1625.
(104) Abadi, A. H.; Abou-Seri, S. M.; Hu, Q.; Negri, M.; Hartmann, R. W. Synthesis and biological evaluation of imidazolylmethylacridones as cytochrome P-450 enzymes inhibitors. *MedChemComm* **2012**, *3* (6), 663−666.
(105) Yin, L.; Lucas, S.; Maurer, F.; Kazmaier, U.; Hu, Q.; Hartmann, R. W. Novel Imidazol-1-ylmethyl Substituted 1,2,5,6-Tetrahydropyrrolo[3,2,1-ij]quinolin-4-ones as Potent and Selective CYP11B1 Inhibitors for the Treatment of Cushing's Syndrome. *J. Med. Chem.* **2012**, *55* (14), 6629−6633.
(106) Bossche, H. V.; Willemsens, G.; Bellens, D.; Roels, I.; Janssen, P. A. J. From 14α-demethylase inhibitors in fungal cells to androgen and oestrogen biosynthesis inhibitors in mammalian cells. *Biochem. Soc. Trans.* **1990**, *18* (1), 10−13.
(107) Bruynseels, J.; De Coster, R.; Van Rooy, P.; Wouters, W.; Coene, M.-C.; Snoeck, E.; Raeymaekers, A.; Freyne, E.; Sanz, G.; Vanden Bussche, G.; Vanden Bossche, H.; Willemsens, G.; Janssen, P. A. J. R 75251, a new inhibitor of steroid biosynthesis. *Prostate* **1990**, *16* (4), 345−357.
(108) Thomas, A. G.; Henry, J. J. Retinoic acid regulation by CYP26 in vertebrate lens regeneration. *Dev. Biol.* **2014**, *386* (2), 291−301.
(109) Wachall, B. G.; Hector, M.; Zhuang, Y.; Hartmann, R. W. Imidazole substituted biphenyls: A new class of highly potent and in vivo active inhibitors of P450 17 as potential therapeutics for treatment of prostate cancer. *Bioorg. Med. Chem.* **1999**, *7* (9), 1913−1924.
(110) Hutschenreuter, T. U.; Ehmer, P. B.; Hartmann, R. W. Synthesis of Hydroxy Derivatives of Highly Potent Non-steroidal CYP 17 Inhibitors as Potential Metabolites and Evaluation of their Activity by a Non Cellular Assay using Recombinant Human Enzyme. *J. Enzyme Inhibition Medicinal Chem.* **2004**, *19* (1), 17−32.
(111) Leroux, F.; Hutschenreuter, T. U.; Charrière, C.; Scopelliti, R.; Hartmann, R. W. N-(4-Biphenylmethyl)imidazoles as Potential Therapeutics for the Treatment of Prostate Cancer: Metabolic Robustness Due to Fluorine Substitution? *Helv. Chim. Acta* **2003**, *86* (7), 2671−2686.
(112) Hu, Q.; Negri, M.; Olgen, S.; Hartmann, R. W. The Role of Fluorine Substitution in Biphenyl Methylene Imidazole-Type CYP17 Inhibitors for the Treatment of Prostate Carcinoma. *ChemMedChem.* **2010**, *5* (6), 899−910.
(113) Johnson, B. M.; Shu, Y.-Z.; Zhuo, X.; Meanwell, N. A. Metabolic and Pharmaceutical Aspects of Fluorinated Compounds. *J. Med. Chem.* **2020**, *63* (12), 6315−6386.
(114) Zhuang, Y.; Wachall, B. G.; Hartmann, R. W. Novel imidazolyl and triazolyl substituted biphenyl compounds: synthesis and evaluation as nonsteroidal inhibitors of human 17α-hydroxylase-C17, 20-Lyase (P450 17). *Bioorg. Med. Chem.* **2000**, *8* (6), 1245−1252.
(115) Hu, Q.; Yin, L.; Jagusch, C.; Hille, U. E.; Hartmann, R. W. Isopropylidene Substitution Increases Activity and Selectivity of Biphenylmethylene 4-Pyridine Type CYP17 Inhibitors. *J. Med. Chem.* **2010**, *53* (13), 5049−5053.
(116) Hille, U. E.; Hu, Q.; Vock, C.; Negri, M.; Bartels, M.; Müller-Vieira, U.; Lauterbach, T.; Hartmann, R. W. Novel CYP17 inhibitors: Synthesis, biological evaluation, structure−activity relationships and modelling of methoxy- and hydroxy-substituted methyleneimidazolyl biphenyls. *Eur. J. Med. Chem.* **2009**, *44* (7), 2765−2775.
(117) Hu, Q.; Negri, M.; Jahn-Hoffmann, K.; Zhuang, Y.; Olgen, S.; Bartels, M.; Müller-Vieira, U.; Lauterbach, T.; Hartmann, R. W. Synthesis, biological evaluation, and molecular modeling studies of methylene imidazole substituted biaryls as inhibitors of human 17α-hydroxylase-17,20-lyase (CYP17)—Part II: Core rigidification and influence of substituents at the methylene bridge. *Bioorg. Med. Chem.* **2008**, *16* (16), 7715−7727.
(118) Jagusch, C.; Negri, M.; Hille, U. E.; Hu, Q.; Bartels, M.; Jahn-Hoffmann, K.; Mendieta, M. A.E. P.-B.; Rodenwaldt, B.; Muller-Vieira, U.; Schmidt, D. Synthesis, biological evaluation and molecular modelling studies of methyleneimidazole substituted biaryls as inhibitors of human 17α-hydroxylase-17,20-lyase (CYP17). Part I: Heterocyclic modifications of the core structure. *Bioorg. Med. Chem.* **2008**, *16* (4), 1992−2010.
(119) Pinto-Bazurco Mendieta, M. A. E.; Negri, M.; Jagusch, C.; Hille, U. E.; Müller-Vieira, U.; Schmidt, D.; Hansen, K.; Hartmann, R. W. Synthesis, biological evaluation and molecular modelling studies of novel ACD- and ABD-ring steroidomimetics as inhibitors of CYP17. *Bioorg. Med. Chem. Lett.* **2008**, *18* (1), 267−273.
(120) Pinto-Bazurco Mendieta, M. A. E.; Negri, M.; Hu, Q.; Hille, U. E.; Jagusch, C.; Jahn-Hoffmann, K.; Müller-Vieira, U.; Schmidt, D.; Lauterbach, T.; Hartmann, R. W. CYP17 Inhibitors. Annulations of Additional Rings in Methylene Imidazole Substituted Biphenyls: Synthesis, Biological Evaluation and Molecular Modelling. *Arch. Pharmazie* **2008**, *341* (10), 597−609.
(121) Pinto-Bazurco Mendieta, M. A. E.; Negri, M.; Jagusch, C.; Müller-Vieira, U.; Lauterbach, T.; Hartmann, R. W. Synthesis, Biological Evaluation, and Molecular Modeling of Abiraterone Analogues: Novel CYP17 Inhibitors for the Treatment of Prostate Cancer. *J. Med. Chem.* **2008**, *51* (16), 5009−5018.
(122) Hu, Q.; Jagusch, C.; Hille, U. E.; Haupenthal, J.; Hartmann, R. W. Replacement of Imidazolyl by Pyridyl in Biphenylmethylenes Results in Selective CYP17 and Dual CYP17/CYP11B1 Inhibitors for the Treatment of Prostate Cancer. *J. Med. Chem.* **2010**, *53* (15), 5749−5758.
(123) Kaku, T.; Tsujimoto, S.; Matsunaga, N.; Tanaka, T.; Hara, T.; Yamaoka, M.; Kusaka, M.; Tasaka, A. 17,20-Lyase inhibitors. Part 3: Design, synthesis, and structure−activity relationships of biphenylylmethylimidazole derivatives as novel 17,20-lyase inhibitors. *Bioorg. Med. Chem.* **2011**, *19* (7), 2428−2442.
(124) Sergejew, T.; Hartmann, R. W. Pyridyl Substituted Benzocycloalkenes: New Inhibitors of 17α-Hydroxylase/ 17,20-Lyase (P450 17α). *J. Enzyme Inhibition* **1994**, *8* (2), 113−122.
(125) Nakajin, S.; Shively, J.; Yuan, P.-M.; Hall, P. F. Microsomal cytochrome P-450 from neonatal pig testis: two enzymic activities (17.alpha.-hydroxalase and C17,20 associated with one protein. *Biochemistry* **1981**, *20* (14), 4037−4042.
(126) Hartmann, R. W.; Bayer, H.; Gruen, G.; Sergejew, T.; Bartz, U.; Mitrenga, M. Pyridyl-Substituted Tetrahydrocyclopropa[a]-naphthalenes: Highly Active and Selective Inhibitors of P450 arom. *J. Med. Chem.* **1995**, *38* (12), 2103−2111.
(127) Wächter, G. A.; Hartmann, R. W.; Sergejew, T.; Grün, G. L.; Ledergerber, D. Tetrahydronaphthalenes: Influence of Heterocyclic

https://doi.org/10.1021/acs.jmedchem.3c00442
J. Med. Chem. 2023, 66, 6542−6566

Substituents on Inhibition of Steroidogenic Enzymes P450 arom and P450 17. *J. Med. Chem.* **1996**, *39* (4), 834−841.
(128) Hartmann, R. W.; Wächter, G. A.; Sergejew, T.; Würtz, R.; Düerkop, J. 4,5-Dihydro-3-(2-pyrazinyl)naphtho[1,2-c]pyrazole: A Potent and Selective Inhibitor of Steroid-17α-Hydroxylase-C17,20-Lyase (P450 17). *Arch. Pharmazie* **1995**, *328* (7−8), 573−575.
(129) Voets, M.; Antes, I.; Scherer, C.; Müller-Vieira, U.; Biemel, K.; Barassin, C.; Marchais-Oberwinkler, S.; Hartmann, R. W. Heteroaryl-Substituted Naphthalenes and Structurally Modified Derivatives: Selective Inhibitors of CYP11B2 for the Treatment of Congestive Heart Failure and Myocardial Fibrosis. *J. Med. Chem.* **2005**, *48* (21), 6632−6642.
(130) Hille, U. E.; Hu, Q.; Pinto-Bazurco Mendieta, M. A. E.; Bartels, M.; Vock, C. A.; Lauterbach, T.; Hartmann, R. W. Steroidogenic cytochrome P450 (CYP) enzymes as drug targets: Combining substructures of known CYP inhibitors leads to compounds with different inhibitory profile. *Comptes Rendus Chimie* **2009**, *12* (10), 1117−1126.
(131) Pinto-Bazurco Mendieta, M. A. E.; Hu, Q.; Engel, M.; Hartmann, R. W. Highly Potent and Selective Nonsteroidal Dual Inhibitors of CYP17/CYP11B2 for the Treatment of Prostate Cancer To Reduce Risks of Cardiovascular Diseases. *J. Med. Chem.* **2013**, *56* (15), 6101−6107.
(132) Hartmann, R. W.; Frotscher, M.; Ledergerber, D.; Wächter, G. A.; Grün, G. L.; Sergejew, T. F. Synthesis and Evaluation of Azole-Substituted Tetrahydronaphthalenes as Inhibitors of P450 arom, P450 17, and P450 TxA2. *Arch. Pharmazie* **1996**, *329* (5), 251−261.
(133) Zhuang, Y.; Zapp, J.; Hartmann, R. W. Synthesis of Z- and E-1-Methyl-2-(1-hydroximinoethyl)-6-methoxy-3,4-dihydronaphthalene and Evaluation as Inhibitors of 17α-Hydroxylase-C17,20-Lyase (P450 17). *Arch. Pharmazie* **1997**, *330* (11), 359−361.
(134) Zhuang, Y.; Hartmann, R. W. Synthesis of Novel Oximes of 2-Aryl-6-methoxy-3,4-dihydronaphthalene and Their Evaluation as Inhibitors of 17α-Hydroxylase-C17,20-Lyase (P450 17). *Arch. Pharmazie* **1998**, *331* (1), 36−40.
(135) Zhuang, Y.; Hartmann, R. W. Synthesis and Evaluation of Azole-substituted 2-Aryl-6-methoxy-3,4-dihydronaphthalenes and -naphthalenes as Inhibitors of 17α-Hydroxylase-C17,20-Lyase (P450 17. *Arch. Pharmazie* **1999**, *332* (1), 25−30.
(136) Matsunaga, N.; Kaku, T.; Ojida, A.; Tanaka, T.; Hara, T.; Yamaoka, M.; Kusaka, M.; Tasaka, A. C17,20-lyase inhibitors. Part 2: Design, synthesis and structure−activity relationships of (2-naphthylmethyl)-1H-imidazoles as novel C17,20-lyase inhibitors. *Bioorg. Med. Chem.* **2004**, *12* (16), 4313−4336.
(137) Kaku, T.; Matsunaga, N.; Ojida, A.; Tanaka, T.; Hara, T.; Yamaoka, M.; Kusaka, M.; Tasaka, A. 17,20-Lyase inhibitors. Part 4: Design, synthesis and structure−activity relationships of naphthylmethylimidazole derivatives as novel 17,20-lyase inhibitors. *Bioorg. Med. Chem.* **2011**, *19* (5), 1751−1770.
(138) Kaku, T.; Hitaka, T.; Ojida, A.; Matsunaga, N.; Adachi, M.; Tanaka, T.; Hara, T.; Yamaoka, M.; Kusaka, M.; Okuda, T.; Asahi, S.; Furuya, S.; Tasaka, A. Discovery of orteronel (TAK-700), a naphthylmethylimidazole derivative, as a highly selective 17,20-lyase inhibitor with potential utility in the treatment of prostate cancer. *Bioorg. Med. Chem.* **2011**, *19* (21), 6383−6399.
(139) Rafferty, S. W.; Eisner, J. R.; Moore, W. R.; Schotzinger, R. J.; Hoekstra, W. J. Highly-selective 4-(1,2,3-triazole)-based P450c17a 17,20-lyase inhibitors. *Bioorg. Med. Chem. Lett.* **2014**, *24* (11), 2444−2447.
(140) Kimura, K.-i.; Itakura, Y.; Goto, R.; Tojima, M.; Egawa, N.; Yoshihama, M. Inhibition of 17α-Hydroxylase/C17,20-Lyase (CYP17) from Rat Testis by Green Tea Catechins and Black Tea Theaflavins. *Biosci., Biotechnol., Biochem.* **2007**, *71* (9), 2325−2328.
(141) Castaño, P. R.; Parween, S.; Pandey, A. V. Bioactivity of Curcumin on the Cytochrome P450 Enzymes of the Steroidogenic Pathway. *Int. J. Mol. Sci.* **2019**, *20* (18), 4606.
(142) Rainey, W. E.; Saner, K.; Schimmer, B. P. Adrenocortical cell lines. *Mol. Cell. Endocrinol.* **2004**, *228* (1), 23−38.
(143) Gazdar, A. F.; Oie, H. K.; Shackleton, C. H.; Chen, T. R.; Triche, T. J.; Myers, C. E.; Chrousos, G. P.; Brennan, M. F.; Stein, C. A.; La Rocca, R. V. Establishment and Characterization of a Human Adrenocortical Carcinoma Cell Line That Expresses Multiple Pathways of Steroid Biosynthesis1. *Cancer Res.* **1990**, *50* (17), 5488−5496.
(144) Rodriguez, H.; Hum, D. W.; Staels, B.; Miller, W. L. Transcription of the Human Genes for Cytochrome P450scc and P450c17 Is Regulated Differently in Human Adrenal NCI-H295 Cells Than in Mouse Adrenal Y1 Cells. *J. Clin. Endocrinol. Metabolism* **1997**, *82* (2), 365−371.
(145) Cloutier, M.; Fleury, A.; Courtemanche, J.; Ducharme, L.; Mason, J. I.; Lehoux, J.-G. Characterization of the Adrenal Cytochrome P450C17 in the Hamster, a Small Animal Model for the Study of Adrenal Dehydroepiandrosterone Biosynthesis. *DNA Cell Biol.* **1997**, *16* (3), 357−368.
(146) Hamilton, J. B. Androgenic Activity Per Milligram of Colorimetrically Measured Ketosteroids in Urine: an Index of the Respective Contributions from Testicular and Extra-Testicular Sources. *J. Clin. Endocrinol. Metabolism* **1954**, *14* (4), 452−471.
(147) Lynn, W. S.; Brown, R. H. the Conversion of Progesterone to Androgens by Testes. *J. Biol. Chem.* **1958**, *232* (2), 1015−1030.
(148) Kreutzmann, D. J.; Silink, M.; Cam, G. R. Celite multi-column chromatography for the simultaneous separation of progesterone, deoxycorticosterone and 17α-hydroxyprogesterone from small plasma or tissue samples. *J. Chromatogr. B: Biomed. Sci. Appl.* **1982**, *228*, 95−101.
(149) Gandy, H. M.; Peterson, R. E. Measurement of Testosterone and 17-Ketosteroids in Plasma by the Double Isotope Dilution Derivative Technique1. *J. Clin. Endocrinol. Metabolism* **1968**, *28* (7), 949−977.
(150) Milewicz, A.; Vecsei, P.; Korth-Schütz, S.; Haack, D.; Rösler, A.; Lichtwald, K.; Lewicka, S.; Mittelstaedt, G. v. Development of plasma 21-deoxycortisol radioimmunoassay and application to the diagnosis of patients with 21-hydroxylase deficiency. *J. Steroid Biochem.* **1984**, *21* (2), 185−191.
(151) Riepe, F. G.; Wonka, S.; Partsch, C. J.; Sippell, W. G. Automated chromatographic system for the simultaneous measurement of plasma pregnenolone and 17-hydroxypregnenolone by radioimmunoassay. *J. Chromatogr. B: Biomed. Sci. Appl.* **2001**, *763* (1), 99−106.
(152) Morineau, G.; Gosling, J.; Patricot, M.-C.; Soliman, H.; Boudou, P.; Halnak, A. A.; Le Brun, G. l.; Brérault, J.-L.; Julien, R.; Villette, J.-M.; Fiet, J. Convenient chromatographic prepurification step before measurement of urinary cortisol by radioimmunoassay. *Clin. Chem.* **1997**, *43* (5), 786−793.
(153) Abraham, G. E. Radioimmunoassay of steroids in biological fluids. *J. Steroid Biochem.* **1975**, *6* (3), 261−270.
(154) Schatzman, G. L.; Laughlin, M. E.; Blohm, T. R. A normal phase high-performance liquid chromatography system for steroid 17α-hydroxylaseC17−20 lyase (cytochrome P-45021SCC) assays. *Anal. Biochem.* **1988**, *175* (1), 219−226.
(155) Potter, G. A.; Barrie, S. E.; Jarman, M.; Rowlands, M. G. Novel Steroidal Inhibitors of Human Cytochrome P45017.alpha.-Hydroxylase-C17,20-lyase): Potential Agents for the Treatment of Prostatic Cancer. *J. Med. Chem.* **1995**, *38* (13), 2463−2471.
(156) Imai, T.; Globerman, H.; Gertner, J. M.; Kagawa, N.; Waterman, M. R. Expression and purification of functional human 17 alpha-hydroxylase/17,20-lyase (P450c17) in Escherichia coli. Use of this system for study of a novel form of combined 17 alpha-hydroxylase/17,20-lyase deficiency. *J. Biol. Chem.* **1993**, *268* (26), 19681−19689.
(157) Shibata, M.; Sakaki, T.; Yabusaki, Y.; Murakami, H.; Ohkawa, H. Genetically Engineered P450 Monooxygenases: Construction of Bovine P450c17/Yeast Reductase Fused Enzymes. *DNA Cell Biol.* **1990**, *9* (1), 27−36.
(158) Kuwada, M.; Sone, Y.; Kitajima, R. Purification from Adult Pig Testicular P-450 and 17α-Hydroxylase Activity of P-450 Containing Liposomal Membranes. *Biochem. Biophys. Res. Commun.* **1993**, *196* (2), 816−824.

https://doi.org/10.1021/acs.jmedchem.3c00442
J. Med. Chem. 2023, 66, 6542−6566

(159) Wudy, S. A.; Wachter, U. A.; Homoki, J.; Teller, W. M.; Shackleton, C. H. L. Androgen metabolism assessment by routine gas chromatography/mass spectrometry profiling of plasma steroids: part 1, unconjugated steroids. *Steroids* **1992**, *57* (7), 319−324.
(160) Wudy, S. A.; Wachter, U. A.; Homoki, J.; Teller, W. M. Determination of Dehydroepiandrosterone Sulfate in Human Plasma by Gas Chromatography/ Mass Spectrometry Using a Deuterated Internal Standard: A Method Suitable for Routine Clinical Use. *Hormone Res. Paediatrics* **1993**, *39* (5−6), 235−240.
(161) Gallagher, L. M.; Owen, L. J.; Keevil, B. G. Simultaneous determination of androstenedione and testosterone in human serum by liquid chromatography-tandem mass spectrometry. *Ann. Clin. Biochem.* **2007**, *44* (1), 48−56.
(162) Shiraishi, S.; Lee, P. W. N.; Leung, A.; Goh, V. H. H.; Swerdloff, R. S.; Wang, C. Simultaneous Measurement of Serum Testosterone and Dihydrotestosterone by Liquid Chromatography−Tandem Mass Spectrometry. *Clin. Chem.* **2008**, *54* (11), 1855−1863.
(163) Caulfield, M. P.; Lynn, T.; Gottschalk, M. E.; Jones, K. L.; Taylor, N. F.; Malunowicz, E. M.; Shackleton, C. H. L.; Reitz, R. E.; Fisher, D. A. The Diagnosis of Congenital Adrenal Hyperplasia in the Newborn by Gas Chromatography/Mass Spectrometry Analysis of Random Urine Specimens. *J. Clin. Endocrinol. Metabolism* **2002**, *87* (8), 3682−3690.
(164) Honour, J. W. Urinary steroid profile analysis. *Clin. Chim. Acta* **2001**, *313* (1), 45−50.
(165) McDonald, J. G.; Matthew, S.; Auchus, R. J. Steroid Profiling by Gas Chromatography−Mass Spectrometry and High Performance Liquid Chromatography−Mass Spectrometry for Adrenal Diseases. *Hormones Cancer* **2011**, *2* (6), 324−332.
(166) Kempná, P.; Hirsch, A.; Hofer, G.; Mullis, P. E.; Flück, C. E. Impact of Differential P450c17 Phosphorylation by cAMP Stimulation and by Starvation Conditions on Enzyme Activities and Androgen Production in NCI-H295R Cells. *Endocrinology* **2010**, *151* (8), 3686−3696.
(167) Zhao, L.; Sun, N.; Tian, L.; Zhao, S.; Sun, B.; Sun, Y.; Zhao, D. Strategies for the development of highly selective cytochrome P450 inhibitors: Several CYP targets in current research. *Bioorg. Med. Chem. Lett.* **2019**, *29* (16), 2016−2024.
(168) Parr, B. T.; Pastor, R.; Sellers, B. D.; Pei, Z.; Jaipuri, F. A.; Castanedo, G. M.; Gazzard, L.; Kumar, S.; Li, X.; Liu, W.; Mendonca, R.; Pavana, R. K.; Potturi, H.; Shao, C.; Velvadapu, V.; Waldo, J. P.; Wu, G.; Yuen, P.-w.; Zhang, Z.; Zhang, Y.; Harris, S. F.; Oh, A. J.; DiPasquale, A.; Dement, K.; La, H.; Goon, L.; Gustafson, A.; VanderPorten, E. C.; Mautino, M. R.; Liu, Y. Implementation of the CYP Index for the Design of Selective Tryptophan-2,3-dioxygenase Inhibitors. *ACS Med. Chem. Lett.* **2020**, *11* (4), 541−549.
(169) Wang, T.; Pulkkinen, O. I.; Aittokallio, T. Target-specific compound selectivity for multi-target drug discovery and repurposing. *Front. Pharmacol.* **2022**, *13*, 1003480.
(170) Danel, T.; Wojtuch, A.; Podlewska, S. Generation of new inhibitors of selected cytochrome P450 subtypes- In silico study. *Comput. Struct. Biotechnol. J.* **2022**, *20*, 5639−5651.
(171) Bird, I. M.; Abbott, D. H. The hunt for a selective 17,20 lyase inhibitor; learning lessons from nature. *J. Steroid Biochem. Mol. Biol.* **2016**, *163*, 136−146.
(172) Liu, Y.; Denisov, I.; Gregory, M.; Sligar, S. G.; Kincaid, J. R. Importance of Asparagine 202 in Manipulating Active Site Structure and Substrate Preference for Human CYP17A1. *Biochemistry* **2022**, *61* (7), 583−594.
(173) Fernández-Cancio, M.; Camats, N.; Flück, C. E.; Zalewski, A.; Dick, B.; Frey, B. M.; Monné, R.; Torán, N.; Audí, L.; Pandey, A. V. Mechanism of the Dual Activities of Human CYP17A1 and Binding to Anti-Prostate Cancer Drug Abiraterone Revealed by a Novel V366M Mutation Causing 17,20 Lyase Deficiency. *Pharmaceuticals* **2018**, *11*, 37.
(174) Bhatt, M. R.; Khatri, Y.; Rodgers, R. J.; Martin, L. L. Role of cytochrome b5 in the modulation of the enzymatic activities of cytochrome P450 17α-hydroxylase/17,20-lyase (P450 17A1). *J. Steroid Biochem. Mol. Biol.* **2017**, *170*, 2−18.
(175) Guengerich, F. P.; Wilkey, C. J.; Glass, S. M.; Reddish, M. J. Conformational selection dominates binding of steroids to human cytochrome P450 17A1. *J. Biol. Chem.* **2019**, *294* (26), 10028−10041.
(176) Child, S. A.; Guengerich, F. P. Multistep Binding of the Non-Steroidal Inhibitors Orteronel and Seviteronel to Human Cytochrome P450 17A1 and Relevance to Inhibition of Enzyme Activity. *J. Med. Chem.* **2020**, *63* (12), 6513−6522.
(177) Zhang, J.; Li, L.; Lv, Q.; Yan, L.; Wang, Y.; Jiang, Y. The Fungal CYP51s: Their Functions, Structures, Related Drug Resistance, and Inhibitors. *Front. Microbiol.* **2019**, *10*, 691.
(178) Jones, J. P.; Joswig-Jones, C. A.; Hebner, M.; Chu, Y.; Koop, D. R. The effects of nitrogen-heme-iron coordination on substrate affinities for cytochrome P450 2E1. *Chem.-Biol. Interact.* **2011**, *193* (1), 50−56.
(179) Frydenvang, K.; Verkade-Vreeker, M. C. A.; Dohmen, F.; Commandeur, J. N. M.; Rafiq, M.; Mirza, O.; Jorgensen, F. S.; Geerke, D. P. Structural analysis of Cytochrome P450 BM3 mutant M11 in complex with dithiothreitol. *PLoS One* **2019**, *14* (5), e0217292.
(180) Doukov, T.; Li, H.; Sharma, A.; Martell, J. D.; Soltis, S. M.; Silverman, R. B.; Poulos, T. L. Temperature-dependent spin crossover in neuronal nitric oxide synthase bound with the heme-coordinating thioether inhibitors. *J. Am. Chem. Soc.* **2011**, *133* (21), 8326−34.
(181) Martell, J. D.; Li, H.; Doukov, T.; Martasek, P.; Roman, L. J.; Soltis, M.; Poulos, T. L.; Silverman, R. B. Heme-coordinating inhibitors of neuronal nitric oxide synthase. Iron-thioether coordination is stabilized by hydrophobic contacts without increased inhibitor potency. *J. Am. Chem. Soc.* **2010**, *132* (2), 798−806.
(182) Blouin, G. C.; Schweers, R. L.; Olson, J. S. Alkyl Isocyanides Serve as Transition State Analogues for Ligand Entry and Exit in Myoglobin. *Biochemistry* **2010**, *49* (24), 4987−4997.
(183) Chen, A. Y.; Adamek, R. N.; Dick, B. L.; Credille, C. V.; Morrison, C. N.; Cohen, S. M. Targeting Metalloenzymes for Therapeutic Intervention. *Chem. Rev.* **2019**, *119* (2), 1323−1455.
(184) Palermo, G.; Spinello, A.; Saha, A.; Magistrato, A. Frontiers of metal-coordinating drug design. *Expert Opinion on Drug Discovery* **2021**, *16* (5), 497−511.
(185) Barrett, J. A.; Yang, W.; Skolnik, S. M.; Belliveau, L. M.; Patros, K. M. Discovery solubility measurement and assessment of small molecules with drug development in mind. *Drug Discovery Today* **2022**, *27* (5), 1315−1325.
(186) Black, S.; Dang, L.; Liu, C.; Wei, H. On the Measurement of Solubility. *Org. Process Res. Dev.* **2013**, *17* (3), 486−492.
(187) Crumbaker, M.; Gurney, H. Dose considerations for anti-cancer drugs in metastatic prostate cancer. *Prostate* **2017**, *77* (11), 1199−1204.
(188) Benoist, G. E.; Hendriks, R. J.; Mulders, P. F. A.; Gerritsen, W. R.; Somford, D. M.; Schalken, J. A.; van Oort, I. M.; Burger, D. M.; van Erp, N. P. Pharmacokinetic Aspects of the Two Novel Oral Drugs Used for Metastatic Castration-Resistant Prostate Cancer: Abiraterone Acetate Enzalutamide. *Clin. Pharmacokinetics* **2016**, *55* (11), 1369−1380.
(189) Das, B.; Baidya, A. T. K.; Mathew, A. T.; Yadav, A. K.; Kumar, R. Structural modification aimed for improving solubility of lead compounds in early phase drug discovery. *Bioorg. Med. Chem.* **2022**, *56*, 116614.
(190) Lovering, F.; Bikker, J.; Humblet, C. Escape from Flatland: Increasing Saturation as an Approach to Improving Clinical Success. *J. Med. Chem.* **2009**, *52* (21), 6752−6756.
(191) Hara, T.; Kouno, J.; Kaku, T.; Takeuchi, T.; Kusaka, M.; Tasaka, A.; Yamaoka, M. Effect of a novel 17,20-lyase inhibitor, orteronel (TAK-700), on androgen synthesis in male rats. *J. Steroid Biochem. Mol. Biol.* **2013**, *134*, 80−91.
(192) Rana, Z.; Diermeier, S.; Hanif, M.; Rosengren, R. J. Understanding Failure Improving Treatment Using HDAC Inhibitors for Prostate Cancer. *Biomedicines* **2020**, *8* (2), 22.
(193) O'Sullivan, S. E.; Kaczocha, M. FABP5 as a novel molecular target in prostate cancer. *Drug Discovery Today* **2020**, *25* (11), 2056−2061.
(194) Ratta, R.; Guida, A.; Scotté, F.; Neuzillet, Y.; Teillet, A. B.; Lebret, T.; Beuzeboc, P. PARP inhibitors as a new therapeutic option in

https://doi.org/10.1021/acs.jmedchem.3c00442
J. Med. Chem. 2023, 66, 6542−6566

metastatic prostate cancer: a systematic review. *Prostate Cancer Prostatic Diseases* **2020**, *23* (4), 549−560.
(195) Salami, J.; Alabi, S.; Willard, R. R.; Vitale, N. J.; Wang, J.; Dong, H.; Jin, M.; McDonnell, D. P.; Crew, A. P.; Neklesa, T. K.; Crews, C. M. Androgen receptor degradation by the proteolysis-targeting chimera ARCC-4 outperforms enzalutamide in cellular models of prostate cancer drug resistance. *Commun. Biol.* **2018**, *1* (1), 100.
(196) Hoang, D. T.; Iczkowski, K. A.; Kilari, D.; See, W.; Nevalainen, M. T. Androgen receptor-dependent and -independent mechanisms driving prostate cancer progression: Opportunities for therapeutic targeting from multiple angles. *Oncotarget* **2017**, *8* (2), 3724.
(197) Shapiro, D.; Tareen, B. Current and emerging treatments in the management of castration-resistant prostate cancer. *Exp. Rev. Anticancer Therapy* **2012**, *12* (7), 951−964.

https://doi.org/10.1021/acs.jmedchem.3c00442
J. Med. Chem. 2023, 66, 6542−6566

Appendix II

Cell Death & Differentiation
https://doi.org/10.1038/s41418-021-00768-1

Cell Death & Differentiation

ARTICLE

Reducing FASN expression sensitizes acute myeloid leukemia cells to differentiation therapy

Magali Humbert[1,2] · Kristina Seiler[1,3] · Severin Mosimann[1] · Vreni Rentsch[1] · Katyayani Sharma[3,4,5] · Amit V. Pandey[4,5] · Sharon L. McKenna[2,6] · Mario P. Tschan[1,2,3]

Received: 13 July 2020 / Revised: 14 February 2021 / Accepted: 1 March 2021

Abstract

Fatty acid synthase (FASN) is the only human lipogenic enzyme available for de novo fatty acid synthesis and is often highly expressed in cancer cells. We found that FASN mRNA levels were significantly higher in acute myeloid leukemia (AML) patients than in healthy granulocytes or $CD34^+$ hematopoietic progenitors. Accordingly, FASN levels decreased during all-*trans* retinoic acid (ATRA)-mediated granulocytic differentiation of acute promyelocytic leukemia (APL) cells, partially via autophagic degradation. Furthermore, our data suggest that inhibition of FASN expression levels using RNAi or (-)-epigallocatechin-3-gallate (EGCG) accelerated the differentiation of APL cell lines and significantly re-sensitized ATRA refractory non-APL AML cells. FASN reduction promoted translocation of transcription factor EB (TFEB) to the nucleus, paralleled by activation of CLEAR network genes and lysosomal biogenesis. Together, our data demonstrate that inhibition of FASN expression in combination with ATRA treatment facilitates granulocytic differentiation of APL cells and may extend differentiation therapy to non-APL AML cells.

Introduction

While traditional chemotherapy and radiotherapy target highly proliferative cancer cells, differentiation-inducing therapy aims to restore differentiation programs to drive cancer cells into maturation and ultimately into cell death. Differentiation therapies are associated with lower toxicity compared to classical cytotoxic therapies. The success of this therapeutic approach is exemplified by the introduction of all-*trans* retinoic acid (ATRA) in 1985 to treat acute promyelocytic leukemia (APL) [1]. The introduction of ATRA into the treatment regimen changed APL from being one of the most aggressive acute myeloid leukemia (AML) subtypes with a fatal course often within weeks only, to a curable disease with a complete remission rate of up to 95% when combined with anthracycline-based chemotherapy or arsenic trioxide [1]. APL is characterized by translocations involving the C-terminus of the retinoic acid receptor alpha (RARA) on chromosome 17 and genes encoding for aggregate prone proteins. Promyelocytic leukemia (PML)-RARA is the most frequently expressed fusion protein. It is encoded by the translocation t(15;17) and has a dominant-negative effect on RARA. RARA transcriptionally regulates multiple biological processes with a key role in differentiation [2]. Several reports suggest a beneficial effect of ATRA in combination therapies in non-APL AML cells [3–5]. Unfortunately, a variety of intrinsic resistance mechanisms in non-APL AML have been identified such as SCL overexpression, expression of PRAME and epigenetic

Edited by H. Ichijo

Supplementary information The online version contains supplementary material available at https://doi.org/10.1038/s41418-021-00768-1.

✉ Magali Humbert
magali.humbert@yahoo.fr

1 Institute of Pathology, Division of Experimental Pathology, University of Bern, Bern, Switzerland

2 TRANSAUTOPHAGY: European Network for Multidisciplinary Research and Translation of Autophagy Knowledge, COST Action, Bern, Switzerland

3 Graduate School for Cellular and Biomedical Sciences, University of Bern, Bern, Switzerland

4 Pediatric Endocrinology, Diabetology, and Metabolism, University Children's Hospital, Bern, Switzerland

5 Department of Biomedical Research, University of Bern, Bern, Switzerland

6 Cancer Research, UCC, Western Gateway Building, University College Cork, Cork, Ireland

silencing or mutation of RARA [6–9]. Deciphering the mechanisms active during ATRA-mediated differentiation at the molecular level will support the translation of differentiation therapy to non-APL AML patients. We and others have demonstrated the importance of autophagy in ATRA induced granulocytic differentiation of APL cells [10–15]. Autophagy is an intracellular degradation mechanism that ensures dynamic recycling of various cytoplasmic contents [16]. We thus aim to understand the role of autophagy in granulocytic differentiation and to define key druggable autophagy targets in this process.

Endogenous synthesis of fatty acids is catalyzed by fatty acid synthase (FASN), the only human lipogenic enzyme able to perform de novo synthesis of fatty acids [17, 18]. FASN is frequently overexpressed in a variety of tumor types including leukemias [19–25] while its expression in healthy adult tissues is low [26], with the exception of the cycling endometrium [27] and lactating breast [28]. Interestingly, FASN is upregulated in tumor-associated myeloid cells where it activates nuclear receptor peroxisome-proliferator-activated receptor beta/delta (PPARβ/δ) [29], a key metabolic transcription factor in tumorigenesis [30, 31]. Of note, activation of PPARβ/δ regulates anti-inflammatory phenotypes of myeloid cells in other biological contexts such as atherosclerosis and obesity [32–35]. We previously reported that (-)-epigallocatechin-3-gallate (EGCG) improved ATRA-induced differentiation of APL cells by increasing the expression of death-associated protein kinase 2 (DAPK2). Furthermore, EGCG treatment reduces FASN expression levels in selected breast cancer cell lines [36]. The increased FASN expression in cancers including leukemias, its function in tumor-associated myeloid cells and its link to the differentiation enhancer DAPK2 prompted us to analyze the regulation and function of FASN during myeloid leukemic differentiation.

In the present study, we demonstrate that FASN expression is significantly higher in AML blasts partially due to low autophagic activity in those cells. We show that inhibiting FASN protein expression, but not its enzymatic activity, promotes differentiation of non-APL AML cells. Lastly, we link FASN expression to mTOR activation and inhibition of the key lysosomal biogenesis transcription factor TFEB.

Material and methods

Primary cells, cell lines and culture conditions

Fresh leukemic blast cells from untreated AML patients at diagnosis were obtained from the Inselspital Bern (Switzerland) were classified according to the French-American-British classification and cytogenetic analysis. All leukemia samples had blast counts of ~90% after separation of mononuclear cells using a Ficoll gradient (Lymphoprep; Axon Lab AG, Switzerland), as described previously [37]. Protocols and use of 67 human samples acquired in Bern were approved by the Cantonal Ethical Committee at the Inselspital. The isolation of primary neutrophils (purity 95%) was performed by separating blood cells from healthy donors using polymorphprep (Axon Lab AG, Switzerland). $CD34^+$ cells from cord blood or bone marrow were isolated as previously described [37].

The human AML cell lines HT93, OCI/AML2, MOLM-13 and NB4 were obtained from the Deutsche Sammlung von Mikroorganismen und Zellkulturen GmbH (DSMZ, Braunschweig, Germany). All cell lines were maintained in RPMI-1640 with 10% fetal calf serum, 50 U/mL penicillin and 50 µg/mL streptomycin in a 5% CO_2-95% air humidified atmosphere at 37 °C. For differentiation experiments, AML cells were treated with 1 µM ATRA (ATRA; Sigma-Aldrich, Switzerland). Successful granulocyte differentiation was evidenced by CD11b surface expression measured by FACS.

293 T cells were maintained in DMEM (Sigma-Aldrich, St. Louis, MO, USA), supplemented with 5% FBS, 1% penicillin/streptomycin, and 1% Hepes (Sigma-Aldrich, Switzerland), and kept in a 7.5%CO_2-95% air humidified atmosphere at 37 °C.

Antibodies

Antibodies used were anti-FASN (3180; Cell Signaling, Switzerland), anti-LC3B (WB: NB600-1384, Novus biological, Switzerland; IF: 3868; Cell Signaling, Switzerland) anti-LAMP1 (14-1079-80; Thermofisher, Switzerland), anti-p62 (HPA003196; Sigma-Aldrich, Switzerland), anti-TFEB (4240; Cell Signaling, Switzerland), anti-p-TFEB (Ser 211) (37681S, Cell Signaling, Switzerland), anti-p-AKT (Ser473) (4060S, Cell Signaling, Switzerland) anti-PTEN (9552, Cell Signaling, Switzerland), anti-ULK1 (4776; Cell Signaling, Switzerland), anti-p-ULK1 (Ser757, equivalent to Ser758 of human ULK1) (6888; Cell Signaling, Switzerland), anti-ATG13 (6940; Cell Signaling, Switzerland), anti-pATG13 (Ser318) (600-401-C49; Rockland, Switzerland), anti p-mTOR (Ser2448) (5536; Cell Signaling, Switzerland), p4E-BP1 (Thr37/46) (2855; Cell Signaling, Switzerland), anti-α-tubulin (3873; Cell Signaling, Switzerland), anti-cleaved PARP (9541; Cell Signaling, Switzerland), anti yH2AX (2577; Cell Signaling, Switzerland) and anti-CD11b-PE (R0841; Dako, Switzerland).

Cell lysate preparation and western blotting

Whole-cell extracts were prepared using UREA lysis buffer and 30–60 µg of total protein was loaded on a 7.5% or 12%

denaturing polyacrylamide self-cast gels (Bio-Rad, Switzerland). Blots were incubated with the primary antibodies in TBS 0.05% Tween-20/5% milk overnight at 4 °C and subsequently incubated with HRP coupled secondary goat anti-rabbit (7074; Cell Signaling, Switzerland) and goat anti-mouse antibody (7076; Cell Signaling, Switzerland) at 1:5–10,000 for 1 h at room temperature. Blots were imaged using Chemidoc (Bio-Rad, Switzerland) and ImageLab software.

Lentiviral vectors

pLKO.1-puro lentiviral vectors expressing shRNAs targeting *FASN* (sh*FASN*_1: NM_004104.x-1753s1c1 and sh*FASN*_2: NM_004104.x-3120s1c1) were purchased from Sigma-Aldrich. A mCherry-LC3B lentiviral vector was kindly provided by Dr. Maria S. Soengas (CNIO, Molecular Pathology Program, Madrid, Spain). All vectors contain a puromycin antibiotic resistance gene for the selection of transduced mammalian cells. Lentivirus production and transduction were performed as previously described [37, 38]. Transduced NB4, MOLM-13 and OCI/AML2 cell populations were selected with 1.5 µg/ml puromycin for 4 days and knockdown efficiency was assessed by western blot analysis.

Immunofluorescence microscopy

Cells were prepared as previously described [14]. Briefly, cells were fixed and permeabilized with ice-cold 100% methanol for 4 min (FASN, mTOR, LC3B and LAMP1 staining) or 2% paraformaldehyde for 7 min followed by 5 min in PBS 0.1% TRITON X-100 (TFEB and tubulin staining) and then washed with PBS. Cells were incubated with primary antibody for 1 h at room temperature followed by washing steps with PBS containing 0.1% Tween (PBS-T). Cells were incubated with the secondary antibody (anti-rabbit, 111-605-003 (Alexa Fluor® 647) 111-096-045 (FITC); anti-mouse, (Cy3) 115-605-003 (Alexa Fluor® 647); Jackson ImmunoResearch, West Grove, PA, USA) for 1 h at room temperature. Prior to mounting in fluorescence mounting medium (S3032; Dako, Switzerland) cells were washed three times with PBS-Tween. Images were acquired on an Olympus FluoView-1000 confocal microscope (Olympus, Volketswil, Switzerland) at ×63 magnification.

Acridine Orange staining

Cells were washed three times with PBS and resuspended in RPMI 10% FBS containing 5ug/mL Acridine Orange (A3568, Invitrogen, Switzerland) to a concentration of 0.2 × 106 cells per ml. Cells were then incubated at 37 °C for 20 min and washed three times with PBS. Acridine Orange staining was measured by FACS analysis using a 488 nm laser with 530/30 (GREEN) and 695/40 (RED) filters on a FACS LSR-II (BD Biosciences, Switzerland). Data were analyzed with FlowJo software (Ashland, OR, USA). The software derived the RED/GREEN ratio and we compared the distribution of populations using the Overton cumulative histogram subtraction algorithm to provide the percentage of cells more positive than the control.

Nitroblue tetrazolium reduction test

Suspension cells (5 × 105) were resuspended in a 0.2% nitro blue tetrazolium (NBT) solution containing 40 ng/ml PMA and incubated 15 min at 37 °C. Cells were then washed with PBS and subjected to cytospin. Counterstaining was done with 0.5% Safranin O for 5 min (HT90432; Sigma-Aldrich, Switzerland). The NBT-positive and negative cells were scored under a light microscope (EVOS XL Core, Thermofisher, Switzerland).

Trypan blue exclusion counting

Trypan blue exclusion cell counting was performed to assess cellular growth. 20 µL of cell suspension was incubated with an equal volume of 0.4% (w/v) trypan blue solution (Sigma-Aldrich, Switzerland). Cells were counted using a dual-chamber hemocytometer and a light microscope (EVOS XL Core, Thermofisher, Switzerland).

Real-time quantitative RT-PCR (qPCR)

Total RNA was extracted using the RNeasy Mini Kit and the RNase-Free DNase Set according to the manufacturer's protocol (Sigma-Aldrich, Switzerland). Total RNA was reverse transcribed using all-in-one RT-PCR (BioTool, Switzerland). Taqman® Gene Expression Assays for *FASN*, *ELOVL6*, *SCD1*, *ACACA*, *BECN1*, *GABARAP*, *STK4*, and *WDR45* were Hs01005632_g1, Hs00907564_m1, Hs01682761_m1, Hs01046047_m1, Hs00186838_m1, Hs00925899_g1, Hs00178979_m1 and Hs01079049_g1, respectively. Specific primers and probes for *HMBS* have been already described [37]. Data represent the mean ± s.d. of at least two independent experiments.

TaqMan low-density array (LDA)

Total RNA was extracted using the Qiagen RNeasy kit and the RNase-Free DNase Set to minimize the risk of contamination with genomic DNA, according to the manufacturer's protocol (Qiagen AG). 1–2 µg of total RNA was reverse transcribed using pd(N)6 random primers (Roche Diagnostics AG, Rotkreuz, Switzerland). Real-time RT-PCR for LDAs was performed using the ABI 7900HT Fast Real-Time PCR

System (Applied Biosystems, Rotkreuz, Switzerland) and 400 ng of cDNA. Taqman® Gene Expression Assays for HMBS, ABL1, and FASN preloaded on LDAs or used in a 96-well format using the ABI PRISM 7700 Sequence Detection System were Hs00609297_m1, Hs00245445_m1, and Hs01005632_g1 respectively (Applied Biosystems).

Measured cycle threshold (Ct) values represent log 2 expression levels. Values were normalized to the expression levels of two housekeeping genes *HMBS* and *ABL1* as described in [39].

Lipid extraction

The protocol was performed as previously described [40]. Briefly, NB4 cells (0.5 × 105 cells/ml) were labelled with 0.5 µCi/ml [^{14}C]-Acetic Acid [American Radiolabeled Chemical Inc., St. Louis, MO, USA] for 6 h in the presence or absence of different concentrations of C75 and Orlistat. Cells were harvested using 0.5 ml PBS and lipids were extracted using chloroform/methanol (3:1, v/v). The chloroform phase was evaporated under nitrogen and concentrated lipids were dissolved in 30 µl dichloromethane. Lipids were separated by thin layer chromatography over silicagel (SIL G/UV254) TLC plates (Macherey-Nagel, Oensingen, Switzerland) using hexane/diethyl ether/acetic acid (70:30:1, v/v) as mobile phase. Palmitic acid (PA) spots were identified using a standard [Sigma-Aldrich, Basel, Switzerland] solution by exposing the TLC to Iodine vapor. The corresponding radiolabeled spots were visualized by autoradiography using a Fuji FLA-7000 PhosphoImager (Fujifilm, Dielsdorf, Switzerland) and quantified using ImageQuant software. The amount of PA formed in the presence of drugs was calculated as a percent of radioactivity incorporated into the control samples.

Statistical analysis

Nonparametric Mann–Whitney-U tests were applied to compare the difference between two groups and Spearman Coefficient Correlation using Prism software (GraphPad Software, Inc., Jolla, CA, USA). P values < 0.05 were considered statistically significant. The error bar on graphs represents the SD of at least two biological replicates performed in two technical replicates.

Results

Primary AML blast cells express significantly higher FASN levels compared to mature granulocytes

Cancer cells frequently express high levels of FASN compared to their healthy counterparts [19–25]. We examined *FASN* mRNA expression in an AML patient cohort. *FASN* mRNA levels in AML samples ($n = 68$) were compared to the levels in granulocytes ($n = 5$) and CD34$^+$ human hematopoietic progenitor cells ($n = 3$) from healthy donors. We found that *FASN* expression was significantly higher in AML patients compared to healthy granulocytes ($p < 0.05$) (Fig. 1A). We obtained similar findings by analyzing *FASN* expression in AML patient data available from the Blood spot gene expression profile data base [41] (Fig. 1B). In addition, hematopoietic stem cells from healthy donors express significantly lower *FASN* mRNA transcript levels than AML blasts (Fig. 1B). Next, we asked if FASN expression was altered during granulocytic differentiation of APL cells. We analyzed FASN protein expression following ATRA-induced differentiation of two APL cell lines, NB4 and HT93. Successful differentiation was confirmed by flow cytometry, using CD11b surface marker expression (Supplementary Fig. 1A-C). ATRA treatment resulted in markedly reduced FASN protein levels from day two onwards (Fig. 1C) whereas FASN mRNA levels did not decrease (Fig. 1D). Interestingly, other transcriptional targets of the sterol regulatory element binding protein 1 (SREBP1), such as *ELOVL6*, *SCD1* and *ACACA*, were upregulated, yet FASN (also a transcriptional target), was not (Supplementary Fig. 1C). Collectively this data suggests that high FASN expression is linked to an immature blast-like phenotype and that the decrease in FASN protein levels during ATRA-induced differentiation is mediated at the protein level, rather than by transcriptional mechanisms.

FASN protein is degraded via macroautophagy during ATRA-induced granulocytic differentiation

We and others have demonstrated that autophagy gene expression is repressed in AML samples compared to granulocytes from healthy donors and that autophagy activity is essential for successful ATRA-induced APL differentiation [10–15, 42]. The marked decrease in FASN protein upon ATRA-induced differentiation is likely to be due to post-transcriptional regulation as transcript levels are unchanged and the protein has a long half-life (1–3 days) [26, 43]. Moreover, FASN has been detected inside autophagosomes, for instance in yeast and in the breast cancer cell line MCF7 [44, 45]. Therefore, we hypothesized that ATRA-induced autophagy participates in the degradation of FASN during differentiation of APL cells. To examine whether autophagy is involved in FASN degradation, we treated NB4 cells for 24 h with different concentrations of Bafilomycin A1 (BafA1), a specific inhibitor of vacuolar-type H$^+$-ATPase [46, 47], alone or in combination with ATRA. FASN protein was found to accumulate in the presence of BafA1 at day 1 and 2 of ATRA treatment in NB4 cells, together with autophagy markers p62 and

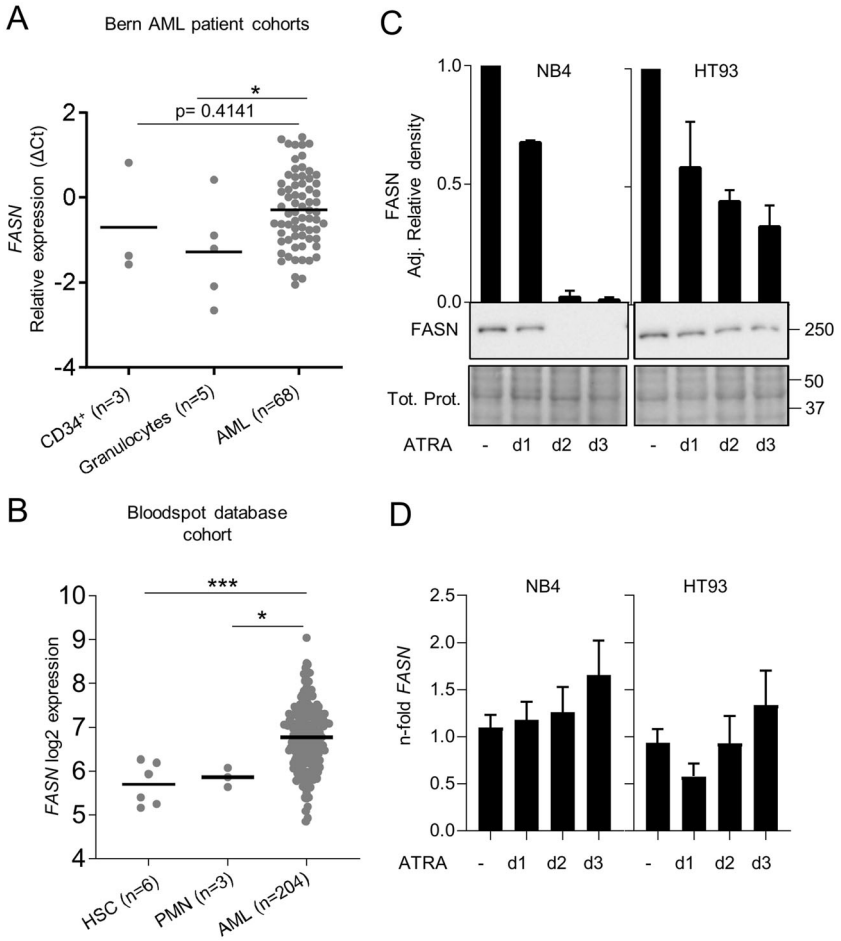

Fig. 1 Increased FASN expression is associated with an immature AML blast phenotype. A FASN mRNA levels in AML blasts, $CD34^+$ progenitor cells and granulocytes from healthy donors were quantified by qPCR. All the samples were obtained from the Inselspital, Bern, Switzerland. AML patient cells and granulocytes were isolated using Ficoll gradient density centrifugation. Values are the differences in Ct-values between FASN and the housekeeping genes HMBS and ABL1. MNW $*p < 0.05$, $**p < 0.0$. **B** Blood spot data bank analysis of FASN expression in AML blasts compared to granulocytes from healthy donors. MNW $*p < 0.05$, $**p < 0.01$. **C** Western blot analysis of FASN regulation in NB4 and HT93 APL cells upon ATRA treatment at different time points (1, 2 and 3 days). Total protein was extracted and submitted to immunoblotting using anti-FASN antibody. Total protein is shown as loading control. The relative protein expressions were normalized to total protein and quantified using ImageJ software (NIH, Bethesda, MD, USA). Data are represented as a mean ($n = 3$), Error bars: SD. **D** Evaluation of *FASN* transcript levels upon ATRA treatment was done by qPCR. Values were normalized to the HMBS housekeeping gene. Results of at least three independent experiments are shown as n-fold regulation compared with non-treated cells.

LC3B-II (Fig. 2A-B). To validate these findings, we utilized NB4 cells stably expressing mCherry-LC3B. Cells were treated with different concentrations of BafA1 with or without ATRA for 24 h and FASN, as well as LC3B localization, was assessed. Endogenous FASN (cyan) showed colocalization with mCherry-LC3B (red) in BafA1 and ATRA treated cells (Fig. 2C). In addition, we found colocalization with endogenous FASN (red) and p62 (green) in NB4 parental cells treated with both ATRA and BafA1 for 24 h (Fig. 2D). It is possible that p62 may help to sequester FASN to the autophagosome. These data suggest that FASN is a target for autophagic degradation during granulocytic differentiation of APL cells.

We have previously shown that EGCG improves the response to ATRA in AML cells by inducing DAPK2 expression, a key kinase in granulocytic differentiation [48]. Furthermore, EGCG was reported to decrease FASN expression [36] and this was reproducible in our APL cell line model (Supplementary Fig. 2A-B). Using different EGCG doses and treatment time points, we confirmed that EGCG improves ATRA-induced differentiation in NB4 cells, as evidenced by increased NBT positive cells and CD11b surface expression (Supplementary Fig. 2C-E). Importantly, increased differentiation when combining ATRA with EGCG was paralleled by enhanced autophagic activity (Supplementary Fig. 2F-G). Autophagy induction

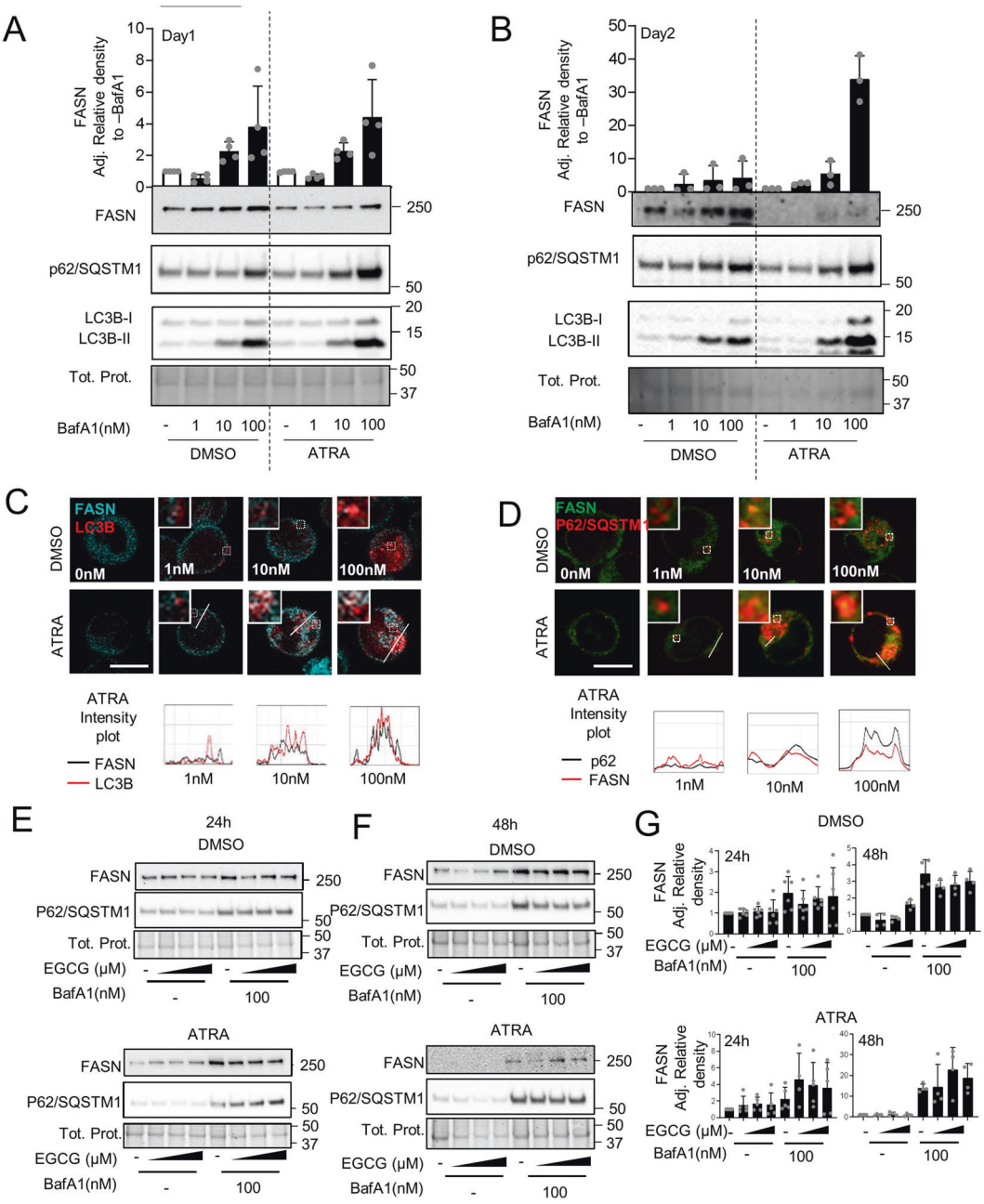

Fig. 2 FASN is degraded via autophagy. A–B NB4 cells were treated with ATRA and three concentrations of Bafilomycin A1 (BafA1) for 24 h (**A**) and 48 h (**B**). NB4 cells were lysed and subjected to western blot analysis as described in 1C. Quantification of the bands was done using ImageJ software and normalized to control-treated cells. Data are represented as a mean of at least three biological replicates, Error bars: SD. **C** NB4 cells stably expressing mCherry-LC3B were treated with ATRA and different concentrations of Bafilomycin A1 (BafA1) for 24 h. NB4 mCherry-LC3B cells were fixed and stained for endogenous FASN. The colocalization analysis was performed using ImageJ software. Scale: 10 μm **D** NB4 cells were treated as in 2 C and fixed and stained for endogenous FASN and p62. The colocalization analysis was performed using ImageJ software. Scale: 10 μm. Results shown are from at least two biological duplicates. **E–G** EGCG potentiate ATRA-induced FASN degradation by autophagy. **E–F** FASN and p62 western blot analysis of NB4 cells treated with DMSO (right panel) or ATRA (left panel), in combination with different EGCG (5–15 μM) and BafA1 (100 nm) concentrations for 24 h (**E**) or 48 h (**F**). Total cell lysates were subjected to western blotting. **G** Quantification of the western blot was done as in Fig. 1C.

was determined by quantifying endogenous, lipidated LC3B-II by western blotting and a dual-tagged mCherry-GFP-LC3B expression construct as described previously [13, 49, 50]. Autophagic flux quantification upon EGCG treatment was performed in the presence or absence of BafA1 [50]. We found no significant changes in cell death or proliferation measured by DAPI staining and trypan blue exclusion, respectively (Supplementary Fig. 2H-I).

Co-treating NB4 parental cells with EGCG and ATRA as well as blocking autophagy using BafA1, resulted in a higher accumulation of FASN protein at 24 h or 48 h (Fig. 2E-G). Together, our data demonstrate that FASN can be degraded via autophagy during APL cell differentiation and that co-treatment with EGCG further promotes FASN protein degradation.

Inhibiting FASN protein expression but not its catalytic function accelerates ATRA-induced granulocytic differentiation in APL cell lines

Next, we evaluated the impact of modulating FASN expression and activity on myeloid differentiation. Therefore, we genetically inhibited FASN expression using lentiviral vectors expressing two independent shRNAs targeting *FASN* in the NB4 APL cell line model. Knockdown efficiency was validated by western blotting (Fig. 3A). We found that ATRA treatment significantly reduced the doubling time (Supplementary Fig. 3A-B) and lowered the accumulation of DNA damage as indicated by yH2AX immunofluorescence staining in NB4 *FASN* depleted cells (Supplementary Fig. 3C-D). Of note, at steady-state conditions, knocking down *FASN* did not affect proliferation compared to control cells. Knocking down *FASN* in NB4 cells resulted in accelerated differentiation into functional granulocytes compared to the control cells as shown by NBT assays (Fig. 3B-C) and by CD11b surface expression analysis (Fig. 3D). We then assessed the effects of two pharmacological FASN inhibitors, C75 and Orlistat. We used C75 and Orlistat concentrations that do not induce significant cell death (Supplementary Fig. 4A-B) or decrease proliferation (Supplementary Fig. 4C-D) to avoid non-specific effects. Of note, FASN protein levels in APL cells were not reduced by C75 or Orlistat treatment (Supplementary Fig. 4E-F) while inhibiting its activity (Supplementary Fig. 4G-H). Unexpectedly, co-treatment of NB4 cells with ATRA and C75 (Fig. 3E-G) or Orlistat (Fig. 3H-J) did not reproduce the phenotype of the *FASN* knockdown cells. Indeed, cells were differentiating similarly or less compared to control-treated cells as demonstrated by NBT assays (Fig. 3E-F and Fig. 3H-I) and CD11b surface expression (Fig. 3G and Fig. 3J). Therefore, we conclude that the catalytic activity of FASN is not involved in impeding ATRA-mediated differentiation in NB4 cells.

FASN attenuates autophagy by increasing mTOR activity

FASN has been previously reported to promote carcinogenesis by activating mTOR, a master negative regulator of autophagy, via AKT signaling in hepatocellular carcinoma [51, 52]. ATRA treatment in APL reduces mTOR activity leading to autophagy activation [10]. We, therefore, hypothesized that FASN may negatively regulate autophagy via mTOR in APL cells, thereby impeding ATRA-induced differentiation. Therefore, we initially confirmed that FASN expression impacts autophagic activity in our system. Autophagy induction was established by quantifying endogenous LC3B dots formation by immunofluorescence microscopy (IF) after ATRA treatment [50]. In order to measure autophagic flux, ATRA treatment was performed in the presence or absence of BafA1 (Fig. 4A-B) [50]. In addition, we looked at the direct consequences of mTOR activity on ULK1 and ATG13 phosphorylation. ULK1 (ATG1), a key autophagy gene of the initiation complex, is inhibited by mTOR-mediated phosphorylation at Ser757, leading to reduced autophagic activity (Fig. 4C) [53]. In line with FASN activating mTOR, lowering *FASN* expression by shRNA (Fig. 4D) resulted in decreased mTOR phosphorylation at Ser2448 (Fig. 4E) and mTOR-mediated downstream phosphorylation of ULK1 at Ser758 (Fig. 4F). Elevated ULK1 activity was confirmed by an increase of ATG13 activating phosphorylation at Ser318 (Fig. 4G) [54, 55].

We then asked how FASN regulates mTOR activity. First, we tested whether FASN is localized to the lysosome by immunofluorescence microscopy upon ATRA treatment in NB4 cells. Interestingly, FASN localized to $LAMP1^+$ vesicles during steady-state conditions. Furthermore, ATRA treatment reduced both protein and FASN localization to $LAMP1^+$ vesicles (Fig. 5A). In addition, lowering FASN expression led to a reduced lysosomal localization of mTOR (Fig. 5B). Next, we asked whether the mTOR upstream regulators AKT and PTEN were influenced by FASN expression. We treated FASN depleted NB4 cells for 3 days with ATRA and quantified AKT protein phosphorylation and PTEN protein levels. Furthermore, we analyzed two additional mTOR downstream targets namely p-4EBP1 (Thr37/46) and p-TFEB (Ser211). Interestingly, we found a compensatory activation of AKT in NB4 *FASN* knockdown cells while no marked differences in PTEN and p-4EBP1 levels were seen. Of note, TFEB was less phosphorylated in FASN depleted than in SHC002 control NB4 cells (Fig. 5C-D).

These results suggest that FASN expression promotes mTOR activity at the lysosomes, which in turn enhances autophagy inhibition in AML cells.

FASN expression negatively affects transcription factor EB (TFEB) activation

mTOR phosphorylates the transcription factor EB (TFEB), a master regulator of lysosome biogenesis, leading to the sequestration of TFEB within the cytoplasm and inhibition of its transcriptional activity [56–59]. TFEB is a key

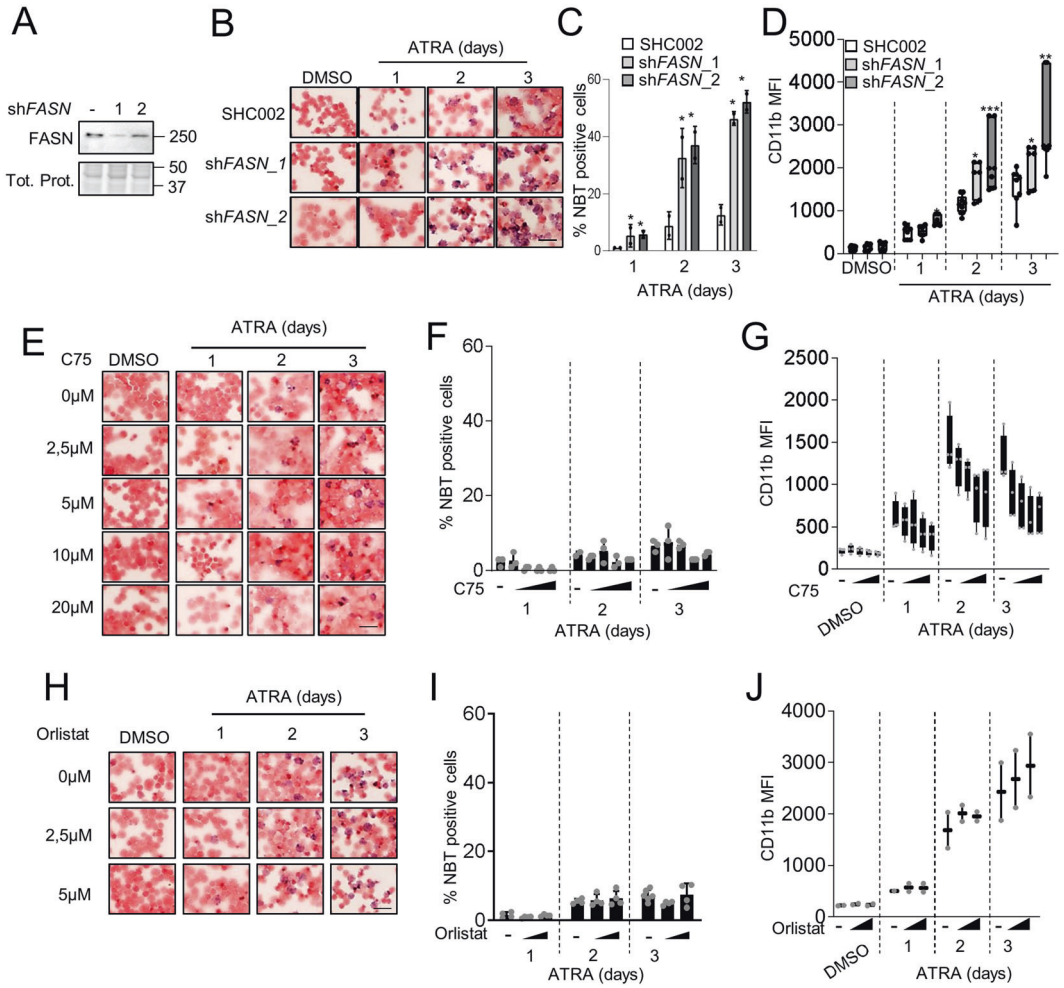

Fig. 3 Reducing FASN protein levels improves ATRA-mediated neutrophil differentiation of APL cells. A–D NB4 cells were stably transduced with non-targeting shRNA (SHC002) or shRNAs targeting *FASN* (sh*FASN*_1 and sh*FASN*_2) lentiviral vectors and differentiated with 1 μM ATRA for 1, 2 or 3 days. **A** FASN western blot analysis of control and sh*FASN* (sh*FASN*_1, _2) expressing NB4 cell populations. **B–C** NBT reduction in ATRA-treated NB4 control (SHC002) and *FASN* knockdown (sh*FASN*_1, _2) cells. **B** Representative images of NBT assays in control and FASN depleted NB4 cells. Scale 20 μM. **C** Quantification of the percentage of NBT^+ cells. **D** Flow cytometry analysis of CD11b surface expression NB4 control (SHC002) and *FASN* knockdown (sh*FASN*_1, _2) NB4 cells upon ATRA treatment. **E–G** NB4 cells were treated with the indicated C75 concentrations for 3 days in combination with ATRA. **E–F** NBT reduction during ATRA-mediated neutrophil differentiation of NB4 control and C75 treated cells. **E** Representative images of NBT assays in control and C75 treated NB4 cells upon ATRA-mediated differentiation. Scale 20 μM. **F** Quantification of the percentage of NBT^+ cells. **G** Flow cytometry analysis of CD11b surface expression in NB4 control and C75 treated cells upon ATRA-mediated differentiation. **H–J** NB4 cells were treated with the indicated Orlistat concentrations for 3 days in combination with ATRA. **H–I** NBT reduction during ATRA-mediated neutrophil differentiation of NB4 control and Orlistat treated cells. **H** Representative images of NBT assays in control and Orlistat treated NB4 cells upon ATRA-mediated differentiation. Scale 20 μM **I** Quantification of the percentage of NBT^+ cells. **J** Flow cytometry analysis of CD11b surface expression in NB4 control and Orlistat treated cells upon ATRA-mediated differentiation. Data are represented as a mean ($n = 3$), Error bars: SD.

transcriptional regulator of more than 500 genes that comprise the CLEAR (Coordinated Lysosomal Expression and Regulation) network of autophagy and lysosomal genes (Supplementary Fig. 5A). A recent study demonstrated a key role of TFEB during ATRA-induced differentiation [15]. We, therefore, investigated the relationship between FASN and CLEAR network gene expression. Interestingly, several TFEB downstream targets from the different categories (lysosomal hydrolases and accessory proteins, lysosomal membrane, lysosomal acidification, non-lysosomal proteins involved in lysosomal biogenesis and autophagy) are negatively associated with FASN transcript levels in two primary AML patient cohorts from TCGA analyzed using the UCSC Xena platform [60] and the Blood spot gene expression profiles data base [41] (Fig. 6A, Supplementary Fig. 5B-C Supplementary Table 1–2). Furthermore, analyzing RNA-seq data of NB4 cells treated with ATRA confirmed a reduction of FASN expression

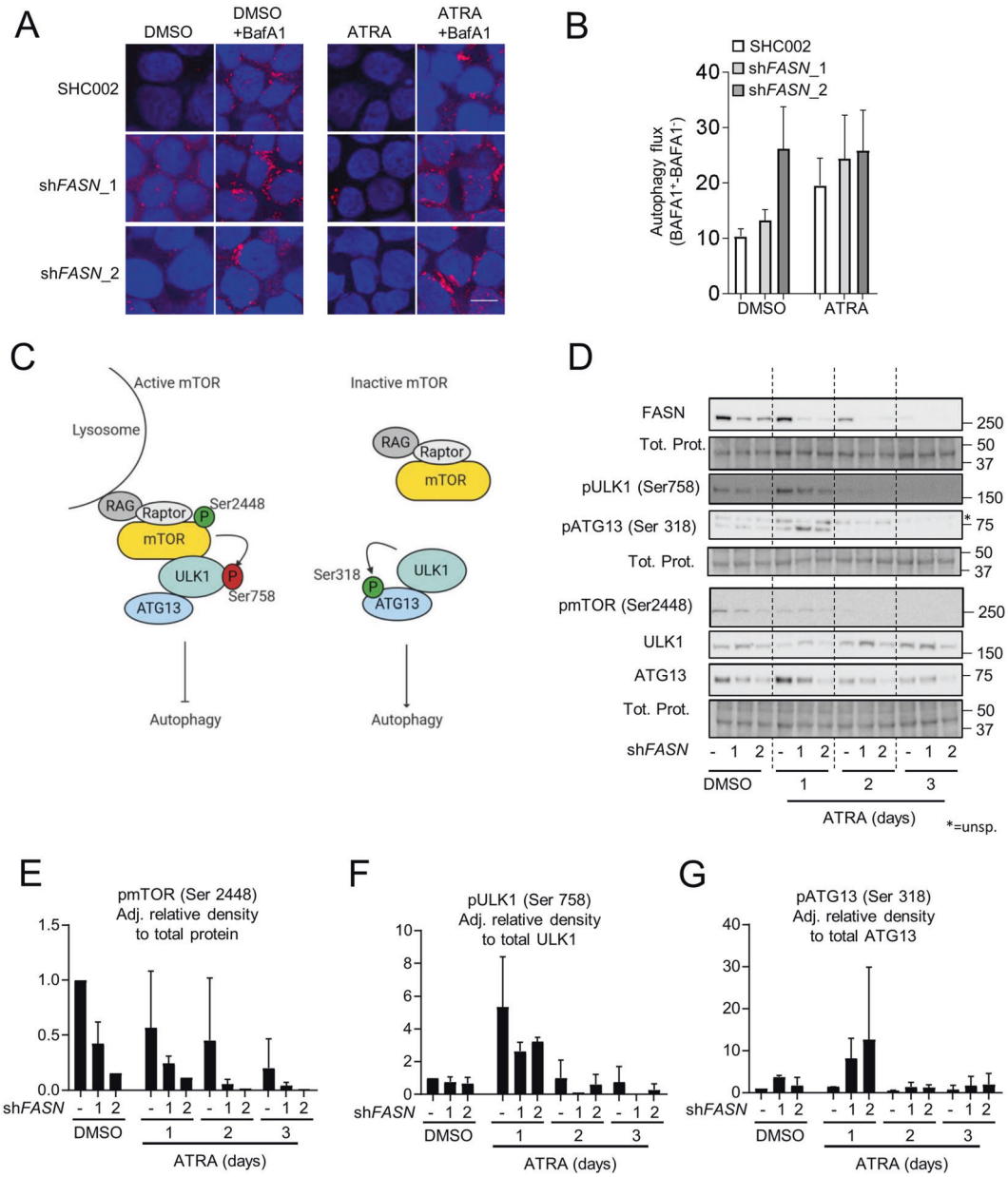

Fig. 4 FASN expression is linked to increased mTOR activity. A–C Autophagy induction in NB4 sh*FASN* cells treated with 1 µM ATRA for 24 h, in the presence or absence of BafA1 during the last 2 h before harvesting. **A–B** NB4 control (SHC002) and FASN knockdown (sh*FASN*_1, _2) cells were subjected to LC3B immunofluorescence. **A** Representative picture of LC3B punctae in NB4 control (SHC002) and FASN knockdown (sh*FASN*_1, _2) cells. Scale: 10 µm. **B** Quantification of autophagy flux. Three independent experiments were quantified as described in [13]. **C** Scheme of mTOR activity on the ULK1 complex. **D** NB4 control (SHC002) and FASN knockdown (sh*FASN*_1, _2) cells were treated for 1–3 days with ATRA. Total protein was extracted and subjected to immunoblotting using anti-FASN, anti-pmTOR(Ser2448), anti- pULK1(Ser757), anti-ULK1, anti-pATG13(Ser318) and anti-ATG13 antibodies. **E–F** Relative protein expressions of two independent experiments were normalized to total protein or the respective non-phosphorylated protein and quantified using ImageJ software (NIH, Bethesda, MD, USA). **E** pmTOR(Ser2448) normalized to total protein. **F** pULK1(Ser758) normalized to total ULK1. **G** pATG13(Ser318) normalized to total ATG13. Results shown are from at least two biological duplicates.

paralleled by increased TFEB and TFEB target gene transcript levels [15] (Fig. 6B). To test if the FASN-mTOR pathway is involved in regulating TFEB activity, we analyzed the cellular localization of TFEB upon ATRA treatment in NB4 control and FASN depleted cells. First, we investigated if TFEB translocates to the nucleus following ATRA treatment and if this translocation is paralleled by an increase in lysosome numbers (LAMP1$^+$ dots), assessed by immunofluorescence microscopy (Supplementary Fig. 6A-B). Indeed, ATRA treatment resulted in increased LAMP1$^+$

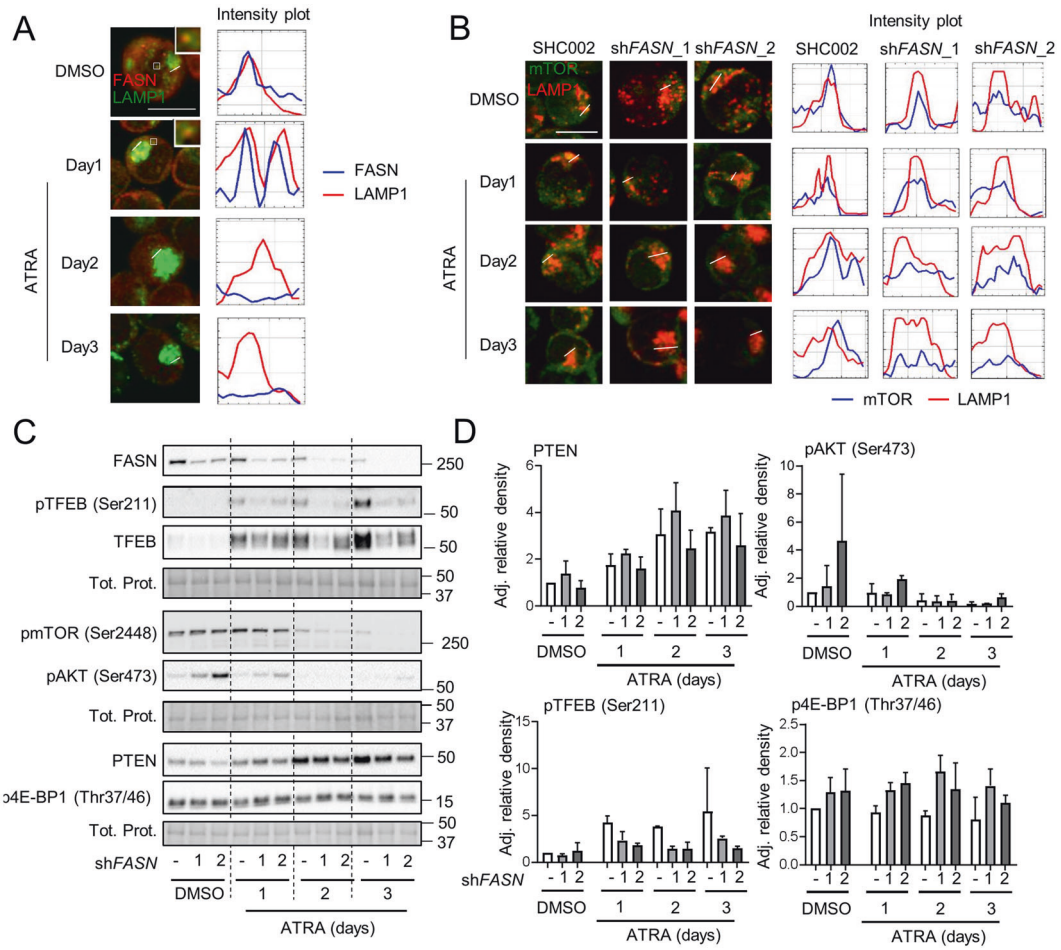

Fig. 5 FASN localizes at the lysosome to increase mTOR activity. **A** NB4 cells were treated as in 2D and fixed and stained for endogenous FASN (red) and LAMP1 (green) protein. The colocalization analysis was performed using ImageJ software. Scale: 10 µm. Results shown are from at least two biological duplicates. **B**–**D** NB4 control (SHC002) and *FASN* knockdown (sh*FASN*_1, _2) cells were treated for 1–3 days with ATRA. **B** Immunofluorescence microscopy of endogenous mTOR (green) and LAMP1 (red). The colocalization analysis was performed using ImageJ software. Scale: 10 µm. **C** Total protein was extracted and subjected to immunoblotting using anti-FASN, anti-pmTOR(Ser2448), anti-pTFEB(Ser211), anti-TFEB, anti-pAKT(Ser473) anti-PTEN and anti-p4E-BP1 (Thr37/46) antibodies. **D** Relative protein expressions of two independent experiments were normalized to total protein or the respective non-phosphorylated protein and quantified using ImageJ software (NIH, Bethesda, MD, USA).

dot formation and nuclear translocation of TFEB. Interestingly, TFEB nuclear translocation occurs faster in FASN depleted NB4 cells compared to control cells (Fig. 6C), consistent with an increase in LAMP1^{+} dot formation (Fig. 6D-E). Furthermore, we treated cells with Acridine Orange to quantify the lysosomal integrity by flow cytometry. Acridine Orange is a cell-permeable fluorescent dye that, when excited at 488 nm, emits light at 530 nm (GREEN) in its monomeric form but shifts its emission to 680 nm (RED) when accumulating and precipitating inside lysosomes. Therefore, we measured the RED/GREEN ratio of Acridine Orange stained cells by flow cytometry as previously described [61]. We found that ATRA treatment shifted the ratio towards the red channel (Supplementary Fig. 6C). Reducing FASN expression further accelerated the increase of the RED/GREEN ratio indicating enhanced lysosome biogenesis (Fig. 6G-H). These results suggest that FASN expression impairs TFEB translocation to the nucleus and therefore reduces lysosome biogenesis

We then evaluated the effect of FASN expression on the transcription of the following TFEB target genes: *BECN1*, *GABARAP*, *STK4* and *WDR45*. All four TFEB targets showed increased expression upon ATRA treatment, in line with previous studies [14, 15, 62] (Fig. 6I). Knock down of *FASN* led to a further increase in the expression of 3/4 TFEB targets analyzed (Fig. 6I). These results suggest that FASN retardation of TFEB translocation to the nucleus attenuates CLEAR network gene transcription.

Then, we tested whether we can obtain similar results by lowering FASN protein levels using EGCG. Using different

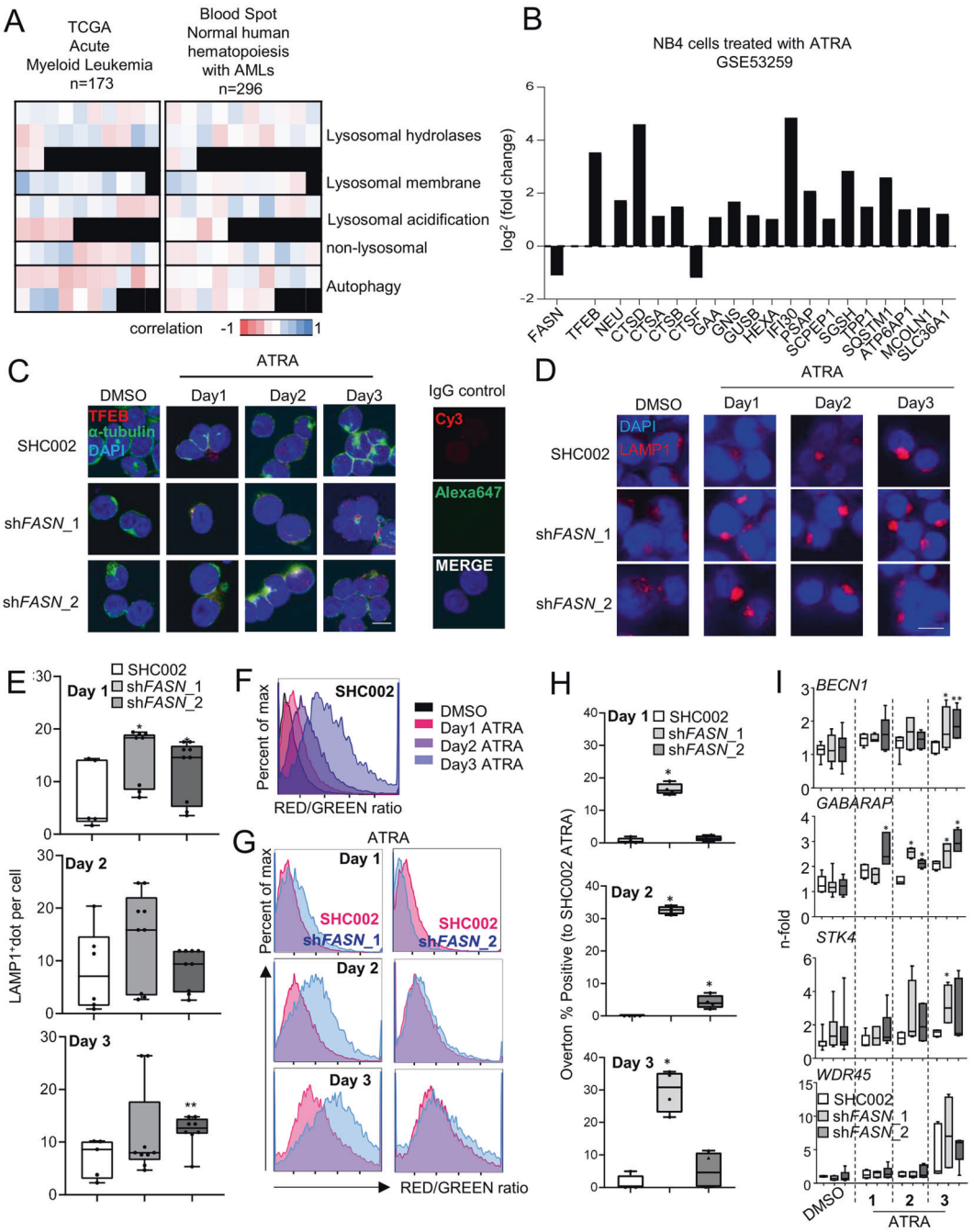

Fig. 6 FASN expression negatively associates with TFEB activity. **A** Heatmaps of the correlation between FASN and TFEB target genes extracted from the TCGA-AML cohort analyzed by the UCSD xena platform and from the blood spot data bank (Spearman, *p* values in Supplementary Table 1 and 2). **B** mRNA sequencing data of NB4 cells treated with ATRA. Relative expression of *FASN*, *TFEB* and TFEB transcriptional targets involved in lysosomal function and biogenesis are shown. **C**–**H** NB4 control (SHC002) and *FASN* knockdown (sh*FASN*_1, _2) cells were treated for 1–3 days with ATRA. **C** Immunofluorescence microscopy of endogenous TFEB (red) and α-tubulin (green). IgG staining was used as negative control. Nuclei were stained with DAPI (blue). **D** Immunofluorescence microscopy of endogenous LAMP1 (red). Nuclei were stained with DAPI (blue). Scale: 10 µm (**E**) LAMP1 punctae quantification of cells shown in (**D**). Scale: 10 µm (**F**–**H**) Acridine Orange staining. **F** Histogram representation of the ratio between RED and GREEN of NB4 control (SHC002) cells treated as described in 6 C. **G** Representative histogram of NB4 control (SHC002) and *FASN* knockdown (sh*FASN*_1, _2) cells treated as in 6 C. **H** Overton percentage positive quantification of the RED/GREEN ratio of NB4 control (SHC002) and *FASN* knockdown (sh*FASN*_1, _2) cells treated with ATRA at indicated times. **I** Evaluation of *BECN1*, *GABARAP*, *STK4* and *WDR45* mRNA transcripts was done by qPCR. Values were normalized to the HMBS housekeeping gene. Results shown are from at least two biological duplicates.

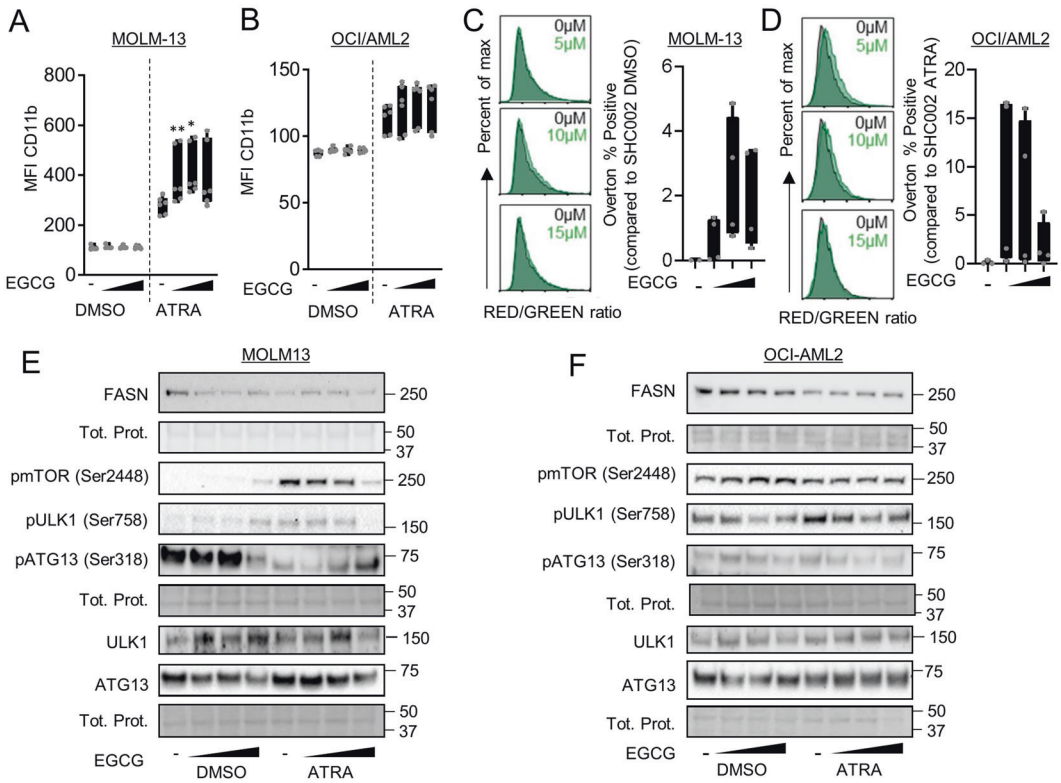

Fig. 7 Lowering FASN protein expression levels improves ATRA therapy in non-APL AML cells. A–F MOLM-13 (**A**, **C**, **E**), and OCI-AML2 (**B**, **D**, **F**) cells were treated with ATRA and different concentrations of EGCG (5 μM, 10 μM and 15 μM) for 3 days ($n = 3$). **A–B** CD11b surface staining was analyzed by flow cytometry. Box blot represent the median fluorescence intensity (MFI) of CD11b positive cells. **C–D** Acridine Orange staining. Analysis was performed as in Fig. 6E-G. **E–F** Total protein extracted from MOLM-13 and OCI-AML2 cells treated as in 7 A/B were subjected to immunoblotting using anti-FASN, anti-pmTOR(Ser2448), anti- pULK1(Ser757), anti-ULK1, anti-pATG13(Ser318) and anti-ATG13 antibodies. Results shown are from at least two biological duplicates.

EGCG concentrations, we found a decrease in mTOR phosphorylation at Ser2448 (Supplementary Fig. 7A), an increase of TFEB translocation to the nucleus (Supplementary Fig. 7B), an increase of LAMP1^{+} vesicles (Supplementary Fig. 8A-B) and an increase of the RED/GREEN ratio in Acridine Orange stained cells similar to the results seen in FASN-depleted APL cells (Supplementary Fig. 8C-E). In addition, we found an upregulation of 3/4 TFEB target genes in presence of EGCG in line with our FASN knockdown experiments (Supplementary Fig. 7C).

Together, these data suggest that high FASN expression results in lower autophagic activity and decreased lysosomal capacity due to increased mTOR activity causing TFEB inhibition.

Lowering FASN expression improves ATRA therapy in non-APL AML cell lines by inhibiting the mTOR pathway

Given the fact that APL cells treated with EGCG demonstrated improved response to ATRA therapy, we asked if EGCG can be beneficial to other AML subtypes that are refractory to ATRA treatment. We and others previously demonstrated a positive impact of co-treating HL60 AML cells, a non-APL AML cell line that responds to ATRA, with EGCG and ATRA [48, 63, 64]. Therefore, we tested if ATRA-refractory AML cell lines with different genetic backgrounds, namely MOLM-13 (FLT3-ITD^{+}) and OCI/AML2 (DNMT3A R635W mutation), would respond to ATRA in combination with EGCG. MOLM-13 showed significantly increased granulocytic differentiation upon the combination treatment as shown by CD11b surface expression while OCI/AML2 cells showed a clear but non-significant trend toward improved granulocytic differentiation (Fig. 7A-B). In addition, MOLM-13 and OCI/AML2-showed an increase in the RED/GREEN ratio when stained with Acridine Orange (Fig. 7C-D). Furthermore, co-treatment with ATRA and EGCG led to a decrease in mTOR activity as seen by a decrease in mTOR (Ser2448) and ULK1 (Ser758) phosphorylation. In MOLM-13 cells, this was paralleled by an increase of ATG13 (Ser318) phosphorylation (Fig. 7E-F). We further confirmed these data by genetically inhibiting *FASN* in MOLM-13 (Fig. 8A) and OCI/AML2 (Fig. 8B) cells. Depleting FASN in both cell lines caused an increase of CD11b surface expression after 3 days of ATRA treatment (Fig. 8C-D), coupled with

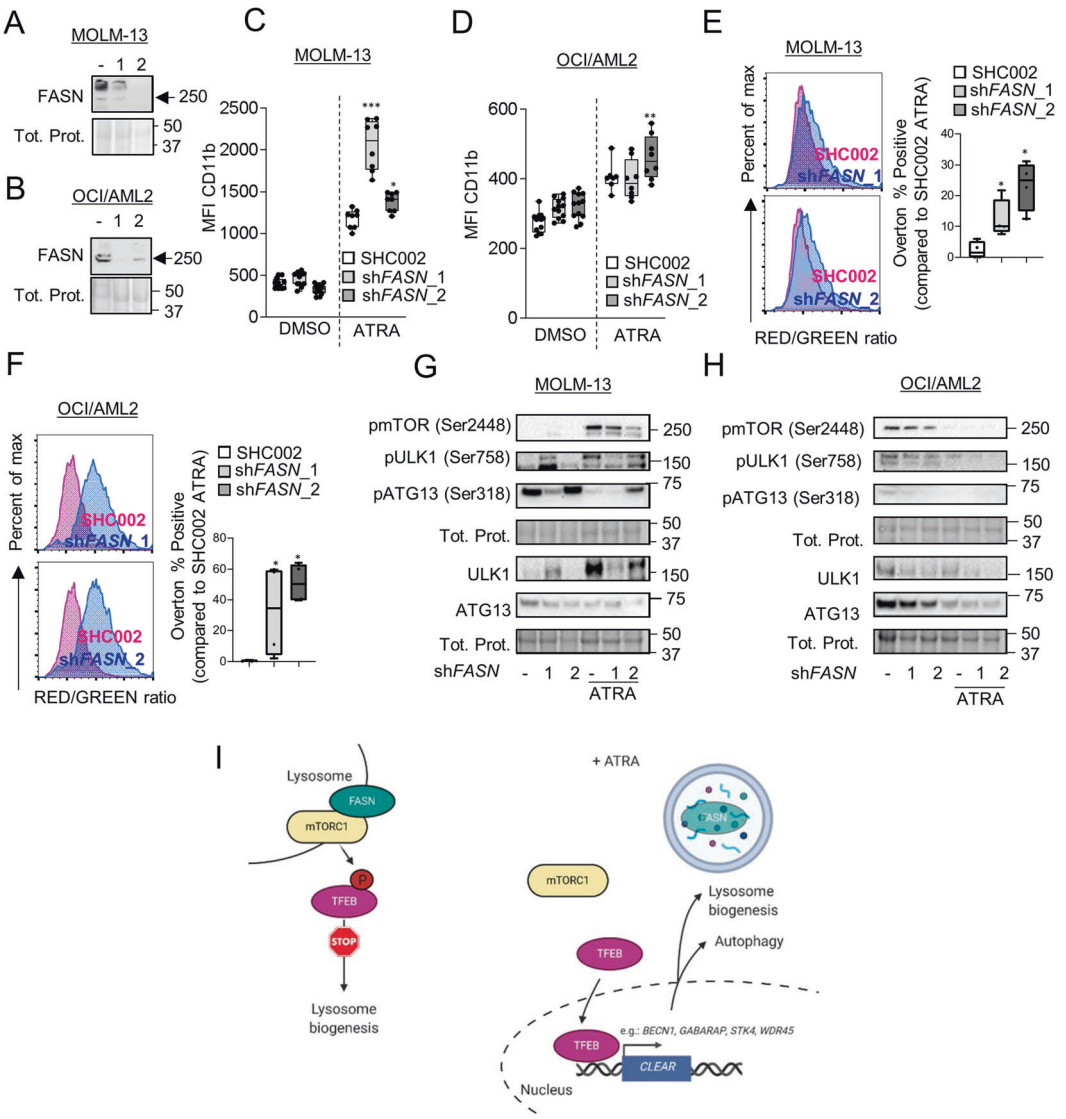

Fig. 8 MOLM-13 and OCI/AML2 were stably transduced with 2 independent shRNA targeting *FASN* ($n = 3$). A–B *FASN* knockdown efficiency was validated in MOLM-13 (**A**) and OCI/AML2 (**B**) by western blotting. **C–H** MOLM-13 and OCI/AML2 control and FASN knockdown cells were treated with ATRA for 3 days. **C–D** CD11b surface marker expression was analyzed as in (**A–B**). **E–F** Acridine Orange staining analysis was performed as in 7E-G. **G–H** Western blot analysis of total protein was extracted and subjected to immunoblotting using anti-FASN, anti-pmTOR(Ser2448), anti- pULK1(Ser757), anti-ULK1, anti-pATG13(Ser318) and anti-ATG13 antibodies. Results shown are from at least two biological duplicates. **I** FASN localizes to lysosomes in AML with mTOR leading to the phosphorylation of TFEB and its sequestration in the cytoplasm. ATRA treatment resulted in FASN degradation by autophagy and thus TFEB translocation to the nucleus and activation of lysosomal biogenesis.

an increased RED/GREEN ratio when stained for Acridine Orange (Fig. 8E-F) and lower mTOR activity (Fig. 8G-H). Interestingly, we found more variation in lysosomal compartment changes between the experimental duplicates upon ATRA when cells were treated with EGCG (Fig. 7D, F) than in the knockdown cells (Fig. 8F, H), perhaps reflecting the lower specificity of EGCG.

Together, our data suggest that reducing FASN expression can increase lysosomal biogenesis and improve the differentiation of non-APL AML cells. We, therefore, propose that FASN is recruited to lysosomes in AML cells resulting in activation of mTOR and sequestration of TFEB in the cytoplasm (Fig. 8I). FASN degradation via autophagy resulted in activation of TFEB and its downstream targets (Fig. 8I).

Discussion

In this study, we aimed at further dissecting the function of FASN in AML cells and, in particular, its potential role in the differentiation of immature AML blasts. We showed

that knocking down *FASN* accelerated ATRA-induced differentiation, while inhibition of its enzymatic function by pharmacological inhibitors such as C75 or Orlistat had no effect. Furthermore, we found that FASN expression activates mTOR resulting in sequestration of TFEB to the cytoplasm. Importantly, inhibiting *FASN* expression, in combination with ATRA treatment, improved differentiation therapy in non-APL AML cells.

Several studies demonstrated a tumor suppressor role of autophagy in AML cells. Autophagy can support degradation of leukemic oncogenes in AML such as FLT3-ITD and PML-RARA [10, 65, 66]. Furthermore, activation of mTORC1 is crucial for leukemia cell proliferation at least partially due to its inhibitory effect on autophagy [42, 67]. Accordingly, inhibition of autophagy leads to acceleration of MLL-ENL AML leukemia progression in vivo [42]. Our results indicate that increased FASN expression might be a key activator of mTORC1 in AML. Surprisingly, we found that reducing FASN protein levels, but not inhibition of catalytic function, promotes ATRA-induced differentiation. Recently, Bueno et al. demonstrated that FASN is key during the transformation from 2- to 3-dimensional growth of cancer cells. This transformation step does not depend on the FASN biosynthetic products palmitate, further hinting to at important non-catalytic functions of FASN in carcinogenesis [68]. Further studies on the interplay between FASN, mTOR and autophagy in AML transformation, progression and therapy resistance are warranted to improve our understanding of cell fate decisions and could potentially open new avenues to tackle this disease with improved differentiation therapies.

We further confirmed that EGCG positively impacts cellular differentiation in additional AML subtypes in vitro [48, 63, 64]. Searching for potential mediators of the positive effects of EGCG observed during ATRA-induced differentiation, we previously found that EGCG induces expression of the Ca^{2+}/calmodulin-regulated serine/threonine kinase DAPK2. DAPK2 plays a major role in granulocytic differentiation and decreased DAPK2 expression in APL cells can be restored by ATRA and EGCG treatment [13, 38, 48]. DAPK2 also negatively regulates mTOR via phosphorylation of raptor at Ser721 as shown in HeLa cells [69]. Therefore, a potential impact of FASN on DAPK2 activity in a leukemic context warrants further investigation.

Interestingly, treating APL cells with ATRA had a negative effect on FASN protein levels (Fig. 1C), and we demonstrated that ATRA-induced autophagy contributes to FASN protein degradation. Furthermore, FASN reduction led to increased lysosomal biogenesis suggesting a negative feedback loop between autophagy and FASN. It is reasonable to hypothesize that the more AML cells differentiate the more they become competent to degrade long-lived proteins including FASN. In addition, inhibiting mTOR using Rapamycin or Everolimus accelerates differentiation of APL cells [10, 12]. While PI3K/AKT/mTOR pathways are activated in about 80% of AML cases, mTOR inhibitors had only modest effects in AML therapy [70, 71]. Furthermore, despite its role in leukemia cells, mTOR activity is crucial for hematopoietic stem cell (HSC) proliferation and self-renewal potential [72]. Therefore, targeting FASN with low expression in healthy progenitor cells would allow activation of autophagy in AML cells sparing healthy HSC cells in the bone marrow. In our hands, EGCG treatment only demonstrated partial effects regarding improved differentiation when compared to knocking down FASN in non-APL AML cells. Therefore, a more specific FASN expression inhibitor is needed to improve differentiation therapy in non-APL AML patients.

Indeed, it would be of interest to study the transcriptional regulation of FASN to influence its expression in autophagy-deficient cells. Consistently, there are several studies showing that *FASN* transcription is positively affected by retinoic acids [73, 74]. However, transcription induction is not mediated by a classic retinoic acid-responsive element but rather by the indirect influence of retinoic acid via *cis*-regulatory elements. Since this involves different cofactors it is tempting to speculate that transcriptional activation might switch to repression depending on the cellular context including specific retinoid-binding proteins and cofactors. We previously found that members of the KLF transcription factor family are often deregulated in primary AML patient samples. Among the different KLF family members downregulated in AML, particularly *KLF5* turned out to be essential for granulocytic differentiation [75, 76]. KLF5 forms a transcriptionally active complex with RAR/RXR heterodimers [77, 78]. Interestingly, ectopic expression of KLF5 in U937 non-APL AML cell line was sufficient to significantly increase ATRA-induced differentiation [79]. We hypothesize that KLF5 negatively regulates *FASN* transcription in AML cells via the RAR/RXR complex.

In summary, our data suggest that inducing FASN protein degradation is likely to be beneficial for differentiation therapy of non-APL AML cells as this will impede mTOR and promote TFEB transcriptional activity and autophagy. Furthermore, high FASN expression in AML is partially based on attenuated autophagy activity in this disease.

Acknowledgements Deborah Shan-Krauer is gratefully acknowledged for excellent technical support. We thank Dr. MS Soengas for providing a mCherry-LC3B lentiviral vector. We thank Dr. Stefan Freigang for his help with the revision experiments. All schematic representations were created with Biorender.com.

Author contributions MH, KS, KS, SM, and VR performed the experimental research. MH, KS, SMCK and MPT drafted the article.

SMCK, and AVP provided essential reagents and data. MH designed the project. MPT gave final approval of the submitted paper.

Funding This study was supported by grants from Swiss Cancer Research (KFS-3409-02-2014 to MPT, MD-PhD 03/17 Scholarship to KS), the Swiss National Science Foundation (31003A_173219 to MPT), the Berne University Research Foundation (45/2018, to MPT), the University of Bern initiator grant, the Bernese Cancer League, "Stiftung für klinisch-experimentelle Tumorforschung", and the Werner and Hedy Berger-Janser Foundation for Cancer Research (to MH). SMCK is supported by Breakthrough Cancer Research. Open Access funding provided by Universität Bern.

Compliance with ethical standards

Conflict of interest The authors declare no competing interests.

Ethical approval Protocols and use of 67 human samples acquired in Bern were approved by the Cantonal Ethical Committee at the Inselspital.

Publisher's note Springer Nature remains neutral with regard to jurisdictional claims in published maps and institutional affiliations.

References

1. Wang Z-Y, Chen Z. Acute promyelocytic leukemia: from highly fatal to highly curable. Blood. 2008;111:2505–15.
2. Germain P, Chambon P, Eichele G, Evans RM, Lazar MA, Leid M, et al. International Union of Pharmacology. LX. Retinoic acid receptors. Pharm Rev. 2006;58:712–25.
3. Su M, Alonso S, Jones JW, Yu J, Kane MA, Jones RJ, et al. All-Trans Retinoic Acid Activity in Acute Myeloid Leukemia: role of Cytochrome P450 Enzyme Expression by the Microenvironment. PLOS ONE. 2015;10:e0127790.
4. Marchwicka A, Cebrat M, Sampath P, Śnieżewski Ł, Marcinkowska E. Perspectives of Differentiation Therapies of Acute Myeloid Leukemia: the Search for the Molecular Basis of Patients' Variable Responses to 1,25-Dihydroxyvitamin D and Vitamin D Analogs. Front Oncol. 2014; 4. https://doi.org/10.3389/fonc.2014.00125.
5. Schenk T, Chen WC, Göllner S, Howell L, Jin L, Hebestreit K, et al. Inhibition of the LSD1 (KDM1A) demethylase reactivates the all-trans-retinoic acid differentiation pathway in acute myeloid leukemia. Nat Med. 2012;18:605–611.
6. Rice AM, Holtz KM, Karp J, Rollins S, Sartorelli AC. Analysis of the relationship between Scl transcription factor complex protein expression patterns and the effects of LiCl on ATRA-induced differentiation in blast cells from patients with acute myeloid leukemia. Leuk Res. 2004;28:1227–37.
7. Bullinger L, Schlenk RF, Götz M, Botzenhardt U, Hofmann S, Russ AC, et al. PRAME-induced inhibition of retinoic acid receptor signaling-mediated differentiation–a possible target for ATRA response in AML without t(15;17). Clin Cancer Res J Am Assoc Cancer Res. 2013;19:2562–71.
8. Petrie K, Zelent A, Waxman S. Differentiation therapy of acute myeloid leukemia: past, present and future. Curr Opin Hematol. 2009;16:84–91.
9. Altucci L, Gronemeyer H. The promise of retinoids to fight against cancer. Nat Rev Cancer. 2001;1:181–93.
10. Isakson P, Bjørås M, Bøe SO, Simonsen A. Autophagy contributes to therapy-induced degradation of the PML/RARA oncoprotein. Blood. 2010;116:2324–31.
11. Wang Z, Cao L, Kang R, Yang M, Liu L, Zhao Y, et al. Autophagy regulates myeloid cell differentiation by p62/SQSTM1-mediated degradation of PML-RARα oncoprotein. Autophagy. 2011;7:401–11.
12. Jin J, Britschgi A, Schläfli AM, Humbert M, Shan-Krauer D, Batliner J, et al. Low Autophagy (ATG) Gene Expression Is Associated with an Immature AML Blast Cell Phenotype and Can Be Restored during AML Differentiation Therapy. Oxid Med Cell Longev. 2018;2018:1482795.
13. Humbert M, Federzoni EA, Tschan MP. Distinct TP73-DAPK2-ATG5 pathway involvement in ATO-mediated cell death versus ATRA-mediated autophagy responses in APL. J Leukoc Biol. 2017;102:1357–70.
14. Brigger D, Proikas-Cezanne T, Tschan MP. WIPI-dependent autophagy during neutrophil differentiation of NB4 acute promyelocytic leukemia cells. Cell Death Dis. 2014;5:e1315.
15. Orfali N, O'Donovan TR, Cahill MR, Benjamin D, Nanus DM, McKenna SL et al. All-trans retinoic acid (ATRA) induced TFEB expression is required for myeloid differentiation in acute promyelocytic leukemia (APL). Eur J Haematol. 2019. https://doi.org/10.1111/ejh.13367.
16. Feng Y, He D, Yao Z, Klionsky DJ. The machinery of macroautophagy. Cell Res. 2014;24:24–41.
17. Asturias FJ, Chadick JZ, Cheung IK, Stark H, Witkowski A, Joshi AK, et al. Structure and molecular organization of mammalian fatty acid synthase. Nat Struct Mol Biol. 2005;12:225–32.
18. Maier T, Jenni S, Ban N. Architecture of mammalian fatty acid synthase at 4.5 \AA resolution. Science. 2006;311:1258–62.
19. Pizer ES, Lax SF, Kuhajda FP, Pasternack GR, Kurman RJ. Fatty acid synthase expression in endometrial carcinoma. Cancer. 1998;83:528–37.
20. Visca P, Sebastiani V, Botti C, Diodoro MG, Lasagni RP, Romagnoli F, et al. Fatty acid synthase (FAS) is a marker of increased risk of recurrence in lung carcinoma. Anticancer Res. 2004;24:4169–73.
21. Bandyopadhyay S, Pai SK, Watabe M, Gross SC, Hirota S, Hosobe S, et al. FAS expression inversely correlates with PTEN level in prostate cancer and a PI 3-kinase inhibitor synergizes with FAS siRNA to induce apoptosis. Oncogene. 2005;24:5389–95.
22. Alo PL, Visca P, Marci A, Mangoni A, Botti C, Di Tondo U. Expression of fatty acid synthase (FAS) as a predictor of recurrence in stage I breast carcinoma patients. Cancer. 1996;77:474–82.
23. Shurbaji MS, Kalbfleisch JH, Thurmond TS. Immunohistochemical detection of a fatty acid synthase (OA-519) as a predictor of progression of prostate cancer. Hum Pathol. 1996;27:917–21.
24. Rashid A, Pizer ES, Moga M, Milgraum LZ, Zahurak M, Pasternack GR, et al. Elevated expression of fatty acid synthase and fatty acid synthetic activity in colorectal neoplasia. Am J Pathol. 1997;150:201–8.

25. Diaz-Blanco E, Bruns I, Neumann F, Fischer JC, Graef T, Rosskopf M, et al. Molecular signature of CD34(+) hematopoietic stem and progenitor cells of patients with CML in chronic phase. Leukemia. 2007;21:494–504.
26. Weiss L, Hoffmann GE, Schreiber R, Andres H, Fuchs E, Körber E, et al. Fatty-acid biosynthesis in man, a pathway of minor importance. Purification, optimal assay conditions, and organ distribution of fatty-acid synthase. Biol Chem Hoppe Seyler. 1986;367:905–12.
27. Pizer ES, Kurman RJ, Pasternack GR, Kuhajda FP. Expression of fatty acid synthase is closely linked to proliferation and stromal decidualization in cycling endometrium. Int J Gynecol Pathol J Int Soc Gynecol Pathol. 1997;16:45–51.
28. Maningat PD, Sen P, Rijnkels M, Sunehag AL, Hadsell DL, Bray M, et al. Gene expression in the human mammary epithelium during lactation: the milk fat globule transcriptome. Physiol Genom. 2009;37:12–22.
29. Park J, Lee SE, Hur J, Hong EB, Choi J-I, Yang J-M, et al. M-CSF from Cancer Cells Induces Fatty Acid Synthase and PPARβ/δ Activation in Tumor Myeloid Cells, Leading to Tumor Progression. Cell Rep. 2015;10:1614–25.
30. Peters JM, Gonzalez FJ. Sorting out the functional role(s) of peroxisome proliferator-activated receptor-β/δ (PPARβ/δ) in cell proliferation and cancer. Biochim Biophys Acta BBA - Rev Cancer. 2009;1796:230–41.
31. Zuo X, Peng Z, Moussalli MJ, Morris JS, Broaddus RR, Fischer SM, et al. Targeted Genetic Disruption of Peroxisome Proliferator–Activated Receptor-δ and Colonic Tumorigenesis. JNCI J Natl Cancer Inst. 2009;101:762–7.
32. Jung-Kyu Han, Hyun-Sook Lee, Han-Mo Yang, Jin Hur, Soo-In Jun, Ju-Young Kim, et al. Peroxisome Proliferator–Activated Receptor-δ Agonist Enhances Vasculogenesis by Regulating Endothelial Progenitor Cells Through Genomic and Nongenomic Activations of the Phosphatidylinositol 3-Kinase/Akt Pathway. Circulation. 2008;118:1021–33.
33. Kang K, Reilly SM, Karabacak V, Gangl MR, Fitzgerald K, Hatano B, et al. Adipocyte-Derived Th2 Cytokines and Myeloid PPARδ Regulate Macrophage Polarization and Insulin Sensitivity. Cell Metab. 2008;7:485–95.
34. Lee C-H, Chawla A, Urbiztondo N, Liao D, Boisvert WA, Evans RM. Transcriptional Repression of Atherogenic Inflammation: Modulation by PPARδ. Science. 2003;302:453–7.
35. Odegaard JI, Ricardo-Gonzalez RR, Red Eagle A, Vats D, Morel CR, Goforth MH, et al. Alternative M2 Activation of Kupffer Cells by PPARδ Ameliorates Obesity-Induced Insulin Resistance. Cell Metab. 2008;7:496–507.
36. Yeh CW, Chen WJ, Chiang CT, Lin-Shiau SY, Lin JK. Suppression of fatty acid synthase in MCF-7 breast cancer cells by tea and tea polyphenols: a possible mechanism for their hypolipidemic effects. Pharmacogenomics J. 2003;3:267.
37. Tschan MP, Fischer KM, Fung VS, Pirnia F, Borner MM, Fey MF, et al. Alternative splicing of the human cyclin D-binding Myb-like protein (hDMP1) yields a truncated protein isoform that alters macrophage differentiation patterns. J Biol Chem. 2003;278:42750–60.
38. Rizzi M, Tschan MP, Britschgi C, Britschgi A, Hügli B, Grob TJ, et al. The death-associated protein kinase 2 is up-regulated during normal myeloid differentiation and enhances neutrophil maturation in myeloid leukemic cells. J Leukoc Biol. 2007;81:1599–608.
39. Tschan MP, Shan D, Laedrach J, Eyholzer M, Leibundgut EO, Baerlocher GM, et al. NDRG1/2 expression is inhibited in primary acute myeloid leukemia. Leuk Res. 2010;34:393–8.
40. Gubern A, Barceló-Torns M, Casas J, Barneda D, Masgrau R, Picatoste F, et al. Lipid Droplet Biogenesis Induced by Stress Involves Triacylglycerol Synthesis That Depends on Group VIA Phospholipase A2. J Biol Chem. 2009;284:5697–708.
41. Bagger FO, Sasivarevic D, Sohi SH, Laursen LG, Pundhir S, Sønderby CK, et al. BloodSpot: a database of gene expression profiles and transcriptional programs for healthy and malignant haematopoiesis. Nucleic Acids Res. 2016;44:D917–24.
42. Watson AS, Riffelmacher T, Stranks A, Williams O, De Boer J, Cain K et al. Autophagy limits proliferation and glycolytic metabolism in acute myeloid leukemia. Cell Death Discov. 2015; 1. https://doi.org/10.1038/cddiscovery.2015.8.
43. Volpe JJ, Vagelos PR. Mechanisms and regulation of biosynthesis of saturated fatty acids. Physiol Rev. 1976;56:339–417.
44. Dengjel J, Høyer-Hansen M, Nielsen MO, Eisenberg T, Harder LM, Schandorff S et al. Identification of Autophagosome-associated Proteins and Regulators by Quantitative Proteomic Analysis and Genetic Screens. Mol Cell Proteomics. MCP 2012; 11. https://doi.org/10.1074/mcp.M111.014035.
45. Suzuki K, Nakamura S, Morimoto M, Fujii K, Noda NN, Inagaki F, et al. Proteomic Profiling of Autophagosome Cargo in Saccharomyces cerevisiae. PLOS ONE. 2014;9:e91651.
46. Yamamoto A, Tagawa Y, Yoshimori T, Moriyama Y, Masaki R, Tashiro Y. Bafilomycin A1 prevents maturation of autophagic vacuoles by inhibiting fusion between autophagosomes and lysosomes in rat hepatoma cell line, H-4-II-E cells. Cell Struct Funct. 1998;23:33–42.
47. Poole B, Ohkuma S. Effect of weak bases on the intralysosomal pH in mouse peritoneal macrophages. J Cell Biol. 1981;90:665–9.
48. Britschgi A, Simon H-U, Tobler A, Fey MF, Tschan MP. Epigallocatechin-3-gallate induces cell death in acute myeloid leukaemia cells and supports all-trans retinoic acid-induced neutrophil differentiation via death-associated protein kinase 2. Br J Haematol. 2010;149:55–64.
49. Gump JM, Thorburn A. Sorting cells for basal and induced autophagic flux by quantitative ratiometric flow cytometry. Autophagy. 2014;10:1327–34.
50. Klionsky DJ, Abdelmohsen K, Abe A, Abedin MJ, Abeliovich H, Acevedo Arozena A, et al. Guidelines for the use and interpretation of assays for monitoring autophagy (3rd edition). Autophagy. 2016;12:1–222.
51. Hu J, Che L, Li L, Pilo MG, Cigliano A, Ribback S, et al. Co-activation of AKT and c-Met triggers rapid hepatocellular carcinoma development via the mTORC1/FASN pathway in mice. Sci Rep. 2016;6:20484.
52. Calvisi DF, Wang C, Ho C, Ladu S, Lee SA, Mattu S, et al. Increased lipogenesis, induced by AKT-mTORC1-RPS6 signaling, promotes development of human hepatocellular carcinoma. Gastroenterology. 2011;140:1071–83.
53. Kim J, Kundu M, Viollet B, Guan K-LAMPK. and mTOR regulate autophagy through direct phosphorylation of Ulk1. Nat Cell Biol. 2011;13:132–41.
54. Joo JH, Dorsey FC, Joshi A, Hennessy-Walters KM, Rose KL, McCastlain K, et al. Hsp90-Cdc37 Chaperone Complex Regulates Ulk1- and Atg13-Mediated Mitophagy. Mol Cell. 2011;43:572–85.
55. Petherick KJ, Conway OJL, Mpamhanga C, Osborne SA, Kamal A, Saxty B, et al. Pharmacological Inhibition of ULK1 Kinase Blocks Mammalian Target of Rapamycin (mTOR)-dependent Autophagy. J Biol Chem. 2015;290:11376–83.
56. Vega-Rubin-de-Celis S, Peña-Llopis S, Konda M, Brugarolas J. Multistep regulation of TFEB by MTORC1. Autophagy. 2017;13:464–72.
57. Peña-Llopis S, Vega-Rubin-de-Celis S, Schwartz JC, Wolff NC, Tran TAT, Zou L, et al. Regulation of TFEB and V-ATPases by mTORC1. EMBO J. 2011;30:3242–58.
58. Roczniak-Ferguson A, Petit CS, Froehlich F, Qian S, Ky J, Angarola B, et al. The transcription factor TFEB links mTORC1 signaling to transcriptional control of lysosome homeostasis. Sci Signal. 2012;5:ra42.

59. Napolitano G, Esposito A, Choi H, Matarese M, Benedetti V, Malta CD, et al. mTOR-dependent phosphorylation controls TFEB nuclear export. Nat Commun. 2018;9:3312.
60. Goldman M, Craft B, Hastie M, Repečka K, McDade F, Kamath A, et al. The UCSC Xena platform for public and private cancer genomics data visualization and interpretation. bioRxiv. 2019;6:326470.
61. Thomé MP, Filippi-Chiela EC, Villodre ES, Migliavaca CB, Onzi GR, Felipe KB, et al. Ratiometric analysis of Acridine Orange staining in the study of acidic organelles and autophagy. J Cell Sci. 2016;129:4622–32.
62. Brigger D, Torbett BE, Chen J, Fey MF, Tschan MP. Inhibition of GATE-16 attenuates ATRA-induced neutrophil differentiation of APL cells and interferes with autophagosome formation. Biochem Biophys Res Commun. 2013;438:283–8.
63. Moradzadeh M, Roustazadeh A, Tabarraei A, Erfanian S, Sahebkar A. Epigallocatechin-3-gallate enhances differentiation of acute promyelocytic leukemia cells via inhibition of PML-RARα and HDAC1. Phytother Res PTR. 2018;32:471–9.
64. Lung HL, Ip WK, Wong CK, Mak NK, Chen ZY, Leung KN. Anti-proliferative and differentiation-inducing activities of the green tea catechin epigallocatechin-3-gallate (EGCG) on the human eosinophilic leukemia EoL-1 cell line. Life Sci. 2002;72:257–68.
65. Larrue C, Saland E, Boutzen H, Vergez F, David M, Joffre C, et al. Proteasome inhibitors induce FLT3-ITD degradation through autophagy in AML cells. Blood. 2016;127:882–92.
66. Rudat S, Pfaus A, Cheng YY, Holtmann J, Ellegast JM, Bühler C, et al. RET-mediated autophagy suppression as targetable co-dependence in acute myeloid leukemia. Leukemia. 2018;32:2189–202.
67. Hoshii T, Tadokoro Y, Naka K, Ooshio T, Muraguchi T, Sugiyama N, et al. mTORC1 is essential for leukemia propagation but not stem cell self-renewal. J Clin Investig. 2012;122:2114–29.
68. Bueno MJ, Jimenez-Renard V, Samino S, Capellades J, Junza A, López-Rodríguez ML, et al. Essentiality of fatty acid synthase in the 2D to anchorage-independent growth transition in transforming cells. Nat Commun. 2019;10:5011.
69. Ber Y, Shiloh R, Gilad Y, Degani N, Bialik S, Kimchi A. DAPK2 is a novel regulator of mTORC1 activity and autophagy. Cell Death Differ. 2015;22:465–75.
70. Mirabilii S, Ricciardi MR, Piedimonte M, Gianfelici V, Bianchi MP, Tafuri A Biological Aspects of mTOR in Leukemia. Int J Mol Sci. 2018; 19. https://doi.org/10.3390/ijms19082396.
71. Tabe Y, Tafuri A, Sekihara K, Yang H, Konopleva M. Inhibition of mTOR kinase as a therapeutic target for acute myeloid leukemia. Expert Opin Ther Targets. 2017;21:705–14.
72. Ghosh J, Kapur R. Regulation of Hematopoietic Stem Cell Self-Renewal and Leukemia Maintenance by the PI3K-mTORC1 Pathway. Curr Stem. Cell Rep. 2016;2:368–78.
73. Roder K, Wolf SS, Schweizer M. Regulation of the fatty acid synthase promoter by retinoic acid. Biochem Soc Trans. 1996;24:233S.
74. Roder K, Schweizer M. Retinoic acid-mediated transcription and maturation of SREBP-1c regulates fatty acid synthase via cis-elements responsible for nutritional regulation. Biochem Soc Trans. 2007;35:1211–4.
75. Humbert M, Halter V, Shan D, Laedrach J, Leibundgut EO, Baerlocher GM, et al. Deregulated expression of Kruppel-like factors in acute myeloid leukemia. Leuk Res. 2011;35:909–13.
76. Diakiw SM, Kok CH, Lewis LB, Brown ID, D'Andrea AL. RJ. The granulocyte-associated transcription factor Krüppel-like factor 5 is silenced by hypermethylation in acute myeloid leukemia. Leuk Res. 2012;36:110–6.
77. Lv X-R, Zheng B, Li S-Y, Han A-L, Wang C, Shi J-H, et al. Synthetic retinoid Am80 up-regulates apelin expression by promoting interaction of RARα with KLF5 and Sp1 in vascular smooth muscle cells. Biochem J. 2013;456:35–46.
78. Kada N, Suzuki T, Aizawa K, Munemasa Y, Matsumura T, Sawaki D, et al. Acyclic retinoid inhibits functional interaction of transcription factors Krüppel-like factor 5 and retinoic acid receptor-alpha. FEBS Lett. 2008;582:1755–60.
79. Shahrin NH, Diakiw S, Dent LA, Brown AL, D'Andrea RJ. Conditional knockout mice demonstrate function of Klf5 as a myeloid transcription factor. Blood. 2016;128:55–59.

Declaration of Originality

Last name, first name:

Matriculation number:

I hereby declare that this thesis represents my original work and that I have used no other sources except as noted by citations.
All data, tables, figures and text citations which have been reproduced from any other source, including the internet, have been explicitly acknowledged as such.
I am aware that in case of non-compliance, the Senate is entitled to withdraw the doctorate degree awarded to me on the basis of the present thesis, in accordance with the "Statut der Universität Bern (Universitätsstatut; UniSt)", Art. 69, of 7 June 2011.

Place, date

Signature